University of Alberta
Department of Civil Engineering

Structural Engineering Report No. 199

THE FLEXURAL CREEP BEHAVIOR OF OSB PANELS UNDER VARIOUS CLIMATIC CONDITIONS

by

Naiwen Zhao

J.J. Roger Cheng

and

Lars Bach

May 1994

Structural Engineering Report No. 199

THE FLEXURAL CREEP BEHAVIOR OF OSB PANELS UNDER VARIOUS CLIMATIC CONDITIONS

by

Naiwen Zhao

J.J. Roger Cheng

and

Lars Bach

Department of Civil Engineering

University of Alberta

Edmonton, Alberta, Canada T6G 2G7

May 1994

Abstract

The major concern of accepting Oriented Strandboard (OSB) as a structural material is its time-dependent performance. The objective of this study is to explore the flexural creep behavior of OSB panel in various climatic conditions. The study was carried out by an experimental and analytical program.

The relative humidity (RH) level, frequency of humidity cycling, panel thickness, and panel surface strand orientation are major variables studied. A total of ten test series were tested under four cyclic humidity, three constant humidity, and three uncontrolled indoor conditions. The creep duration was twelve and six weeks for the uncontrolled and controlled (constant/cyclic humidity) tests, respectively, except that the duration for one cyclic test series (14 days/cycle) was twenty-five weeks. The applied load was at a 20% stress level and the cyclic humidity changed between 35% and 85%. Plywood was tested along with OSB for comparison.

The panel deflection, as well as panel thickness and moisture movement, was measured during the creep test. Observations regarding the test results are made in this study. Analysis of variance and regression analysis are carried out here-in to demonstrate the significant variable(s) affecting the OSB creep.

For the constant and indoor environments, the creep prediction equations are obtained on a logarithmic time scale. A bilinear model, with parameters determined by the regression analysis, is established for OSB creep in cyclic humidity environments. The prediction results agree with the European code.

In one-dimensional analysis, the OSB diffusion coefficient is calculated and the moisture movement is analyzed by the finite difference method. A mechano-sorptive

model, which relates the panel creep to its moisture situation is constructed and the model result is compared with the creep prediction made by the regression equations. Furthermore, a parametric study using the creep model is carried out to speculate upon the OSB creep for panel thicknesses and environmental situations which are not studied in the experimental program.

ACKNOWLEDGEMENTS

This report is a reprint of a thesis by the first author under the supervision of the second and third author. Financial support for the project was provided mainly by the Natural Sciences and Engineering Research Council of Canada to Dr. L. Bach under grant No. A4656 and partially by the same funding source to Dr. J.J. Cheng under grant No. A4727.

The authors wish to express their thanks to the assistance of the technical staffs of the I.F. Morrison Structural Laboratory at the University of Alberta and of the Forest Products Testing Laboratory at the Alberta Research Council.

TABLE OF CONTENTS

LIST OF TABLES

LIST OF FIGURES

LIST OF SYMBOLS

• LATIN CHARACTERS

a	hydroviscoelastic constant
A	material constant
b	width of rectangular cross section
b_1, b_2	partial regression coefficients
B	material constant
C	material constant
D	material constant
D_m	diffusion coefficient
e_i	experimental error or residual in regression analysis
$E(u)$	elastic modulus at moisture content u
E_c	compressive elastic modulus
E_t	tensile elastic modulus
$f(t)$	creep function
$f_C(t)$	creep function for compression
$f_t(t)$	creep function for tension
F_i	observed fractional deflection in regression analysis
$\overline{F}$	mean of the observed fractional deflection in regression analysis
$\hat{F}$	expected fractional deflection in regression analysis
$F(t)$	fractional deflection at creep time t
F_{65}	fractional deflection under 65% RH/20 ^{o}C
F_{ms}	mechano-sorptive fractional deflection
$G(t)$	relaxation modulus
h	nominal thickness of OSB panels

h_c	height of area in compression
h_t	height of area in tension
H	measured thickness of OSB panels
$H0$	measured thickness of OSB panels at 65%RH/20 ^{o}C
$J, J(t)$	creep compliance
J_{00}	instantaneous elastic compliance at 0% moisture content
$J_E(u)$	elastic compliance at the current MC level u
J_N	basic master curve under constant MC and constant load
J_R	reduced creep compliance
J_c	creep compliance corresponding to the creep deflection increment at 65% RH/20 ^{o}C environment
J_e	elastic compliance of a specimen at equilibrium condition as 65% RH/20 ^{o}C
J_{ms}	mechano-sorptive creep compliance
K	slope
$L/2$	half thickness of wood panel
m	material constant
M	moment
MC	moisture content (%)
MC_{65}	panel's equilibrium MC at 65%RH/20 ^{o}C
MC_i	initial equilibrium moisture content
MC_0	outside surface moisture content
MC_{m-1}	moisture contents at the point $(m-1)\delta x$ at time $n\delta t$
MC_m	moisture content at the point $m\delta x$ at time $n\delta t$
MC_{m+1}	moisture content at the point $(m+1)\delta x$ at time $n\delta t$
MC_m^+	moisture content at the point $m\delta x$ at time $(n+1)\delta t$
MC_m^-	moisture content at the point $m\delta x$ at time $(n-1)\delta t$

MOE	modulus of elasticity
n	number of moisture content changes
$\bar{n}$	number of RH cycles
N_1 , N_2	characteristic cycle number
N_c	resultant compressive force
N_t	resultant tensile force
p	period of cyclic RH
p_i , q_i	parameters in differential equation describing mechanical response under applied load
Q	rate of transfer of diffusion substance per unit area of section
t	time
u	moisture content level
V	concentration of diffusion substance
W	mass of wood sample
W_0	oven-dry mass of the sample
W_{65}	panel's equilibrium weight at 65%RH/20 ^{o}C
x	space coordinate
X	dimensionless space coordinate
Z	fractional moisture content
$\bar{Z}$	average fractional moisture content of panel
Z_{m-1}	fractional moisture contents at the point $(m-1)\delta x$ at time $n\delta t$
Z_m,	fractional moisture content at the point $m\delta x$ at time $n\delta t$
Z_{m+1}	fractional moisture content at the point $(m+1)\delta x$ at time $n\delta t$
Z_m^+	fractional moisture content at the point $m\delta x$ at time $(n+1)\delta t$

• GREEK CHARACTERS

$\alpha(u)$	moisture shift factor
β	free shrinking or swelling coefficient
σ	stress
σ_0	applied constant stress
σ_c	maximum compressive stress along bending cross section
σ_t	maximum tensile stress along bending cross section
σ_u	short-term ultimate strength
ε	strain
ε_c	basic creep strain under constant load and climatic condition
ε_e	elastic strain
ε_s	strain induced by moisture fluctuation
$\dot{\varepsilon}_{s0}$	free moisture induced strain rate
$\dot{\varepsilon}^{ms}$	mechano-sorptive strain rate
$\dot{\varepsilon}^{msr}$	mechano-sorptive recovery rate
$\dot{\varepsilon}^{st}$	shrinkage-swelling rate
ε_C'	maximum compressive strain along bending cross section
ε_t	maximum tensile strain along bending cross section
Φ	curvature
τ	relative time
δt	time interval
δx	distance interval
Δ	total bending deflection
Δ_c	pure creep deflection due to the sustained loading and constant climatic condition
Δ_e	elastic bending deflection

Δ_{ms}	mechano-sorptive deflection
χ	material constant
$\xi(t)$	material time

Chapter 1 Introduction

1.1 General

Most mechanical properties of building materials are based on the assumption of elastic behavior under which the stress and strain have a unique relationship. However, the time-dependency of building materials is very important in many cases. Creep and stress relaxation are two important aspects of the time-dependency. The strain of most materials does not remain constant and additional strain develops with the passage of time under the application of a given constant stress; this phenomenon is often referred to as creep. The time-dependent deformation may lead to undesired deflection. Under constant maintained strain, the associated stress gradually decreases, and is called stress relaxation. The stress relaxation phenomenon can be observed in many cases. For instance, the reduction of pressure due to stress relaxation could result in low-quality bonding for some types of glued assemblies.

Furthermore, the time-dependency of materials could cause a column to buckle under a sustained compressive load that is much lower than the elastic buckling load; beams or columns could fail under sustained loads which are less than the ultimate static load, which means that the ultimate strength of a material decreases with the duration of the applied load. This is referred to as duration of load.

Wood and wood based materials exhibit noticeable time-dependent behavior. The time-dependent behavior of building materials is influenced by loading conditions, as well as by the environment to which the material is exposed. Under a low stress level, most materials behave linearly. Under a high stress level, most materials behave nonlinearly, that is, the time-dependent deformation is not proportional to the applied load. In addition, the time-dependency of wood is affected by the type of stress. Under

compression or tension, creep may be different. The time-dependency of the mechanical behavior of wood is also affected by the rate of loading. Usually, faster loading results in less deformation when stress reaches the same level.

The influence of environment is very important to the time-dependent behavior of wood and wood based materials. Under high environmental humidity and/or temperature, the time-dependent deformations will increase. The variations in humidity combined with mechanical loading have a very significant influence on the time-dependent behavior of wood materials. A large amount of deformation is produced under the interaction between humidity variations and mechanical loading when compared with constant humidity environment. This interaction effect is often referred to as mechanical-sorption in the pertinent literature. Much of the research in this area is summarized in the next chapter.

An example of the interaction between the applied sustained load and environmental humidity changes is shown in Fig. 1.1. The plot is the result reported by Hearmon and Paton (1964) for small sized beams. As shown in the figure, the time-dependent deflection of the solid wood beams under humidity changes is much larger than that of the high constant humidity. The beams failed at the load much less than their short-term ultimate strength.

1.2 Oriented Strandboard and Plywood

1.2.1 Oriented Strandboard

Oriented strandboard is an engineering product made by processing small, fast growing trees, such as aspen, into strands which are bonded together under heat and pressure with a waterproof and boilproof resin. The surface layers of strands of OSB are aligned in the panel length direction. The inner layers may be cross or random

aligned. Greater strength and dimension stability are obtained through such arrangement. The bending strength of OSB is larger in the parallel direction than in the perpendicular direction.

The basic manufacturing steps include preparing strands, blending, forming, pressing, cooling, and trim sawing. The thickness of a strand is usually controlled and its length along the grain direction is at least twice, and usually many times, its width. The strand size used by most mills is approximately 83 mm (3 1/4") long, 25 mm (1") wide and 0.7 mm thick. The strength of OSB comes mainly from the uninterrupted wood fiber, the interleaving of the long strands, and the degree of strand orientation of surface layers. The waterproof and boilproof resin combined with the strands provides the panels with internal strength, rigidity, and moisture resistance. The waterproof and boilproof resin is a thermosetting adhesive binder which is not softened by heat or moisture at the condition normally encountered in service when it is fully cured. Phenol-formaldehyde is the most commonly used resin in manufacturing OSB.

Although regular OSB panels are unsanded, they have solid uniform faces, with surfaces and interiors free of knots and large voids. The thickness of OSB panels ranges from 6 mm (1/4") to 32 mm (1 1/4") and their size is usually 1220 mm by 2440 mm (4' x 8').

In Canada OSB is manufactured to meet the requirements of CAN/CSA-O437.0-M93 "Strandboard and Waferboard". The standard specifies the minimum mechanical and physical properties for each grade, including workability, nailability, gluability, paintability, permeability, weight, and thermal resistance. The panels may also be manufactured according to a performance based standard that identifies the needs of specific uses. The standard for construction sheathing panels is CAN/CSA-O325.0-M88 "Construction Sheathing" (1988).

According to CAN/CSA-O437.0-M93, the OSB grade O-2 panel is specifically recognized by the 1990 National Building Code of Canada (NBCC) as being structurally equivalent to plywood when used as roof, wall, and floor sheathing. The OSB conforming to CAN/CSA O325.0-M88 is included in the general reference for Construction Sheathing products in the 1990 NBCC.

In the fall 1993, the Canadian Standards Association proposed a new standard: "Design Rated OSB" (CSA/Standard Series O452). The CSA Standard O452 provides a means to use performance rated OSB in engineered structures covered by Part 4 of the NBCC. The Standard covers these 3 types of Design Rated OSB panels; that is, Type 1 (STARNDARD), Type 2 (PLUS), and Type 3 (PROPRIETARY). The constituent materials or processes used in the manufacture of the OSB are not specified by the standard. However, the basic structural capacities of Type 1 and 2 Design Rated OSB are classified according to qualification tests. The Standard provides for the assignment of engineering design values to Type 3 Design Rated OSB (CAN/CSA-O452.0, 1994) as they appear in the new CSA O86 edition in 1994.

With the dwindling supply of mature softwood, the prospect of OSB as a structural material is good. The product is made from small, fast growing hardwood trees which used to be valueless. The cost of OSB is relatively low in comparison to other wood composite products such as plywood, and the short-term mechanical properties of OSB are almost the same as other composites. OSB has been rapidly accepted as a structural material since its entrance into the market. However, like other wood based materials, OSB exhibits significant time-dependent behavior. The time-dependent behavior is affected by the environmental conditions to which OSB is exposed. OSB will be more competitive if its time-dependent behavior (which is always influenced by climate) is known and/or improved. This fact leads to the major reason for this research project;

not much information is available and little research has been done about OSB.

1.2.2 Plywood

Plywood is a panel product of wood veneers glued together so that the grain directions of some veneers is along the length of the panel. In most cases, the grain of every other layer is laid parallel to the first and an odd numbers of veneers is usually used. Most plywood is made from softwood veneer. Production technology, grades, and uses of the softwood and hardwood plywood differ greatly.

Softwood plywood is primarily used as a construction material. Hardwood plywood is used for paneling, industrial parts, furniture, and as a construction material as well.

The basic manufacturing steps include heating the wood block, cutting the veneer, storaging and clipping the veneer, drying the veneer, laying-up and pressing the veneer. The adhesives used in the production of plywood are thermosetting synthetic resins, of which the two most important types are phenol-formaldehyde and urea-formaldehyde. Phenol-formaldehyde is used for both interior and exterior grades of softwood and exterior grades of hardwood plywood and it is water-proof. Urea-formaldehyde is used exclusively for interior grades of hardwood plywood because it is not water-proof.

Softwood plywood has four categories according to the durability of the glue line: Exterior, Interior, Exposure 1, Exposure 2. The Exterior could be used for severe wetting and drying situations. The quality of veneer in the core of Exterior plywood is higher than that for Interior plywood. Exposures 1 and 2 are durability categories for performance-rated panels. Exposure 2 and Interior panels are comparable.

The duaribility of hardwood plywood is indicated by Type 1, 2, or 3. The durability of Type 1 is similar to that of the Exterior softwood category. Type 3 is designed for noncritical uses.

With the decreasing availability of timber, the production of plywood cannot depend on large, high-quality logs. The average diameter of the logs utilized by mills is 10 to 12 inches (Haygreen and Bowyer, 1989). Fortunately, the technology for producing veneer from small logs has improved. However, utilizing hardwood for panel production is an alternative. The OSB panels introduced previously are one of these options.

Plywood exhibits time-dependent behavior which, like OSB, is affected by the environment. Research carried out in this area is reviewed in Chapter 2.

1.3 Serviceability Limit States Design of Wood Structure

With a limit states design method, a building structure should fulfill the functions for which it was designed. The limit states include ultimate limit states and serviceability limit states. Ultimate limit states concern safety which includes exceeding the load carry capacity, fracture, fatigue etc.. Serviceability limit states are those states which restrict the intended use and occupancy of the building. They include deflection, vibration, permanent deflection and cracking (1990 National Building Code of Canada).

For the wood or wood based building materials, the serviceability limit states often govern the structural design due to the significant time-dependency of the material as discussed in the previous section.

In the Canadian wood design code (CAN/CSA-O86.1-M89), the elastic deflection

under a specified load is limited to avoid damage to structural elements or attached nonstructural elements. The limit for elastic deflection is 1/180 of the span. The permanent deformations should be limited when they can result in unsightly appearance or potential damage to adjacent elements of the structure. However, the code does not provide a method to calculate the time-dependent deformation. The Canadian code does require that when the continuously applied loads are in excess of 50% of the total specified loads, an upper limit of 1/360 of the span shall be imposed on the elastic deflection due to continuously applied loads.

Because of the influence of service conditions, the long-term deformation of wood panels under sustained loads could be several times larger than that of the elastic deformation under the same loads. In such cases, the 1/360 limitation on the elastic deflection may become inadequate.

The European code (Eurocode, 1991) gives an explicit equation for calculating long-term deflection. A creep factor (K_{def}) accounting for creep deflection is given for various wood products under three different service conditions. The creep factor for composite products such as OSB remains untabulated when the environmental humidity is higher than 85%.

To reach a more rational and economic structural design for wood composites, research on the time-dependent behavior under different service conditions is in demand.

Consequently, the following summary outlines reasons for this research project:

1. For proper structural engineering design with OSB, it is necessary to know both the short term elastic properties and the time-dependent behavior. Lack of knowledge of the time-dependent properties will negatively effect the competitiveness of OSB

with other building materials.

2. The Canadian wood engineering design code CAN/CSA-O86 has recently accepted design values for CAN/CSA-O452 "Design Rated OSB" for dry service condition only. Opportunities exist to get acceptance in CAN/CSA-O86 for semi-dry service conditions in the 1999 code pending availability of reliable data.

3. The time-dependent properties of OSB must be more carefully researched to identify the process variables that can improve the time-dependent properties more effectively, perhaps with less cost.

1.4 Objectives and Scope

The objectives of this study are:

1. To experimentally explore the time-dependent flexural behavior in OSB panels exposed to cyclic and constant humidity conditions and normal indoor environment at sustained load.

2. To predict creep development of OSB panels exposed to constant, cyclic humidity or normal indoor environment.

3. To construct numerical models to model the moisture movement in wood panels and the creep of the panels, along with the creep test process.

The scope of this research includes the study of the effect of variables on the long-term deformation of OSB panels. The variables studied are thickness of panels , frequency of humidity cycling, surface strand orientation, and RH level. For comparison, plywood panels with the same nominal thicknesses as OSB are also tested under the same environmental conditions.

The moisture movement in panels exposed to various climates is observed during tests. Moisture diffusion coefficients are determined from test recordings of the panel moisture content changes. The numerical analysis of moisture diffusion is carried out and the results are compared with test results.

The study also provides long-term predictions for various OSB panels under various climates according to the results obtained from creep tests with relatively short creep duration. A creep development model is constructed upon moisture diffusion analysis results.

1.5 Outline of the Thesis

Chapter 1 is a general introduction of the research project. General ideas about time-dependency of building materials are presented. The concept of OSB, which is the building material studied in this research project, is introduced. The advantage of the product and the existing time-dependent problem of OSB are emphasized. The current codes dealing with the problems are also described. Finally, the objectives and scope of the research is identified. The outline of the thesis is given in this section.

Chapter 2 reviews the studies done elsewhere in the area of creep of wood and wood composites. A general concept about rheology is given. The basic techniques used in viscoelasticity, including creep compliance and superposition principle, are briefly introduced. The time-dependency of wood is interpreted on the molecular structure level, and is based on a highly simplified model. The chapter reviews experimentally based research regarding the creep of solid wood and wood composites. The influence of constant and cyclic humidity, and the influence of environmental temperature on the time-dependency are also included. Furthermore, the literature review includes the analytical methods modeling the creep deformation development.

Review of the analysis of moisture diffusion in wood panels are presented in Chapter 7.

Chapter 3 describes the experimental program design for the experimental study of the creep behavior of OSB. First of all, the experimental materials and the preparation procedures are described. Next, the methods for measurement of the moisture content and the thickness of panels are given. Then, the test procedures to obtain materials' short-term bending stiffness and ultimate strength are briefly described. Finally, the long-term flexural creep test is presented in detail, and includes the test set-up, the applied load level, the environmental treatment, the creep duration, and the experimental instrumentation. Procedures for the flexural creep tests are also provided in this chapter.

Chapter 4 provides the experimental results. The short-term mechanical properties, including bending stiffness and ultimate bending strength, are summarized. The environmental conditions are recorded for both the controlled and normal indoor conditions. The measurements of moisture content and panel thickness, along with the creep tests, are also included. Most importantly, this chapter presents creep deflection development and creep recovery for all panels in all creep test series.

Chapter 5 is the discussion of the test results summarized in Chapter 4. The short-term properties of the panels are discussed for both plywood and OSB. A discussion of the effects of RH level, cyclic RH frequency, panel thickness, and strand orientation on wood panel creep is based on the results obtained from the constant and cyclic creep tests. The statistical procedures, including analysis of variance (ANOVA) and regression analysis, are adopted to testify to the significant factors affecting the OSB panels' creep behavior. The correlation between creep and those variables are calculated.

Chapter 6 provides tools to predict OSB long-term deflection under various climatic conditions. Such prediction is useful for practical purposes. A curve fitting method is used for the creep test data under various constant RH levels and indoor climates on a logarithmic time scale. Because of the use of the logarithmic time scale, the long-term creep predictions based on curve fitting equations are extrapolated close to the existing test data. The predictions are therefore reasonably reliable. One advantage of the curve fitting method is that the long-term creep can be calculated directly by the predicting equation rather than by considering each individual factor which might affect the creep. A bilinear prediction model (see Sect. 6.3.1) is proposed in this chapter for cyclic humidity environment on a logarithmic time scale. To determine parameters in the bilinear model, a stepwise regression analysis procedure is adopted. The achieved prediction model includes the significant variables affecting panel creep. The validation of the prediction model is checked through comparing the prediction with the creep test results for 150 days.

Chapter 7 describes moisture movement in wood panels by using diffusion equations. A finite difference method is used to solve the differential equation of diffusion. Both accuracy and convergence of the finite difference method are discussed. The numerical analysis results are compared with the moisture content measurements from the experiment. The method used to calculate moisture diffusion coefficients from adsorption or desorption is given and the panels' moisture diffusion coefficients are calculated from the moisture content measurements taken during all test series. Some characteristics of the moisture diffusion coefficient are also discussed in the chapter.

Chapter 8 presents the constitutive relation describing the time-dependent flexural behavior of OSB panels under the influence of moisture changes. A number of assumptions and simplifications are made to derive the model. The related material

parameters in the model are evaluated from test results. The derived model is verified by comparing the model prediction with the test results. The restrictions and limitations of the model are also discussed, and a parametric study is carried out to predict the possible creep development of the variables with values other than those tested in the experimental program.

Chapter 9 summarizes the research documented in this thesis. Conclusions are drawn from both the experimental and analytical studies, and recommendations are proposed for the future studies and engineering applications of creep knowledge to OSB.

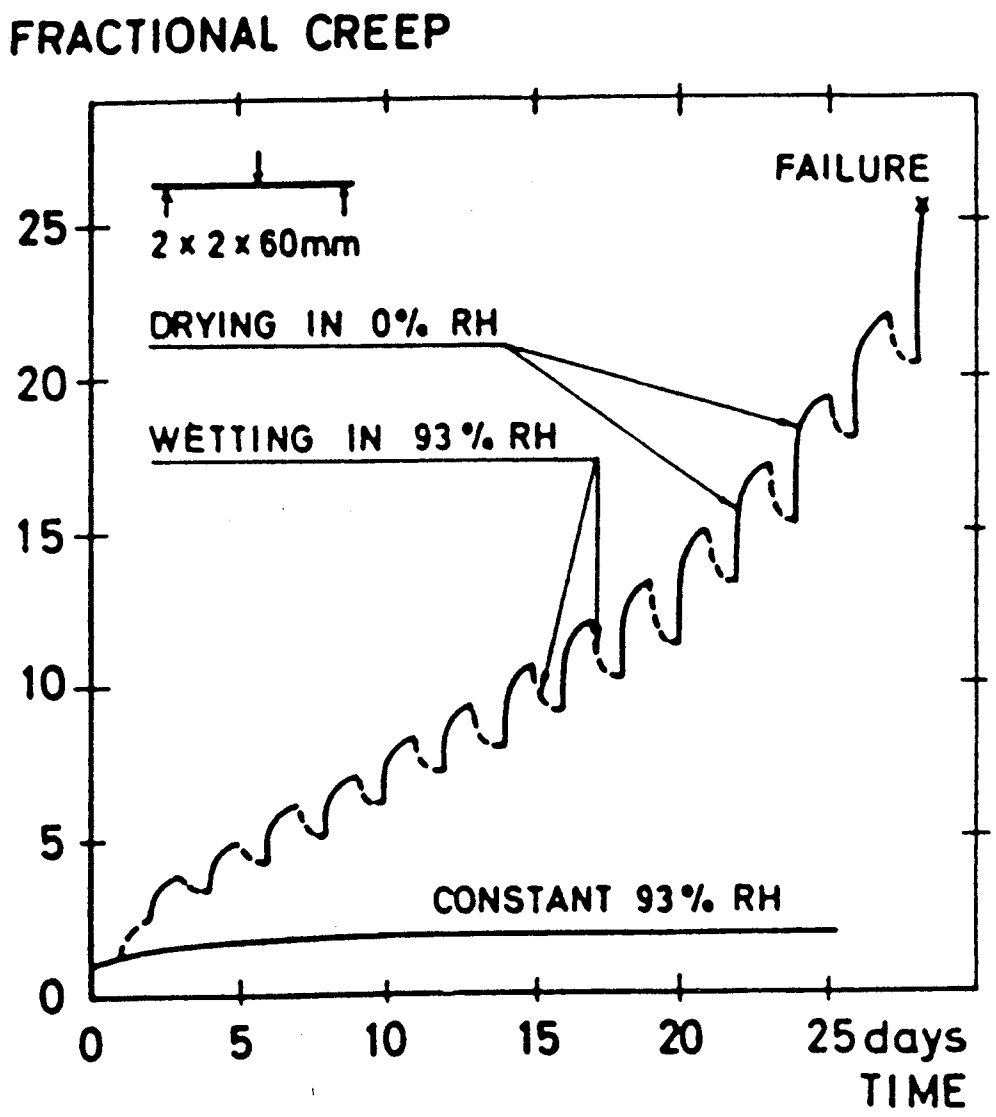

Fig. 1.1 Fractional Deflection vs. Time Curves for Small Wood Beam at Constant and Cyclic Humidity Changes (Hearmon and Paton, 1964)

Chapter 2 Literature Review

2.1 General Theory

Rheology is the science of the time dependent stress-strain behavior of materials. During this century, rheology has been concerned largely with polymeric solids, materials which exhibit large time-dependent behaviors. When such materials are exposed to mechanical loading, the mechanical response can be characterized by three components: elastic deformation, viscoelastic deformation, and viscous deformation.

Elastic deformation happens instantaneously upon loading, and it is recoverable; the stress-strain relationship of such behavior is governed by Hooke's law in linear elasticity theory. Viscoelastic deformation is a type of delayed elastic deformation because it produces a time-dependent response and that is also recoverable. Although viscous deformation is time-dependent, it produces an irrecoverable response.

The three components of deformation are illustrated in Fig. 2.1, which shows the results of a sustained load applied for a period of time. Theoretically, mechanical response of materials under the applied load could be described by the following differential equation with the sufficient number of parameters p_i and q_i (Flügge, 1967)

$$\sigma + p_1\dot{\sigma} + p_2\ddot{\sigma} + \cdots = q_0\varepsilon + q_1\dot{\varepsilon} + q_2\ddot{\varepsilon} + \cdots \tag{2.1}$$

where σ and ε are stress and strain, respectively. Such a complex differential equation may become a simple algebraic equation through Laplace transformation.

Creep and stress relaxation are two major ways to study the time-dependent behavior of materials. Creep is defined as the time-dependent deformation of a material under constant load (only σ term left on the left side of Eqn. (2.1)). Stress relaxation is

defined as the change in resistance for forces in a material subjected to a constant deformation (only ε term left on the right side of Eqn. (2.1)). The maximum stress occurs as soon as the deformation takes place, and the stress decreases gradually with time from this maximum value.

Section 2.1.1 introduces the basic concept about the creep compliance and the superposition principle used in viscoelasticity. The rheology phenomena of wood behavior are interpreted on the molecular structural level through a simplified model.

2.1.1 Creep Compliance and Boltzmann's Principle of Superposition

In creep tests, the time-dependent strain $\varepsilon(t)$ is proportional to the applied stress σ_0 for linear viscoelastic materials. The relationship can be written as

$$\varepsilon(t) = \sigma_0 J(t) \tag{2.2}$$

where $J(t)$ is called the creep compliance, which has three components: elastic viscoelastic, and viscous. For $t < 0$, $J(t) \equiv 0$, and $J(t)$ is a monotonically increasing function for $t > 0$. The creep compliance is a material property. When $J(t)$ is known, the time-dependent strain can be calculated.

When several loads are applied, the time-dependent strain can be calculated by using the rule of linear superposition called the Bolztmann's Principle of Superposition. According to Aklonis and MacKnight (1983), upon a continuous stress application, $\sigma(t)$, the time-dependent strain $\varepsilon(t)$ is :

$$\varepsilon(t) = \int_{-\infty}^{t} \frac{\partial \sigma(v)}{\partial v} J(t - v)dv \tag{2.3a}$$

where $J(t)$ is a creep compliance and v is the variable. Assuming σ equal zero within [-∞, 0), then

$$\varepsilon(t) = J(0)\sigma(t) + \int_0^{\infty} \frac{\partial J(v)}{\partial v}\sigma(t-v)dv$$
$$= J(0)\sigma(t) + \int_0^{t} \frac{\partial J(t-v)}{\partial (t-v)}\sigma(v)dv \qquad (2.3b)$$

Similarly, for the imposed strain in strain relaxation cases, the time-dependent stress could be obtained by

$$\sigma(t) = \int_{-\infty}^{t} \frac{\partial \varepsilon(v)}{\partial v}G(t-v)dv$$
$$= G(0)\varepsilon(t) + \int_0^{\infty} \frac{\partial G(v)}{\partial v}\varepsilon(t-v)dv \qquad (2.4)$$
$$= G(0)\varepsilon(t) + \int_0^{t} \frac{\partial G(t-v)}{\partial (t-v)}\varepsilon(v)dv$$

where $G(t)$ is a relaxation modulus of the material.

By using the superposition principle, the time-dependent strain can be predicted under any type of applied stress history, assuming that the creep compliance of the material is known and that the two assumptions given earlier are satisfied. For example, when the sustained stress σ_0 in a creep test is unloaded at time t_1, the remaining strain during the creep recovery can be obtained by applying stress $-\sigma_0$ at time t_1. Using Boltzmann's superposition principle, the strain during creep recovery can be expressed as

$$\varepsilon(t) = J(t)\sigma_0 - J(t-t_1)\sigma_0 \qquad (2.5)$$

The use of the superposition method is also illustrated in Fig. 2.1.

2.1.2 Structural Interpretation of Time-Dependency of Wood

Like many polymeric materials, the macroscopic rheological behavior of wood is believed to be largely governed by the molecular structure. Therefore, it is important to

understand the essentials of wood structure. The following section introduces the molecular composition of wood cells and briefly summarizes some simplified interpreting models for time-dependency.

Molecular Composition of Wood

The structure of wood is described by many authors, such as Stamm (1964), Bodig and Jayne (1982). Wood is composed primarily of carbon, hydrogen, and oxygen. The elemental constituents of wood are combined into a number of polymers: cellulose, hemicellulose, and lignin. There are also compounds such as extractives that have little effect on mechanical behavior, but that do affect the moisture diffusion in the wood.

Cellulose is composed of glucose molecules ($C_6H_{12}O_6$) which are joined together end-to-end through linkages. The ensuing linear long-chain polymer, cellulose $(C_6H_{12}O_6)n$, has n as large as 30,000. Cellulose in wood is partially crystalline and partially amorphous. Water (H_2O) can be joined by its hydrogen bond to the hydroxyl groups in the noncrystalline zones in the cellulose. However, it can't move into the crystalline cellulose.

Most hemicelluloses are branched-chain polymers, in contrast to straight-chain polymer cellulose, and have fewer degrees of polymerization. The degree of crystallization of the hemicellulose is low.

Lignin is a high molecular weight polymer. It is a noncrystalline net polymer that is stable and difficult to isolate. Lignin produces a rigidity, like cement in concrete, which is important to the properties of wood, because it binds the cellulose cells fibers together.

Although all wood is mainly composed of the three components (cellulose,

hemicellulose, and lignin), the different wood macrostructures resulted from various wood species are important.

Anisotropic Nature of Wood

A material that has the same mechanical properties in each direction is termed isotropic. A material that has different mechanical properties in different directions is termed anisotropic (not isotropic). When mechanical properties of a material are symmetric about three mutually perpendicular planes, it is called an orthotropic material.

Wood has distinctively different properties (strength and elastic properties) in longitudinal, radial, and tangential directions, and is considered an anisotropic material. The modulus of elasticity parallel to grain (longitudinal direction) is about 20 to 30 times as large as modulus of the elasticity perpendicular to the grain (transverse directions). However, the properties in the radial and tangential directions do not differ greatly. In engineering practice, a common strength value for the tangential and radial direction is used.

Most wood composites such as plywood and OSB are orthotropic. The orthotropy of composite wood panel products will be further discussed later.

A Structural Interpretation of Time-Dependency of Wood

The time-dependent behavior of polymers is governed to a great extent by their molecular structure. Nielsen (1962) discusses the effects of molecular weight and chain entanglements on the materials' rheological behavior, and also summarizes the rheological behavior of uncrosslinked, crosslinked, and crystalline polymers.

A highly simplified two-dimensional molecular network is illustrated by Bodig and

Jayne (1982). The plot in Fig. 2.2 represents two polymers, each composed of four monomers. The solid lines are atomic and molecular bonds; the broken lines are secondary bonds. The three components of deformation upon applied load are described by the model as follows:

1. Because of the elastic nature of atomic and molecular bonds, the elastic component is believed traceable largely to elastic deformation of primary and secondary chemical bonds. This is schematically shown in Fig. 2.3.

2. The viscous component, or non recoverable deformation, is assumed to be the result of sections of molecules, and perhaps whole molecules, shifting from one position to another. Failure and reconstitution of secondary bonds are associated with the viscous deformation shown in Fig. 2.4.

3. The time-dependent or delayed elastic deformation is associated with the straightening of molecules and occasionally with secondary bond breakage and reformation. This process is shown in Fig. 2.5.

When environmental humidity is changed, the migration of water molecules through micropores may increase the rate of bond breakage. The creep deformation may therefore be accelerated (Bazant 1985; Haygreen and Bowyer 1989), and is the so called mechano-sorptive creep. Such creep deformation will be further discussed in the later sections of this chapter.

2.1.3 Short-term Mechanical Properties and Climatic Conditions

As mentioned earlier, the time-dependent behavior of wood is affected by climatic conditions such as temperature and humidity. The related research will be reviewed in the next few sections. The short-term elastic mechanical properties of wood are also

affected by environmental conditions and they are briefly reviewed in this section.

The moisture content (MC) of wood product is the ratio of the weight of the water to the wood's oven-dry weight. The method to measure moisture content will be discussed in Chapter 3. The level of the moisture adsorbed by wood at a particular time is affected by temperature and humidity, and the level of moisture alters all physical properties. Adsorbed moisture also causes dimensional change which can alter the stiffness of a bending member by changing its geometrical dimensions.

When wood dries, its modulus of elasticity and strength increase. When water is removed from the cell wall of clear wood, the long-chain molecules move together and become tightly bonded. The modulus of elasticity and strength are therefore increased. However, the influence of MC on ultimate strength is more significant than that on the modulus of elasticity. For wood resin composites like OSB, the moisture, particularly that at high levels of relative humidity, tends to weaken the bonds between fibers and between wood particles. Consequently, moisture not only changes the properties of the fibers or particles, it also degrades internal binding. The short-term stiffness and strength of wood composites decrease significantly at high moisture levels (Bodig 1966; Bryan and Schniewind 1965).

The effects of the change in the MC on the change in the modulus of elasticity have been reported by many researchers. The relation between modulus of elasticity and wood moisture content is assumed to be linear or bilinear by Hunt and Shelton (1987) in bending test on Ponderosa and Scots pine, and in tension test on Beech wood. In the bilinear model, the decrease of the modulus of elasticity is more rapid in higher moisture content levels with the increase of the moisture content. In other words, the effect of the moisture content level is more severe when high moisture levels are reached.

An increase in the temperature of wood is reflected by two internal changes: a transitory change in internal energy levels and a permanent structural reorganization. The former results in transitory change in mechanical properties, and the later causes permanent effects.

With few exceptions, elastic properties decline as temperature increases, and temperature decreases have the opposite effect. High temperatures (exceeding 100 °C) can cause permanent loss of stiffness in wood (Haygreen and Bowyer 1989). More attention should be paid to high temperatures because the effect of exposing wood to high temperatures tends to be cumulative.

The interaction of moisture content and temperature also affect the short-term stiffness. In general, the higher the moisture content of the wood, the greater its sensitivity to high temperature.

2.2 Basic Experimental Research on Wood Creep

The influences of climatic conditions on the short-term mechanical properties of wood have been introduced in the previous sections. The time-dependent behavior of wood is also affected by environmental conditions. The related experimental study is reviewed in this section.

Scientific studies on the rheological behavior of solid wood began about 50 years ago, and many works have been produced since then. With the structural application of wood composites to replace solid wood, more and more attention is being paid to the rheological behavior of wood composite products. The experimental study about solid wood and wood composites at various environmental conditions, is briefly reviewed in the following two sections.

2.2.1 Rheological Behavior of Solid Wood

Because of the structural complexity of wood, the rheological study of wood has been approached through extensive experimental studies from a phenomenological point of view since the 1950s. Despite the existence of inconsistency between different studies, some general rheological behaviors of wood have been identified. Detailed reviews of the literature were made by Schniewind Richmond (1968) and Holzer et al. (1989). Those studies, summarized in the following discussion, are about the creep behavior of solid wood at different humidity conditions.

Constant Relative Humidity/Moisture Content

Moisture content of wood is very important for the rheological properties of solid wood. The increase of MC will usually result in the increase of creep. This is observed in tension/compression tests when the load is parallel/perpendicular to wood grain (Bach 1965, Youngs 1957). The total creep compliance and its components (elastic, viscoelastic, and viscous) are found to be proportions of quadratic terms of MC in tension (Bach, 1965). In the bending test, the total deflection and the rate of creep development are found to increase with increases of MC (Ota and Tsubota 1966).

Variable Relative Humidity

Armstrong and Kingston (1962) find that the creep rate of small green beams is higher when they are allowed to dry under loading compared with the situation where they are kept green during the creep test. Even larger creep is observed when cyclic humidity changes are encountered. Cyclic humidity changes result in a large deflection increment during desorption, and in some deflection recovery during adsorption in bending. The total time-dependent deflection increases more at cyclic conditions than at the constant higher level of humidity during cycling (Armstrong and Christensen 1961;

Armstrong and Kingston 1962; Hearmon and Paton 1964; Christensen 1962). The deflection recovery during adsorption may become a reduction of creep rate if the applied load is high and the cyclic changes are small (Schniewind 1967).

The deflection under cyclic humidity changes cannot alone be predicted directly from constant humidity tests. The phenomenon of the mechanical influences combined with moisture sorption is often referred to as the "mechano-sorptive effect" in literature. Extensive work has been undertaken to discuss the source of the effect during the last fifteen years (Hunt and Shelton 1987, 1988, Ranta-Maunus 1990, Toratti 1990). However, the results from these studies are sometimes confusing, and even contradictory, because the mechano-sorptive behavior is affected by many factors, such as wood species and loading modes. Some important aspects of the mechano-sorptive behavior of solid wood observed from literature is reviewed as follow.

The shrinking/swelling of wooden specimens is affected by the applied load. In uniaxial creep tests, the deformations developed during moisture sorption and mechanical loading include both shrinking/swelling and the mechano-sorptive effect. To study the mechano-sorptive effect, the shrinking/swelling of a specimen must somehow be separated from the total deformation changes. However, the shrinking/swelling of a specimen under loading may be different from that of a zero-load specimen. It was found that the stress needed to prevent a specimen from swelling during a humidity change was less than the stress applied to a specimen after its swelling to retain the zero deformation (Kingston and Perkitny 1972). On the other hand, the equilibrium moisture content of a wooden specimen under compressive stress at a specific humidity is lower compared with the unloaded specimen at the same humidity level. Tension gives a higher equilibrium moisture content than does compression. The phenomena were shown by Libby and Haygreen (1967), Hunt and

Shelton (1988). Since it is difficult to tell the shrinking/swelling of a loaded specimen from the total deformation change during moisture sorptions, the mechano-sorptive creep in uniaxial tests is usually taken as the difference between the total deformation change and the free shrinking/swelling (Martensson 1992). For a bending beam, free shrinking/swelling does not influence the curvature, which will be discussed in detail in Chapter 8 . The deflection oscillations of a bending beam are caused only by the mechano-sorptive effect.

The mechano-sorptive effect may be different for different loading modes. During moisture desorptions, the deformation after zero-load compensation increases for both tension and compression. During adsorptive phases, there are some confusing results. The zero-load compensated strain decreases in tension (Eriksson and Norén 1965) and compression (Armstrong and Kingston 1962, Martensson 1992). Some other studies give opposite results for both tension (Mohageer 1987) and compression (Cheng and Schniewind 1985). When the first sorption is an adsorption or when the moisture content reaches values not attained earlier, the zero-load compensated strain always increases in tension specimens.

In bending beams (see Fig. 1.1), the first adsorption and all desorptions cause increases in deflection, while later adsorptions decrease the deflection. When the moisture content changes beyond the previously attained limits, the deflection increases.

Regarding the magnitude of the mechano-sorptive effect for different loading modes, Armstrong and Kingston (1962) show that there are differences between the compression and the tension for Australian wood species. Martensson (1988) shows that the tensile creep is surprisingly small during moisture changes, but Hunt (1986) finds that the mechano-sorptive effect in tension and bending on two species of

softwood is similar. The results by Mohager (1987) indicate that the behavior in tension and compression is similar at low stress level.

The recovery of wood after unloading is accelerated by moisture cycling (Christensen 1962; Arima and Grossman 1978) and is larger during adsorption than during desorption.

The size effect on the interaction of moisture content changes and mechanical loading is also studied. Armstrong and Christensen (1961) conclude that the behavior of the two beams with a different size is similar. The mechano-sorptive creep is also found in structural timber (Hoyle et al. 1986; Mohager 1987). The relative creep of a full size beam is found to be as large as that of a small beam (Mohager 1987). However, the mechano-sorptive creep is reported to decrease with the increase of specimen size by Schniewind and Lyon (1973).

The non-linearity begins at 20-40% of ultimate strength for constant RH dependent on the level of the RH shown by Bach (1965). The non-linearity of creep deformation in constant humidity started around 50% of ultimate strength (Kingston and Budgen 1972). The linearity during mechano-sorptive creep is studied by Hunt (1989). The non-linearity started at total strain around 0.14% to 0.15% for compression and bending test pieces, while the tensile pieces were approximately linear up to 0.18% strain.

2.2.2 Rheological Behavior of Wood Composite Panels

The rheological behavior of wood based panel products is important to their engineering application. Due to the increasing structural application of such products, much research has been going on recently, although the early rheological studies about wood composites date back to the 1960s. The following review is mainly concerned

with the flexural creep behavior of composite panels with respect to the influence of environmental humidity condition. Other factors such as applied load level and resin type, which may also affect the creep behavior of composite panels, are briefly reviewed later.

Moisture content level is important to the creep of wood composite panels. At a high constant level, wood panels creep considerably. Bryan and Schniewind (1965) report that the relative creep of the urea-bonded Douglas-fir particleboard is more than 10 times greater at 18 than 6 percent nominal moisture content. Haygreen et al. (1975) test several types of panels in four RH environments: 65%, 70%, 75%, and 80%. They find that the flexural creep of shavings/residue type-particleboard is accelerated if the RH exceeds about 75%. In plywood and oriented particleboard, creep increases as RH is increased, but no definite point where the acceleration of creep rate occurs is noted in the results of their tests. The relative creep of commercial oriented strandboard after 1 month loading is reported to be as high as 7 at 95% RH/75 ^{o}F (23.9 ^{o}C) environment (Pu et al. 1992 a). If the temperature increases to 95 ^{o}F (35 ^{o}C), tertiary creep is observed (Pu et al. 1992 b). The severe influence of high moisture content or humidity to composite wood panels is not observed in whole wood.

In changing RH or moisture content environments, the mechano-sorptive effect is also observed in wood composites (Bryan and Schniewind 1965; Sauer and Haygreen 1968; Armstrong and Grossman 1972; Yeh et al. 1990). The creep deflection of wood panels increases in cyclic RH environment, especially when high moisture content level is reached (Bryan and Schniewind 1965; Haygreen et al. 1975; Yeh et al. 1990). It is reported that relative creep is considerably greater in specimens subjected to the fluctuating RH rather than to the constant RH of average value. The 40-80% RH cyclic condition yielded about 2 to 3 times creep of a 60% RH constant condition in the study

of Haygreen et al. (1975). McNatt and Hunt (1982) had similar results. In their tests, the creep of a 25-85% RH cyclic environment is found to be 3 to 4 times of that of a 65% RH constant condition. The creep was reported many times larger at 6-18% moisture content cycling than at 6% moisture content constant (Armstrong and Grossman 1972).

The test results about the creep development during sorptions vary from study to study ; sometimes they are inconsistent, or even contradictory. Bryan and Schniewind (1965) test urea- and phenol-formaldehyde Douglas-fir particleboard under cyclic RH conditions. In contrast to solid wood, creep deflection increased during adsorption and some recovery is observed during desorption. The studies by Haygreen et al. (1975) and Hall et al. (1977), involving creep of changing RH conditions, give the same creep development trend during adsorption and desorption.

However, different creep behavior is reported during sorptions (Armstrong and Grossman 1972; Hearmon and Paton 1964; Yeh et al. 1990). In these studies, the creep deflection is found increasing during desorption and decreasing during adsorption, but the first sorption, whether showing a gain or loss of moisture, always gives a large increase in deflection (Armstrong and Grossman 1972). In addition, when the first sorption is adsorption, far more creep is introduced than that of constant or desorption cases (Sauer and Haygreen 1968). The creep behavior during cyclic RH described in these studies is the same as that of solid wood, as described previously.

The effect of the duration of cyclic RH on creep is studied by Yeh et al. (1990). When the RH oscillates between 65 and 95 percent, the test results show that more creep develops in a fast cyclic test (4 days/cycle) than in a slow cyclic test (66 days) for the creep duration of 100 days. Since there is only 1.5 full cycles involved in the slow cyclic test, the information regarding the effect of the cyclic rate is limited. Haygreen et

al. (1975) report that increasing the rate of sorption at the surface of the panels has only a small effect on the creep rate as long as high humidity levels are not encountered.

When the stiffness and strength loss after sustained loading are also studied., the stiffness and strength of panels after long-term loading under 95% RH are substantially lost (Pu et al. 1992a), while the instantaneous recovery upon unloading is found to be about 16 to 70 percent more than that of the initial elastic deflection upon loading; the strength loss is about 40%. A similar "fatigue effect" that weakens the elastic properties and is caused by cyclic RH is also reported by Yeh at. al (1990). The bending strength and stiffness after 90 days of loading are 74 to 99 percent of that for control specimens not subjected to long-tern loading (McNatt and Hunt 1982). However, an analysis of variance shows no significant differences between the control strengths and residual strengths of the creep specimens (McNatt and Laufenberg 1991).

The linearity of creep deflection exists until a certain load level is reached. When the applied load is below 20% of the ultimate strength, the creep deflection is linear in a 95% RH constant environment (Pu et al. 1992a). Haygreen et al. (1975) come to the same conclusion of 20% load level for both cyclic and constant RH conditions. The deflections of 100 and 200 pound concentrated loading panels are linear except for wet-dry conditions (Hall et al. 1977). Pu et al. (1992b) indicates that the level of applied load has substantial effects on the creep behavior of the OSB under a 95% RH/95 ^{o}F environment.

The thickness swelling is one of the direct effects of moisture content changes. Thickness swelling is affected by moisture content increase, panel density, resin level, production process etc.. Halligan and Schniewind (1972) correlate creep to the thickness swelling for panels with different density and resin levels, and find that the thickness swelling is a good indication of how exposure to high RH affects the creep.

Panels with high thickness swelling also have high creep. Lee and Biblis (1976) also report that panels exposed to high RH have irrecoverable thickness swelling. The irrecoverable changes also happen to other properties such as strength and stiffness.

The loading condition of most studies about wood panel creep behavior is simple bending. When concentrated load is applied on a 32" x 43" floor (Haygreen et al. 1975), the flexural behavior under the concentrated load is reported qualitatively, similar to that under simple flexural stress. Martensson and Thelanderson (1987) study the creep behavior of hardboard in tension, and find that the creep pattern in tension during RH cycling is different from the creep pattern reported for bending. The zero-load compensated strain has an abrupt change at the beginning of each RH change. Fridley and Tang (1992) study shear effect on the creep behavior of wood composite I-beams. They indicate that the in-plane shear creep behavior of the web must be included to consider the creep performance of the I-beams.

The effect of resin type and resin level on the creep behavior composite wood panels has also been studied by researchers. Some find no difference in the creep of urea- and phenolic-bonded panel regarding the moisture and sorption effect (Bryan and Schniewind 1965; Haygreen et al. 1975). However, Pu et al. (1992a) test 6 types of commercial Stud-I-Floor OSB products under a 95% RH/75 ^{o}F environment, and the creep resistance of OSB under high RH was found different for various resin types (liquid phenol-formaldehyde, isocyanate, powder phenol-formaldehyde) and wood species. Another study by Pu et al. (1992b) about commercial OSB indicates that research about the types of adhesive and resin contents is in demand to evaluate the creep of OSB. The flexural test by Yeh et al. (1988) finds no significant effect on creep resistance when the resin content is increased from 5 to 7 percent in a constant humidity environment (95% RH/75 ^{o}F and 65% RH/75 ^{o}F), but Yeh et al. (1990) show that the

long-term performance of flakeboards under changing environments could be moderately improved when liquid phenol-formaldehyde resin content is increased from 5 to 7 percent.

The strandboard with various flake alignment was studied by McNatt et al. (1992); they analyze the contributions of flake alignment to bending strength, bending stiffness, internal bond strength, thickness swelling and linear expansion. The alignment contribution to long-term performance is presented in an earlier paper by Bach and McNatt. (1990), where the time-dependent deformation under sustained loading relative to initial deformation is reported almost independent of the degree of strand alignment in OSB panels. The creep of both parallel and perpendicular commercial OSB in a 95% RH constant condition is studied by Pu et al. (1992 a), and shows that the parallel specimens have much better creep resistance (absolute creep) than perpendicular specimens.

2.3 Analytical Methods Modeling Wood Creep

Many of the studies about the time-dependent properties of wood are empirical and their validity is limited to a specific species, specimen geometry, and loading and environmental condition. A review paper by Holzer et al. (1989) states that the time-dependent behavior of wooden structures should be examined at several levels, including 1) polymer, 2) microstructure, 3) continuum, 4) structural element, and 5) structure levels. The influence of each level on the time-dependent behavior is briefly discussed in that paper.

Most creep models found in the literature are based on the test results of uniaxial stress under constant environments. Within linear range, such creep model could be incorporated into a finite element process to analyze a structure. For variable

environments, modeling becomes more complicated and difficult. Lists of requirements to model mechano-sorptive creep are given by Grossman (1976), Hoffmeyer (1990), and Hunt (1989). The listed requirements are not all the same because of the differences in the authors' test results, and in their interpretations of the results. The following review is mainly directed to the modeling of mechano-sorptive creep during RH changes. The creep modeling methods found in literature are summarized in three categories: creep compliance (J) methods, constitutive equation methods, and curve fitting methods. The discussion of the first two modeling methods is related to the creep with mechano-sorptive effects only. The third method also covers the constant environment condition.

2.3.1 Creep Compliance (J) Methods

In summary, there are three aspects of Mechano-Sorptive (M-S) creep for solid wood:

1. Decrease of moisture content , the creep deflection increases;

2. When moisture increases at levels not reached before, the creep deflection increases much more than that which occurred in other sorptive process;

3. When moisture increases at levels reached for the second or subsequent times, the creep deflection decreases.

The above three aspects of M-S creep may be in agreement with solid wood creep test data, but may not be true for composite wood products. Based on the above described creep behavior, Ranta-Maunus (1975) proposed the following equation to describe the strain history:

$$\varepsilon = \sigma_0[J(t) + \sum_{i=1}^{n} aJ_{00}(u_i - u_{i-1})] \qquad (2.6)$$

where ε is the strain at a constant stress level σ_0; J_{00} is the instantaneous elastic compliance at 0% MC; $JJ(t)$ is the integrated cumulative creep and elastic compliance which is a function of the elapsed time at the MCs sustained during the test; n is the number of moisture content changes between u_{i-1} and u_i, and a is known as the hydroviscoelastic constant obtained from test results and has three values: a^- for decrease in MC, a^{++} for first moisture increases at any MC level, and a^+ for subsequent moisture increase.

The above equation is based on the assumption that there is no interaction between normal creep, corresponding to J term, and M-S creep. This assumption may not be exactly true.

Hunt (1986), rewrites the above equation in a more general way. The total creep compliance is expressed as:

$$J_{total} = J + \sum_{i=1}^{n} \frac{dJ^*}{du}(u_i - u_{i-1})] \tag{2.7}$$

where J^* takes the value of J^{++}, J^+ or J^- according to the type of moisture changes: first MC increment, subsequent MC increment, and MC decrease, respectively. His tests on two species of pine showed that low stress bending and tension give similar M-S creep. The $\Delta J^*/\Delta u$ is calculated from Hunt's creep test data as a in Eqn. (2.6). The value is different in different tests. No quantitative creep calculation method has been found which could fit all test results.

The total creep compliance J_{total} is separated into components in several ways by Hunt, and a reduced creep compliance concept is proposed by Hunt and Sheltonχ(1987):

$$J_R = J + J_E(u) \tag{2.8}$$

where J is the creep compliance , $J_E(u)$ is the elastic compliance at the current MC level u, and J_R is the reduced creep compliance. The relationships between J_E and MC are assumed to be linear or bilinear. The J_R could be taken as the results of creep during the moisture changing history or the results of normal creep and the M-S creep. Attempt is made to relate J_R with dJ_R/du, and the correlation between dJ_R/du and β (free shrinking or swelling coefficient) as a function of MC are also obtained. The relation of dJ_R/du and β obtained from tests is presented by fitted curves.

Later, Hunt and Sheltonχ(1988) proposed that M-S creep has a limit, and postulate that humidity cycling is merely a means of accelerating normal creep. The total creep compliance is written by Huntχ(1989) as

$$J_R = J_E + J_N + J_1(1-e^{-n/N_1}) + J_2(1-e^{-n/N_2}) \tag{2.9}$$

where J_∞ $(=J_1+J_2)$ is the M-S creep limit; J_N $(J_N = f(logt,(logt)^2,\cdots))$ is the normal creep from constant MC, which is based on the least-square analysis of the test data. J_N is a basic master curve under constant MC and constant load. With different elastic compliance and moisture content value, a horizontal shift H_E or H_M is applied to the master curve. N_1 and N_2 are characteristic cycle numbers given by the paper, and n is the number of cycle. Although the existence of a creep limit is proved to some extend, it is not fully verified, especially when humidity reaches values not attained earlier. Whether or not the creep limit is changed in such cases remains unknown.

In this type of creep modeling method, total deflection or compliance is divided into several components in different ways. In most cases, each component is obtained by fitting it into the test data somehow. The model results may agree with some test results, but not with others. No general method has been achieved to quantitatively predict the creep compliance under cyclic humidity conditions.

2.3.2 Constitutive Equation Methods

The constitutive type of models, describing the combined effects of mechanical and moisture loading, are proposed by Leicester (1971), Ranta-Maunus (1975), Rybarczyk and Ganowics (1974), Bazant (1985) and Martensson (1988, 1992), but the range of validity for these models under general stress and moisture variations are not known.

Martensson (1988, 1990) adopted a formulation in which the strain rate is expressed as :

$$\dot{\varepsilon}_x = \dot{\varepsilon}_x(\dot{\sigma}_x, \sigma_x, \dot{u}, u) \tag{2.10}$$

where $\dot{\varepsilon}_x$ is the strain rate, σ_x and $\dot{\sigma}_x$ are the current stress and its rate of change, and u and $\dot{u}$ are the moisture content and its rate of change, respectively. The explicit form of the above equation is

$$\dot{\varepsilon}_x = \dot{\varepsilon}_e + \dot{\varepsilon}_c + \dot{\varepsilon}_s \tag{2.11}$$

where $\dot{\varepsilon}_e$, $\dot{\varepsilon}_c$ and $\dot{\varepsilon}_s$ are the strain rates corresponding to elastic strain component, basic creep strain component, and the strain component induced by moisture fluctuations, respectively. The elastic component of strain can be expressed as

$$\varepsilon_e = \frac{\sigma_x}{E(u)} \tag{2.12}$$

$E(u)$ is the elastic modulus at moisture content u. By applying the linear viscoelastic formulation, the basic creep component can be expressed as

$$\varepsilon_c = J(t)\sigma_x = \int_0^t J(\xi(t) - \xi(t'))d\sigma(t') \tag{2.13}$$

for arbitrary vary stress σ and moisture content u. $\xi(t)$ is a material time concerning the accelerating effect of high moisture content level, which accounts for the horizontal

shift of creep time due to a high moisture content level. $\xi(t)$ is defined by $d\xi(t) = dt/\alpha(u)$, where $\alpha(u)$ is a moisture shift factor.

The moisture induced strain rate component can be expressed as

$$\dot{\varepsilon}_s = \dot{\varepsilon}_{s0} + \chi \frac{\sigma_x}{\sigma_u} |\dot{\varepsilon}_{s0}| \tag{2.14}$$

where χ is a material constant which may depend on current stress; and different values corresponding to compression and tension are assigned to the constant ; σ_u is the short-term ultimate strength, and $\dot{\varepsilon}_{s0}$ is the free moisture induced strain rate given by

$$\dot{\varepsilon}_{s0} = \beta(u)\dot{u} \tag{2.15}$$

where $\beta(u)$ is the free swelling-shrinkage coefficient of the material.

Later, Martensson (1992) derived a general three-dimensional formulation based on representation theorems. The constitutive relation for uniaxial stress is expressed as

$$\dot{\varepsilon} = \dot{\varepsilon}^e + \dot{\varepsilon}^{st} + \dot{\varepsilon}^c + \dot{\varepsilon}^{ms} + \dot{\varepsilon}^{msr} \tag{2.16}$$

where $\dot{\varepsilon}^e$ is the elastic strain rate, $\dot{\varepsilon}^{st}$ is the shrinkage-swelling rate, $\dot{\varepsilon}^c$ is the basic creep rate, $\dot{\varepsilon}^{ms}$ is the mechano-sorptive strain rate, and $\dot{\varepsilon}^{msr}$ is the mechano-sorptive recovery rate. The model is verified by Martensson's uniaxial test results.

The normal, or basic, creep component is neglected by some researchers (Ranta-Maunus 1990, Torati 1990); only elastic and M-S creep are included in their creep models.

Torati (1990) analyzes the cross section creep with a constant bending moment where the diffusion of moisture was taken into account by the finite difference method

and the creep was calculated simultaneously. Only mechano-sorptive creep is included in the calculation. The constitutive relations are based on Ranta-maunus (1975) and Hunt (1988). The results show that the full size cross section creep is also significantly increased under humidity fluctuations.

2.3.3 Curve Fitting Methods

There are two types of curve fitting methods commonly used in literature. One method is to choose a mathematical or empirical equation with some unknown parameters, where the parameters are determined by regression analysis based on the creep data and the developed equation is used to portray the time-dependent deflection development or long-term prediction. The other method of curve fitting is based on some physical models which can include elements such as springs, dashpots, or other M-S elements. The characteristic properties of these elements are also obtained by fitting them into the test data.

Nine empirical creep equations are summarized by Bodig and Jayne (1982). The commonly used empirical equations for compliance are

$$J(t) = J_0 + A_1 log(t+1) \tag{2.17}$$

$$J(t) = J_0 + A_1 log(t+1) + A_2 log^2(t+1) \tag{2.18}$$

$$J(t) = J_0 + mt^n \tag{2.19}$$

Models such as Eqns. (2.17) to (2.19) can work well over the limited time domains within the primary and secondary regions of creep. The power law form (Eqn. (2.19)) may have some predictive capacity (Holzer et al. 1989).

Kliger (1991) compares seven different mathematical expressions and uses

weighted and unweighed input data, and concludes that the use of the weighted values at the end of the observed creep data can significantly improve the predictive capacity of a model.

Nielsen (1972) lists some rheology models. For the creep of wood panels, Pierce and his colleagues (1977,1979,1985) study 3, 4, and 5 element models, and find that the 5-element model seems to give better long-term results than do the other two models.

In a more general sense, the methods discussed in sections 2.3.1 and 2.3.2 are also curve fitting methods, since many material parameters need to be obtained from creep test data. Usually, the values of material parameters are different for different creep tests.

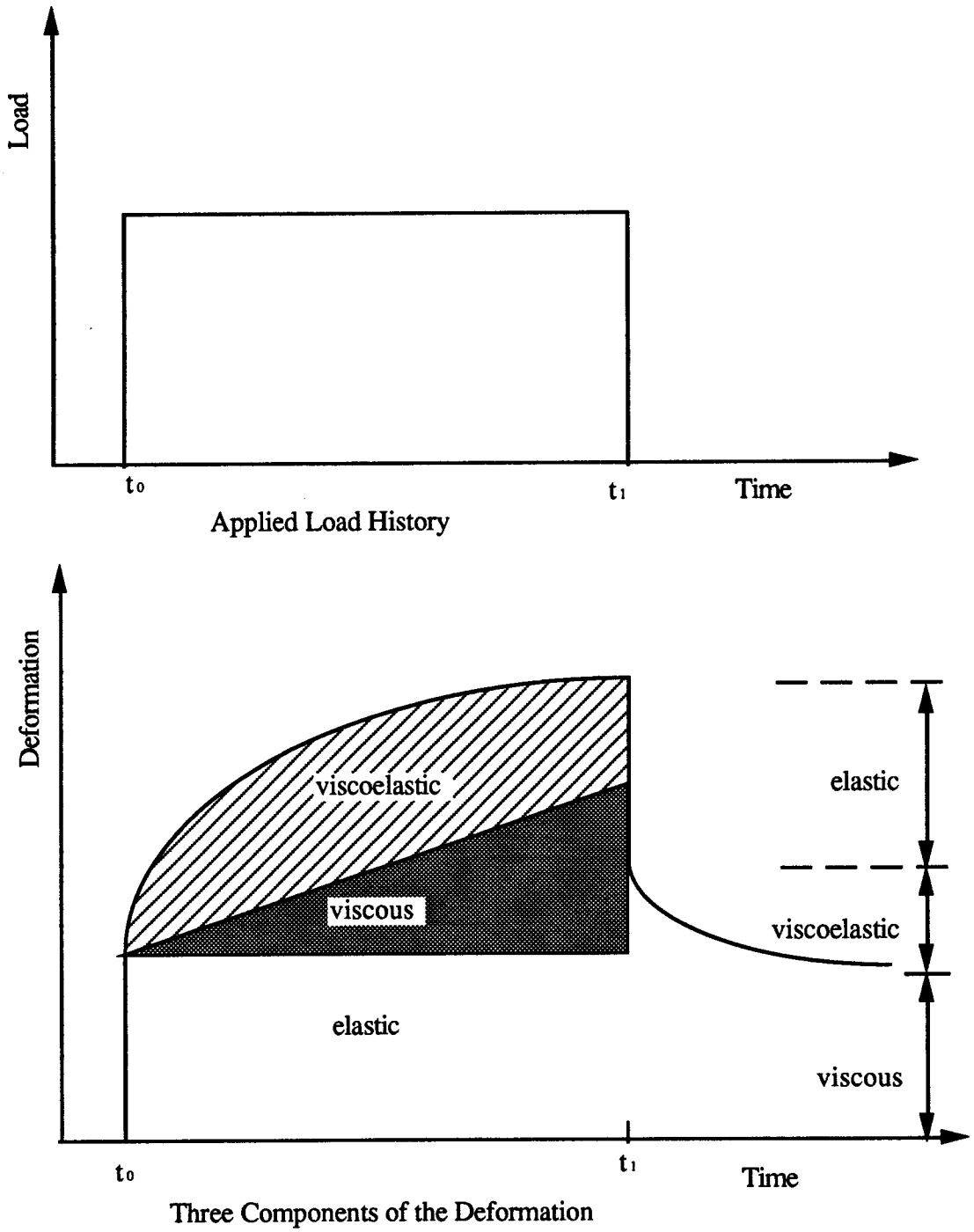

Fig. 2.1 Illustration of Response of a Material to Applied Load

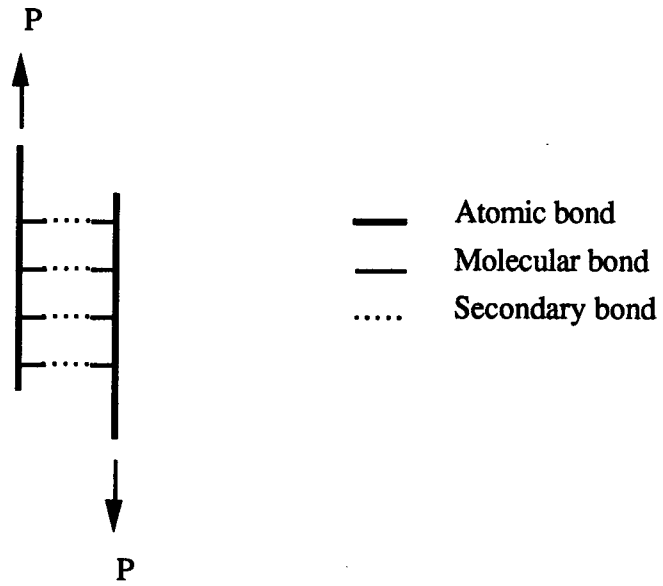

Fig. 2.2 A Simplified Chemical Bond Model of the Rheological Behavior of Wood (Bodig and Jayne, 1982)

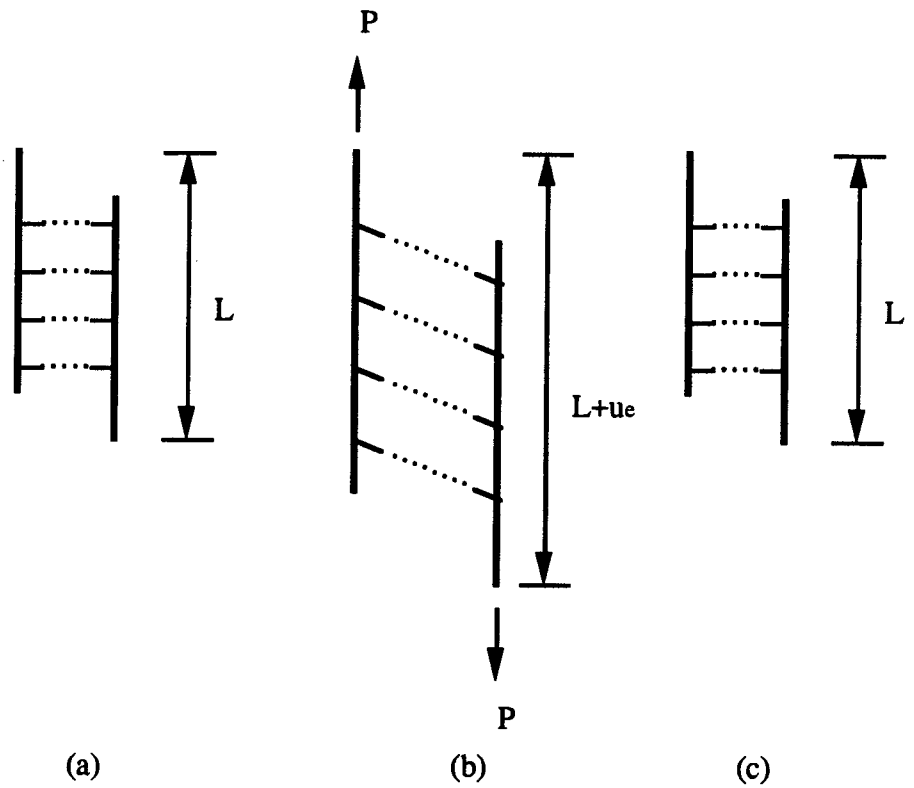

(a) initial condition, (b) elastic deformation, (c) recovery shape

Fig. 2.3 Schematic Representation of Elastic Deformation (Bodig and Jayne, 1982)

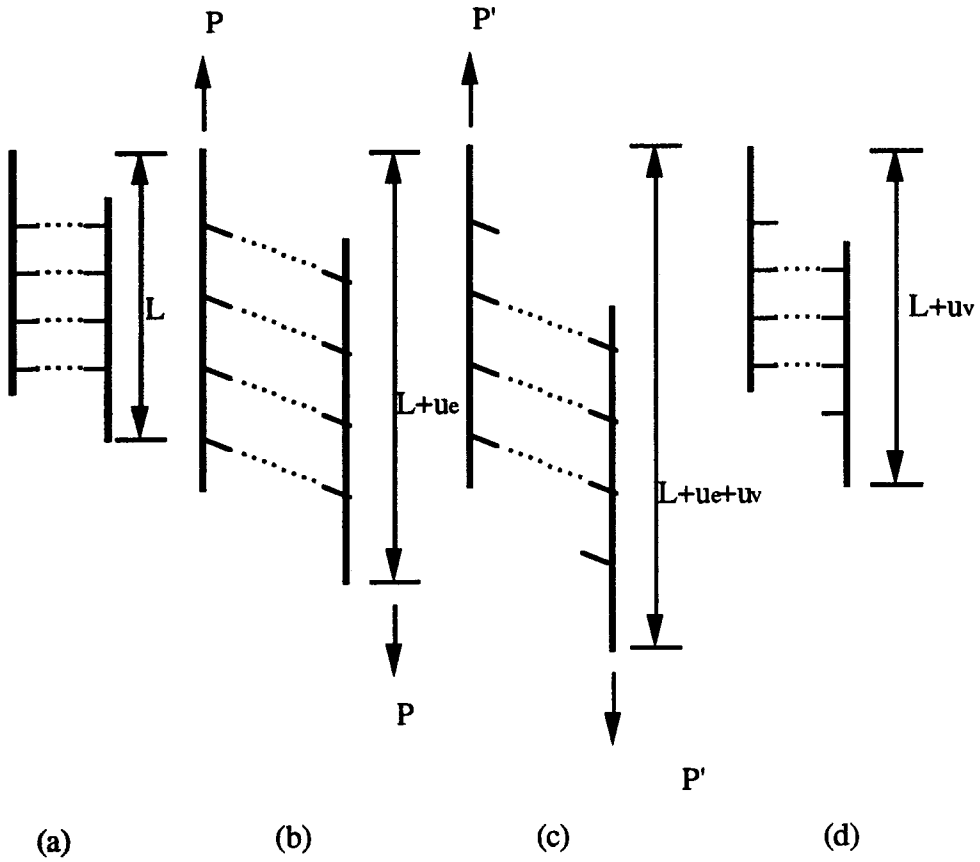

(a) initial condition, (b) elastic deformation, (c) bond breakage,

(d) newly formed bonds

Fig. 2.4 Schematic Representation of Viscous Flow (Bodig and Jayne, 1982)

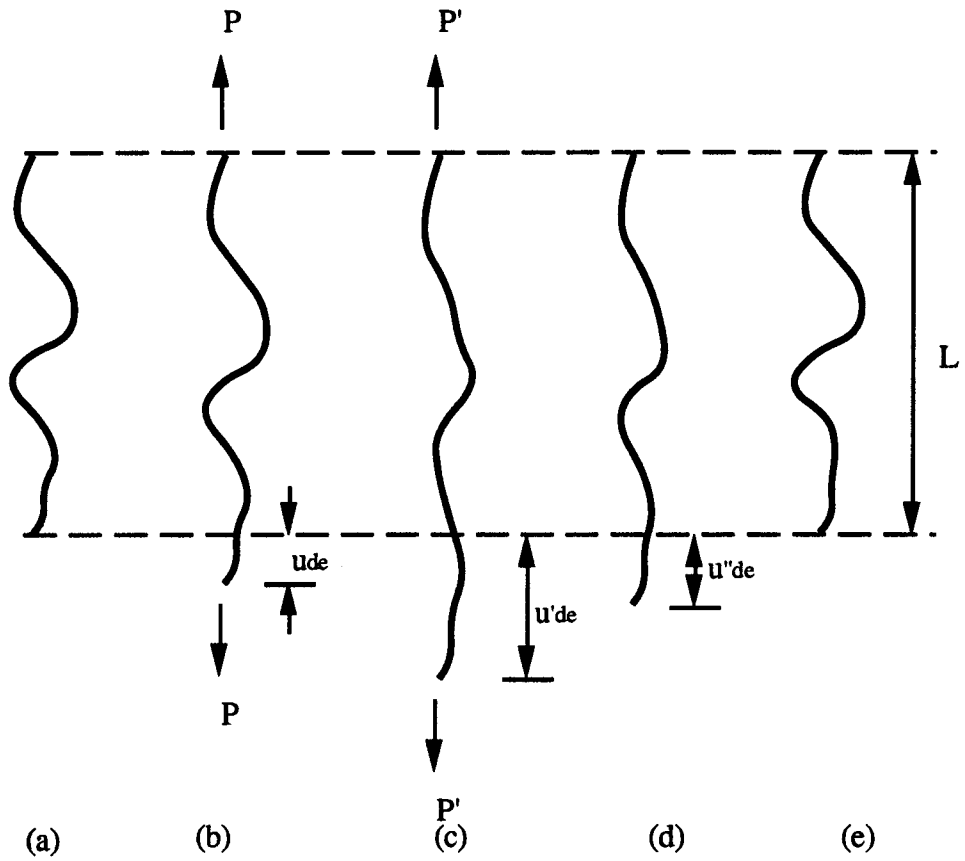

(a) original shape, (b) early stages of deformation, (c) final stages of elongation, (d) early stages of recovery, (e) recovered shape

Fig. 2.5 Schematic Representation of Delayed Elastic (Viscoelastic) Deformation (Bodig and Jayne, 1982)

Chapter 3 Experimental Program

3.1 General Test Plan

The experimental program was composed of two major parts. The first part, the short-term test, was conducted to determine the material properties (modulus of elasticity and modulus of rupture) of OSB and plywood panels. The other part, long-term test, was conducted to study the time-dependent deflection behavior of OSB and plywood panels under various climatic conditions. Along with long-term tests, some matched unloaded OSB and plywood panels were exposed to the same environment as creep specimens. The moisture gain/loss of the panels and swelling/shrinkage of the panel thickness were observed during the time period of creep testing.

The short-term test was carried out at the Forest Products Testing Laboratory, at the Alberta Research Council. The long-term creep test was carried out in Building F-34 located in the Edmonton Research Station, University of Alberta.

3.1.1 Short-term Experiment

All test specimens were cut from full size wood panels (2440mm x 1220mm). The size of the specimen is 1200mm x 300mm. Specimens were placed in a conditioning room (65%RH/20 ^{o}C) at the Alberta Research Council to get moisture equilibrium. Short-term properties (stiffness and ultimate strength) were determined after the conditioning. The test procedure for short-term tests is described in Section 3.4.1.

3.1.2 Long-term Experiment

A total of ten series of creep tests, each with 24 specimens, was conducted in the program. It consists of three series of constant RH controlled conditions, four cyclic

RH controlled conditions, and three normal indoor environmental conditions, as summarized in Table 3.1. In each series, two thicknesses (9.5 mm and 15.9 mm) and two strand orientations (surface strands parallel or perpendicular to the span direction) were chosen as study variables, as listed in Table 3.2. There were four replications for OSB panels and two for plywood in each variable studied. The OSB used in the test program was commercially manufactured in November 1990, in Alberta, Canada. The OSB was manufactured according to the standard CAN/CSA O437 from Alberta aspen trees; the plywood was manufactured according to the standard CAN/CSA O121 from Alberta white spruce trees.

3.2 Test Materials and Sample Preparations

3.2.1 Test Materials

The size of the test specimens was 300 mm wide and 1220 mm long. There were two cut plans, as shown in Fig. 3.1, to get strand/grain orientations parallel to the long or short direction of the specimens. Specimens cut as shown in Fig. 3.1 (a) are referred to as parallel bending specimens or parallel specimens; Specimens cut as shown in Fig. 3.1 (b) are referred to as perpendicular bending specimens or perpendicular specimens.

In the long-term creep test, there were 4 replications of OSB creep samples for each combination of thickness and strand orientation, and 2 replications for plywood creep specimens. For each combination of thickness and strand orientation, one unloaded OSB and plywood panel was for measurement of moisture content changes. The quantity of panels tested in each long-term creep test series is summarized in Table 3.2. There were 24 specimens for sustained creep loading and 8 specimens for moisture movement observation without loading in each of the ten long-term test series.

3.2.2 Specimen Preparation

Experimental specimens were prepared as follows:

1. Specimens were cut from full size panel as shown in Fig. 3.1. No treatment, such as painting or panel edge sealing, was given to the specimens.

2. All specimens were placed in a conditioning room (65%RH/20 ^{o}C) at the laboratory for at least five weeks to allow specimens to reach their equilibrium moisture contents.

3. When the equilibrium was reached, all the specimens were nondestructively tested to determine their short-term stiffness. The test procedure is discussed in Section 3.4.1.

4. After stiffness determination, some specimens were destructively tested to determine their short-term ultimate strength. Two panels from each whole sheet (4' x 8') were destructively tested. The test procedure is described in Section 3.4.1. The remaining specimens were long-term tested in Building F-34.

3.3 Moisture Content and Panel Thickness Measurement

3.3.1 Moisture Content Measurement

Moisture Content (MC) is defined as the quantity of moisture in the sample and is expressed as a percentage of oven-dry mass of the sample

$$MC = \frac{W - W_0}{W_0} \times 100\% \qquad (3.1)$$

where W = mass of sample at test

W_0 = oven-dry mass of the sample.

The oven-dry mass is defined as the mass obtained after the sample has been dried at 102 ± 3 °C for 24 hours according to ASTM D4442-92 (1992).

The equilibrium MC of OSB and plywood panels under the environment of 65%RH/20 °C was obtained, based on the broken wood pieces from the short-term destructive test: one small wood piece was cut from each destructive testing panel; the original weight under 65%RH/20 °C, as well as the oven-dry weight, of every small wood piece was recorded. The MC of each wood piece can be calculated according to Eqn. (3.1). The average of MCs from OSB or plywood pieces with the same nominal thickness was taken as the value of equilibrium MC at 65%RH/20 °C for that type of panel.

To monitor the moisture changes in panels during creep tests under various humidity conditions, the weights of unloaded dummy reference specimens (called moisture content measurement samples) were followed during the tests. To obtain the MC of wood panels during creep tests, the weight of MC measurement samples were recorded after they were conditioned at 65%RH/20 °C for longer than five weeks. Sample MC was calculated as follows:

$$MC = \frac{W(1+MC_{65}) - W_{65}}{W_{65}} \times 100\% \qquad (3.2)$$

where W = weight of panel exposed to a creep test environment

W_{65} = panel's equilibrium weight at 65%RH/20 °C

MC_{65} = panel's equilibrium MC at 65%RH/20 °C.

3.3.2 Panel Thickness Measurement

As water enters the cell wood structure, the wood swells; but as wood loses moisture, it shrinks. When panel is exposed to environmental RH changes, the thickness of panel, as well as the dimensions in the other two directions, swells or shrinks. The thickness of the panels was measured on the MC samples at the same time as they were weighed for MC determination. Since the thickness was not perfectly even throughout the specimens, the thickness measurement was taken each time at the same two different points of each MC measurement panel by a micrometer. An average taken from the two points represented the panel's thickness for that moment.

3.4 Mechanical Test Equipment and Procedure

3.4.1 Short-term Flexural Test

The short-term flexural test was carried out on specimens conditioned at 65% RH/20 ^{o}C for more than five weeks. Prior to destructive or long-term flexure testing, all panels were non-destructively tested by the Machine Stress Rated (MSR) method to determine the Modulus of Elasticity (MOE) according to CAN/CSA 0325.1-88. The apparent MOE was determined by a "three-point" loading system.

Matched samples (1' x 4') cut from each whole sheet as in Fig. 3.1, were destructively tested according to ASTM D 3043-87 to determine Modulus of Rupture (MOR). These specimens were tested to failure under a four-point loading configuration (two applied loads and two supports). The maximum load was recorded. The maximum stress in the specimens was calculated according to the geometric information of loading and panel. The maximum stress was the panel's MOR value. The MOR was not able to obtained for 9.5 mm perpendicular plywood panels due to excessive deformation during the post flexural test.

3.4.2 Long-term Flexural Test

Flexural Test Set-up

The test set-up for flexural creep tests is shown in Fig. 3.2. The creep specimen was simply supported on two round bars. The sustained load was applied by lead bricks through two aluminum bars. One of the aluminum bars had a round cross section, which could move outward easily when the deflected panel had a large curvature. The other bar was round but with a cut flat surface. The flat surface was put on the creep specimen. A picture of a tested specimen during the long-term test is shown in Fig. 3.3. The sustained load applied to the creep panel was a two-line load. The span between the line loads was almost unchanged with the increase of creep deflection because of the moveable round cross section of the aluminum bar.

With this type of set-up, the span between two loading lines had a maximum constant moment and was shear free. When the self-weight of the creep panel was excluded, the measured deflection, which will be discussed later, was flexural deflection only. The observed creep data represented the flexural creep behavior of all panels

Applied Load

The load applied to a creep panel was about 20% of the ultimate short-term strength (at 65% RH/20 ^{o}C) except for 9.5 mm perpendicular plywood panels. The ultimate strength was MOR value for the same type of panels obtained from the destructive test as described in Section 3.4.1. The stress produced by the self-weight of panel (65% RH/20 ^{o}C) was also counted as part of the sustained loading effect. The nominal values of the total applied load are listed in Table 3.3. For parallel bending cases, the applied load for OSB was 51% and 70% that of the plywood for 9.5 mm and 15.9 mm panels,

respectively.

The sustained load, which was produced by lead bricks, was applied manually. The loading time varied from 5 to 30 seconds depending on the magnitude of the applied load or the number of lead bricks.

The maximum stress in 9.5 mm perpendicular bending plywood panels was 1.3 MPa, which was 8% of the ultimate short-term strength of 15.9 mm perpendicular plywood panels. Though the applied load was very low, the panel's deflection was very large because of the low stiffness of the panel. After tests C35 and I1 (as defined in Table 3.1), the loading span for 9.5 mm perpendicular bending plywood panels was shortened to reduce the overall deflection, while the maximum bending moment was kept unchanged. Compared with the set-up shown in Fig. 3.2, the total span between two supports was 610 mm (24") instead of 1067 mm (42"), and the distance between loading and reaction was 152 mm (6") instead of 254 (10"). Although the span was changed for the rest of the eight test series for the 9.5 mm perpendicular plywood panels, the deflection was still large.

Environment Treatment and Creep Duration

The long-term creep tests were carried out in both controlled and uncontrolled environments. For the controlled environment, the creep tests were conducted in an enclosed chamber. Beside the enclosed chamber, the other half of the building was set up for the uncontrolled environmental creep tests.

The controlled environment creep tests consisted of three series of constant RH conditions, and four series of cyclic RH conditions at 20 ^{o}C. For the three constant RH tests, named C35, C65, and C85, the RH was kept constant at 35%, 65%, or 85%, respectively. The designed RH for the three constant RH creep tests is shown

schematically in Fig. 3.4. During four cyclic RH tests, named V1 (1 day/cycle), V2 (2 days/cycle), V7 (7 days/cycle), and V14 (14 days/cycle), the RH fluctuated between 35% and 85% and started from a 35% RH duration at 20 °C. The cyclic frequencies were 1 day/cycle, 2 days/cycle, 7 days/cycle, and 14 days/cycle. The stepwise cycling is shown in Fig. 3.5. Besides the specified RH, the temperature was also kept constant at about 20 °C.

The creep duration of these controlled series was six weeks, except for test V14 (14 days/cycle) that lasted for 25 weeks (175 days).

The "uncontrolled environment" for creep tests was conducted at indoor environmental conditions in a normal heated laboratory. Three series of creep tests, I1, I2, and I3, were carried out under indoor environment conditions. The temperature fluctuated between 18 °C and 27 °C and the RH fluctuated between 15% and 60% in the uncontrolled environment. Since the three test series were carried out one after another, they took place during different seasons. The RH and temperature were a little different for the three series. During summer, the RH and temperature were a little higher than during the other seasons. The creep duration was 12 weeks for the three test series.

In Table 3.1 all the ten series of creep tests carried out inside and outside the chamber are summarized. For each creep test series, both environmental conditions and creep duration are also shown in the table. Specimens were unloaded when the creep duration specified in Table 3.1 was reached. All specimens were allowed to recover for 3 days.

Experimental Instrumentation

Instrumentation for environment control - All the creep tests were carried out in a

laboratory equipped with a gas fired furnace. The lower temperature limit was set at 18 ^{o}C. In summer, an air conditioner was used to keep the temperature of the chamber down to about 20 ^{o}C.

The environmental control of the tests was realized by a computer. A DASCON board with four channels was used to record the chamber's RH, temperature, and the deflections of specimens measured by two Linear Variable Differential Transformers (LVDT).The computer used a circuit board and program developed by the electronics shop of the Department of Civil Engineering. The RH and temperature of the chamber were sensed by a humidity sensor and a temperature sensor. These two sensors were calibrated before the experiment and signals from the two sensors were sent to the computer. The humidifier and dehumidifier were activated by the computer to adjust the RH inside the chamber. (A circuit board was used to activate the connection between the computer and the humidifier or dehumidifier). Either humidifier or dehumidifier would start to work when the difference between sensed actual RH and the test specified RH was larger than $\pm$ 1% RH. There was one humidifier and one dehumidifier for adjusting the chamber's RH during the creep tests C35, C85, and V1. There were two humidifiers and two dehumidifiers for adjusting the chamber's RH during the later creep tests C65, V2, V7, and V14. The air circulation of the chamber was maintained with four 12" oscillating fans. The controlling of the chamber's environment is illustrated in Fig. 3.6.

The RH and temperature for the indoor uncontrolled environment creep tests were recorded continuously by a mini hygrothermograph. They were also recorded manually when the deflections of creep specimens in the same environment were measured.

Instrumentation for deflection measurement - A dial gauge fixed to an aluminum tripod was used to measure the deflection over the 406 mm (16") span in the middle of panels,

as is shown in Fig. 3.7. The measured deflection was resulted mainly from bending deformation in the central part of panel. The deflection was measured manually on both sides of the panels to eliminate any possible warping deformation. The accuracy of the dial gauge was .0245 mm (.001"). The weight of the tripod and dial gauge was small compared with the load applied to the panels. In addition, this weight was applied whenever the deflection was measured.

Since creep developed very fast shortly after loading and the creep rate gradually decreased with time, short intervals for deflection measuring were used at the beginning of creep test, and longer intervals were used for the rest of the creep test duration. After a specimen was loaded, the deflection was measured at the following elapsed times: 1 minute, 3 minutes, 10 minutes, 30 minutes, 100 minutes, 200 minutes, 1 day. Later, the measurements were taken at longer intervals depending on individual creep test series. When the creep duration as shown in Table 3.1 was reached, specimens were unloaded. The creep recovery was also observed for 3 days. The recovery deflection was measured at the following elapsed times after unloading: 1 minute, 10 minutes, 100 minutes, 1 day, 3 days.

In addition to the manual deflection measurement, mid-span deflection of two OSB specimens in each test series (one was 9.5 mm parallel panel and the other was 15.9 mm parallel panels) was measured by two LVDTs which were connected to the computer in small data collecting intervals. This set-up is also shown in Figs. 3.3 and 3.7.

Experimental Procedures for the Creep Test

1. Readings were taken by the dial gauge when panels were lying on the ground (without any load and weight).

2. Readings were taken by the dial gauge 1 minute after panels were put on the two round bar supports. The difference between the first two measurements was considered as the elastic deflection under the self-weight of the panel.

3. Readings were taken by the dial gauge one day after the panels began lying on the supports. Later on, these readings were recorded as the initial reading before the loads were applied to the specimens.

4. Loads (most was lead bricks) were applied on creep panels. Once a specimen was loaded, the deflection was measured at the following elapsed times: 1 minute, 3 minutes, 10 minutes, 30 minutes, 100 minutes, 200 minutes, 1 day. Later, with longer intervals were adopted.

5. The sustained load was taken off when the creep duration (as shown in Table 3.1) was reached. The panel deflection was measured at elapsed times: 1 minute, 10 minutes, 100 minutes, 1 day, 3 days.

Table 3.1 Summary of Ten Series of the Creep Tests

Test ID	RH Condition	Temperature	Creep Duration
C35	35% Constant	20 °C	6 weeks
C65	65% Constant	20 °C	6 weeks
C85	85% Constant	20 °C	6 weeks
V1	35-85-35%, 1 day/cycle	20 °C	6 weeks
V2	35-85-35%, 2 days/cycle	20 °C	6 weeks
V7	35-85-35%, 7 days/cycle	20 °C	6 weeks
V14	35-85-35%, 14 days/cycle	20 °C	25 weeks
I1	uncontrolled, 10-30%	19 °C-22 °C	12 weeks
I2	uncontrolled, 20-60%	19 °C-27 °C	12 weeks
I3	uncontrolled, 10-45%	18 °C-22 °C	12 weeks

Table 3.2 List of Specimens Tested in Each Long-term Test Series

Materials	Nominal Thickness(mm)	Strand Direction	No. of Specimens: Creep Specimen	No. of Specimens: MC Specimen
OSB	9.5	Parallel [a]	4	1
		Perpendicular [b]	4	1
	15.9	Parallel	4	1
		Perpendicular	4	1
Plywood	9.5	Parallel	2	1
		Perpendicular	2	1
	15.9	Parallel	2	1
		Perpendicular	2	1

[a] Parallel refers to specimen cut according to cut plan shown in Fig. 3.1a.

[b] Perpendicular refers to specimen cut according to cut plan shown in Fig. 3.1b.

Table 3.3 Nominal Loads Applied to the Test Specimens

Materials	Nominal Thickness(mm)	Applied Load (N): Parallel [a]	Applied Load (N): Perpendicular [b]
OSB	9.5	169.5	114.7
	15.9	469.4	335.2
Plywood	9.5	334.2	41.2 (98.1) [c]
	15.9	668.4	272.4

[a] Parallel refers to specimen cut according to cut plan shown in Fig. 3.1a.

[b] Perpendicular refers to specimen cut according to cut plan shown in Fig. 3.1b.

[c] The applied load was 41.2 N for tests C35 and I1, and 98.1 N for the rest of tests.

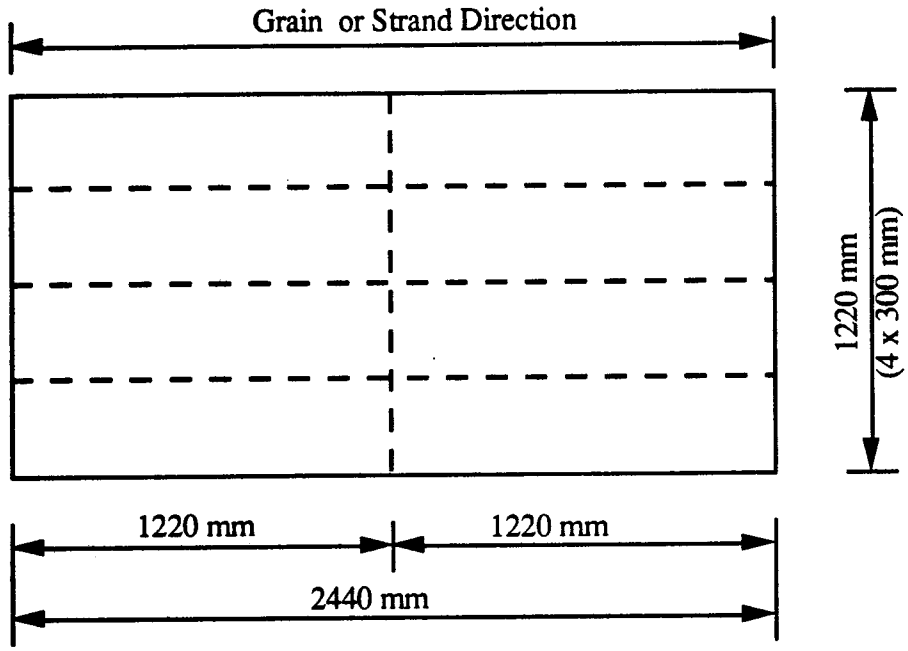

(a) Specimen Cutting Plan (Strand Parallel to Specimens' Long Direction)

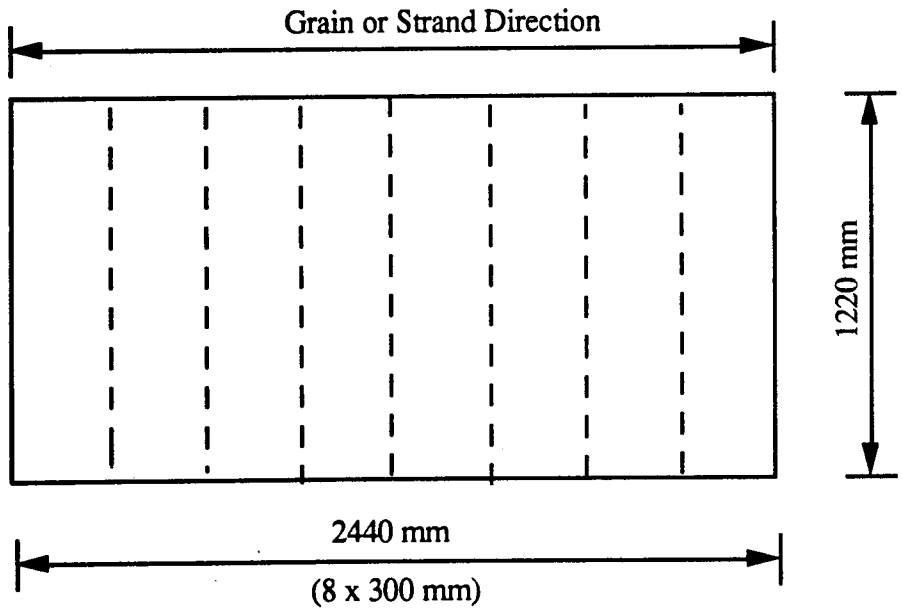

(b) Specimen Cutting Plan (Strand Perpendicular to Specimens' Long Direction)

Fig. 3.1 Specimen Cutting Plan (Parallel or Perpendicular)

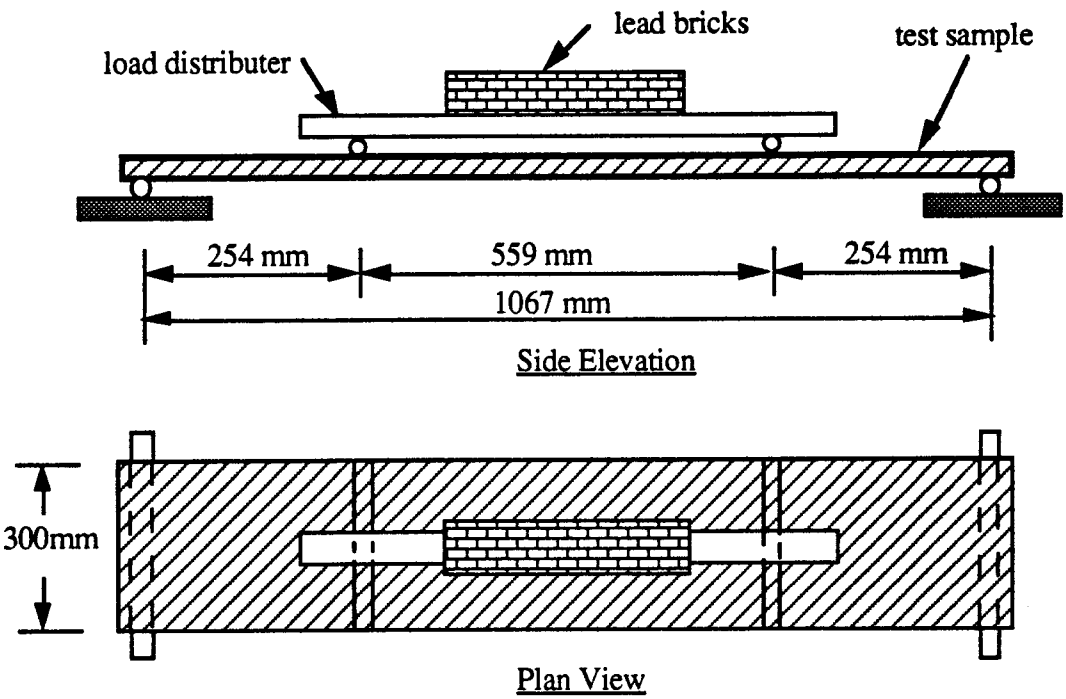

Fig. 3.2 Experimental Apparatus for Flexural Creep Test

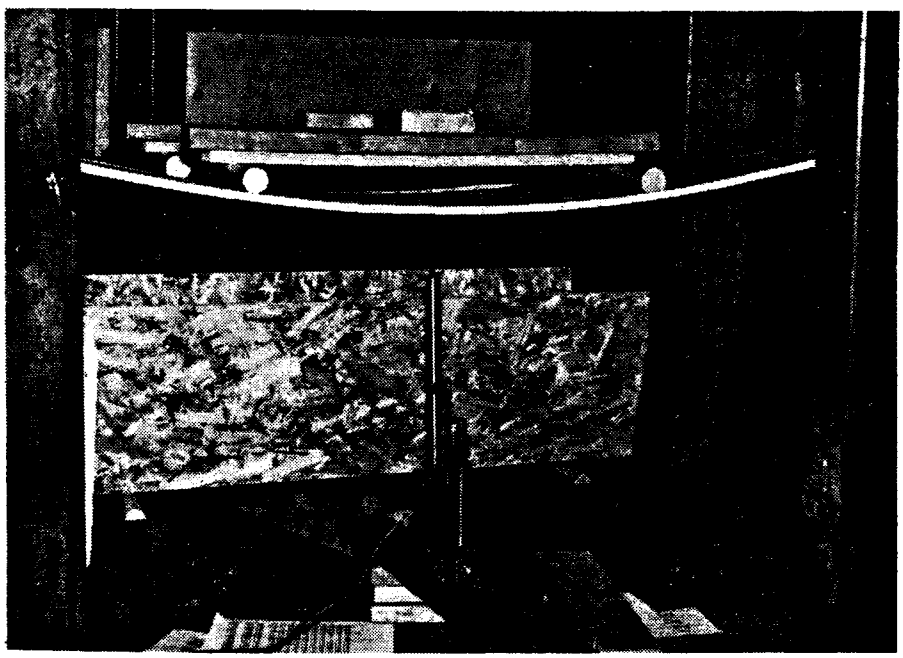

Fig. 3.3 Picture of 9.5 mm OSB Specimen with Sustained Load during Creep Test inside the Controlled Chamber

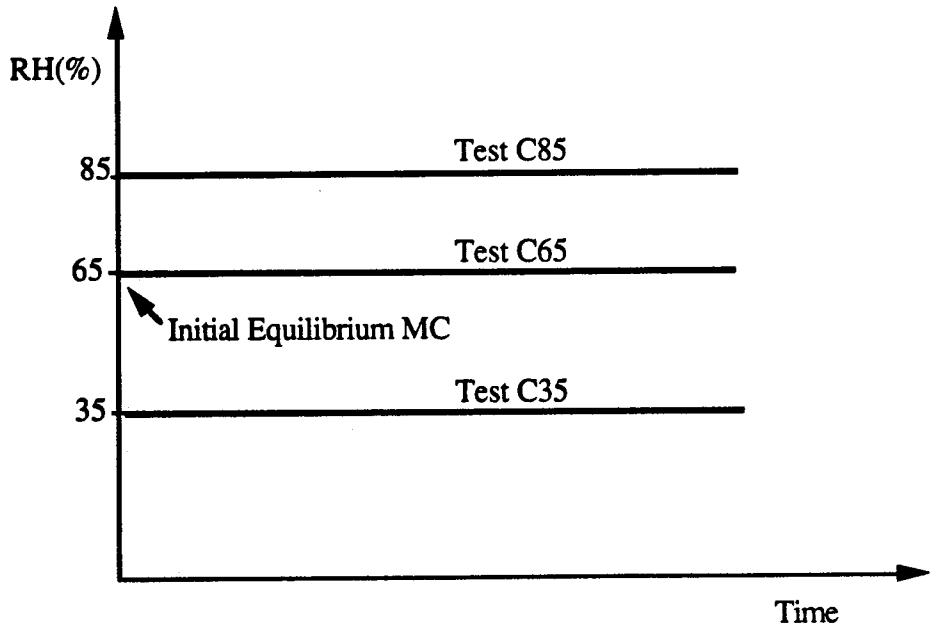

Fig. 3.4 Schematic Plots of Designed RH for Three Constant RH Creep Tests

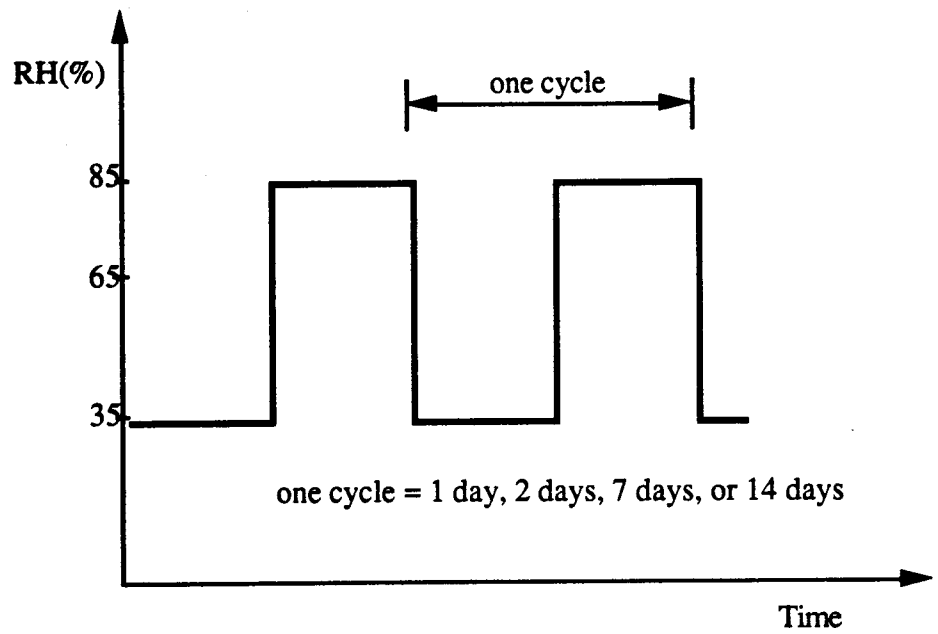

Fig. 3.5 Schematic Plot of The Designed Stepwise RH Cycling for Four Cyclic Creep Tests (V1, V2, V7, and V14)

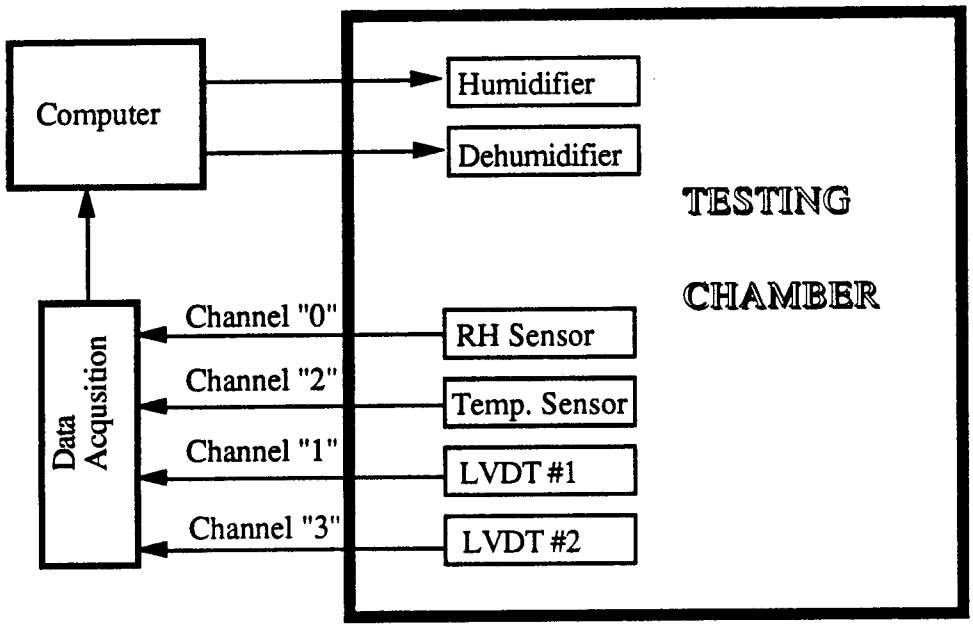

Fig. 3.6 Illustration of Instrumentation for the Chamber's Environment Control

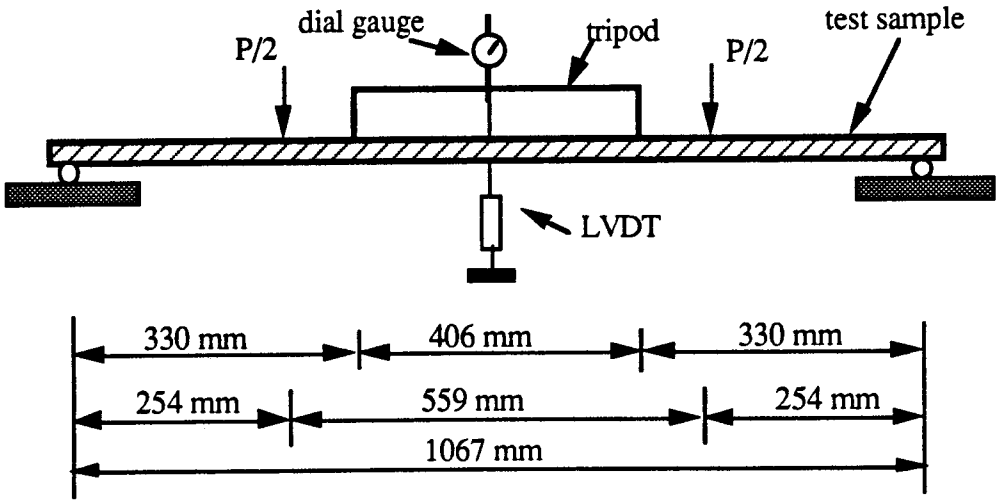

Fig. 3.7 Instrumentation for Deflection Measurement

Chapter 4 Experimental Results

The results of the experimental program are summarized in this chapter, which demonstrates the panel's short-term mechanical properties, the MC, the thickness, the time-dependent deflection, and the actual creep test environmental conditions.

The short-term mechanical properties from nondestructive and destructive tests are presented in Section 4.1. The RH and temperature for creep tests inside the enclosed chamber and outside the chamber are shown in Section 4.2. The MC and panel thickness changes of unloaded panels exposed to the same environment as the creep panels are reported in Section 4.3. The long-term flexural creep test results are summarized in Section 4.4.

4.1 Short-term Material Properties

4.1.1 Short-term Bending Stiffness of Materials

As described in chapter 3, there were seven creep test series carried out inside an enclosed chamber with specified environmental RH conditions. The panels for the tests were all preconditioned (65%RH/20 ^{o}C) for about five weeks in seven batches, one after another. The panels used for the three indoor uncontrolled environment test series were preconditioned with three of the seven batches described above: test I1 with test C35, test I2 with testV1, and test I3 with test V2. After the preconditioning, the panels in each batch were MSR tested all together. The MSR test results are summarized in Tables 4.1-4.7 for all seven batches. The calculation of the MOE values in the tables is based on the nominal panel width (304.8 mm) and the measured panel thicknesses.

It should be noted that the MOE values from all batches are consistent, which means that the panels for all creep test series were homogeneous. One exception was

the batch shown in Table 4.4 for creep tests V1 (1 day/cycle) and I2 (indoor environment). The MOE values in the table seem lower than for the other batches. It was also found that the measured panel thicknesses in the batch were larger than that of other batches. Since the calculation of MOE values was based on the measured panel thickness, the possible thickness measuring errors (such as non-zero reading of the micrometers and different applied pressure during measuring) would cause errors in the MOE values. Larger measured thicknesses would result in smaller calculated MOE values. The MOE values in Table 4.4 would be consistent with the other batches if the panel thicknesses were given the same values as other batches. Therefore, the actual panel stiffness of this batch might be consistent with others if the error due to thickness measuring did exist. This speculation was later verified by comparing the panels' instantaneous deflections with that of the other creep series under the applied creep loads. The consistency of the instantaneous deflections implied that the panel short-term stiffness in that batch had no significant difference with other batches.

In Tables 4.1 - 4.7, the standard deviations used for calculating coefficients of variation are based on the degree of freedom equal to the sample number. These tables show that the short-term stiffness is close for panels with the same material and surface orientation. The perpendicular plywood panels were the only exception. The MOE of the perpendicular OSB panels was a little more than one-third that of the parallel OSB panels. The MOE of perpendicular plywood panels was very little. The variations of 9.5 mm plywood panels with smaller thickness were larger than that of the OSB panels.

The results listed in Tables 4.1 - 4.7 are summarized in Table 4.8. The MOE values in the table are the average values for the panels used in the entire experimental program.

4.1.2 Short-term Ultimate Bending Strength of Materials

Some panels from the batch listed in Table 4.1 were destructively tested to obtain the short-term ultimate bending strength right after their MSR test. The panels used for creep tests were assumed to have the same ultimate strength as the destructively tested panels when the creep load was at a 20% stress level. The post-flexure testing results for the first batch are listed in Table 4.9. The coefficients of variation are not reported for the plywood panels in the table because of the limited number of test samples.

To carry out the post flexure test more efficiently, the destructive test was not done immediately after the MSR tests for all other batches listed in Tables 4.2 to 4.7. The panels for the destructive test were kept in a normal indoor environment until all the destructive testing specimens from the other six batches were available. The wood panels for the destructive test were placed in the conditioning room (65%RH/20 ^{o}C) for six weeks before the destructive test was carried out. It should be noted that these panels for destructive testing were never creep tested. The post flexure test results are listed in Table 4.10.

During the post-flexure tests, the 9.5 mm perpendicular plywood panels slipped. The MOR for this type of panel could not be obtained. The values are missing in Tables 4.9 and 4.10.

The results from two of the post flexure testing batches listed in Tables 4.9 and 4.10 are consistent. They are put together in Table 4.11, which shows that the short-term ultimate strengths, like MOE, were close for the panels with the same material and surface orientation, except for the perpendicular plywood panels. The ultimate strengths of the perpendicular OSB panels were approximately three-quarters that of the parallel OSB panels; the coefficients of variation for OSB panels were about 10% and the

coefficients of variation for plywood panels were about 20%.

4.2 Environmental Records

4.2.1 Uncontrolled Environment

The temperature and RH of the uncontrolled indoor environment were recorded during the three flexure creep test series (I1, I2, and I3). The creep test series I1 was tested from January to April. The weather was characterized by low humidity, and the RH fluctuated between 10% and 30%. The creep test series I2 was tested from April to July. The environment for this creep test duration had a high RH and a high temperature; the highest recorded RH was near 60%, and the highest temperature was about 27 ^{o}C. Creep test I3 was carried out from September to November. The environment was mostly very dry. The RH ranged between 10 to 30% except for the first week, during which the RH was a little higher, between 30 to 45%.

The records of temperature and RH are shown in Figs. 4.1 to 4.3 for the three indoor test series.

4.2.2 Controlled Environment

The RH of the controlled chamber was designed as shown in Figs. 3.4 and 3.5 for the seven creep test series with constant or cyclic RH environment. The temperature was kept around 20 ^{o}C. The actual RH of the chamber was recorded by the computer at every two hour intervals.

As described in the Chapter 3, there were only one humidifier and one dehumidifier to control the chamber's RH during the constant RH creep test C35, C85, and the cyclic RH creep test V1 (1 day/cycle). It took about 60 minutes to raise the chamber's RH from 35% to 85%. It was difficult to lower the RH with one dehumidifier, and it

took about 120 minutes to change from 85% to 35%. In addition, the specified RH cycles changed relatively fast in creep test V1 where each RH level lasted for 12 hours in one cycle. Rephrased that means that the actual RH of the chamber was not quite a square wave cycle as shown in Fig. 3.5. An actual RH recording taken during test V1 is shown in Fig. 4.4.

For the later cyclic RH creep tests, V2 (2 days/cycle), V7 (7 days/cycle), and V14 (14 days/cycle), a second humidifier and dehumidifier were brought in to adjust the chamber's RH. The two dehumidifiers altered the RH in a much shorter time, taking about 90 minutes to decrease the chamber's RH from 85% to 35%, and about 30 minutes to raise the RH back to 85%. The actual RH in these three creep test series was very close to a square wave cycle as designed in Fig. 3.5. Part of the actual RH recording taken from test V7 is shown in Fig. 4.5.

4.3 Moisture Content and Panel Thickness

4.3.1 Equilibrium Moisture Content

The panels preconditioned at 65%RH/20 ^{o}C for more than 5 weeks reached a constant weight. The MC of the panels therefore also reached equilibrium. The equilibrium MC of the panels under 65%RH/20 ^{o}C was obtained from the broken wood pieces immediately after the post-flexure test as described in Chapter 3. The results of the measured MC are summarized in Table 4.12.

The MC for OSB, and for plywood, with two nominal thicknesses is given separately in the table . Further examination by a "Student's t Test" shows that the mean equilibrium MC for 9.5 mm (3/8") OSB is not significantly different from that of 15.9 mm (5/8") OSB at a 10% confidence level. The Student's t Test gives the same conclusion for 9.5 mm (3/8") and 15.9 mm (5/8") plywood. Therefore, the population

mean for OSB can be considered as the equilibrium MC for all OSB at 65%RH/20 ^{o}C. The population mean for plywood is taken as the equilibrium MC for all plywood at 65%RH/20 ^{o}C.

In both tests C35 and C85, the weights of unloaded panels were unchanged towards the end of the tests. The panel equilibrium MC at 35%RH/20 ^{o}C could be obtained from test C35, and the panel equilibrium MC at 85%RH/20 ^{o}C could be obtained from test C85. The MCs of the unloaded panels were calculated as described in Section 3.3.1 using Eqn. (3.2).The equilibrium MC at three constant RH levels (35%, 65%, and 85%) are listed in Table 4.13, which shows that panels with two nominal thicknesses give very close equilibrium MC at 35% or 85% RH level, except for the plywood panels at 35% RH level; the MC of 15.9 mm plywood panels was 2% points higher than that of 9.5 mm plywood panels.

The equilibrium MC at 65%RH/20 ^{o}C was taken as a reference value for the calculation of MC at other environmental conditions. The equilibrium MC at 65%RH/20 ^{o}C is taken as 9.4% and 11.2% for OSB and plywood panels, respectively. The equilibrium MC of OSB and plywood panels at the three RH levels are also plotted in Fig. 4.6. The values used for the plot are the averages of panels with two nominal thicknesses. The figure shows that the plywood has about 2% points higher equilibrium MC than OSB at same RH levels.

4.3.2 Moisture Content Fluctuation during Creep Tests

During cyclic RH creep tests, the MC in panels fluctuated. The MC changes were different for different panel thicknesses and different cyclic RH frequencies. The panels' MC fluctuation, as measured during the creep test process, is reported in Table 4.14 to Table 4.22.

The moisture content situations of panels with different thicknesses were different. The measured panel's average MC for the 9.5 mm and 15.9 mm OSB panels in creep test V7 (7 days/cycle) is plotted in Fig. 4.7. The dashed lines in the figure are the panel's surface MC in the cyclic RH environment, assuming that the surfaces could respond to the surrounding RH changes immediately. As shown, the thicker panels have less MC change than the thinner panels have during the same RH cycling. The thinner panels have higher MC in the wetting duration and lower MC in the drying duration than do the thicker panels. The MC of the 9.5 mm OSB panels changed by about 3.4% within one full cycle, but only by 2.7% for the 15.9 mm OSB panels. The average MC levels in one full cycle are close for both thicknesses.

Panels have different MC changes in cyclic RH environments with different frequencies. The MC of the 9.5 mm OSB panels in test V2 and V7 is shown in (a) and (b) of Fig. 4.8. The dashed lines in the figure have the same meaning as in Fig. 4.7, and represent the environmental RH changes. The figure shows that the panels have a higher average MC as well as a larger MC fluctuation in test V7 than in test V2. The lower MC level during drying is close for both frequencies. The peak MC for test V7 during wetting is about 1 % more than for test V2. The average MC levels in one full cycle are higher at slower cyclic conditions.

4.3.3 Panel Thickness

When environmental RH changes, the wood panel dimensions also change because of swelling or shrinking. One major purpose of measuring panel thickness is to know how much the moment of inertia of the panel's cross section will change during creep tests. The thickness of the unloaded panel was measured during creep tests. The ratio between the measured panel thickness during creep tests and the initial thickness, H/H_0, was calculated. The ratios for all panels are listed in Tables 4.14 to 4.22.

In test C35, the panel thickness decreased due to the environmental RH changing from 65% to 35%. The shrinkage of panel thickness happened gradually until the panel MC attained equilibrium. This stable panel thickness is herein called equilibrium panel thickness. The ratio between the measured equilibrium thickness at 35% RH and the initial equilibrium thickness at 65% RH was about 0.97 for OSB. In test C85, the panel thickness increased because the environmental RH changed from 65% to 85%. The ratio between the equilibrium thickness at 85% RH and the initial equilibrium thickness at 65% RH was about 1.07 for OSB. These ratios are plotted in Fig. 4.9, where H/H_0 refers to the thickness ratio.

During cyclic RH creep tests, panel thickness also varied during different sorptive processes. The thickness changes were around 4% between the two RH levels (35% and 85%) in test V14 and 2% in test V7. The thickness changes in test V1 and V2 were negligible. Since wood panel does not have a perfectly even thickness, the thickness measurement was not always accurate enough to represent the wood panel's thickness change, but the general trend should be satisfactory.

4.4 Long-term Deflection and Creep Recovery

To present long-term test results about panels' creep behavior, the fractional deflection is chosen to describe the long-term performance of panels under various climatic conditions. The fractional deflection is defined as the ratio of the total deflection to the instantaneous deflection. The deflection at one minute after loading is selected as the instantaneous deflection.

For the same type of panels, the variations among the replications are smaller when the creep behavior is presented by the fractional deflection instead of by actual deflection. This is shown in Figs. 4.10 and 4.11. Fig. 4.10 shows the actual measured

deflection vs. time curves for the four 15.9 mm OSB panels in cyclic test V7 (7 days/cycle); and Fig. 4.11 shows fractional deflection vs. time curves for the same panels.

During the experiment it was found that the fractional deflection of the four OSB specimen replications, as well as for the two plywood specimens, in each creep test was very consistent. Therefore, the results presented shown an average of the four or two replications. The panels' fractional deflection obtained from the ten creep test series are summarized in Tables 4.23 to 4.29 in tabulated format. The fractional deflection vs. time curves are plotted from Fig. 4.12 to Fig. 4.25 for various types of panels tested in controlled or uncontrolled indoor environments. The time or elapsed time for deflection data in the figures was based on the instant that the full load was applied to the test specimens. The unit of time was in minutes.

Fractional deflections for ten creep test series after 6 weeks of sustained loading are summarized in Table 4.30. It should be noted that although 12 weeks load duration is used for the 3 indoor uncontrolled series and 25 weeks for the cyclic RH creep test V14 (14 days/cycle), the 6 weeks creep data are used in Table 4.30 for comparison. The fractional deflections in the table are the averages of four specimens for OSB and two specimens for plywood, as described before. 9.5 mm or 15.9 mm represents the nominal thickness of creep specimens, and parallel or perpendicular is the relative orientation between bending and surface strand orientation as shown in Fig. 3.1. The 9.5 mm perpendicular plywood samples were also creep tested, but the results are not reported in the table since some panels slipped down to the floor during creep tests because of excessive creep deflections.

The results and observations from the long-term creep tests are given in the following sections and are based on the test environments.

4.4.1 Constant RH Tests

4.4.1.1 Long-term Deflection of Constant RH Tests

As shown in Table 4.30, the fractional deflection of most OSB panels in constant RH at medium levels (test C35 and C65) are between 1.5 to 2.0 after 6 weeks of sustained loading. When panels were exposed to a high RH environment (test C85), much more creep developed. The OSB fractional deflections ranged between 3.6 and 4.9 after six weeks in a high RH environment (85% RH).

Creep curves for 15.9 mm parallel OSB panels are plotted in Fig. 4.26. The figure shows that the creep curve for 85% RH is much higher than the creep curves for 35% and 65% RH; the creep curve for 65% RH is a little lower than that of 35% in the early duration of the creep test. The creep curve for 65% RH starts to catch up later on, which means that the slope of the creep curve or creep rate for a 65% RH environment is larger than that of the 35% RH environment in the later creep duration (Figs. 4.13 to 4.15). This observation is true for all OSB panels, with the exception of the 9.5 mm parallel OSB panels (Fig. 4.12), while the slopes of the 35% and 65% RH creep curves are close after the early creep duration; the creep curve under 65% RH is always lower than that of 35% RH in the entire creep test duration.

4.4.1.2 Creep Recovery of Constant RH Tests

The instantaneous fractional deflection recoveries upon unloading for all creep test series are listed in Table 4.31. The instantaneous fractional deflection recovery upon unloading is referred to as the deflection recovery at one minute after unloading.

For constant RH conditions, the instantaneous fractional deflection recoveries listed in Table 4.31 for OSB panels are all close to 1.00, but a little less than 1.00. They are

between 0.92 to 0.99.

Wood panel recovery continues with time after the sustained load is removed; the recovered deflection is the viscoelastic component developed under sustained loading. In the experiment, the recovery lasted at least 3 days for all test series. The panel recovery curves are also shown in Fig. 4.26. Although the recovery would continue after the fist 3 days, the trend of the recovery curves shows that most of the time-dependent deformation would remain irrecovered. The remaining fractional deflection after unloading and 3 days' recovery is listed in Table 4.32; it is about 3 times of the instantaneous deflection for the OSB. However, the plywood has much less irrecoverable deformation compared with the OSB.

As creep was affected by RH level, the recovery (viscoelastic deflection) was different for different RH levels; the OSB panel in test C85 recovered more than in test C35 and C65 in the first 3 days. However, the panel in test C85 still had much more irrecovered or permanent deflection (which is the viscous deflection developed during creep) than tests C35 and C65.

4.4.2 Cyclic RH Tests

4.4.2.1 Long-term Deflection of Cyclic RH Tests

As summarized in Table 4.30, the fractional deflection of OSB panels has different values in cyclic RH tests. Within the range of the four cyclic frequencies conducted in the experiment, the slower the cycling, the more the creep developed in the OSB panels. The slowest cycling (14 days/cycle) gave the OSB panels the most creep during six weeks. The fractional deflection of OSB was up to about 4.0 within only six weeks in the test V14.

This observation is also shown in Fig. 4.27, in which the fractional deflection vs. time curves under four cyclic RH conditions are plotted for 15.9 mm parallel OSB panels. Although the test V14 continued for 25 weeks, only the creep curve for the first 6 weeks is plotted in Fig. 4.27. The figure shows that the creep curves of the slower RH cycles are higher than those of faster cycles.

A typical OSB creep curve measured by an LVDT and recorded by the computer from one specimen in creep test V7 is shown in Fig. 4.28. It is clear that large creep increments occur in the first desorption and adsorption. The creep developed during the first full cycle (one desorption and one adsorption) was about 30-65% of the total creep in a 6 week duration for all cyclic tests. In addition, the creep curve during the first adsorption was close to a straight line (Fig. 4.28), which was much steeper than the creep curve during the first desorption. The deformation of the first adsorption was about twice of the first desorption. Then the curve leveled off during the subsequent desorptions and accelerated during the subsequent adsorptions. The creep accelerating rates in the subsequent adsorptions decreased gradually.

Since much creep developed during the first adsorption, slower RH cycling yielded less panel creep before the first adsorption took place. It can be observed in Fig. 4.27 that the creep curve of test V14 is lowest in the early stage. The curve begins crossing the creep curves of all other tests during the first adsorption, and later on, the overall creep rate is also larger than that for the other tests. Therefore, the curve becomes the highest among the four cyclic tests.

In addition, it is found in Table 4.30 that in cyclic RH environment, the thinner panels (9.5 mm) tend to creep more than the thicker panels (15.9 mm) in cyclic RH tests. The creep difference caused by panel thickness is clearly showed in Fig. 4.29.

Because of the time limitation, all the creep test series - except test V14 (14 days/cycle) - were creep tested for only 6 weeks. The long-term creep behavior of wood panels was observed up to about 6 months (25 weeks) in test V14. The fractional deflections vs. time curve for the OSB panels are plotted in Fig. 4.30 for the entire creep test duration in test V14; and the curves for the plywood are plotted in Fig. 4.31. After the creep test was conducted for about 10^5 minutes, the panels' deflection was measured once in each RH duration. The readings were usually taken when the RH was about to change to the next RH level. In Fig. 4.30, the up and down changes in the creep curve correspond to adsorptive and desorptive processes, respectively.

All of the OSB panels in test V14 developed very large deflections after 25 weeks, as Table 4.30 shows. The fractional deflection after 25 weeks was up to 5.94 and 4.87 for 9.5 mm and 15.9 mm parallel OSB panels, respectively. One 9.5 mm perpendicular OSB panel fell on floor due to excessive creep deflection during the 8th week, and another two fell during the 12th and 13th weeks. The 9.5 mm perpendicular OSB panels all fell before the last week of the 25 week creep test duration.

4.4.2.2 Creep Recovery of Cyclic RH Tests

The instantaneous fractional deflection recovery for cyclic RH tests is shown in Table 4.31. The recovery of 9.5 mm perpendicular OSB panels was not available for test V14 since all four of those panels fell on the floor during the test.

In this table, the most instantaneous fractional deflection recovery of the four cyclic RH tests is around 1.00. Although the values for cyclic tests are generally larger than those of the constant RH tests, the absolute differences are very small.

Panel recoveries are different in cyclic RH tests. The recovery curves in Fig. 4.27 shows the different recovery rates. The 3 day recovery data shows that the slowest RH

cycling (test V7) gave the most recovery among the three RH tests (V1, V2, and V7), but the differences between each recovery are not big. Further, the panels of test V7 still have the most irrecovered or permanent deflection, even though their recovery is the largest among the three tests in the first 3 days.

As is summarized in Table 4.32, the remaining fractional deflection (most are irrecoverable) is about 1 and 4 times of the instantaneous deflection for the OSB in test V1 and V4, respectively. However, the plywood has much less irrecoverable deformation compared with the OSB.

4.4.3 Uncontrolled Indoor Environment Tests

The indoor environment changes during the four seasons, and is also different from day to night, but those changes are very gentle when compared with cyclic RH changes. As shown in Table 4.30, the fractional deflections of panels in indoor environments are obviously less than those of the cyclic RH environment and the 85% constant RH tests. The panel creep in the indoor environment is close to that of tests C35 and C65.

The fractional deflection vs. time curves for all type of the panel in three indoor environment tests are plotted in Fig. 4.19 to Fig. 4.25. The creep curves are relatively smooth compared to the creep curves of the cyclic conditions in Fig. 4.27. The creep curve difference among the three indoor tests is attributed to the indoor climatic changes of the seasons.

The instantaneous fractional deflection recovery upon unloading for three indoor environment tests are listed in Table 4.31. The values are very close to 1.00; for OSB panels, they are between 0.96 and 1.01. The recovery within the first 3 days was also less than that of cyclic or 85% constant RH tests.

Table 4.1 MSR Test Results for the Panel in Test Series C35 and I1

Materials	Measured Thickness(mm)	Number of Specimens		MOE(GPa) Parallel [a]	MOE(GPa) Perpendicular [b]
OSB	10.5	2 x 16 [d]	Mean	6.61	2.60
			COV [c]	4.9%	8.0%
	16.7	2 x 16	Mean	6.27	2.70
			COV	2.6%	3.9%
Plywood	9.6	2 x 8 [d]	Mean	8.73	0.52
			COV	6.0%	10.7%
	15.4	2 x 8	Mean	7.46	2.35
			COV	4.1%	3.6%

[a] Parallel refers to specimen cut according to cut plan shown in Fig. 3.1a.

[b] Perpendicular refers to specimen cut according to cut plan shown in Fig. 3.1b.

[c] COV = coefficient of variation = standard deviation / mean x 100%.

[d] 16 or 8 specimens in each strand orientation.

Table 4.2 MSR Test Results for the Panel in Test Series C65

Materials	Measured Thickness(mm)	Number of Specimens		MOE(GPa) Parallel [a]	MOE(GPa) Perpendicular [b]
OSB	10.4	2 x 8 [d]	Mean	6.72	2.59
			COV [c]	5.9%	3.7%
	16.9	2 x 8	Mean	6.59	2.82
			COV	5.3%	4.2%
Plywood [e]	9.6	2 x 8	Mean	9.16	0.59
			COV	3.9%	24.5%
	15.4	2 x 8	Mean	7.80	2.26
			COV	2.2%	6.7%

[a] Parallel refers to specimen cut according to cut plan shown in Fig. 3.1a.

[b] Perpendicular refers to specimen cut according to cut plan shown in Fig. 3.1b.

[c] COV = coefficient of variation = standard deviation / mean x 100%.

[d] 8 specimens in each strand orientation.

[e] Plywood panels in creep test V14 were also from this batch.

Table 4.3 MSR Test Results for the Panel in Test Series C85

Materials	Measured Thickness(mm)	Number of Specimens		MOE(GPa) Parallel [a]	MOE(GPa) Perpendicular [b]
OSB	10.2	2 x 8 [d]	Mean	6.49	2.60
			COV [c]	7.3%	4.2%
	16.9	2 x 8	Mean	6.36	2.55
			COV	4.2%	4.4%
Plywood	9.7	2 x 8	Mean	8.86	0.64
			COV	5.8%	18.6%
	15.6	2 x 8	Mean	7.63	2.44
			COV	4.1%	4.8%

[a] Parallel refers to specimen cut according to cut plan shown in Fig. 3.1a.

[b] Perpendicular refers to specimen cut according to cut plan shown in Fig. 3.1b.

[c] COV = coefficient of variation = standard deviation / mean x 100%.

[d] 8 specimens in each strand orientation.

Table 4.4 MSR Test Results for the Panel in Test Series V1 and I2

Materials	Measured Thickness(mm)	Number of Specimens		MOE(GPa) Parallel [a]	MOE(GPa) Perpendicular [b]
OSB	10.7	2 x 16 [d]	Mean	5.28	2.11
			COV [c]	4.6%	5.1%
	17.3	2 x 16	Mean	5.41	2.24
			COV	6.2%	4.1%
Plywood	10.1	2 x 8 [d]	Mean	5.71	0.42
			COV	8.4%	21.5%
	15.8	2 x 8	Mean	6.63	2.12
			COV	4.22%	9.9%

[a] Parallel refers to specimen cut according to cut plan shown in Fig. 3.1a.

[b] Perpendicular refers to specimen cut according to cut plan shown in Fig. 3.1b.

[c] COV = coefficient of variation = standard deviation / mean x 100%.

[d] 16 or 8 specimens in each strand orientation.

Table 4.5 MSR Test Results for the Panel in Test Series V2 and I3

Materials	Measured Thickness(mm)	Number of Specimens		MOE(GPa) Parallel [a]	MOE(GPa) Perpendicular [b]
OSB	10.4	2 x 16 [d]	Mean	6.97	2.74
			COV [c]	5.3%	6.9%
	17.0	2 x 16	Mean	6.65	2.75
			COV	4.1%	2.5%
Plywood	9.5	2 x 8 [d]	Mean	8.03	0.58
			COV	10.5%	11.7%
	15.5	2 x 8	Mean	6.57	2.39
			COV	13.3%	10.0%

[a] Parallel refers to specimen cut according to cut plan shown in Fig. 3.1a.

[b] Perpendicular refers to specimen cut according to cut plan shown in Fig. 3.1b.

[c] COV = coefficient of variation = standard deviation / mean x 100%.

[d] 16 or 8 specimens in each strand orientation.

Table 4.6 MSR Test Results for the Panel in Test Series V7

Materials	Measured Thickness(mm)	Number of Specimens		MOE(GPa) Parallel [a]	MOE(GPa) Perpendicular [b]
OSB	10.2	2 x 8 [d]	Mean	6.87	2.70
			COV [c]	4.2%	4.0%
	17.2	2 x 8	Mean	6.52	2.70
			COV	4.9%	3.9%
Plywood	9.6	2 x 8	Mean	7.51	0.54
			COV	2.6%	19.2%
	15.3	2 x 8	Mean	7.55	2.23
			COV	2.8%	7.5%

[a] Parallel refers to specimen cut according to cut plan shown in Fig. 3.1a.

[b] Perpendicular refers to specimen cut according to cut plan shown in Fig. 3.1b.

[c] COV = coefficient of variation = standard deviation / mean x 100%.

[d] 8 specimens in each strand orientation.

Table 4.7 MSR Test Results for the Panel in Test Series V14

Materials [e]	Measured Thickness(mm)	Number of Specimens		MOE(GPa) Parallel [a]	MOE(GPa) Perpendicular [b]
OSB	10.2	2 x 8 [d]	Mean	6.89	2.61
			COV [c]	6.8%	5.2%
	17.2	2 x 8	Mean	6.83	2.78
			COV	2.6%	2.9%

[a] Parallel refers to specimen cut according to cut plan shown in Fig. 3.1a.

[b] Perpendicular refers to specimen cut according to cut plan shown in Fig. 3.1b.

[c] COV = coefficient of variation = standard deviation / mean x 100%.

[d] 8 specimens in each strand orientation.

[e] MOE results for plywood panels in test series V14 are shown in Table 4.2.

Table 4.8 Summary of Modulus of Elasticity of the Test Panel

Materials	Nominal Thickness(mm)		Number of Specimens	MOE(GPa) Mean	MOE(GPa) COV [c]
OSB	9.5	Parallel [a]	80	6.47	11.1%
		Perpendicular [b]	80	2.54	10.6%
	15.9	Parallel	80	6.29	8.7%
		Perpendicular	80	2.57	9.1%
Plywood	9.5	Parallel	48	8.00	16.1%
		Perpendicular	48	0.55	22.4%
	15.9	Parallel	48	7.27	9.0%
		Perpendicular	48	2.30	8.8%

[a] Parallel refers to specimen cut according to cut plan shown in Fig. 3.1a.

[b] Perpendicular refers to specimen cut according to cut plan shown in Fig. 3.1b.

[c] COV = coefficient of variation = standard deviation / mean x 100%.

Table 4.9 Post Flexure Test Results for Test Series C35 and I1

Materials	Nominal Thickness(mm)		Number of Specimens	MOR(MPa) Mean	MOR(MPa) COV [c]
OSB	9.5	Parallel [a]	6	21.96	6.2%
		Perpendicular [b]	6	15.69	6.7%
	15.9	Parallel	6	22.74	3.0%
		Perpendicular	6	15.94	3.1%
Plywood	9.5	Parallel	2	47.94	-
		Perpendicular	2	-	-
	15.9	Parallel	2	36.75	-
		Perpendicular	2	15.62	-

[a] Parallel refers to specimen cut according to cut plan shown in Fig. 3.1a.

[b] Perpendicular refers to specimen cut according to cut plan shown in Fig. 3.1b.

[c] COV = coefficient of variation = standard deviation / mean x 100%.

Table 4.10 Post Flexure Test Results for Test Series Other than C35 and I1

Materials	Nominal Thickness(mm)		Number of Specimens	MOR(MPa) Mean	MOR(MPa) COV [c]
OSB	9.5	Parallel [a]	8	21.62	14.8%
		Perpendicular [b]	8	15.35	10.1%
	15.9	Parallel	7 [d]	23.11	11.8%
		Perpendicular	8	14.06	7.9%
Plywood	9.5	Parallel	5	40.53	22.5%
		Perpendicular	5	-	-
	15.9	Parallel	5	35.48	9.4%
		Perpendicular	5	16.56	22.6%

[a] Parallel refers to specimen cut according to cut plan shown in Fig. 3.1a.

[b] Perpendicular refers to specimen cut according to cut plan shown in Fig. 3.1b.

[c] COV = coefficient of variation = standard deviation / mean x 100%.

[d] Due to mistake during the post flexure test, one panel's MOR was missed. The actual tested panel number was 7 for this group.

Table 4.11 Summary of the Panel Short-term Bending Strength

Materials	Nominal Thickness(mm)		Number of Specimens	MOR(MPa) Mean	MOR(MPa) COV [c]
OSB	9.5	Parallel [a]	14	21.77	12.3%
		Perpendicular [b]	14	15.50	8.8%
	15.9	Parallel	13	22.94	9.3%
		Perpendicular	14	14.87	8.7%
Plywood	9.5	Parallel	7	42.65	21.2%
		Perpendicular	7	-	-
	15.9	Parallel	7	35.84	8.8%
		Perpendicular	7	16.29	21.2%

[a] Parallel refers to specimen cut according to cut plan shown in Fig. 3.1a.

[b] Perpendicular refers to specimen cut according to cut plan shown in Fig. 3.1b.

[c] COV = coefficient of variation = standard deviation / mean x 100%.

Table 4.12 The Measured Equilibrium MC of the Materials under 65% RH at 20 °C

Materials	Nominal Thickness(mm)	Number of Specimens	MC(%) Mean	MC(%) COV [c]
OSB [a]	9.5	16	9.2	4.7%
	15.9	16	9.5	4.2%
Plywood [b]	9.5	10	11.5	7.8%
	15.9	10	10.9	4.7%

[a] The population mean of the equilibrium MC under 65% RH at 20 °C for OSB is 9.4%.

[b] The population mean of the equilibrium MC under 65% RH at 20 °C for plywood is 11.2%.

[c] COV = coefficient of variation = standard deviation / mean x 100%; the degree of freedom = number of sample - 1.

Table 4.13 Equilibrium MC of the Material under 35, 65, and 85% RH at 20 °C

Materials	Nominal Thickness(mm)	MC(%) at 35% RH	MC(%) at 65% RH	MC(%) at 85% RH
OSB	9.5	7.1	9.2	16.1
	15.9	7.0	9.5	15.9
Plywood	9.5	6.5	11.5	18.6
	15.9	8.8	10.9	18.4

Table 4.14 Moisture Content and Thickness Swelling of the OSB and Plywood Panels in Constant RH Test C35

Time		Moisture Content (%) and Thickness Swelling (H/Ho)							
		OSB				Plywood			
		9.5 mm		15.9 mm		9.5 mm		15.9 mm	
(minutes)	(days)	MC	H/Ho	MC	H/Ho	MC	H/Ho	MC	H/Ho
0	0.0	9.4	1.00	9.4	1.00	11.2	1.00	11.2	1.00
1800	1.3	8.6	0.99	8.2	0.99	7.8	1.00	10.4	1.00
4630	3.2	8.1	0.98	8.1	0.99	7.2	0.99	9.7	1.00
11890	8.3	7.7	0.98	7.6	0.98	6.9	1.00	9.1	1.00
23480	16.3	7.4	0.00	7.4	0.00	6.7	0.99	8.9	0.99
51030	35.4	7.1	0.00	7.1	0.00	6.7	0.99	8.6	0.99
60550	42.0	7.1	0.97	7.0	0.98	6.5	0.98	8.8	0.99

Table 4.15 Moisture Content and Thickness Swelling of the OSB and Plywood Panels in Constant RH Test C85

Time		Moisture Content (%) and Thickness Swelling (H/Ho)							
		OSB				Plywood			
		9.5 mm		15.9 mm		9.5 mm		15.9 mm	
(minutes)	(days)	MC	H/Ho	MC	H/Ho	MC	H/Ho	MC	H/Ho
0.0	0.0	9.4	1.00	9.4	1.00	11.2	1.00	11.2	1.00
1690.0	1.2	11.2	1.01	10.4	1.00			12.7	1.00
4950.0	3.4	12.7	1.03	11.0	1.01	16.6	1.00	14.6	1.00
10350.0	7.2	14.1	1.05	11.8	1.02	18.5	1.00	16.4	1.01
20310.0	14.1	15.7	1.07	13.1	1.04	19.0	1.00	18.2	1.01
32100.0	22.3	15.8	1.08	14.3	1.05	18.6	0.99	18.1	1.02
42030.0	29.2	16.0	1.08	15.0	1.06	18.6	0.99	18.3	1.01
51960.0	36.1	16.0	1.08	15.5	1.07	18.6	0.99	18.3	1.01
60630.0	42.1	16.1	1.08	15.9	1.07	18.6	0.99	18.4	1.01

Table 4.16 Moisture Content and Thickness Swelling of the OSB and Plywood Panels in Cyclic RH Test V1

Time		Moisture Content (%) and Thickness Swelling (H/Ho)							
		OSB				Plywood			
		9.5 mm		15.9 mm		9.5 mm		15.9 mm	
(minutes)	(days)	MC	H/Ho	MC	H/Ho	MC	H/Ho	MC	H/Ho
0.0	0.0	9.4	1.000	9.4	1.000	11.2	1.00	11.2	1.00
4300.0	3.0	8.2	0.991	8.8	0.997	8.8	0.99	9.9	0.99
10080.0	7.0	8.0	0.991	8.8	0.997	8.5	0.99	9.9	0.99
19440.0	13.5	9.2	0.992	9.5	1.001	11.6	0.99	11.2	1.00
30240.0	21.0	7.9	0.985	8.8	0.996	8.4	0.99	9.8	0.99
39600.0	27.5	9.0	0.993	9.6	1.002	11.2	0.99	11.2	1.00
50390.0	35.0	7.8	0.985	8.8	0.997	8.3	0.98	9.7	0.99
60470.0	42.0	7.8	0.987	8.9	0.998	8.3	0.98	9.7	0.99

Table 4.17 Moisture Content and Thickness Swelling of the OSB and Plywood Panels in Cyclic RH Test V2

Time		Moisture Content (%) and Thickness Swelling (H/Ho)							
		OSB				Plywood			
		9.5 mm		15.9 mm		9.5 mm		15.9 mm	
(minutes)	(days)	MC	H/Ho	MC	H/Ho	MC	H/Ho	MC	H/Ho
0	0.0	9.4	1.00	9.4	1.00	11.2	1.00	11.2	1.00
1460	1.0	8.6	1.00	8.9	1.00	9.2	0.99	10.1	1.00
4335	3.0	8.5	0.99	8.9	1.00	9.4	0.99	10.1	1.00
10085	7.0	8.6	0.99	9.0	1.00	9.5	0.99	10.2	1.00
11535	8.0	10.0	1.00	10.0	1.00	12.8	1.00	12.1	1.00
15855	11.0	8.5	0.99	9.0	1.00	9.3	0.99	10.2	1.00
20175	14.0	10.1	1.00	10.0	1.00	13.0	1.00	12.3	1.00
30255	21.0	8.6	0.99	9.2	1.00	9.6	0.99	10.3	1.00
40335	28.0	10.1	1.00	10.3	1.01	13.3	1.00	12.4	1.00
50415	35.0	8.6	0.99	9.3	1.00	9.6	0.99	10.4	1.00
60470	42.0	10.2	1.00	10.3	1.01	13.4	1.00	12.5	1.00

Table 4.18 Moisture Content and Thickness Swelling of the OSB and Plywood Panels in Cyclic RH Test V7

Time		Moisture Content (%) and Thickness Swelling (H/Ho)							
		OSB				Plywood			
		9.5 mm		15.9 mm		9.5 mm		15.9 mm	
(minutes)	(days)	MC	H/Ho	MC	H/Ho	MC	H/Ho	MC	H/Ho
0	0.0	9.4	1.00	9.4	1.00	11.2	1.00	11.2	1.00
1483	1.0	8.7	0.99	8.9	1.00	9.7	0.99	10.2	0.99
5033	3.5	8.1	0.99	8.5	0.99	8.9	0.99	9.3	0.98
10093	7.0	10.9	1.01	10.4	1.01	14.9	1.00	13.4	1.02
20168	14.0	11.1	1.02	10.7	1.01	15.4	1.01	13.9	1.02
20893	14.5	9.8	1.01	9.8	1.01	11.9	1.00	11.8	1.00
30238	21.0	11.3	1.02	10.9	1.02	15.7	1.01	14.1	1.03
35283	24.5	8.7	1.00	9.1	1.00	9.6	0.99	9.9	0.99
41043	28.5	10.1	1.01	10.1	1.02	12.1	0.99	12.1	1.01
50403	35.0	11.6	1.02	11.2	1.02	15.8	1.01	14.4	1.03
51138	35.5	10.2	1.01	10.2	1.02	12.0	0.99	12.1	1.01
60478	42.0	11.5	1.02	11.2	1.02	15.8	1.01	14.5	1.03

Table 4.19 Moisture Content and Thickness Swelling of the OSB and Plywood Panels in Cyclic RH Test V14

Time		Moisture Content (%) and Thickness Swelling (H/Ho)							
		OSB				Plywood			
		9.5 mm		15.9 mm		9.5 mm		15.9 mm	
(minutes)	(days)	MC	H/Ho	MC	H/Ho	MC	H/Ho	MC	H/Ho
0.0	0.0	9.4	1.00	9.4	1.00	11.2	1.00	11.2	1.00
1470.0	1.0	8.7	1.00	9.0	1.00	9.5	1.00	9.8	1.00
5010.0	3.5	8.2	0.99	8.6	0.99	8.8	0.99	9.1	0.99
10090.0	7.0	7.9	0.99	8.3	0.99	8.8	0.99	8.8	0.99
20160.0	14.0	12.1	1.02	11.6	1.02	17.1	1.01	14.5	1.01
30240.0	21.0	8.4	1.00	8.9	1.00	9.3	0.99	9.3	0.99
40320.0	28.0	12.8	1.03	12.1	1.03	17.4	1.01	15.5	1.01
50400.0	35.0	8.7	1.01	9.2	1.01	9.4	0.98	9.5	0.99
60480.0	42.0	12.9	1.04	12.4	1.04	17.8	1.00	15.9	1.01
70560.0	49.0	8.8	1.01	9.5	1.02	9.6	0.98	9.6	0.99
90720.0	63.0	8.9	1.02	9.6	1.02	9.5	0.98	9.7	0.99
100800.0	70.0	12.9	1.05	12.7	1.04	17.9	1.00	16.1	1.01
120960.0	84.0	13.1	1.05	12.9	1.05	17.9	1.00	16.2	1.01
131040.0	91.0	9.0	1.02	9.7	1.02	9.6	0.98	9.8	0.99
151200.0	105.0	9.0	1.02	9.8	1.03	9.6	0.98	9.8	0.99
221760.0	154.0	13.2	1.04	12.9	1.05	17.5	1.00	16.2	1.01
252000.0	175.0	9.1	1.03	8.7	1.03	10.0	0.98	9.0	1.00

Table 4.20 Moisture Content and Thickness Swelling of the OSB and Plywood Panels in Indoor Test I1

Time		Moisture Content (%) and Thickness Swelling (H/Ho)							
		OSB				Plywood			
		9.5 mm		15.9 mm		9.5 mm		15.9 mm	
(minutes)	(days)	MC	H/Ho	MC	H/Ho	MC	H/Ho	MC	H/Ho
0	0.0	9.4	1.00	9.4	1.00	11.2	1.00	11.2	1.00
4984	3.5	7.1	0.98	8.4	0.99	6.6	0.98	9.6	0.99
12134	8.0	6.0	-	7.6	0.98	5.7	0.98	8.4	0.98
19134	13.0	5.5	-	7.1	-	5.4	-	7.9	-
31680	22.0	5.3	-	6.8	-	5.7	-	7.7	-
37440	26.0	5.2	-	6.7	-	5.6	-	7.6	-
46080	32.0	5.0	-	6.5	-	5.4	-	7.5	-
56160	39.0	5.2	0.96	6.6	0.97	5.6	0.98	7.6	0.98
60480	42.0	4.9	0.96	6.4	0.97	5.2	0.97	7.4	1.04
70560	49.0	4.5	0.96	6.0	0.97	4.7	0.97	6.9	0.98
79200	55.0	4.6	0.96	6.1	0.97	5.0	0.97	7.0	0.93
89280	62.0	4.6	0.95	5.9	0.97	5.0	0.97	7.0	0.98
100800	70.0	4.8	3.29	6.2	0.97	5.5	0.97	7.3	0.98
110880	77.0	5.0	0.96	6.2	0.97	5.6	0.97	7.4	0.98
120960	84.0	5.3	0.96	6.4	0.96	6.1	0.97	7.8	0.98

Table 4.21 Moisture Content and Thickness Swelling of the OSB and Plywood Panels in Indoor Test I2

Time		Moisture Content (%) and Thickness Swelling (H/Ho)							
		OSB				Plywood			
		9.5 mm		15.9 mm		9.5 mm		15.9 mm	
(minutes)	(days)	MC	H/Ho	MC	H/Ho	MC	H/Ho	MC	H/Ho
0	0.0	9.4	1.00	9.4	1.00	11.2	1.00	11.2	1.00
3810	2.6	6.3	0.97	7.9	0.97	4.8	0.96	8.4	0.96
12960	9.0	5.2	0.96	7.0	0.96	3.9	0.95	7.2	0.96
23040	16.0	4.1	0.95	6.1	0.95	2.9	0.95	6.2	0.96
32970	22.9	4.7	0.96	6.4	0.96	4.3	0.95	7.1	0.96
38880	27.0	4.9	0.96	6.5	0.96	4.4	0.95	7.2	0.96
53250	37.0	5.0	0.96	6.5	0.96	4.5	0.95	7.3	0.96
64250	44.6	4.8	0.95	6.4	0.96	4.1	0.95	7.2	0.96
74145	51.5	5.3	0.96	6.8	0.96	5.1	0.95	7.7	0.96
84600	58.8	5.3	0.96	6.9	0.96	5.0	0.95	7.7	0.96
91950	63.9	5.6	0.96	7.0	0.96	5.3	0.95	8.0	0.96
105090	73.0	6.5	0.96	7.8	0.96	6.6	0.95	9.0	0.96
115140	80.0	6.0	0.96	7.5	0.96	5.6	0.95	8.4	0.96
123140	85.5	6.6	0.96	7.9	0.96	6.7	0.95	9.1	0.96

Table 4.22 Moisture Content and Thickness Swelling of the OSB and Plywood Panels in Indoor Test I3

Time		Moisture Content (%) and Thickness Swelling (H/Ho)							
		OSB				Plywood			
		9.5 mm		15.9 mm		9.5 mm		15.9 mm	
(minutes)	(days)	MC	H/Ho	MC	H/Ho	MC	H/Ho	MC	H/Ho
0	0.0	9.4	1.00	9.4	1.00	11.2	1.00	11.2	1.00
1425	1.0	9.0	1.00	9.1	1.00	10.2	1.00	10.6	1.00
5380	3.7	8.4	0.99	8.8	1.00	9.1	0.99	9.8	0.99
11130	7.7	8.1	0.99	8.6	0.99	9.0	0.99	9.6	0.99
21220	14.7	7.4	0.99	8.0	0.99	8.0	0.99	8.7	0.99
31300	21.7	7.2	0.98	7.9	0.99	8.0	0.99	8.6	0.99
39940	27.7	6.7	0.98	7.5	0.99	7.3	0.98	8.1	0.99
51460	35.7	6.5	0.98	7.3	0.98	7.2	0.98	7.9	0.99
61580	42.8	6.4	0.98	7.2	0.98	7.3	0.98	7.9	0.99
71930	50.0	5.7	0.97	6.7	0.98	6.1	0.98	7.1	0.99
82250	57.1	5.2	0.97	6.2	0.98	5.4	0.98	6.4	0.98
92290	64.1	5.2	0.97	6.2	0.98	5.9	0.98	6.6	0.98
102290	71.0	5.5	0.97	6.3	0.98	6.4	0.98	6.9	0.99
112180	77.9	5.3	0.97	6.2	0.97	6.0	0.98	6.7	0.98
122220	84.9	5.1	0.97	5.9	0.97	5.5	0.98	6.4	0.98

Table 4.23 Fractional Deflection of the 9.5 mm Parallel OSB Panels under the Sustained Moment (20% of M_{max})

(MOE = 6.47 GPa from Table 4.8)

	Fractional Deflection									
	OSB Parallel 9.5mm									
Time	C35	C65	C85	V1	V2	V7	V14	I1	I2	I3
1 min	1.00	1.00	1.00	1.00	1.00	1.00	1.00	1.00	1.00	1.00
10 min	1.04	1.03	1.03	1.05	1.04	1.04	1.03	1.04	1.04	1.03
100 mins	1.11	1.07	1.11	1.17	1.12	1.11	1.11	1.11	1.12	1.08
1 day	1.37	1.13	1.57	1.51	1.29	1.29	1.26	1.36	1.37	1.21
3 days	1.48	1.19	2.23	1.83	1.53	1.46	1.39	1.49	1.55	1.31
1 week	1.57	1.22	2.74	2.05	1.80	2.33	1.48	1.63	1.66	1.38
2 weeks	1.65	1.28	3.17	2.23	2.16	2.80	3.05	1.72	1.82	1.55
3 weeks	1.71	1.32	3.42	2.34	2.28	3.13	3.33	1.81	1.92	1.61
4 weeks	1.74	1.35	3.56	2.41	2.47	3.34	3.70	1.81	1.95	1.66
5 weeks	1.76	1.38	3.64	2.47	2.50	3.53	3.95	1.84	1.98	1.70
6 weeks	1.78	1.41	3.71	2.52	2.63	3.69	4.15	1.84	2.00	1.73
12 weeks	-	-	-	-	-	-	5.02	1.82	2.25	1.93

Table 4.24 Fractional Deflection of the 9.5 mm Perpendicular OSB Panels under the Sustained Moment (20% of M_{max})

(MOE = 2.54 GPa from Table 4.8)

	Fractional Deflection									
	OSB Perpendicular 9.5mm									
Time	C35	C65	C85	V1	V2	V7	V14	I1	I2	I3
1 min	1.00	1.00	1.00	1.00	1.00	1.00	1.00	1.00	1.00	1.00
10 min	1.05	1.04	1.05	1.07	1.05	1.05	1.04	1.05	1.06	1.04
100 mins	1.15	1.11	1.14	1.20	1.14	1.14	1.12	1.13	1.14	1.12
1 day	1.46	1.23	1.57	1.54	1.33	1.35	1.28	1.41	1.42	1.27
3 days	1.65	1.38	2.25	1.81	1.63	1.56	1.45	1.57	1.66	1.41
1 week	1.78	1.50	2.94	2.04	1.91	2.30	1.58	1.79	1.79	1.44
2 weeks	1.93	1.67	3.70	2.23	2.28	2.79	2.92	1.93	2.00	1.72
3 weeks	2.01	1.79	4.19	2.35	2.46	3.20	3.25	2.05	2.13	1.79
4 weeks	2.06	1.88	4.51	2.42	2.64	3.44	3.66	2.08	2.18	1.86
5 weeks	2.09	1.95	4.81	2.49	2.71	3.66	3.93	2.12	2.21	1.92
6 weeks	2.11	2.02	4.93	2.55	2.81	3.84	4.18	2.12	2.23	1.98
12 weeks	-	-	-	-	-	-	5.12	2.12	2.49	2.21

Table 4.25 Fractional Deflection of the 15.9 mm Parallel OSB Panels under the Sustained Moment (20% of M_{max})

(MOE = 6.29 GPa from Table 4.8)

	Fractional Deflection									
	OSB Parallel 15.9mm									
Time	C35	C65	C85	V1	V2	V7	V14	I1	I2	I3
1 min	1.00	1.00	1.00	1.00	1.00	1.00	1.00	1.00	1.00	1.00
10 min	1.04	1.04	1.03	1.04	1.04	1.03	1.03	1.03	1.04	1.06
100 mins	1.14	1.08	1.09	1.14	1.11	1.09	1.08	1.09	1.10	1.08
1 day	1.32	1.21	1.58	1.44	1.26	1.22	1.17	1.30	1.30	1.18
3 days	1.39	1.35	2.21	1.67	1.51	1.37	1.28	1.42	1.46	1.26
1 week	1.47	1.47	2.70	1.86	1.79	2.11	1.36	1.55	1.55	1.33
2 weeks	1.54	1.64	3.08	2.02	2.16	2.51	2.84	1.64	1.69	1.45
3 weeks	1.61	1.73	3.31	2.10	2.26	2.73	2.98	1.75	1.79	1.50
4 weeks	1.65	1.82	3.44	2.16	2.46	2.95	3.47	1.76	1.83	1.53
5 weeks	1.66	1.87	3.53	2.21	2.46	3.09	3.57	1.79	1.84	1.57
6 weeks	1.68	1.93	3.58	2.25	2.61	3.22	3.82	1.79	1.89	1.60
12 weeks	-	-	-	-	-	-	4.38	1.89	2.14	1.74

Table 4.26 Fractional Deflection of the 15.9 mm Perpendicular OSB Panels under the Sustained Moment (20% of M_{max})

(MOE = 2.57 GPa from Table 4.8)

	Fractional Deflection									
	OSB Perpendicular 15.9mm									
Time	C35	C65	C85	V1	V2	V7	V14	I1	I2	I3
1 min	1.00	1.00	1.00	1.00	1.00	1.00	1.00	1.00	1.00	1.00
10 min	1.05	1.04	1.04	1.05	1.06	1.04	1.05	1.05	1.05	1.03
100 mins	1.14	1.11	1.12	1.15	1.15	1.12	1.12	1.12	1.12	1.09
1 day	1.37	1.26	1.56	1.43	1.33	1.30	1.28	1.34	1.34	1.22
3 days	1.47	1.41	2.14	1.62	1.58	1.48	1.43	1.47	1.51	1.33
1 week	1.56	1.54	2.72	1.79	1.83	2.09	1.54	1.62	1.62	1.42
2 weeks	1.66	1.73	3.31	1.96	2.20	2.49	2.73	1.74	1.79	1.56
3 weeks	1.74	1.86	3.74	2.05	2.32	2.74	3.03	1.88	1.92	1.62
4 weeks	1.78	1.95	3.97	2.12	2.51	2.96	3.37	1.90	1.95	1.67
5 weeks	1.80	2.03	4.17	2.18	2.53	3.12	3.59	1.96	1.97	1.73
6 weeks	1.83	2.10	4.28	2.24	2.69	3.26	3.78	1.96	2.00	1.79
12 weeks	-	-	-	-	-	-	4.52	2.10	2.20	1.96

Table 4.27 Fractional Deflection of the 9.5 mm Parallel Plywood Panels under the Sustained Moment (20% of M_{max})

(MOE = 8.00 GPa from Table 4.8)

	Fractional Deflection									
	Plywood Parallel 9.5mm									
Time	C35	C65	C85	V1	V2	V7	V14	I1	I2	I3
1 min	1.00	1.00	1.00	1.00	1.00	1.00	1.00	1.00	1.00	1.00
10 min	1.05	1.01	1.01	1.04	1.03	1.02	1.02	1.04	1.02	1.01
100 mins	1.09	1.04	1.05	1.17	1.08	1.09	1.06	1.08	1.06	1.04
1 day	1.17	1.07	1.32	1.41	1.17	1.26	1.16	1.22	1.19	1.09
3 days	1.17	1.10	1.57	1.63	1.32	1.35	1.22	1.24	1.28	1.12
1 week	1.18	1.12	1.67	1.77	1.47	1.68	1.24	1.26	1.32	1.13
2 weeks	1.19	1.14	1.77	1.89	1.68	1.89	1.74	1.28	1.41	1.15
3 weeks	1.20	1.16	1.82	1.96	1.70	2.21	1.99	1.31	1.44	1.16
4 weeks	1.21	1.17	1.84	2.02	1.82	2.15	1.99	1.31	1.46	1.16
5 weeks	1.21	1.18	1.86	2.06	1.81	2.28	2.25	1.32	1.47	1.17
6 weeks	1.21	1.19	1.87	2.08	1.89	2.36	2.19	1.31	1.50	1.17
12 weeks	-	-	-	-	-	-	2.68	1.34	1.58	1.18

Table 4.28 Fractional Deflection of the 15.9 mm Parallel Plywood Panels under the Sustained Moment (20% of M_{max})

(MOE = 7.27 GPa from Table 4.8)

	Fractional Deflection									
	Plywood Parallel 15.9mm									
Time	C35	C65	C85	V1	V2	V7	V14	I1	I2	I3
1 min	1.00	1.00	1.00	1.00	1.00	1.00	1.00	1.00	1.00	1.00
10 min	1.02	1.01	1.00	1.02	1.02	1.02	1.01	1.02	1.01	1.02
100 mins	1.06	1.02	1.03	1.08	1.06	1.05	1.03	1.06	1.04	1.06
1 day	1.20	1.06	1.19	1.17	1.13	1.09	1.09	1.25	1.11	1.13
3 days	1.24	1.08	1.40	1.28	1.23	1.12	1.15	1.34	1.15	1.18
1 week	1.27	1.11	1.56	1.34	1.34	1.64	1.19	1.43	1.16	1.21
2 weeks	1.31	1.14	1.69	1.39	1.42	1.79	1.48	1.50	1.19	1.30
3 weeks	1.33	1.15	1.77	1.42	1.51	1.79	1.63	1.50	1.22	1.31
4 weeks	1.34	1.16	1.81	1.45	1.51	1.93	1.56	1.51	1.23	1.35
5 weeks	1.34	1.18	1.84	1.46	1.58	1.97	1.72	1.52	1.24	1.37
6 weeks	1.35	1.18	1.85	1.45	1.56	1.99	1.61	1.53	1.25	1.38
12 weeks	-	-	-	-	-	-	1.70	1.51	1.37	1.49

Table 4.29 Fractional Deflection of the 15.9 mm Perpendicular Plywood Panels under the Sustained Moment (20% of M_{max})

(MOE = 2.30 GPa from Table 4.8)

	Fractional Deflection									
	Plywood Perpendicular 15.9mm									
Time	C35	C65	C85	V1	V2	V7	V14	I1	I2	I3
1 min	1.00	1.00	1.00	1.00	1.00	1.00	1.00	1.00	1.00	1.00
10 min	1.02	1.02	1.02	1.02	1.02	1.02	1.02	1.02	1.02	1.02
100 mins	1.06	1.05	1.06	1.06	1.07	1.05	1.06	1.07	1.07	1.05
1 day	1.19	1.10	1.24	1.19	1.21	1.15	1.17	1.23	1.19	1.13
3 days	1.24	1.15	1.49	1.25	1.27	1.28	1.28	1.32	1.26	1.18
1 week	1.28	1.19	1.68	1.29	1.34	1.51	1.32	1.40	1.30	1.21
2 weeks	1.32	1.23	1.81	1.35	1.44	1.63	1.56	1.48	1.34	1.28
3 weeks	1.34	1.26	1.87	1.36	1.48	1.66	1.94	1.45	1.41	1.29
4 weeks	1.35	1.28	1.91	1.38	1.52	1.75	1.75	1.45	1.40	1.32
5 weeks	1.35	1.30	1.94	1.40	1.54	1.80	1.98	1.45	1.40	1.32
6 weeks	1.35	1.31	1.95	1.39	1.53	1.81	1.88	1.48	1.41	1.34
12 weeks	-	-	-	-	-	-	2.13	1.43	1.52	1.40

Table 4.30 Summary of Fractional Deflection of the Panel after Six Weeks of Sustained Loadings

	OSB				Plywood		
	9.5 mm		15.9 mm		9.5 mm	15.9 mm	
Test ID	Para.	Perpen.	Para.	Perpen.	Para.	Para.	Perpen.
C35	1.78	2.11	1.68	1.83	1.21	1.35	1.35
C65	1.41	2.02	1.93	2.10	1.19	1.18	1.31
C85	3.71	4.93	3.58	4.28	1.87	1.85	1.95
V1	2.52	2.55	2.25	2.24	2.08	1.45	1.39
V2	2.63	2.81	2.61	2.69	1.89	1.56	1.53
V7	3.69	3.84	3.22	3.26	2.36	1.99	1.81
V14	4.15	4.18	3.82	3.78	2.19	1.61	1.88
	(5.94)[a]	(-)	(4.87)	(5.30)	(3.31)	(1.99)	(2.85)
I1	1.84	2.12	1.79	1.96	1.31	1.53	1.48
I2	2.00	2.23	1.89	2.00	1.50	1.25	1.41
I3	1.73	1.98	1.60	1.79	1.17	1.38	1.34

[a] The values in brackets are the fractional deflections of the panels in test V14 after 25 weeks of sustained loadings.

Table 4.31 Summary of the Instantaneous Fractional Deflection Recovery

	OSB				Plywood		
	9.5 mm		15.9 mm		9.5 mm	15.9 mm	
Test ID	Para.	Perpen.	Para.	Perpen.	Para.	Para.	Perpen.
C35	0.98	0.96	0.99	0.97	0.95	0.98	0.98
C65	0.99	0.98	0.99	0.98	0.99	0.99	0.98
C85	0.92	1.09	0.94	0.98	1.01	0.99	1.02
V1	1.00	0.98	0.97	0.98	1.01	0.99	0.98
V2	1.02	1.02	1.02	1.04	1.07	1.03	1.03
V7	1.04	1.09	1.06	1.04	1.08	1.02	1.03
V14	1.00	-	0.96	0.96	1.04	1.05	1.08
I1	0.98	0.98	0.98	0.99	0.95	0.98	0.97
I2	1.00	0.98	1.01	0.97	0.99	1.00	1.02
I3	0.97	0.96	0.98	0.97	1.00	0.98	0.99

Table 4.32 Summary of the Remaining Fractional Deflection after Unloading and Three Day Recovery

	OSB				Plywood		
	9.5 mm		15.9 mm		9.5 mm	15.9 mm	
Test ID	Para.	Perpen.	Para.	Perpen.	Para.	Para.	Perpen.
C35	0.66	0.96	0.55	0.68	0.19	0.31	0.29
C65	0.29	0.83	0.76	0.88	0.14	0.14	0.23
C85	2.50	3.36	2.30	2.81	0.74	0.72	0.74
V1	1.15	1.17	0.88	0.93	0.68	0.29	0.28
V2	1.16	1.30	1.14	1.21	0.46	0.38	0.34
V7	2.06	2.13	1.62	1.64	1.02	0.57	0.51
V14	3.99	-	3.23	3.59	1.32	0.48	0.84
I1	0.79	0.98	0.72	0.94	0.30	0.47	0.38
I2	0.96	1.16	0.84	0.88	0.41	0.25	0.34
I3	0.76	1.00	0.57	0.76	0.07	0.44	0.32

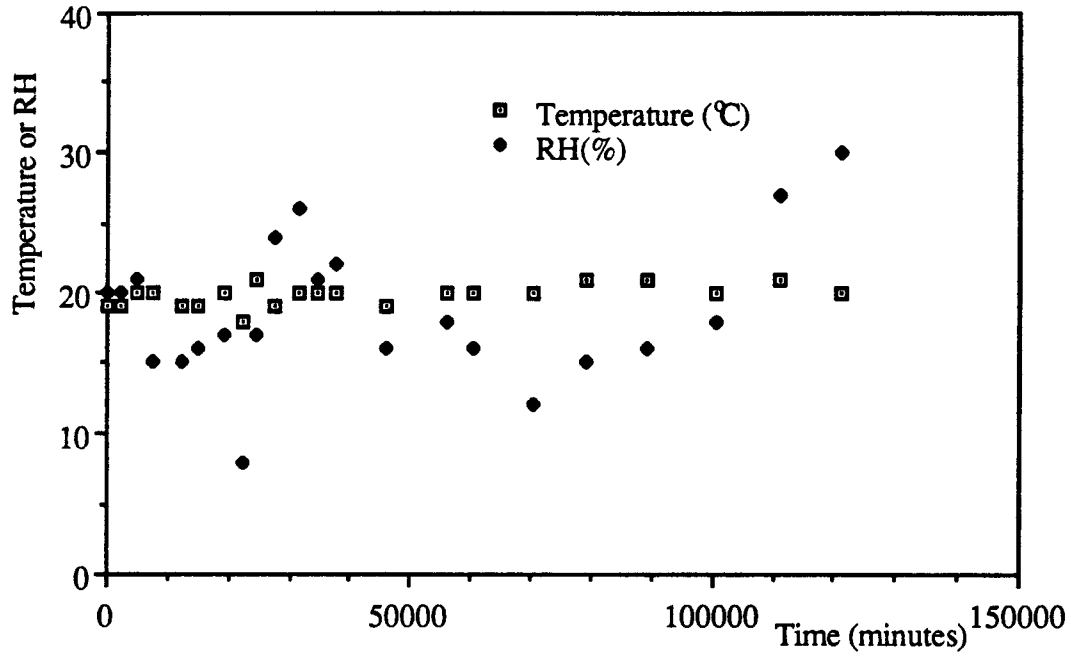

Fig. 4.1 The Environmental Record for Indoor Creep Test I1

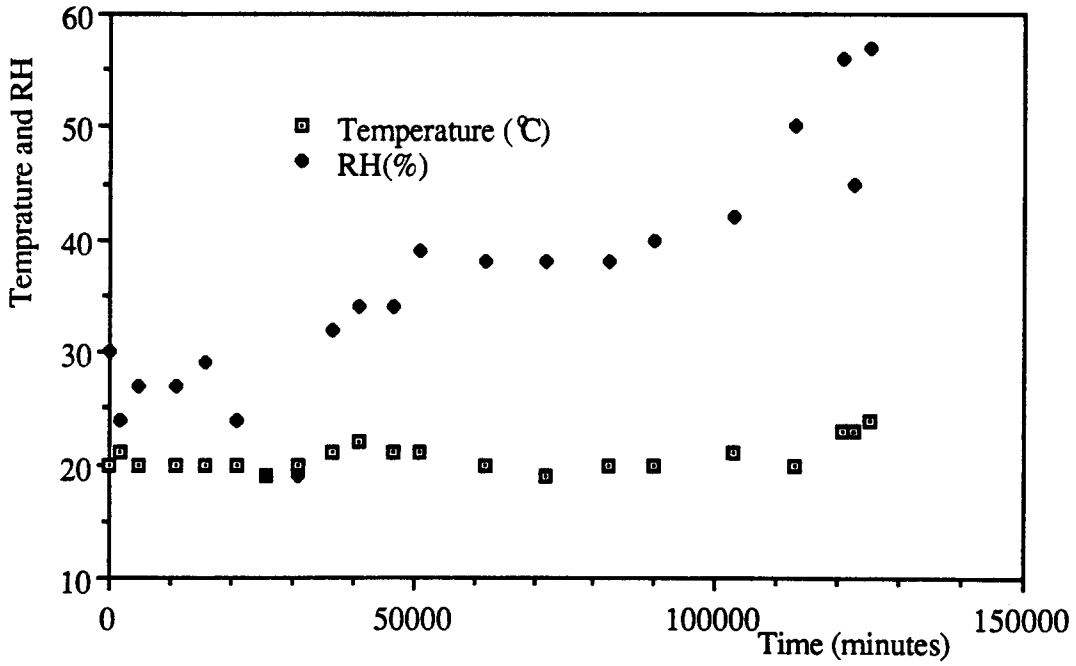

Fig. 4.2 The Environmental Record for Indoor Creep Test I2

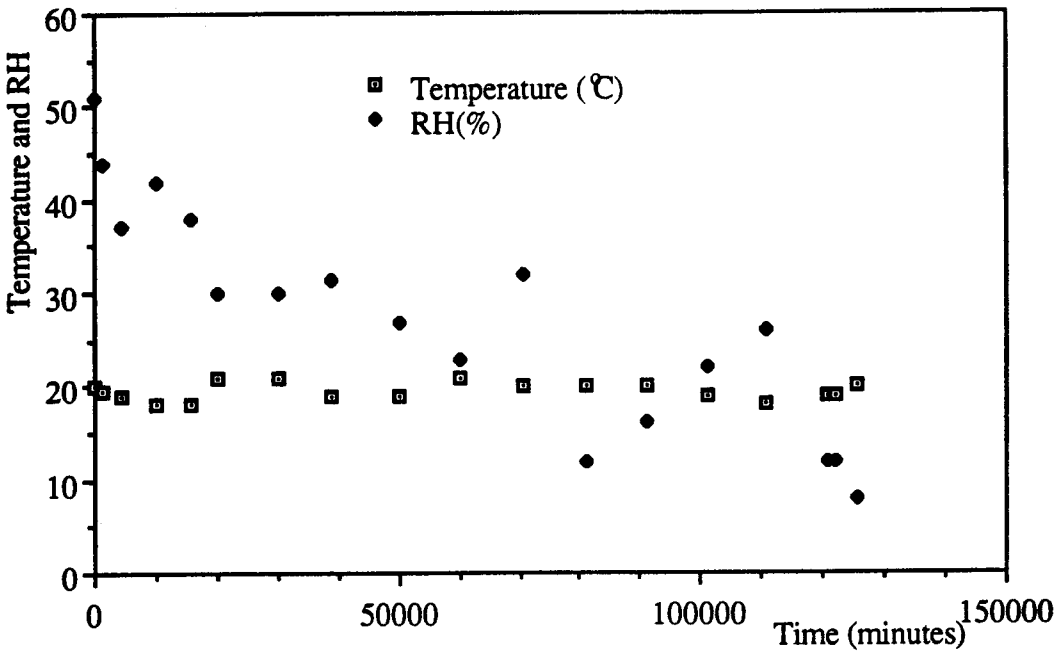

Fig. 4.3 The Environmental Record for Indoor Creep Test I3

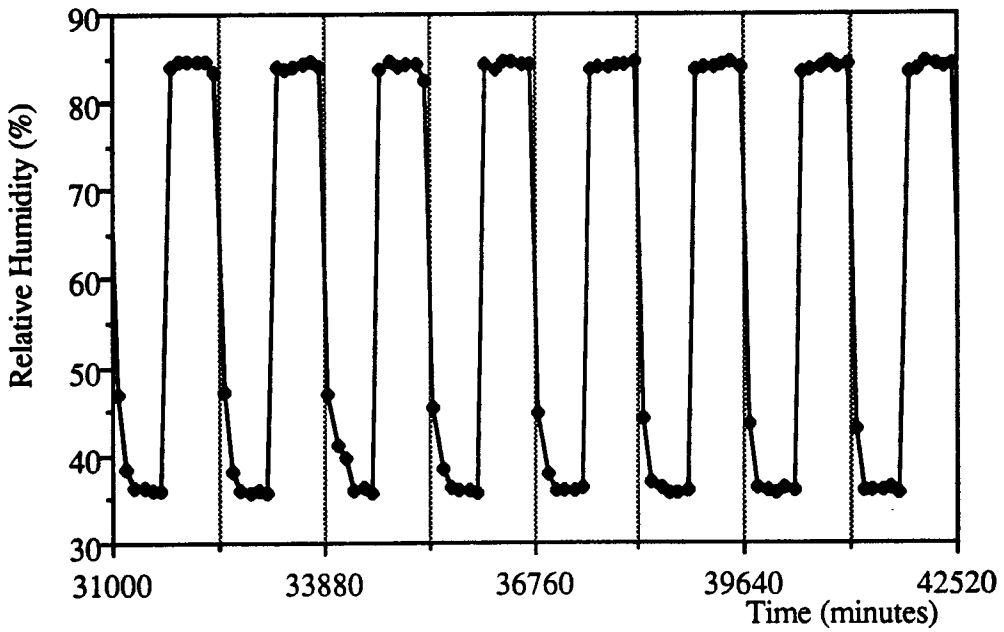

Fig. 4.4 Chamber's Relative Humidity Recorded from Cyclic Creep Test V1

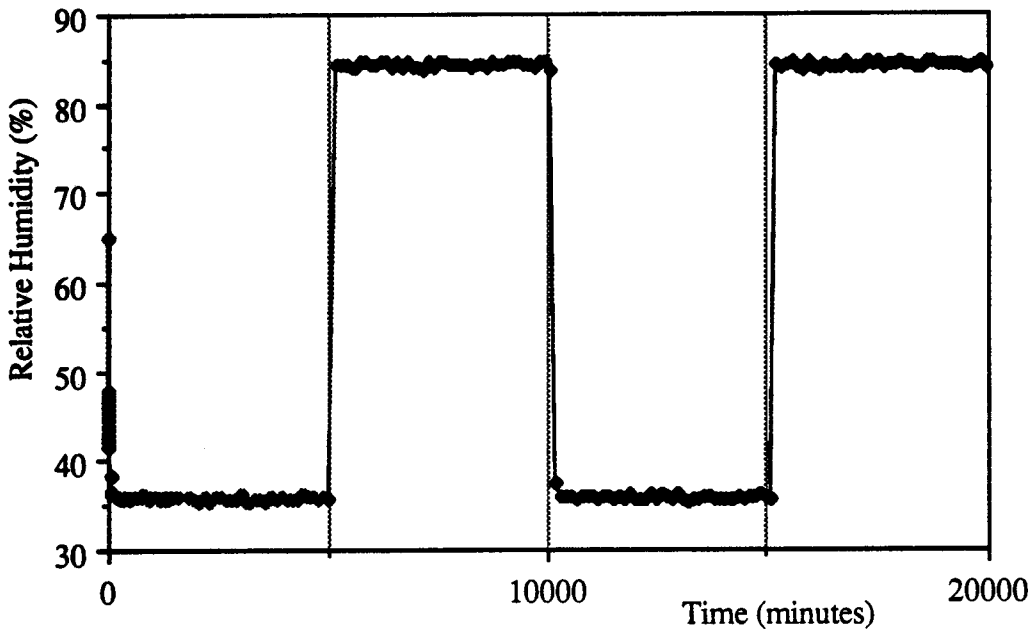

Fig. 4.5 Chamber's Relative Humidity Recorded from Cyclic Creep Test V7

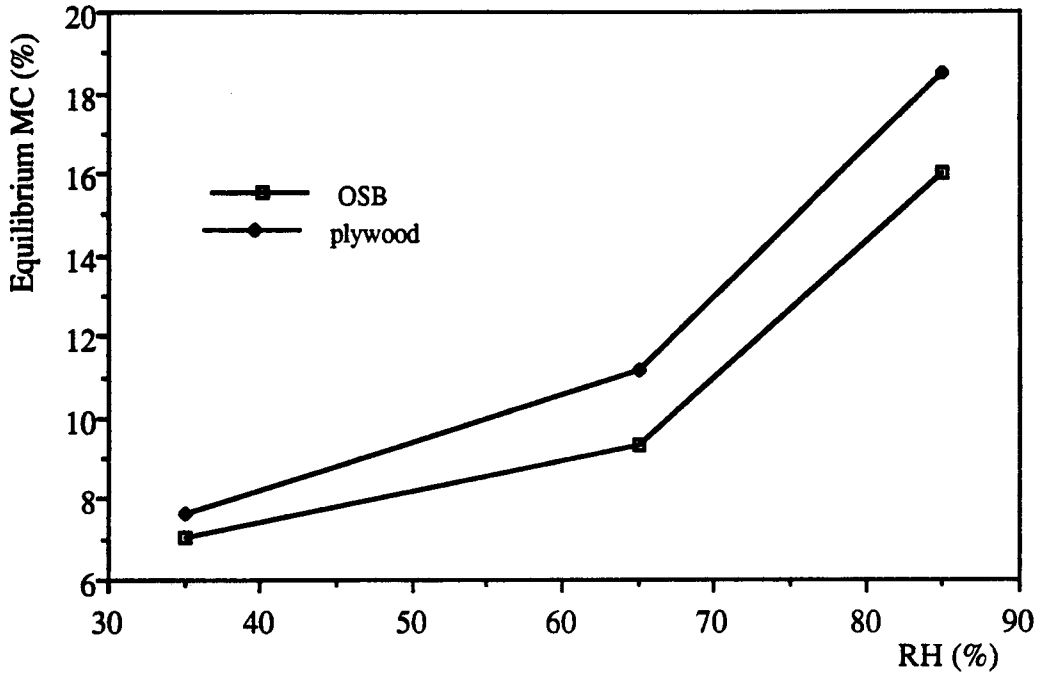

Fig. 4.6 Equilibrium MC of Materials under 35, 65, and 85% RH at 20 °C

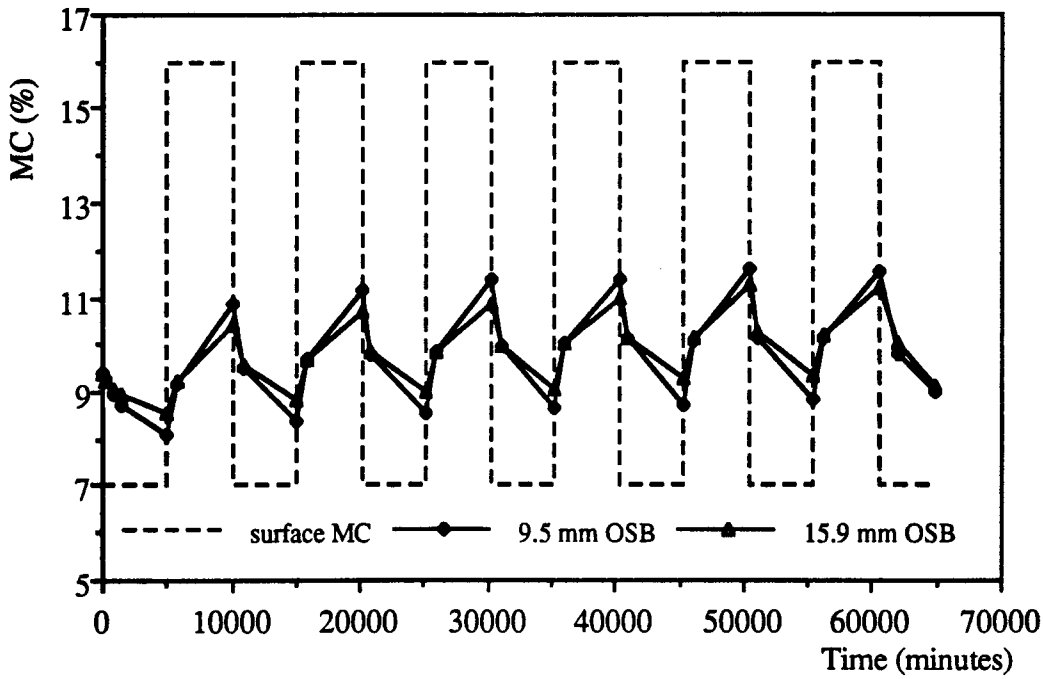

Fig. 4.7 MC of OSB Panels with the Two Thicknesses during Test V7

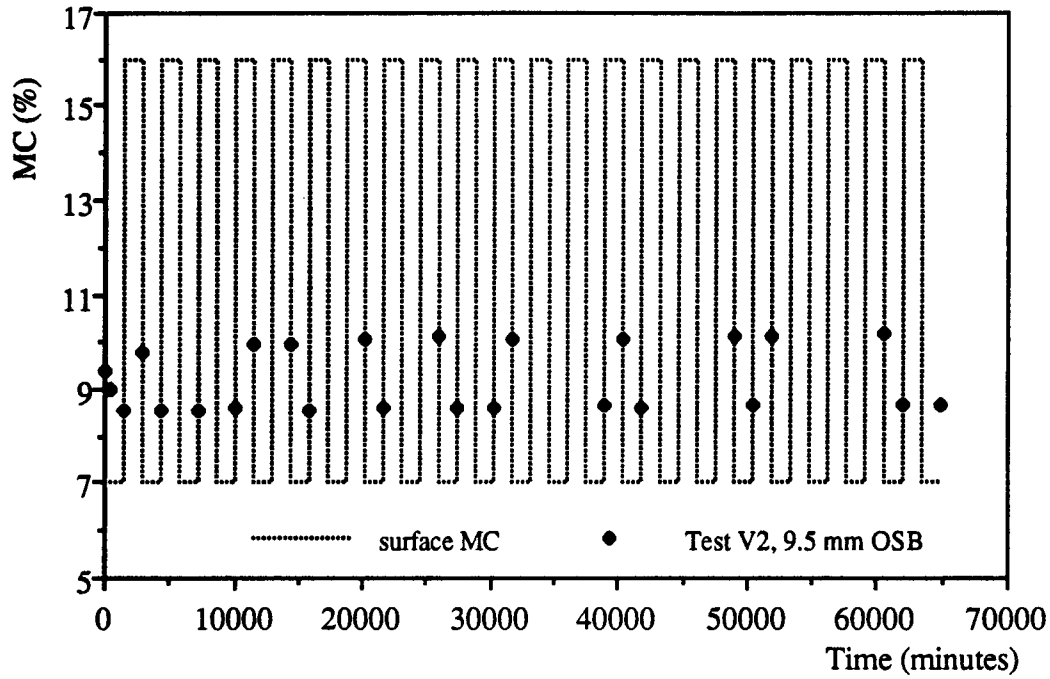

(a) The Measured Panel's Average MC in Cyclic Test V2

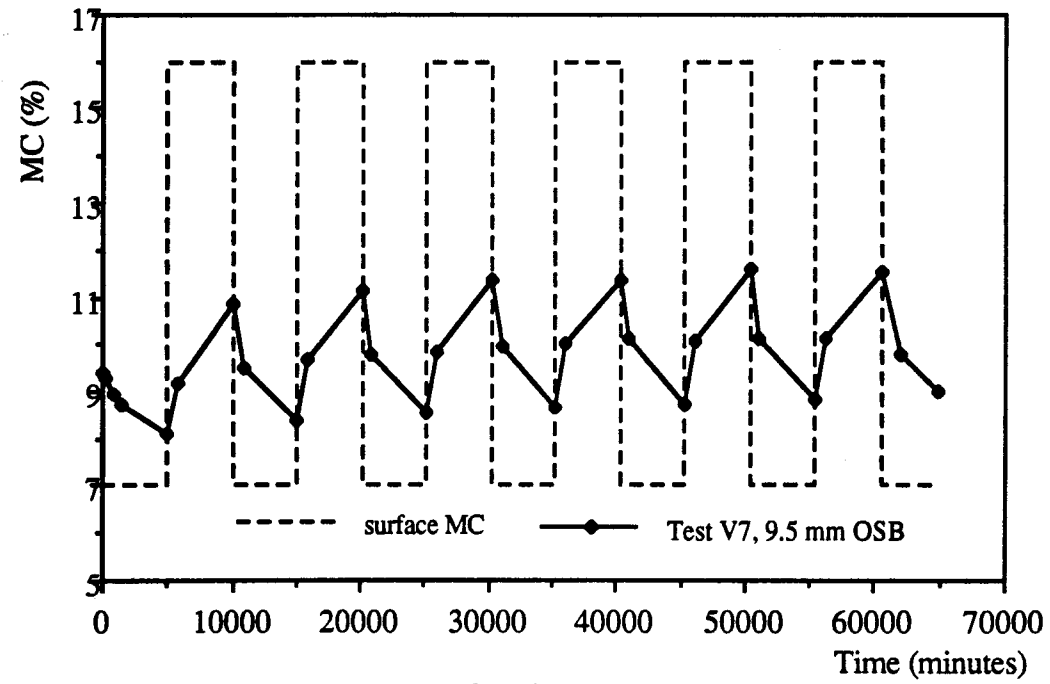

(b) The Measured Panel's Average MC in Cyclic Test V7

Fig. 4.8 MC of the 9.5 mm OSB Panels in Two Cyclic RH Tests V2 and V7

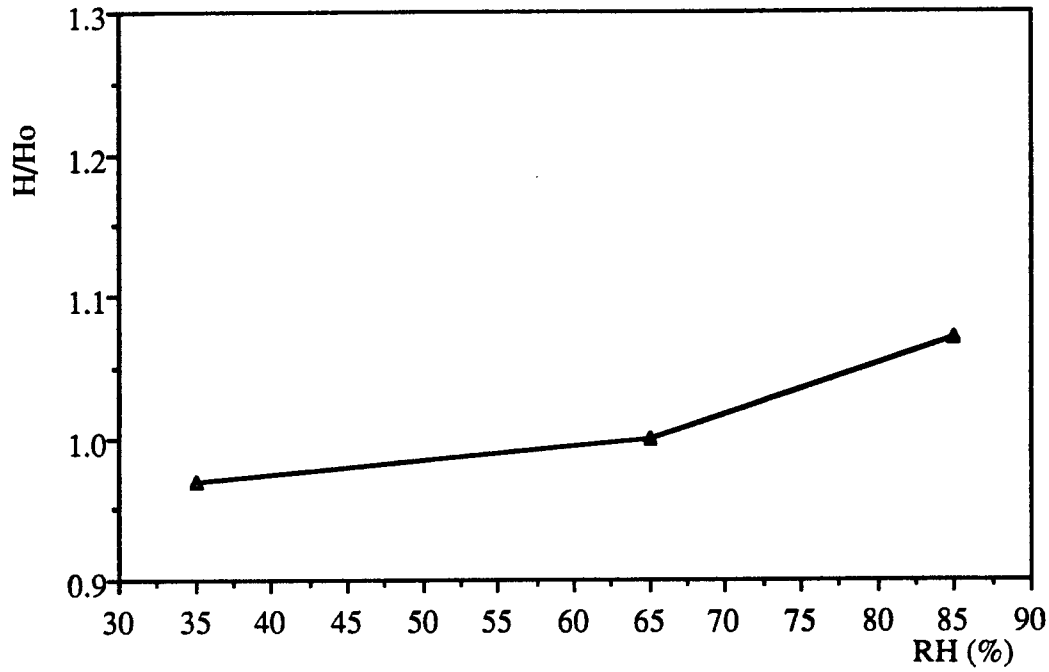

Fig. 4.9 Ratios of OSB Panels' Equilibrium Thickness under 35, 65, and 85% RH at 20 °C to Their Initial Values at 65%RH/20 °C

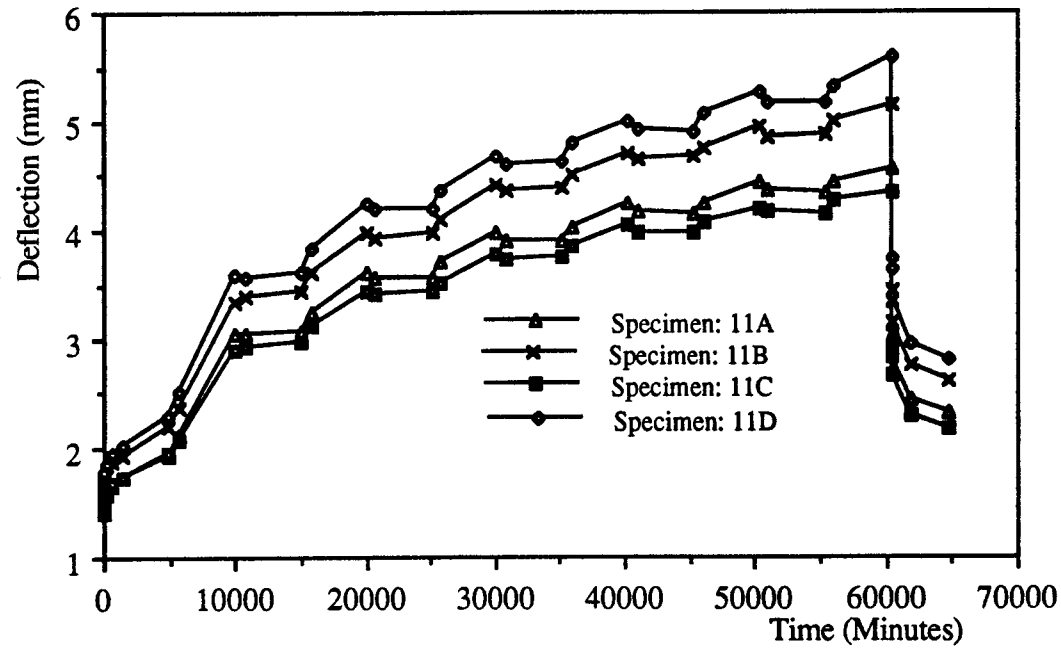

Fig. 4.10 The Measured Deflection (mm) vs. Time Curves for the Four 15.9 mm Parallel OSB Panels in Cyclic RH Test V7 under Sustained Loading for Six Weeks

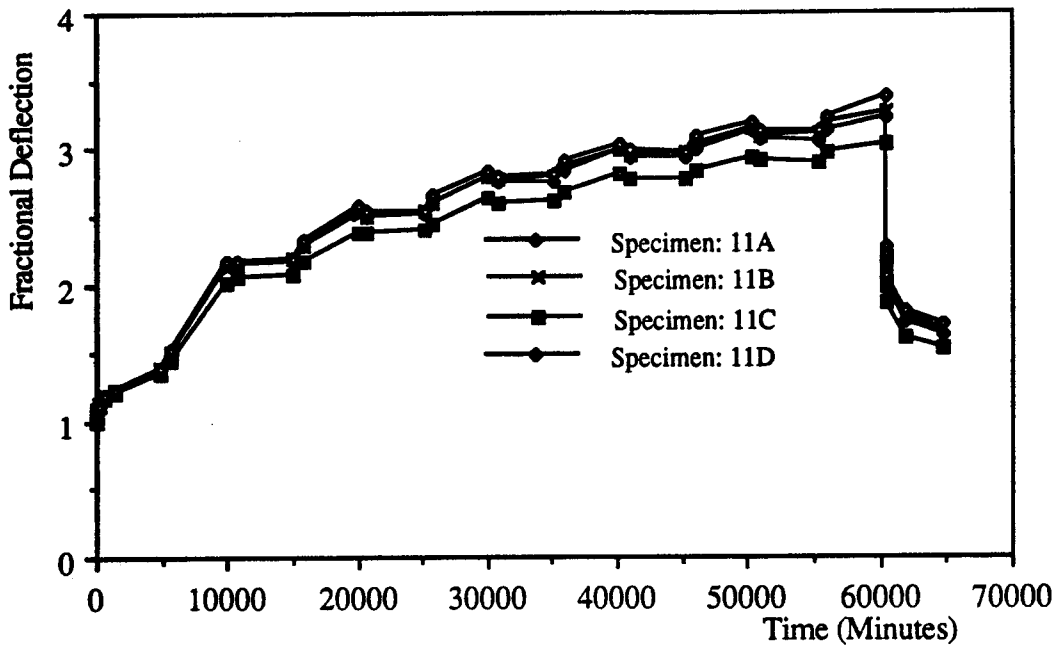

Fig. 4.11 Fractional Deflection vs. Time Curves for the Four 15.9 mm Parallel OSB Panels in Cyclic RH Test V7 under Sustained Loading for Six Weeks

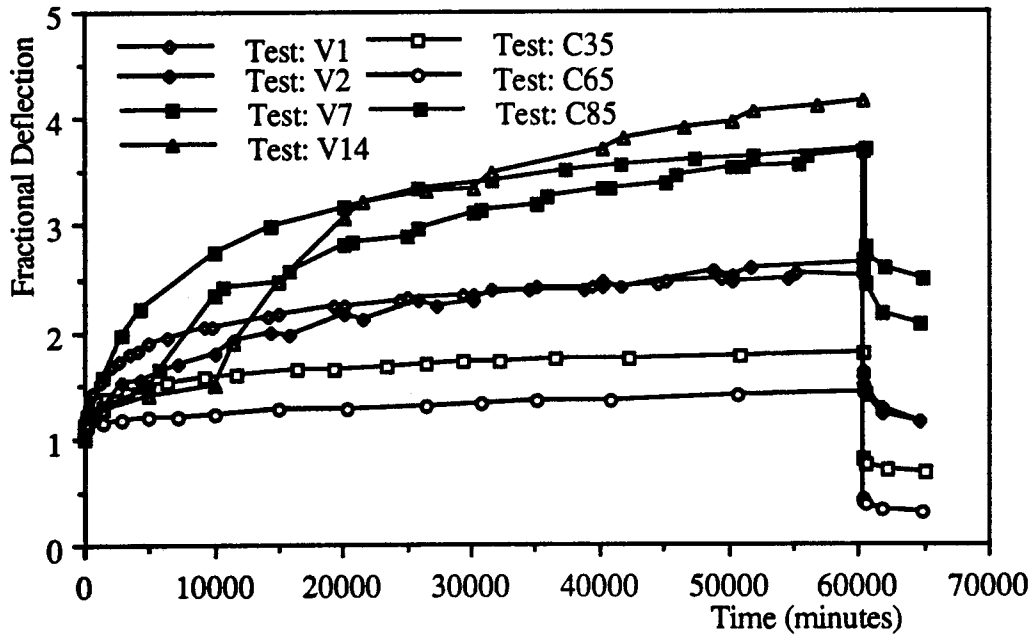

Fig. 4.12 Fractional Deflection vs. Time curves for the 9.5 mm Parallel OSB Panels under Sustained Loading for Six Weeks in Environment Controlled Tests

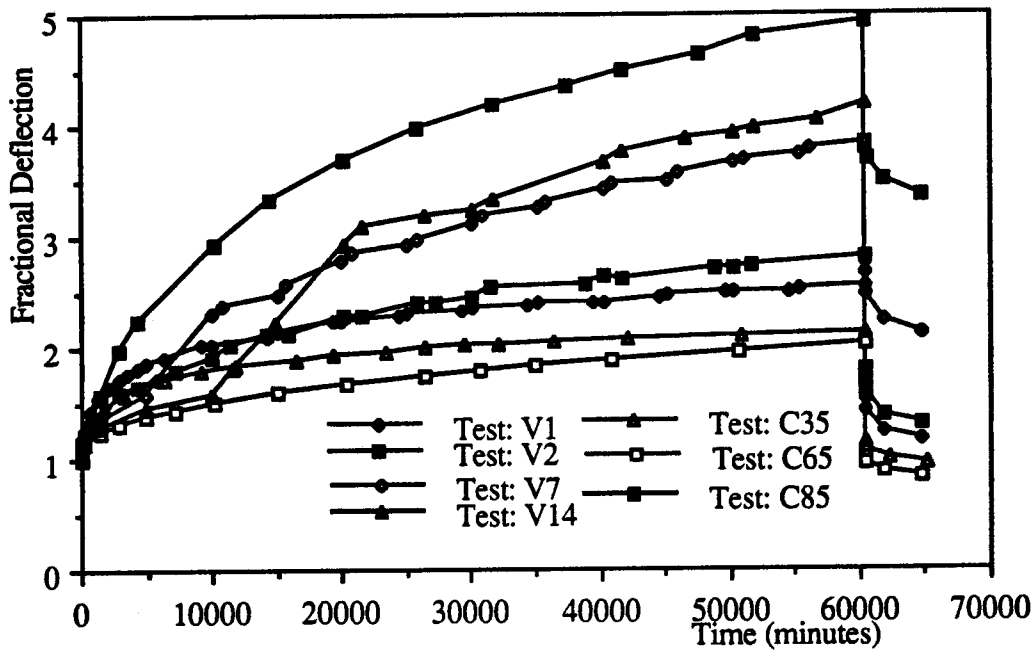

Fig. 4.13 Fractional Deflection vs. Time curves for the 9.5 mm Perpendicular OSB Panels under Sustained Loading for Six Weeks in Environment Controlled Tests

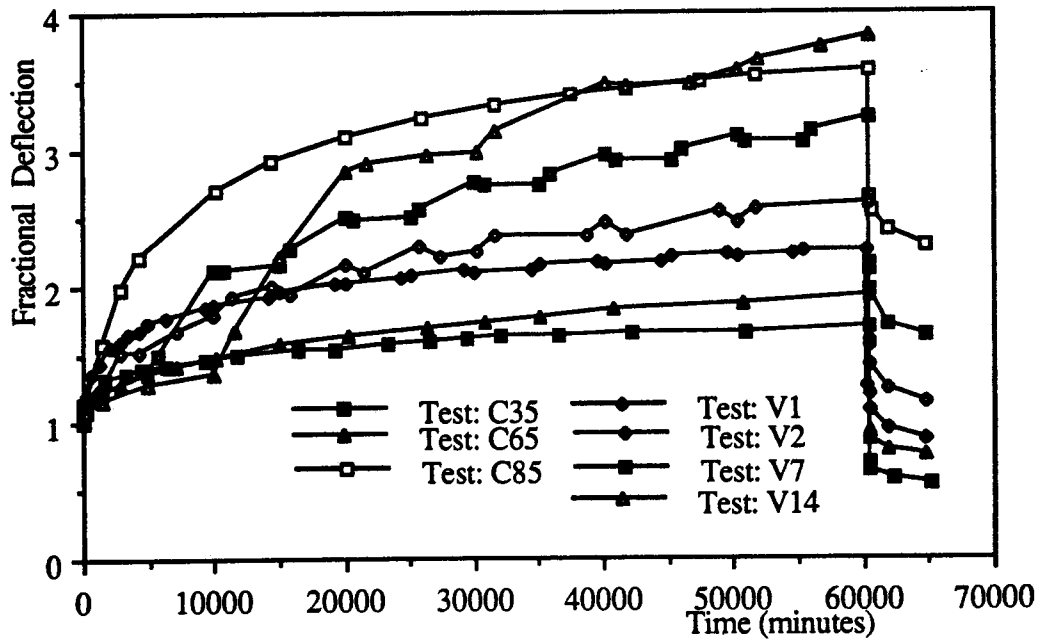

Fig. 4.14 Fractional Deflection vs. Time curves for the 15.9 mm Parallel OSB Panels under Sustained Loading for Six Weeks in Environment Controlled Tests

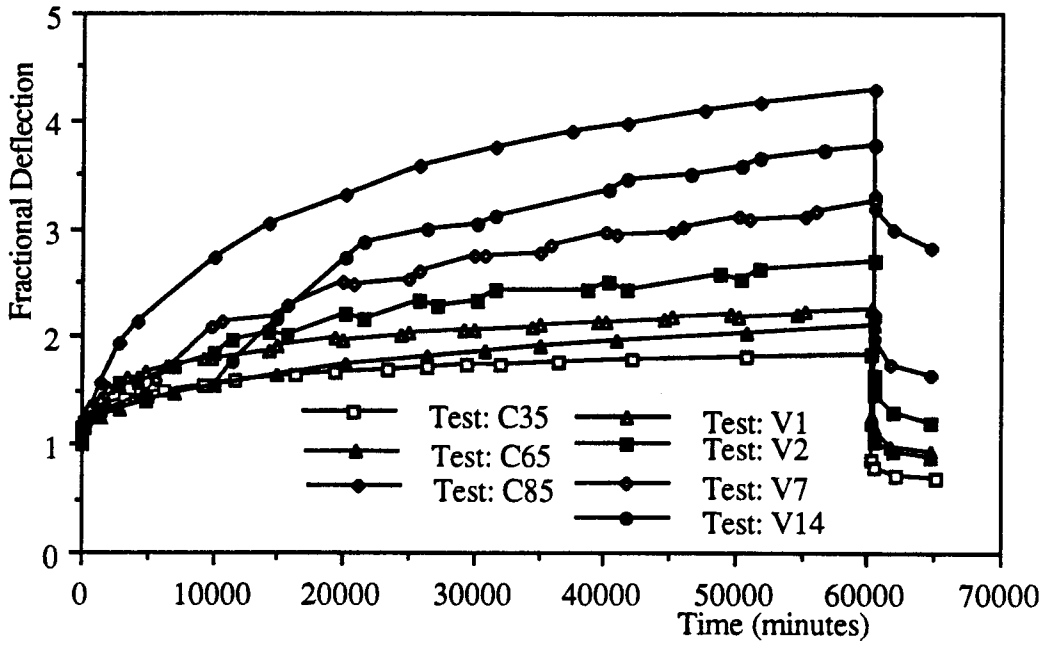

Fig. 4.15 Fractional Deflection vs. Time curves for the 15.9 mm Perpendicular OSB Panels under Sustained Loading for Six Weeks in Environment Controlled Tests

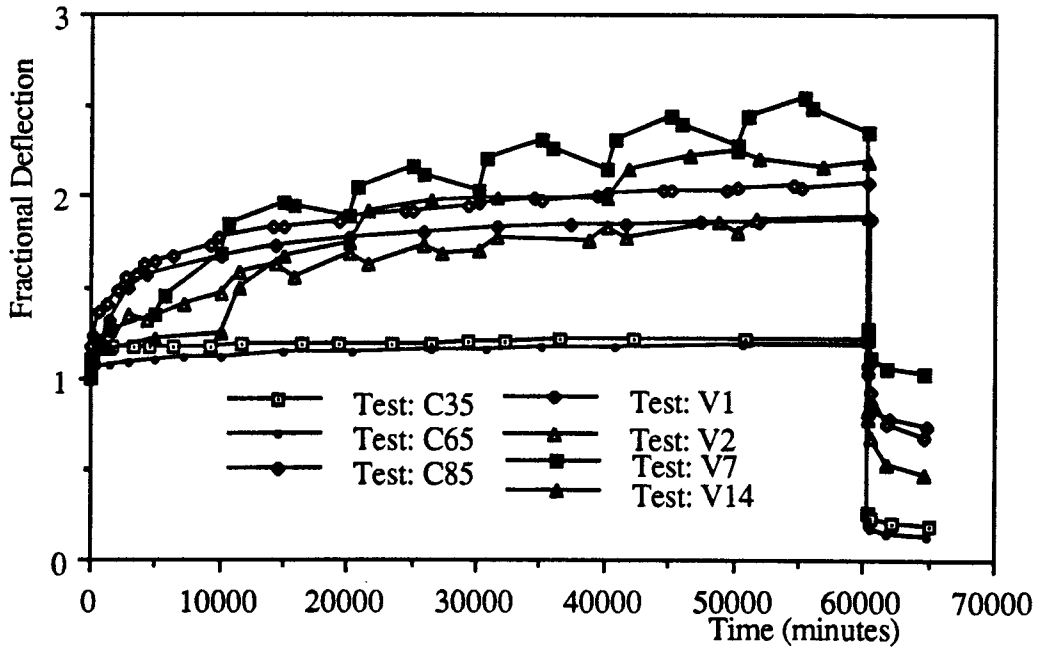

Fig. 4.16 Fractional Deflection vs. Time curves for the 9.5 mm Parallel Plywood Panels under Sustained Loading for Six Weeks in Environment Controlled Tests

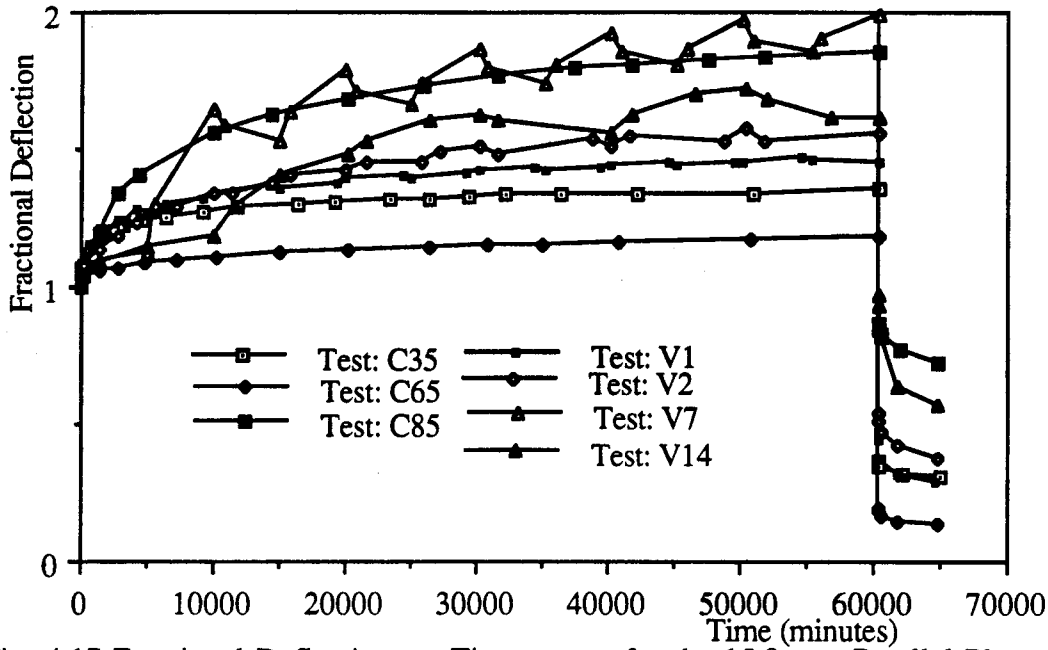

Fig. 4.17 Fractional Deflection vs. Time curves for the 15.9 mm Parallel Plywood Panels under Sustained Loading for Six Weeks in Environment Controlled Tests

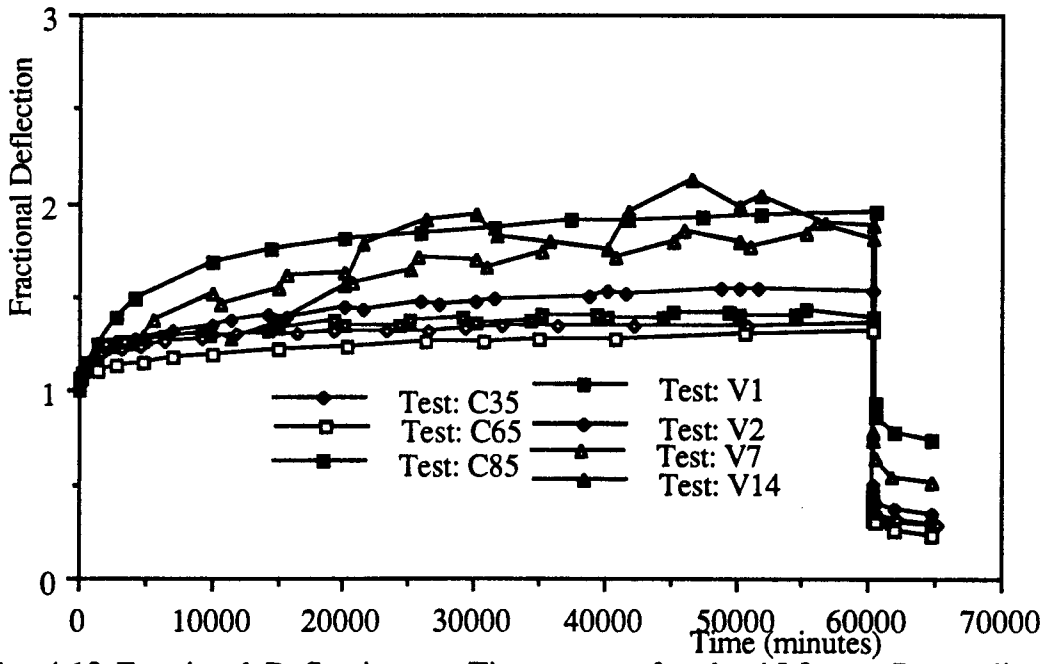

Fig. 4.18 Fractional Deflection vs. Time curves for the 15.9 mm Perpendicular Plywood Panels under Sustained Loading for Six Weeks in Environment Controlled Tests

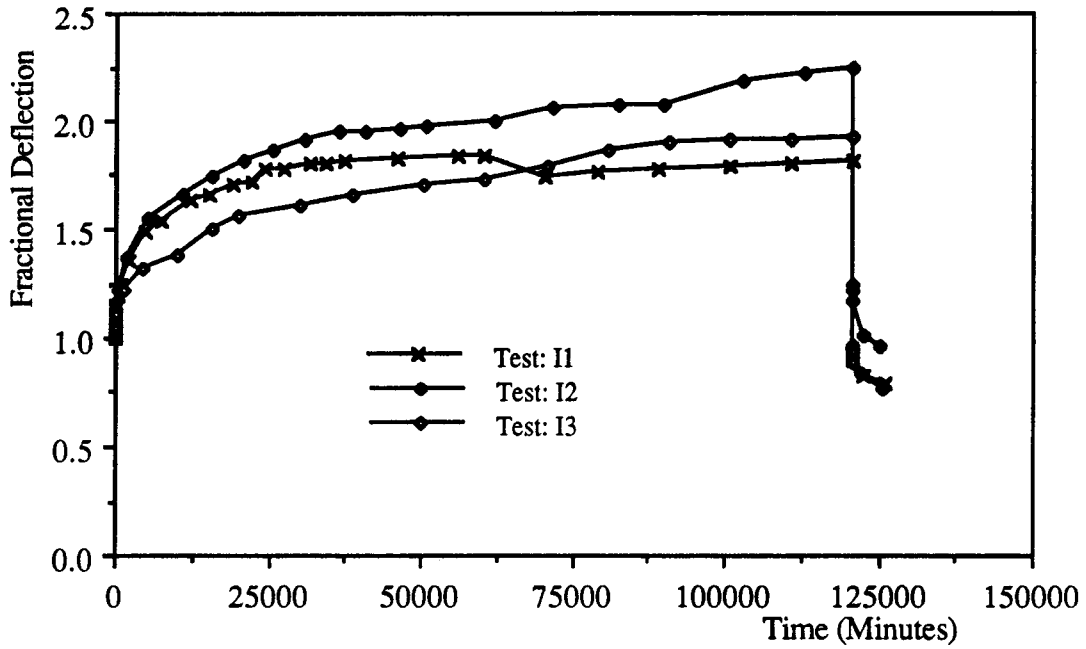

Fig. 4.19 Fractional Deflection vs. Time curves for the 9.5 mm Parallel OSB Panels under Sustained Loading for Twelve Weeks in Three Indoor Environment Tests

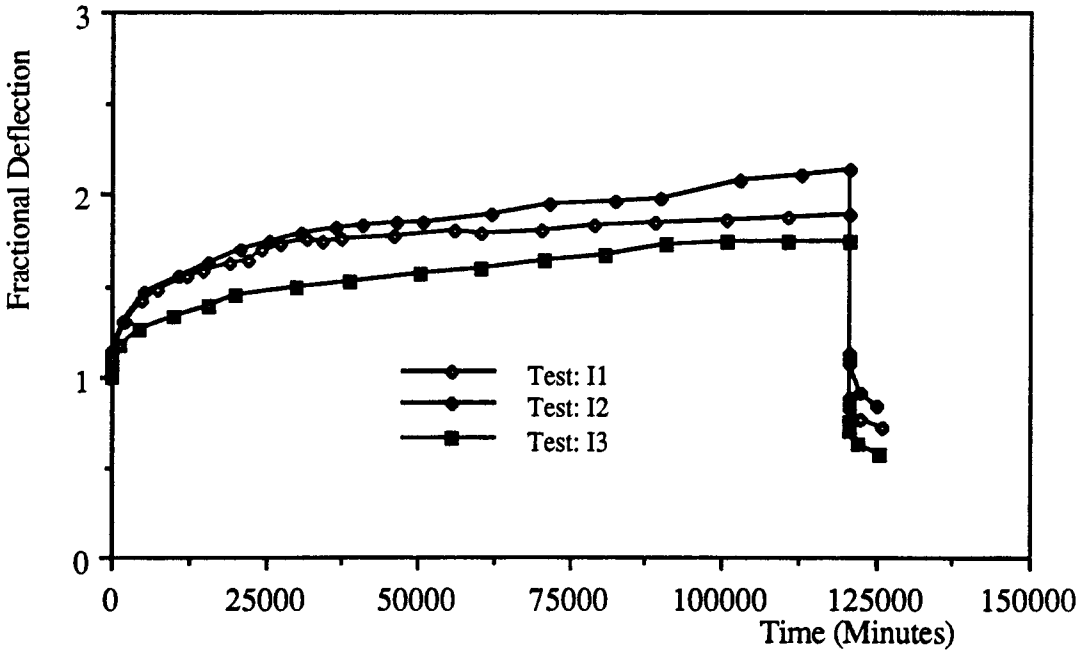

Fig. 4.20 Fractional Deflection vs. Time curves for the 9.5 mm Perpendicular OSB Panels under Sustained Loading for Twelve Weeks in Three Indoor Environment Tests

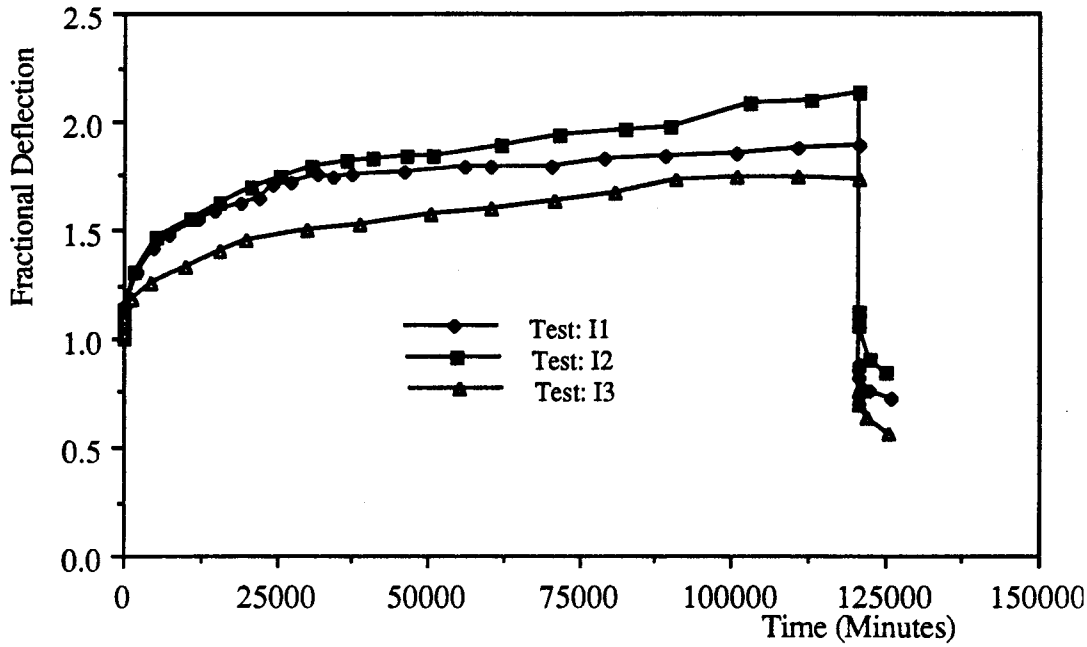

Fig. 4.21 Fractional Deflection vs. Time curves for the 15.9 mm Parallel OSB Panels under Sustained Loading for Twelve Weeks in Three Indoor Environment Tests

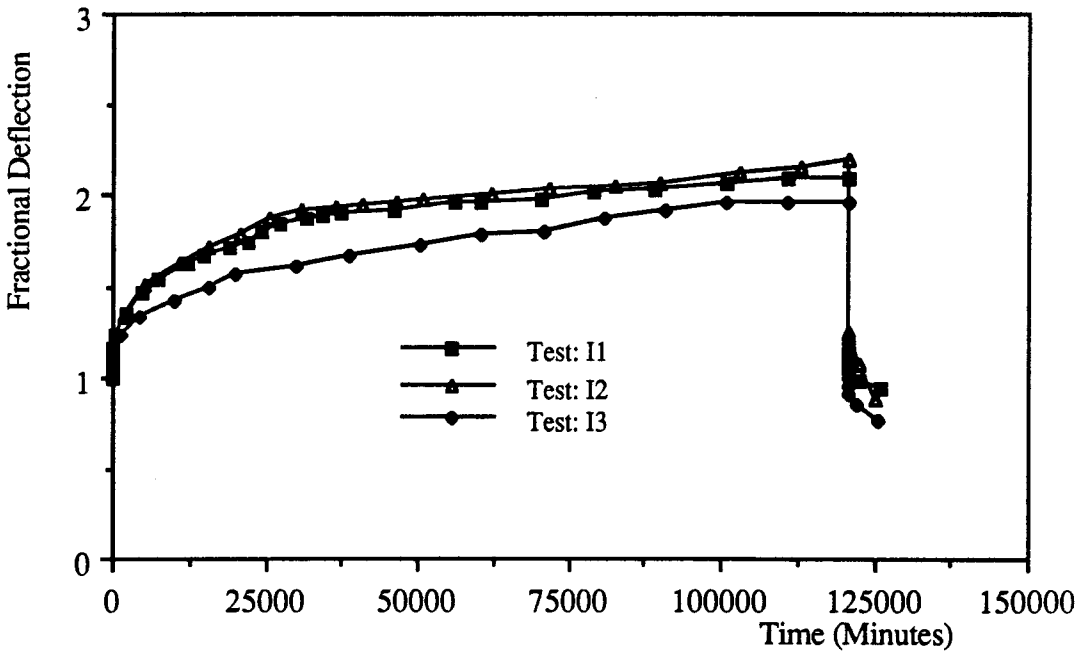

Fig. 4.22 Fractional Deflection vs. Time curves for the 15.9 mm Perpendicular OSB Panels under Sustained Loading for Twelve Weeks in Three Indoor Environment Tests

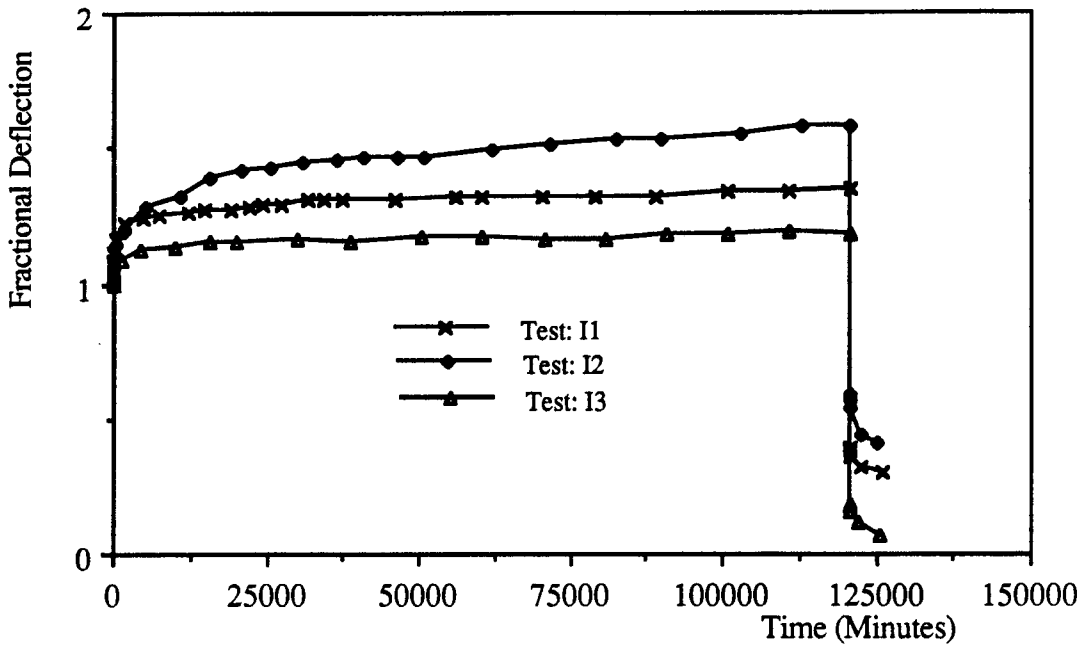

Fig. 4.23 Fractional Deflection vs. Time curves for the 9.5 mm Parallel Plywood Panels under Sustained Loading for Twelve Weeks in Three Indoor Environment Tests

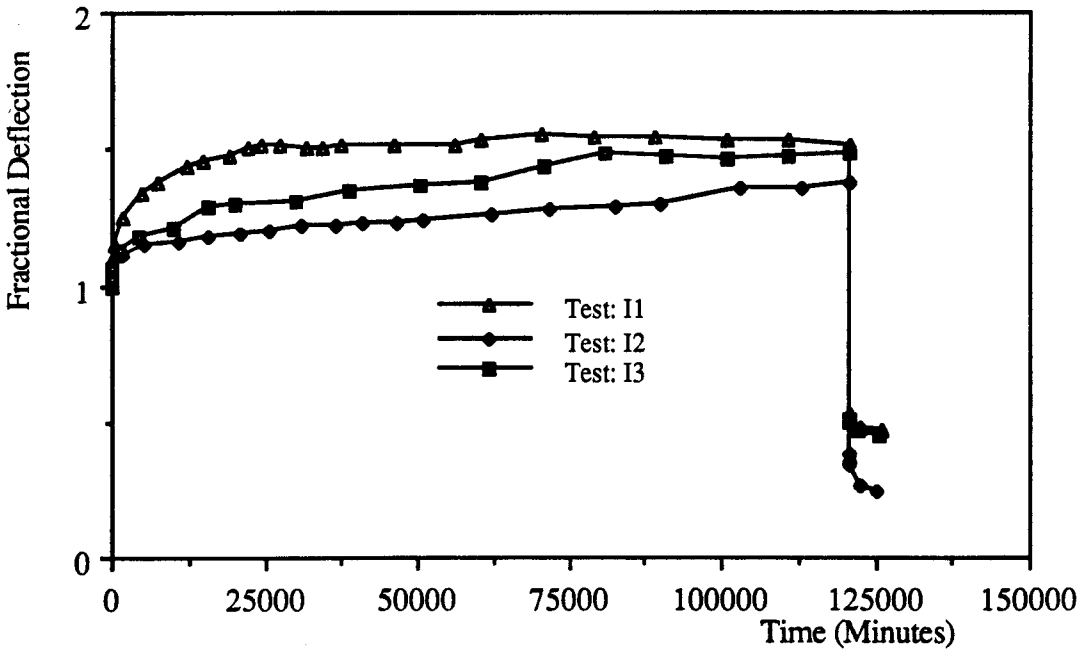

Fig. 4.24 Fractional Deflection vs. Time curves for the 15.9 mm Parallel Plywood Panels under Sustained Loading for Twelve Weeks in Three Indoor Environment Tests

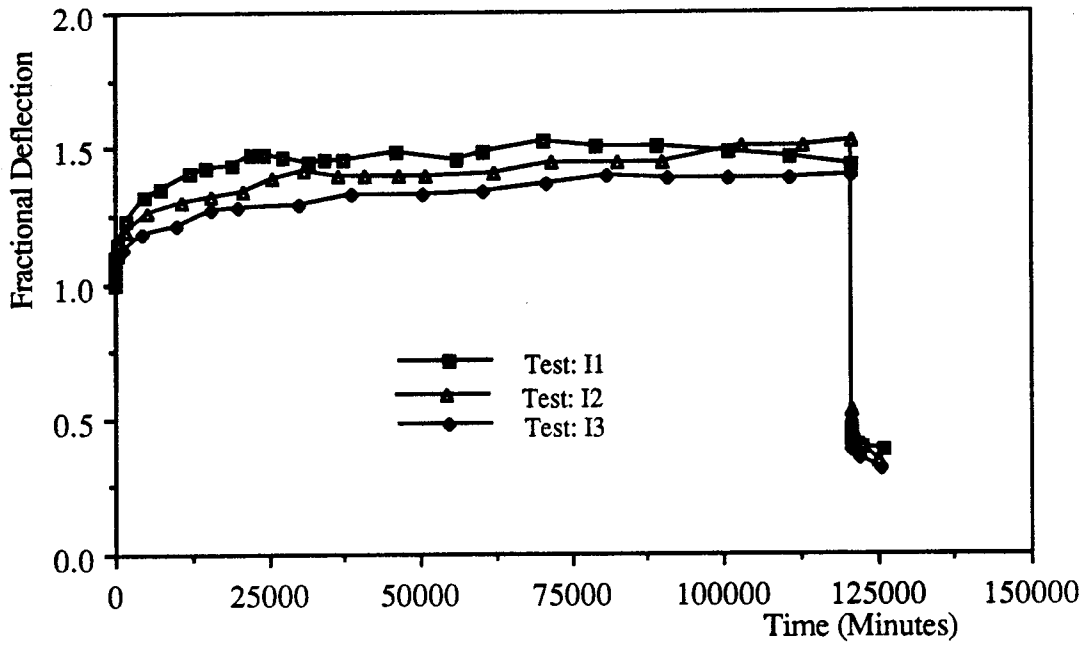

Fig. 4.25 Fractional Deflection vs. Time curves for the 15.9 mm Perpendicular Plywood Panels under Sustained Loading for Twelve Weeks in Three Indoor Environment Tests

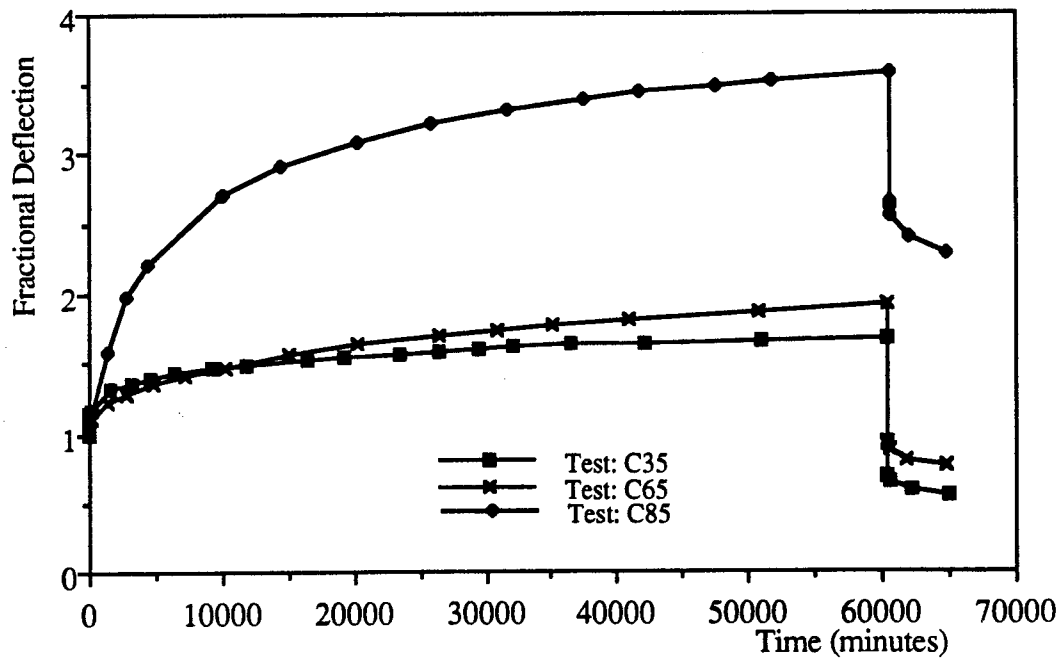

Fig. 4.26 Fractional Deflection vs. Time curves for the 15.9 mm Parallel OSB Panels under Sustained Loading for Six Weeks in the Three Constant RH Conditions

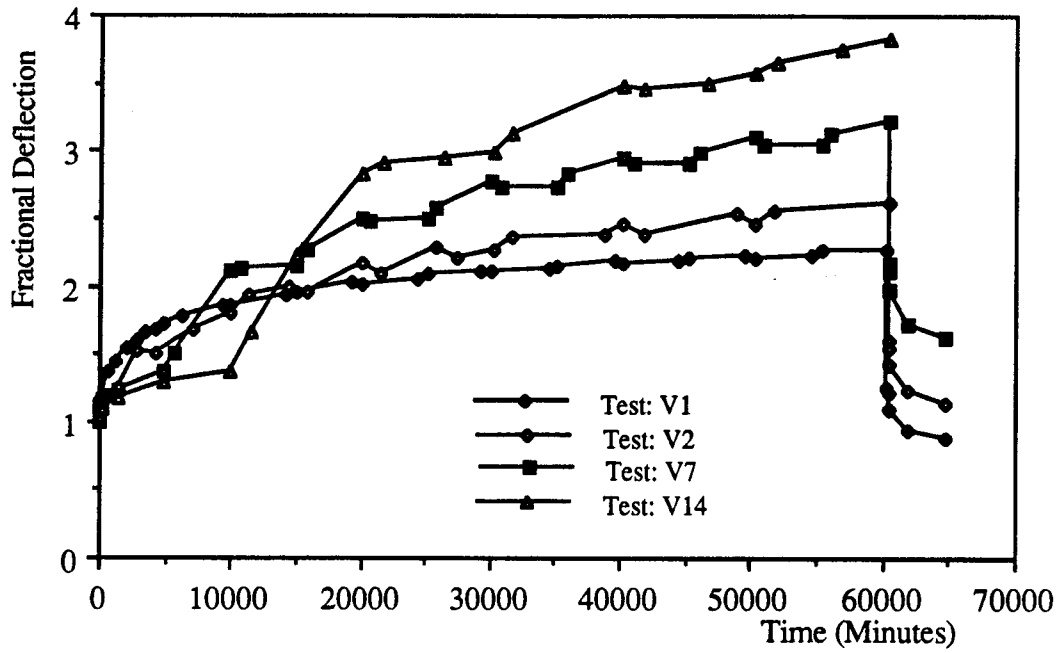

Fig. 4.27 Fractional Deflection vs. Time curves for the 15.9 mm Parallel OSB Panels under Sustained Loading for Six Weeks in the Four Cyclic RH Tests

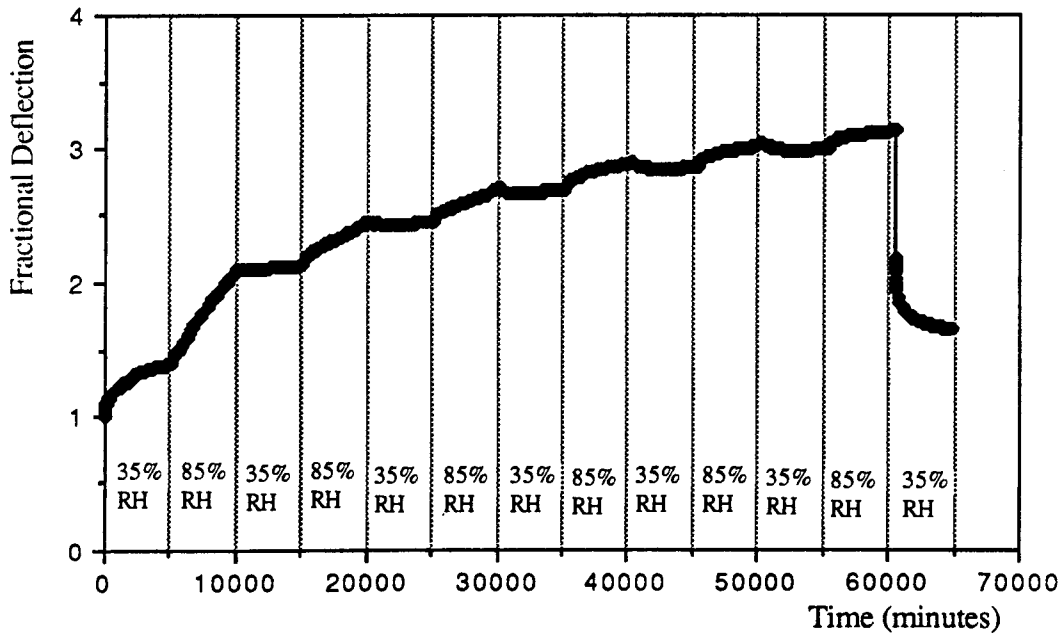

Fig. 4.28 Fractional Deflection vs. Time curves for the 15.9 mm Parallel OSB Panels under Sustained Loading for Six Weeks in Test V7 Measured by LVDT

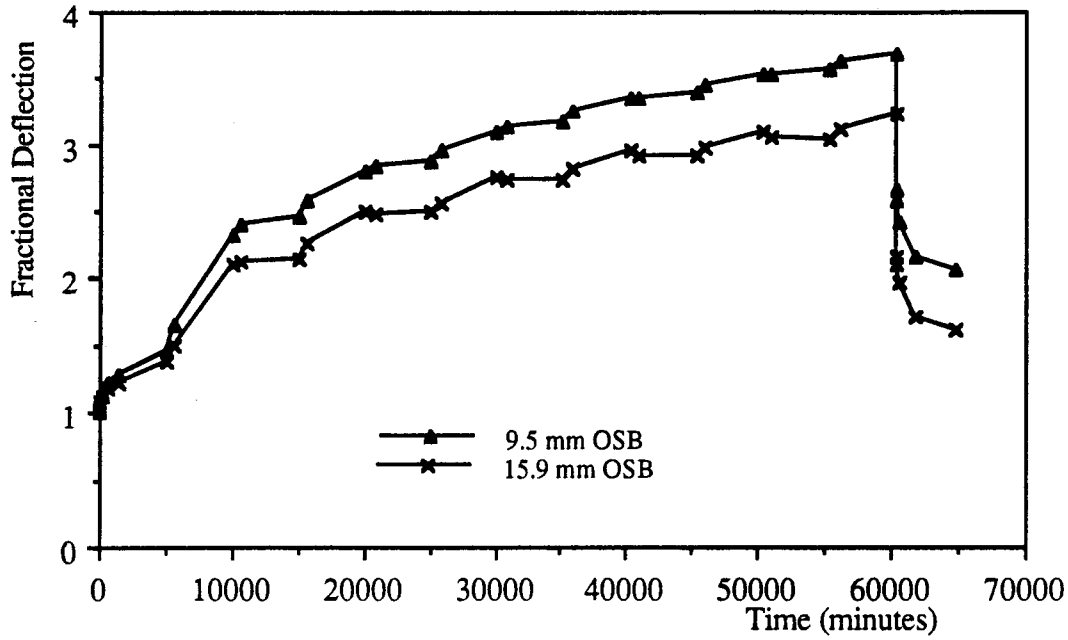

Fig. 4.29 Fractional Deflection vs. Time curves for the Parallel OSB Panel with Two Thicknesses under Sustained Loading for Six Weeks in Test V7

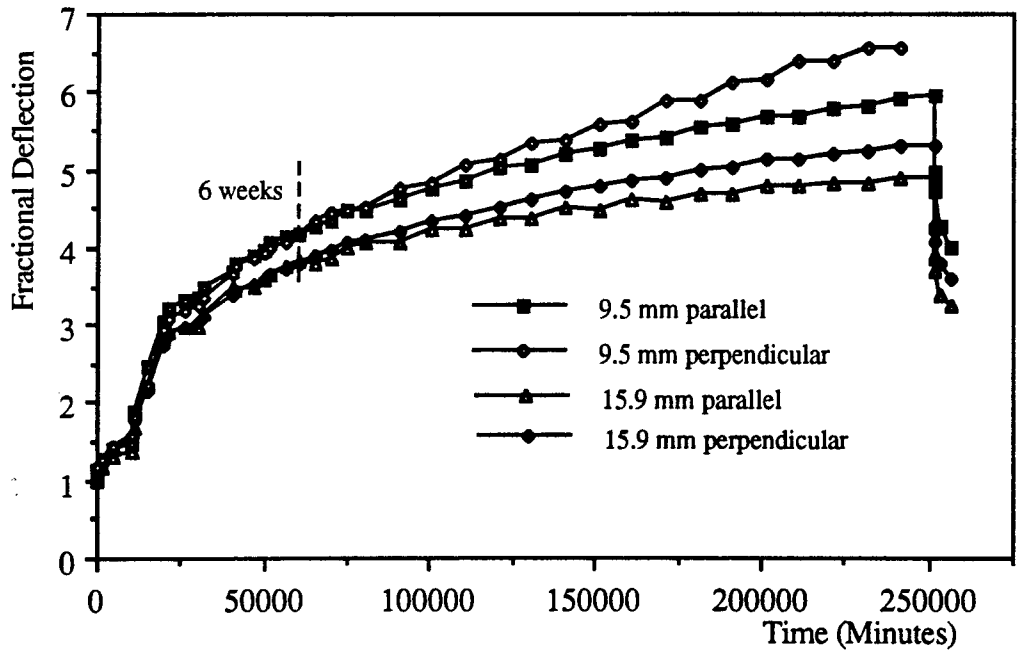

Fig. 4.30 Fractional Deflection vs. Time curves for the OSB Panels under Sustained Loading for 25 Weeks in Cyclic Test V14

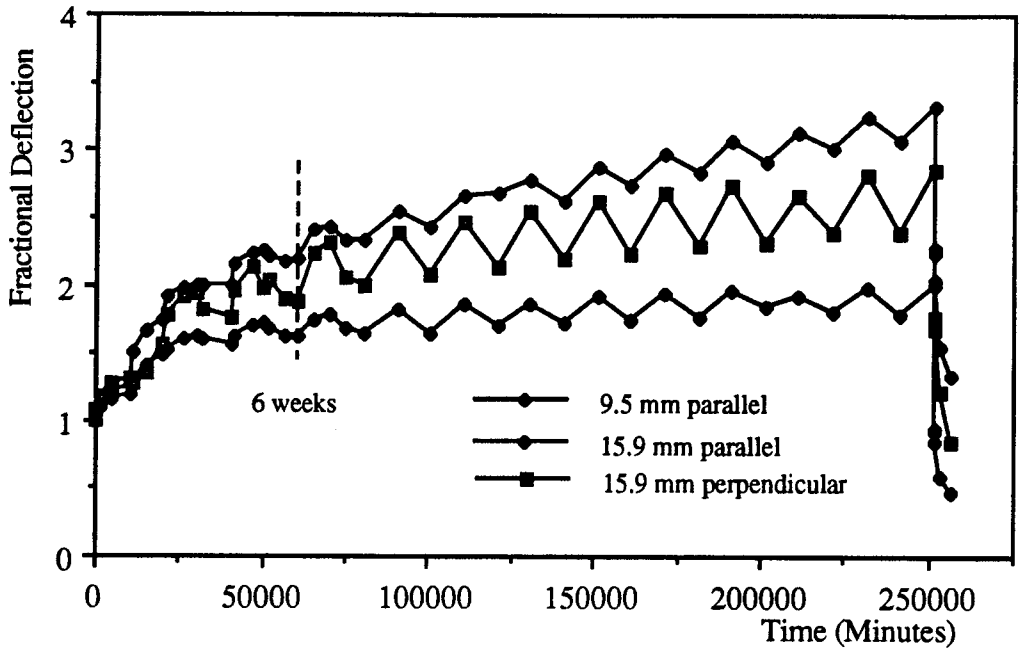

Fig. 4.31 Fractional Deflection vs. Time curves for the Plywood Panels under Sustained Loading for 25 Weeks in Cyclic Test V14

Chapter 5 Discussion of Experimental Results

Test results from the experimental program are summarized in chapter 4. In this chapter, the short-term mechanical properties of wood panels are discussed. The discussion about the effects of RH level, cyclic RH, panel thickness, and strand orientation on wood panel creep is based on the results obtained from the constant and cyclic creep tests. The influence of these factors are also evaluated by two statistic procedures: analysis of variance (ANOVA) and regression analysis. The ANOVA shows the significance of creep differences between panels with various thicknesses, with two strand orientations, and with various periods of RH cycling. The regression analysis gives the statistical significance of the variables affecting the wood panel creep. The correlation between panel creep and other variables is also presented.

5.1 Short-term Material Properties

As described in chapter 3, all of the wood panels were nondestructively tested to determine their short-term bending stiffness. The obtained MOE values are summarized in Tables 4.1 to 4.8. The ultimate bending strength of wood panel was evaluated from some of the matched panels. The results are listed in Tables 4.9 to 4.11. All of the short-term tests were carried out when the panels were in equilibrium at 65% RH/20 ^{o}C.

Strand orientations of the bending panels made differences in the panel stiffness and strength. Wood panels with surface strands parallel to the bending direction are much stiffer and stronger than panels with strands in the perpendicular direction. This phenomenon is especially true for plywood panels. For 9.5 mm plywood, the bending stiffness in the perpendicular direction is very small; it is about 0.5 GPa compared with 8 GPa for the corresponding parallel direction. The perpendicular stiffness of OSB or

15.9 mm plywood is about 1/3 that of the parallel panels. The ultimate strength of the perpendicular panels is about 3/4 that of the parallel panels for OSB, and about 1/2 that of the parallel panels for plywood.

The modulus of elasticity of 15.9 mm plywood is about 20% larger than that of OSB in parallel bending. In perpendicular bending, the MOE of OSB is close to that of plywood for 15.9 mm thick panel. The MOE for 9.5 mm perpendicular plywood is very small (0.55 GPa). The ultimate strengths in parallel bending are about 20 and 40 MPa for OSB and plywood, respectively. In perpendicular bending, the ultimate strengths are around 15 MPa for both OSB and plywood. The property variations among plywood panels are, in general, larger than those for OSB.

5.2 Effect of Constant Maintained Relative Humidity and Moisture Content Levels on Creep

5.2.1 Effect of Constant Maintained Humidity Levels on Creep Deflections

When exposed to various RH environments, wood panels reach different MC levels, and the creep developed is also different. The panels' creep development under various constant RH levels is presented in Sec. 4.4.1. After 6 weeks' of sustained loading, the fractional deflections of OSB panels are usually less than 2 for a low and medium RH (35% and 65% RH), which means that the time-dependent deflections developed within the 6 weeks are less than the instantaneous deflections. However, the fractional deflections are up to about 4.0 for a high RH (85%) environment. The long-term deflections of plywood are also larger in a higher RH level, but the influence of a high RH level on the creep of plywood is not as significant as to OSB panels based on the fractional deflection values listed in Table 4.30. The values for plywood are usually

less than those for OSB panels under the same constant RH environment. Especially when the RH is high (85%), the fractional deflection of plywood is about 2 at sixth week, but is around 4 for OSB.

The results obtained in this study are consistent with test results given by McNatt and Laufenberg (1991). The fractional deflections of OSB and plywood are calculated by the author according to the data provided in their paper. After 6 month creep, the fractional deflection of OSB is 1.45 and 4.4 for 50% and 85% constant RH, respectively. The values for plywood are 1.29 and 1.91 for the two RH levels. The stress level is 30%. Several commercial OSB specimens were creep tested under high RH (95%) by Pu et al. (1992a). After one month of sustained loading, the fractional deflection was as high as 3.2 to 7.3 for various commercial OSB products. The results of the above two papers and the results from this experimental program all show that the OSB panels creep a great amount in a high RH environment.

The effects of constant maintained RH level on OSB creep are shown in Figs. 5.1-5.4, where the creep curves for 35% and 65% constant RH are much lower than that of 85%RH. This fact indicates that a high RH level would accelerate the creep of OSB. Although there is more creep in higher RH conditions for solid wood panels, the influence of high RH on composite wood products is much severer than on solid wood products.

The effect of RH level on creep is studied by comparing both the magnitude and rate of creep. Within the range of low to medium RH , the OSB panels tend to creep more when the environmental RH is higher. In Fig. 5.1, both the magnitude and rate of creep of 15.9 mm parallel OSB panels at 65% RH are larger than that of 35% RH. This is also true for the 15.9 mm perpendicular OSB panels. In Fig. 5.2, the creep rate of 9.5 mm perpendicular OSB panels in a 65% RH environment is larger than that of 35%

RH after the first week, but the magnitude of creep deflection is less than that in 65% RH. In Fig. 5.3, the creep deflection of 9.5 mm parallel OSB panels after 6 weeks is also less in 65% RH than that of 35% RH, but the creep rates in the two RH levels are close. For all the OSB panels, as shown in Figs. 5.1 - 5.3, the creep rate under 35% RH is not more than that under 65% after 6 weeks of sustained loading. However, the curves in the figures also show that the 35% constant RH environment gives more creep than 65% RH constant environment in the early loading stage. This may be caused by creep acceleration in the first desorption in test C35 when RH changes from 65% to 35% at the beginning of the creep test. The desorption creates additional creep in test C35 because of the desorptive process in the wood panels. When the MC approaches equilibrium in test C35 after a certain time period, the creep rate then reflects the actual influence of RH level on the panel creep development.

When the wood panels were unloaded after a 6 week creep duration, the recovery lasted for at least 3 days in all test series. The recovery curves are shown in Figs. 5.1 to 5.4. Panel deflection in a high RH (85%) environment recovers more than that in a lower RH environment. However, the remaining unrecoverable (or permanent) deflections are also more in a higher RH environment. These factors demonstrate that the large creep deflections developed in a high RH (85%) environment consist of both more viscoelastic (recoverable) and viscous (unrecoverable) deflections than those developed in low and medium RH environments.

5.2.2 Effect of RH Level on Panel Stiffness after Sustained Loading

Upon unloading, an instantaneous deflection recovery was observed and recorded. As presented in Sec. 4.4.1.2, the instantaneous recovery is almost equal to the instantaneous deflection upon loading, which implies that the wood panels did not lose their elastic stiffness after the 6 week creep test in either low or high RH environments.

When the swelling/shrinking of the panel thickness is taken into account, the panel has higher/lower MOE after a creep test conducted in low/high RH (35% and 85% RH, respectively) environments. Since wood panel has higher MOE in a drier environment without any loading history, the change of the panel MOE might be caused by the environmental RH changes only. It is therefore concluded that the wood panel does not lose stiffness or MOE through the sustained loading history with low stress level.

However, Pu et al. (1992a) give different conclusions. They report that the OSBs subjected to one month of creep under 95% RH lose about 50% of their MOE. They believe that the OSBs lose their MOE because of the creep history, but the OSB panel MC level for the "no creep" samples and for the creep samples is not clearly stated in the paper. If the MC levels of "no creep" samples and creep samples were different at the time the MOE was measured, the smaller MOE of creep samples may be due to a higher MC level but not due to the loading history. Therefore, the conclusion by Pu et al. (1992a) that MOE is lost because of the creep loading history may not be correct at low stress levels.

5.3 Effect of Cyclic RH on Creep

The results obtained from creep tests under cyclic RH conditions show that the creep deflections were accelerated by the cyclic RH. The general creep behavior during cyclic RH changes, that is, the effects of cyclic frequency of RH, the panel MC, the panel thickness, and surface strand orientation on the panel creep development will be discussed in the following sections.

In Fig. 5.5, the fractional deflections of 15.9 mm parallel OSB panels vs. time curves in four cyclic RH and 65% and 85% constant RH environments are shown. The creep curve of test C65 (65% constant RH), in which no sorption happened during the

entire creep period, is used as the basic curve to discuss the effect of cyclic RH on creep. All creep curves of cyclic RH conditions are higher than the 65% constant RH creep curve. In Fig. 5.5, the creep of test V14 is about 3 times that of test C65. This shows that the cyclic RH conditions significantly accelerated creep deflections.

The accelerating effect of cyclic RH on creep is reported by many researchers on both solid wood and wood composites; for example, Bryan and Schniewind (1965), Sauer and Haygreen (1968), Haygreen et al. (1975), McNatt and Hunt (1982). In the first desorption and adsorption, the accelerating effect of sorptive processes is very pronounced as shown in Figs. 4.28 and 5.5. A large amount of creep developed in the first RH cycle. The creep yielded during the first desorption and adsorption is about 30%-65% of the total creep developed during the 6 week creep duration. The first sorptive process is desorption when the environmental RH changes from 65% to 35% in the cyclic creep test series. Creep deflection develops rapidly during this period, as shown by the creep curves in Fig. 5.5. The second sorptive process is adsorption; when RH changes from 35% to 85%, the creep increases very rapidly during this first adsorption. The creep curve is almost a straight line that hardly levels off in the first high RH duration. The creep rate at this stage is much higher than that of the previous desorption. As shown in Fig. 5.5, slopes of the straight lines, or the creep rates, are very close in the first adsorptions for the four cyclic test series even though the absolute amount of creep produced in that period is quite different.

In subsequent sorptions, the creep rate of OSB is accelerated during adsorptions and is reduced during desorptions. There is even a partial recovery of deflection during desorption. The overall creep rate in the subsequent adsorptions decreases gradually with increasing of creep duration.

The pronounced effect of the first RH cycle on creep is also reported by Armstrong

and Grossman (1972). However, there are inconsistencies among publications about the creep development during the subsequent RH cycling. As described previously, the creep deflection of OSB is increased during adsorption (35%-85% RH) and decreased during desorption (85% - 35%). The results of this study are consistent with some results (Sauer and Haygreen 1968, Hall, et al. 1977, Bryan and Schniewind 1965, Haygreen et al. 1975), but different from others (Yeh et al. 1990, Armstrong and Grossman 1972, Schniewind 1968, etc.) which report that the creep deflection increases during desorption and decreases during adsorptions. It seems that different wood species, moisture level, moisture movement, and moisture distribution of panels may cause the different response in cyclic RH.

Although creep of OSB panel is strongly accelerated by constant maintained high RH (such as 85% RH), the creep in cyclic RH is usually larger. In Fig. 5.5, the creep curve of the cyclic environment in test V14 crossed the creep curve of test C85 at about 4th week. Creep curves of other cyclic RH environments were not as high as that of test C85 in 6 weeks. Therefore, it can be concluded that the cyclic RH environment within a certain cyclic period range produces more creep in OSB than in a high RH environment such as 85% RH.

As for the constant RH creep tests discussed in the previous section, the instantaneous recovery in the cyclic RH tests upon unloading is found to be close to the instantaneous deflection upon loading. The recovery curves, like the creep curves, also fluctuate up and down during desorptions and adsorptions, respectively. As shown in Fig. 5.5, the slowest cyclic RH, test V14, yields the most creep, the most recovered deflection, and the most unrecoverable deflection among the four test series (V1, V2, V7, and V14). It can therefore be concluded that the slower cyclic RH yields both more viscoelastic and viscous deflections.

The creep curves can also be plotted on logarithmic scale as shown in Fig. 5.6 for four cyclic RH tests. On logarithmic time schedule, it is easy for long-term predictions. They are presented in Chapter 6.

5.4 Effect of Cyclic Frequency on Creep

Four series of cyclic RH creep tests were conducted in the experiment. The only environmental difference among the four series was the frequency of the RH changes; that is, the duration of each RH level was different. The yielded creep deflections of OSB and plywood panels were found to be different in the four series. As the fractional deflections listed in Table 4.30 show, the slowest cyclic test, V14 (14 days/cycle), yielded the most creep deflections among the four test series.

The six week fractional deflections of OSB panels vs. RH cyclic period is plotted in Fig. 5.7, which clearly shows that the developed creep deformation is related to the rate of cyclic RH changes. The differences of creep deflection caused by the cyclic frequency are very large. The creep deflections developed in the slower cyclic RH test can be several times more than those of the fast cyclic RH tests within only a six week creep duration. In the range of cyclic frequencies adopted in the experiment, from 1 day/cycle to 14 days/cycle, the final fractional deflections at the sixth week are approximately proportional to the period of RH cycling, as shown in Fig. 5.7. Therefore, it is appropriate to conclude that the slower cyclic RH changes yield more creep deflections in OSB within the cyclic periods ranging from of 1 to 14 days per cycle.

Yeh et al. (1990) tried to explore the effect of cyclic RH frequency on the creep behavior of structural flakeboard. They tested two cyclic frequencies, 66 days/cycle and 4 days/cycle. Their creep test duration is 100 days. During the time less creep is

reported in the slower cyclic test (66 days/cycle). They reach the conclusion that the slower RH cycles give less creep. However, it seem that there is not sufficient evidence to reach this conclusion. First of all, the difference between the two cyclic frequencies adopted in their experiment was very large. Secondly, the total creep duration of 100 days allowed only 1.5 full cycles in the slow cyclic test. The accelerating effects of cyclic RH on creep might not be fully demonstrated in the slow cyclic test within such a short duration. Therefore, it is not appropriate to report the conclusion that fast cyclic RH gives more creep.

5.5 Effect of Panel Thickness on Creep

The creep differences between the panels in each individual test series are attributed to the difference in panel thickness. To indicate the effect of panel thickness on creep, the fractional deflection vs. time curves for OSB panels with both thicknesses in test V1 and V7 are shown in Figs. 5.8 and 5.9, respectively. The thinner panels (9.5 mm thick) creep more than the thicker panels (15.9 mm thick) in both tests. This was true for all the cyclic RH tests conducted in the experiment. The figures also show that the creep differences between two thicknesses are also affected by the cyclic frequency. The creep differences between two panel thicknesses are larger in test V7 than those in test V1. The slower the frequency, the larger the creep differences between two thicknesses. In other words, the effect of panel thickness on creep in a cyclic RH environment is more pronounced with slower cycling. The effect of panel thickness on creep is correlated with the environmental cyclic RH changes.

Although more creep is found in thinner panels, careful study of the test data also shows that the thinner panels creep less during adsorptions and recover less during desorptions when compared with the thicker panels. However, the overall creep increment after one full cycle is larger in thinner panels. A schematic plot is given in

Fig. 5.10, where FD_3 is the fractional deflection increment after one full cycle for 9.5 mm OSB panels. FD_5 has the same meaning but for 15.9 mm OSB panels. These phenomena may be caused by the MC situations in the panels. The moisture diffusion analysis results (will be presented in Section 7.4.2) show that the gradients of moisture distribution along panel thickness are close for both thicknesses during the RH cycles, and the average MC or the MC in the middle of thinner panels are close to that of the thicker panels. Because the same moisture changes in the panel surfaces causes more stiffness changes in thicker panels due to the larger distance from the neutral axis, the fluctuations of creep deflection are larger in thicker panels.

5.6 Effect of Strand Orientation on Creep

The strand orientation of OSB panels at the two outside layers is at right angles with that of the core layer. (Three layer plywood has a similar arrangement). With such arrangement, the bending stiffness of the panels parallel to the surface strand is much larger than that of the panels perpendicular to the surface strand. This fact is demonstrated by the short-term flexural test results listed in Table 4.8. Therefore, both instantaneous and creep deflections of perpendicular panels are much larger than those of parallel panels. When considering the fractional deflections as shown in Table 4.30 or Fig. 5.7, which are the ratios of total deflection to instantaneous deflection, there is no significant difference in general between the two bending directions. This shows that the fractional creep development has little correlation with the bending direction, although the absolute stiffness is several times different between the two bending directions. The results obtained here are consistent with those reported by Bach and McNatt (1990).

Creep compliance is usually used to present the time-dependent flexibility of a panel. As stated before, a panel's creep compliance is very different when it is bending

in two different directions, even though the fractional deflections of a panel bending in the two directions are close. The creep compliance can be calculated as

$$J(t) = F(t)/MOE \tag{5.1}$$

Where $J(t)$ = creep compliance at creep time t

$F(t)$ = fractional deflection at creep time t

MOE = modulus of elasticity from short-term test as in Table 4.8.

The creep compliance of 15.9 mm OSB panel for both bending directions are plotted in Fig. 5.11. The big stiffness difference between the two bending directions can be clearly identified from the two curves shown in the figure.

In some cases, the fractional deflection of perpendicular panel also appears to be a little larger than that of parallel panel, especially when the total creep deflection is large, such as in test C85. This may be attributed to the large absolute deflection in perpendicular panel during creep tests. Since horizontal reactions from the two supports did exist (due to friction) during the experiment (although the reactions were theoretically supposed to be zero), a bending moment - which resulted from the reactions and the panel deflection - was imposed upon the sustained load. This extra bending moment could have lead to extra deflection, which could have resulted in larger total deflection.

The creep compliance of 15.9 mm parallel OSB and plywood panels is plotted in Fig. 5.12 and Fig. 5.13 for cyclic test V7 and indoor test I3, respectively. The creep compliance curves plotted in those two figures can represent the actual creep deflection of OSB and plywood. With combination of larger MOE and less fractional deflection, the actual time-dependent deflection of plywood can be much less than that of OSB,

especially in high or cyclic humidity environment.

5.7 Effect of Panels' MC Level and MC fluctuations on Creep

As described in the previous sections, the wood panel creep was strongly affected by environmental RH level, frequency of cyclic RH, and panel thickness. In fact, all these factors are related to the wood panel moisture content saturation during creep, which includes the MC level and moisture movement in the panels. The following discussion deals with some aspects of the relationship between the panel creep and the panel MC. A creep analysis model is constructed in Chapter 8, and is based upon the relationships summarized here .

As discussed in Sec. 5.2, the wood panels creep is severely affected by a high environmental RH or a high MC in the panel. The cyclic RH creep test results discussed in Sects. 5.3 and 5.4 conclude that both slower cyclic frequency and thinner panel thickness yield more long-term deflection. Much more creep develops during the first RH cycle than during the subsequent cycles. To explore the effect of MC on panel creep, the average MC, the MC fluctuation range during cyclic RH, and the fractional deflection after six weeks of sustained loading are all taken from the experimental measurements, and are presented in Table 5.1.

When comparing results about MC and creep listed in Table 5.1, a higher overall panel MC level and a larger MC fluctuation are found in the slower cyclic RH tests. In the mean while, more creep deformation is also found in slower cyclic RH. Although a close average MC level is found for panels with different thickness during cyclic RH, larger MC fluctuations and more creep deflections are found in thinner wood panels. This factor indicates that not only the overall MC level of panel, but also the ranges of MC fluctuation affect wood panel creep. Both the higher overall MC and the larger MC

fluctuation produce more creep. Test series V1 (1 day/cycle) and V2 (2 days/cycle) show relatively closer MC fluctuation ranges (ΔMC in Table 5.1) than test series V7 (7 days/cycle) and V14 (14 days/cycle), and the resultant creep deflections are also close in the first two tests when compared with those of the later two tests.

The correlation between the panels' MC situation and creep deformation is also demonstrated by the deformation development in the panels' first desorptive and adsorptive processes as discussed in Sec. 5.3. Creep develops quickly when the panels' MC is lost or gained for the first time, and the first adsorption produces even more creep deflection than the first desorption.

The results of the three creep test in indoor environmental conditions also show the influence of the panel MC on creep deflection. Panels in test series I2 had a higher MC compared with the other two series since it was carried out during the summer. The panels' creep deflection in test I2 was also found to be the largest among the three indoor test series.

5.8 Discussion Based on Statistical Analysis Procedures

In this section the importance of each variable designed in the experiment , such as cyclic period and panel thickness, is analyzed by statistical procedures. The analysis of variance (ANOVA) and the regression analysis are carried out to provide the significance level of all the variables which might affect the wood panel creep. The validity of the analysis procedures is examined, and the correlation coefficients between creep and the variables are also provided.

5.8.1 Variables Affecting Creep under Cyclic RH by ANOVA

When comparing variables affecting the 6 week OSB panel creep , the experimental

layout is as follows: There were four test series with different RH cyclic periods. Within each test series, the nominal thickness of panels was tested. In each panel thickness group, there are two bending directions, parallel and perpendicular. For each combination of panel thickness and bending direction, four samples/replications were tested. Therefore, the experiment was a $4 \times 2 \times 2$ factorial experiment. To test the significance of the variables which may affect wood panel creep, the ANOVA is carried out by a statistical software program, SAS (1990), on the population means of the six week fractional deflections, and the number of observations in the data set (available in Table 4.30) is 64 ($4 \times 4 \times 2 \times 2 = 64$). The analysis results are listed in Table 5.2.

In the ANOVA, the null hypothesis to be tested is that population means are equal. In Table 5.2, the numbers in the column under "$P_r > F$" show the probability when the null hypothesis of no difference between population means is true. When the number of "P_r" is small, which means that the probability of equal population means in the corresponding variation source is small, it is concluded that the variation source is significant. On the other hand, when the number of "P_r" is large, the null hypothesis cannot be rejected. In most cases, 5 and 1 percent significance levels are customarily used. If the probability (that the null hypothesis is true) is less than 5 but not less than 1 percent, the difference between the means is said to be *significant* (*). If the probability is less than 1%, the difference is said to be *highly significant* (**). Acceptance of the null hypothesis may be indicated by the letters "ns" (*not significant*).

The ANOVA results listed in Table 5.2 show that the cyclic RH period (P), the panel thickness (T), and the interaction between cyclic period and panel thickness (P*T) are highly significant. The strand orientation (O) is significant. Other factors such as interaction between cyclic period and strand orientation (P*O) are not significant. The conclusions reached here are consistent with those reported in the previous discussions

except for strand orientation, which is significant according to the ANOVA. However, it was taken as having only slight difference in the discussion of Sec. 5.7. There are two explanations for the inconsistent conclusions. Firstly, because of large deflections in the perpendicular bending panels and the friction from supports, an extra bending moment could lead to extra deflection; consequently, the creep difference might not come from the strand orientation itself. Secondly, the absolute fractional deflection differences between the two bending directions are small, even though the differences do exist according to the ANOVA. The "no creep difference" between the two bending directions can still be used in practice.

Similar ANOVA is carried out using the data of parallel bending panels so as to study the influence of the cyclic period and the panel thickness. The results will be discussed in Sec. 5.8.4.

5.8.2 Variables Affecting Creep under Cyclic RH by Regression Analysis

Another method of determining the factors affecting the OSB panel creep is regression analysis. The regression analysis is carried out when six week fractional deflections are taken as the dependent variable. When all variables (cyclic period, panel's thickness, and strand orientation) are included in the analysis, the independent variable, strand orientation, is found not significant at a 25% level.

A stepwise regression analysis is carried out, the significance level chosen is at a 25% level; the variables tested are cyclic RH period, panel thickness, and strand orientation. After running SAS (1990), a regression equation including variables of period and thickness is reached. The strand orientation is not entered into the regression model because it does not meet the 25% significance level for entry into the model. The

R^2 of the final regression equation is 0.91. The variables in the regression equation are very significant with the significance level of 0.01%.

The validity of the regression analysis carried out in this study has been proved by the following facts; that is, the normal probability plot of residuals is close to a straight line, and the residuals are homogeneous with respect to the variables entered in the regression model.

5.8.3 The Correlation Coefficients

The results of the calculation of the correlation between cyclic period, panel thickness, strand orientation, and panel's fractional deflection after six weeks are listed in Table 5.3. There is no correlation between cyclic period, panel thickness, and strand orientation since they are all parameters arbitrarily chosen in the experiment. The correlation between cyclic period and the final fractional deflection is positive and strong; the correlation between panel thickness and the fractional deflection is negative; the correlation between bending directions and the fractional deflections is weak. The results are consistent with the conclusions reported in the previous sections.

5.8.4 Statistical Analysis for Parallel Bending Panels

As discussed earlier, the experimental results for the perpendicular bending panels may not be adequate to present the creep deflections of the panels because of the possible errors that arose in the experiment. Therefore, only the 6 week creep test results for parallel bending panels are further analyzed here.

When the ANOVA was carried out on the six week' fractional deflections of parallel bending panels, the experiment was a 4×2 factorial experiment. For each cyclic RH period and panel thickness combination, there were four replications. The number of

observation in the data set is 32 ($4 \times 4 \times 2 = 32$), and the ANOVA results are listed in Table 5.4.

From the ANOVA table, the fractional deflection differences between the population means for the cyclic period, for the panel thickness, and for their interactions are all highly significant. This conclusion is consistent with the ANOVA results obtained from the data set including both parallel and perpendicular panels.

When a regression analysis is carried out, the cyclic period, panel thickness, and the regression equation itself are all highly significant. The regression equation has $R^2 = 0.93$.

The correlation coefficients are calculated and listed in Table 5.5. The correlation coefficients are close to the values obtained from the data including both parallel and perpendicular panels.

The agreement between the analysis results from the two data sets (parallel plus perpendicular and parallel only) shows that either data set could be used to present the test results. The effects of the cyclic period and the panel thickness on 6 week panel creep behavior are mathematically shown here by the statistic analysis procedures. Further long-term predictions based on the regression analysis of the creep data are reported in the next chapter.

Table 5.1 OSB Panels' Fractional Deflection and Their MC at Sixth Week

Test ID	Nominal Thickness					
	9.5 mm			15.9 mm		
	FD [a]	ΔMC (%) [b]	$(MC)_{ave}$ (%) [c]	FD	ΔMC (%)	$(MC)_{ave}$ (%)
V1	2.52	1.4	9.0	2.25	0.7	9.2
V2	2.63	1.5	9.4	2.61	1.0	9.8
V7	3.69	3.4	10.2	3.22	2.7	10.3
V14	4.15	4.2	11.2	3.82	3.2	11.4

[a] FD = Fractional deflection of parallel bending panels at 6 week's creep duration, taken from Table 4.14.

[b] ΔMC = MC fluctuation during the last cycle in 6 week duration.

[c] $(MC)_{ave}$ = the average value of panel MC during the last cycle

Table 5.2 Analysis of Variance (ANOVA) Table for Sixth Week Fractional Deflections of OSB Panels in Cyclic RH Tests

Source of Variation	Degree of Freedom	Mean Square	$P_r > F$
Period (P)	4-1=3	8.5607	0.0001**
Thickness (T)	2-1=1	1.5570	0.0001**
Strand Orientation (O)	2-1=1	0.0495	0.0190*
P*T	3x1=3	0.1399	0.0001**
P*O	3x1=3	0.0175	0.1154 ns
T*O	1x1=1	0.0264	0.0826 ns
P*T*O	3x1x1=3	0.0015	0.9106 ns
Error: Sample/P*T*O	(4-1)x4x2x2=48	0.0084	

Table 5.3 Correlation Coefficients between OSB Panels' Sixth Week Fractional Deflections and other Variables

Correlation Coefficient	P	T	O	FD
Period (P)	1.00	0.00	0.00	0.9255
Thickness (T)	0.00	1.00	0.00	-0.2350
Strand Orientation (O)	0.00	0.00	1.00	0.0419
Fractional Deflection (FD)	0.9255	-0.2350	0.0419	1.00

Table 5.4 Analysis of Variance (ANOVA) Table for Sixth Week Fractional Deflections of Parallel Bending OSB Panels in Cyclic RH Tests

Source of Variation	Degree of Freedom	Mean Square	$P_r > F$
Period (P)	4-1=3	4.3801	0.0001**
Thickness (T)	2-1=1	0.5888	0.0001**
P*T	3x1=3	0.0690	0.0013**
Error: Sample/P*T	(4-1)x4x2=24	0.0096	

Table 5.5 Correlation Coefficients between Parallel Bending OSB Panels' Sixth Week Fractional Deflections and other Variables

Correlation Coefficient	P	T	FD
Period (P)	1.00	0.00	0.9415
Thickness (T)	0.00	1.00	-0.2039
Fractional Deflection (FD)	0.9415	-0.2039	1.00

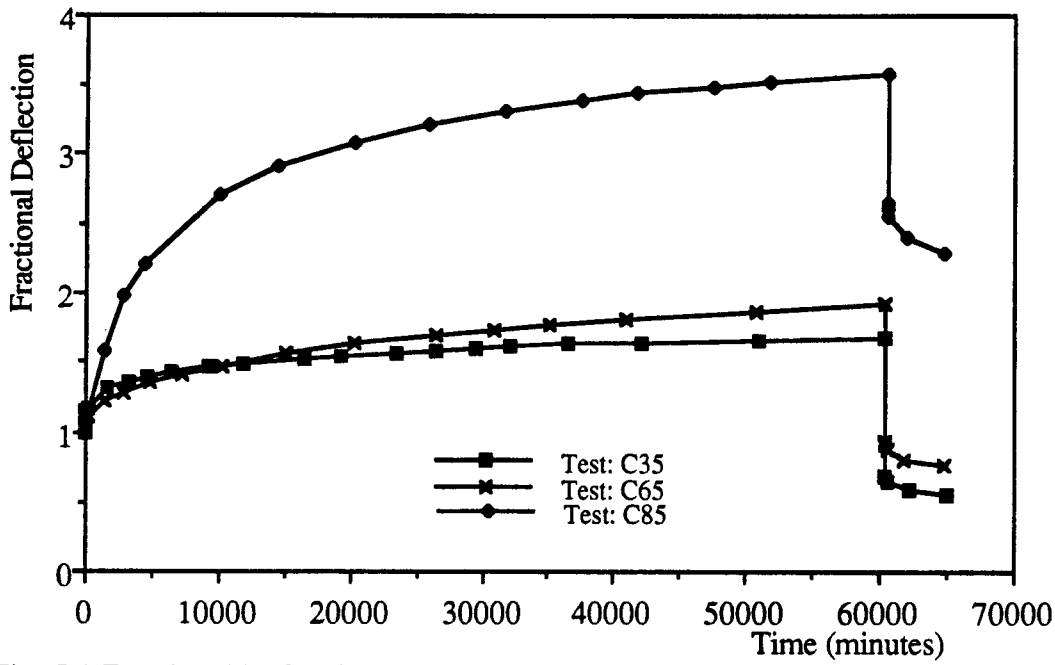

Fig. 5.1 Fractional Deflection vs. Time Curves for the 15.9 mm Parallel OSB Panels under Sustained Loading for Six Weeks in the Three Constant RH Conditions

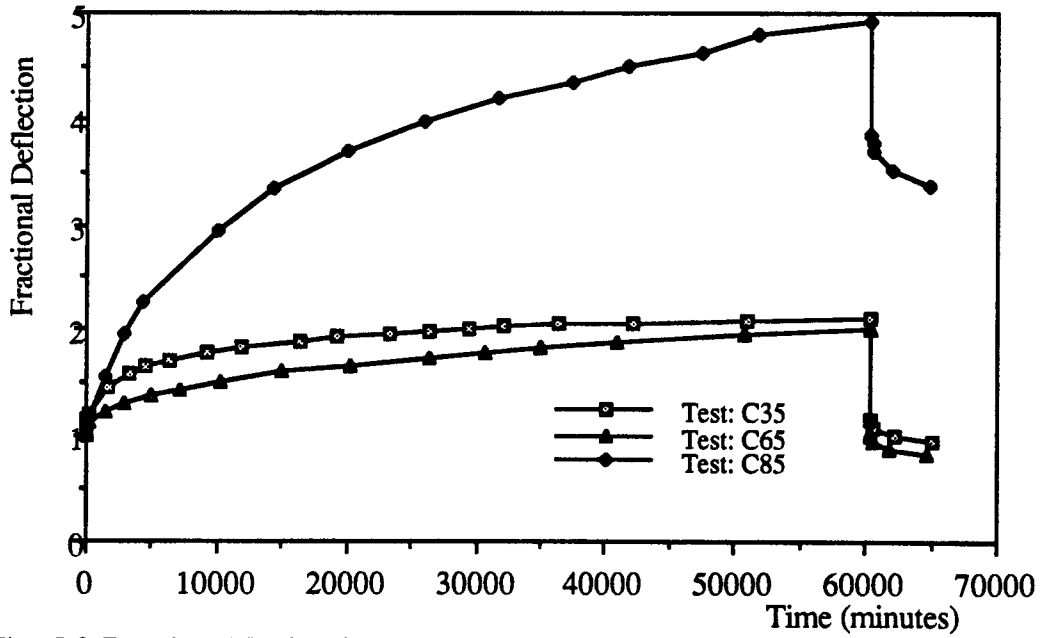

Fig. 5.2 Fractional Deflection vs. Time Curves for the 9.5 mm Perpendicular OSB Panels under Sustained Loading for Six Weeks in the Three Constant RH Conditions

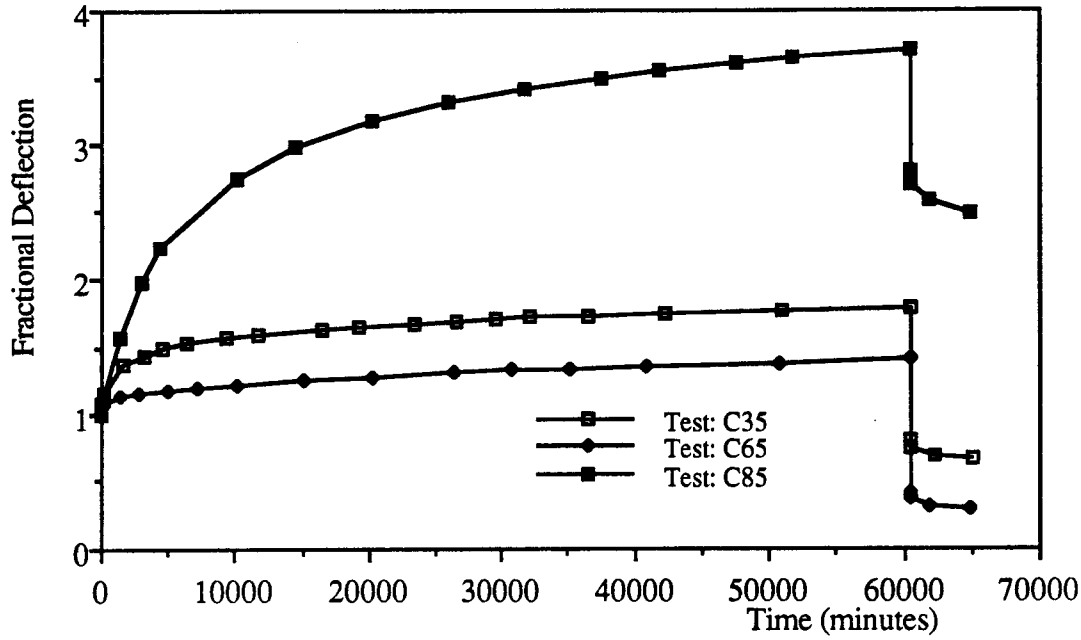

Fig. 5.3 Fractional Deflection vs. Time Curves for the 9.5 mm Parallel OSB Panels uunder Sustained Loading for Six Weeks in the Three Constant RH Conditions

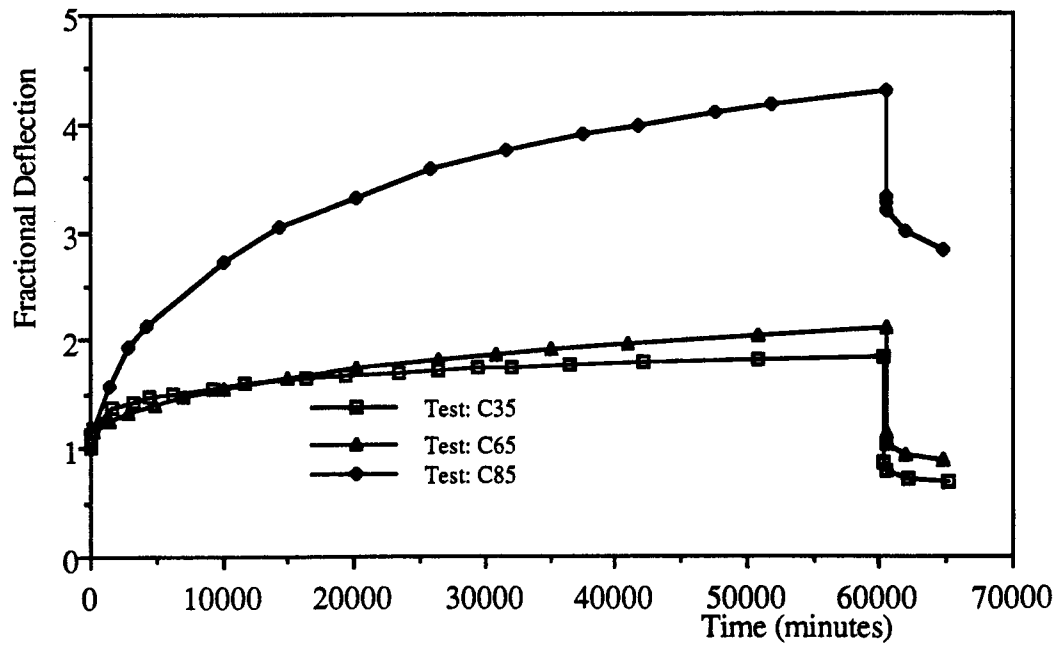

Fig. 5.4 Fractional Deflection vs. Time Curves for the 15.9 mm Perpendicular OSB Panels under Sustained Loading for Six Weeks in the Three Constant RH Conditions

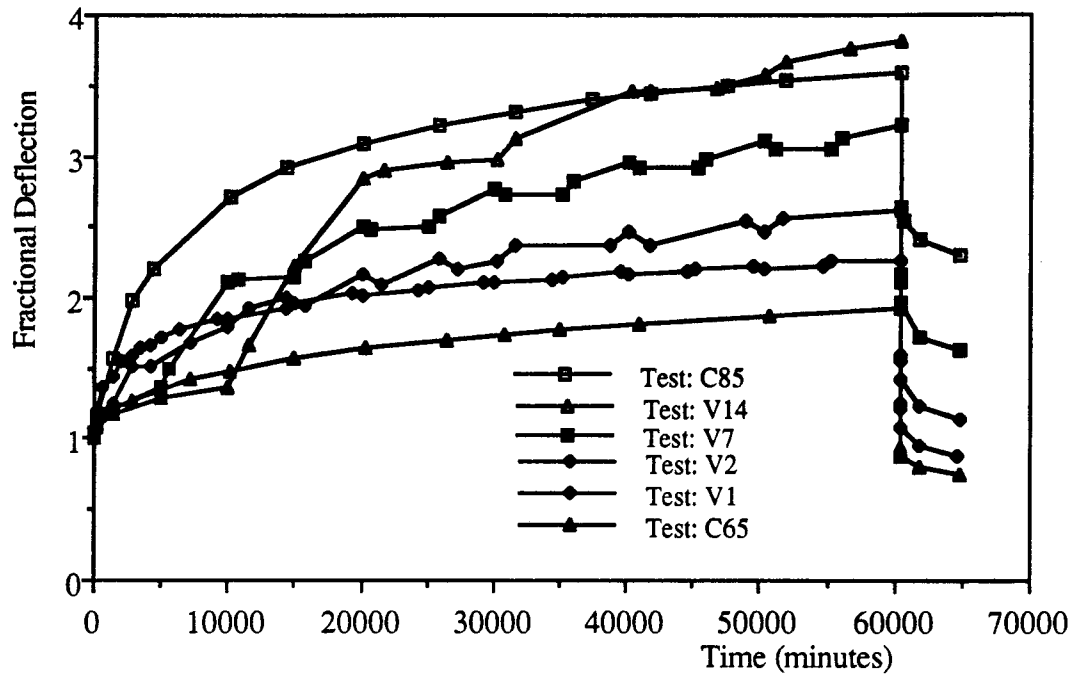

Fig. 5.5 Fractional Deflection vs. Time Curves for the 15.9 mm Parallel OSB Panels under Sustained Loading for Six Weeks in the Four Cyclic RH and 65% and 85% Constant RH Conditions

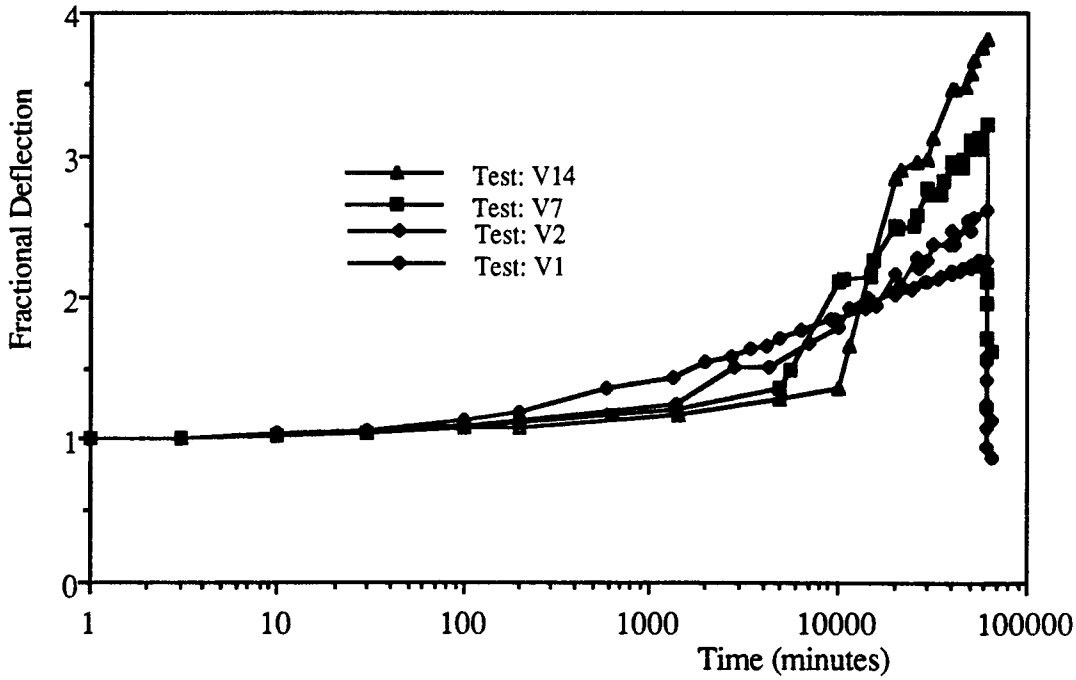

Fig. 5.6 Fractional Deflection vs. Time Curves for the 15.9 mm Parallel OSB Panels under Sustained Loading for Six Weeks in the Four Cyclic RH on Logarithmic Time Scale

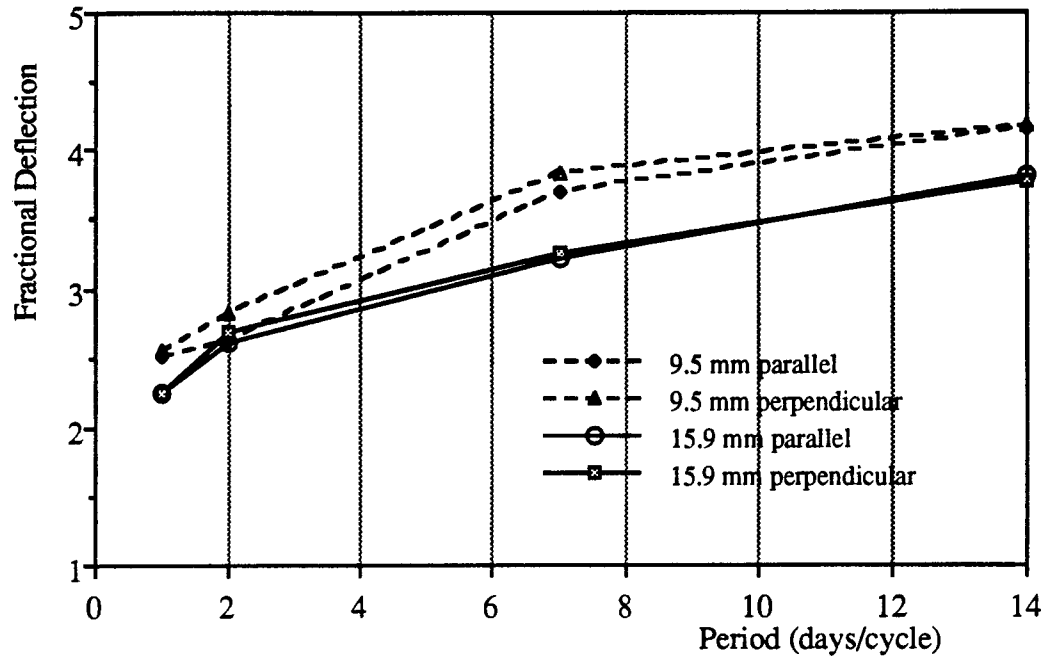

Fig. 5.7 Six Weeks' Fractional Deflection vs. Cyclic Period for OSB Panels under Sustained Loading for Six Weeks in the Cyclic RH Conditions

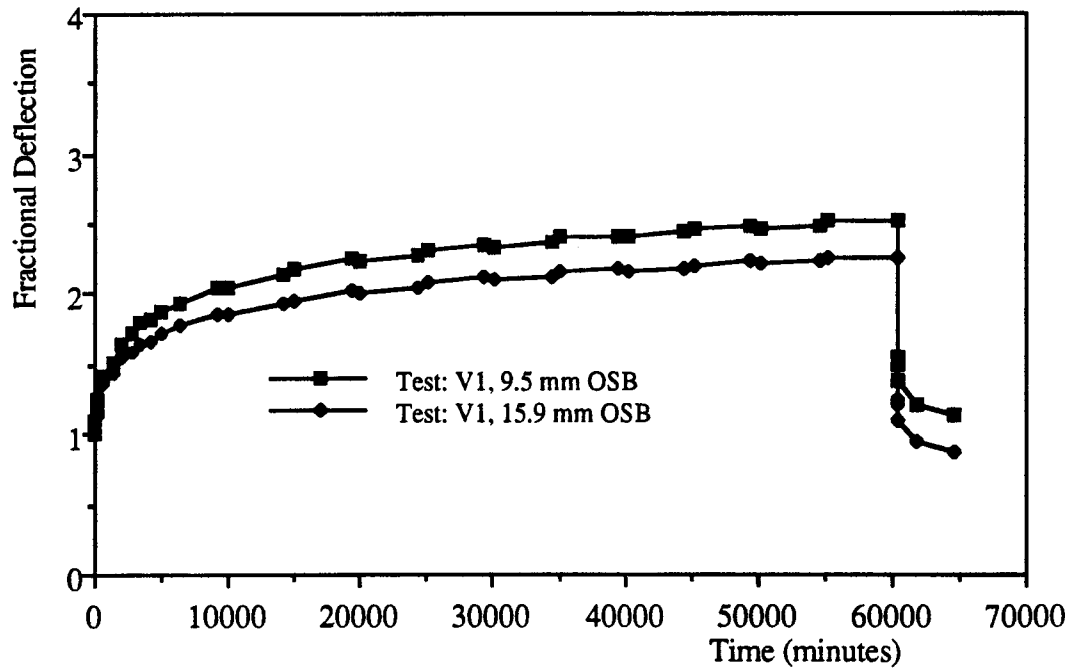

Fig. 5.8 Fractional Deflection vs. Time Curves for the Parallel OSB Panels with Two Thicknesses under Sustained Loading for Six Weeks in Test V1 (1 day/cycle)

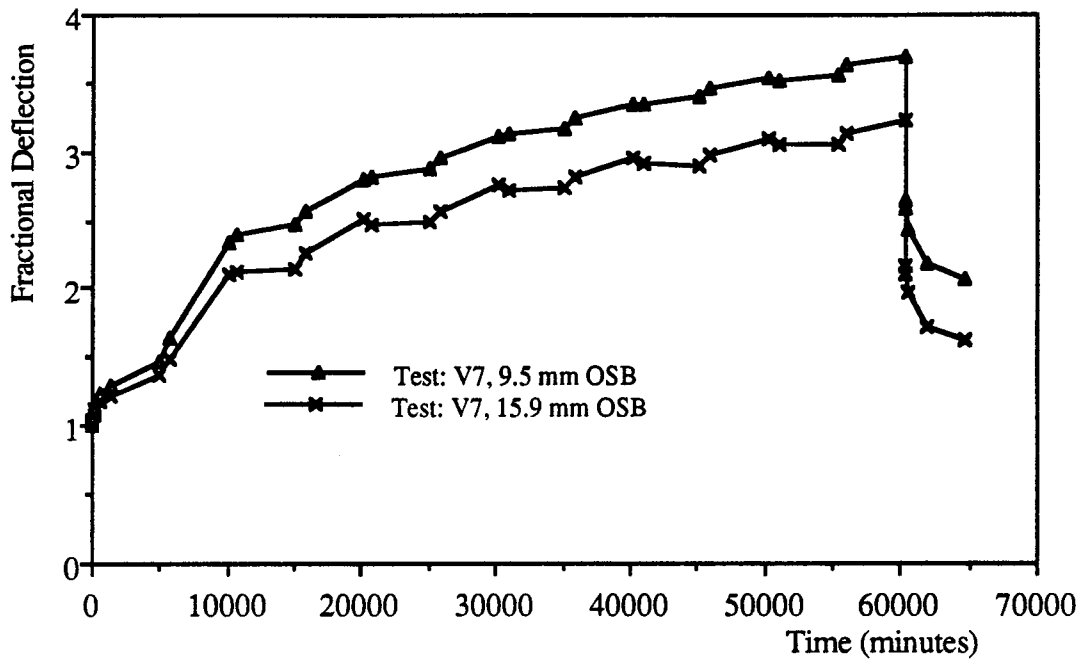

Fig. 5.9 Fractional Deflection vs. Time Curves for the Parallel OSB Panels with Two Thicknesses under Sustained Loading for Six Weeks in Test V7 (7 days/cycle)

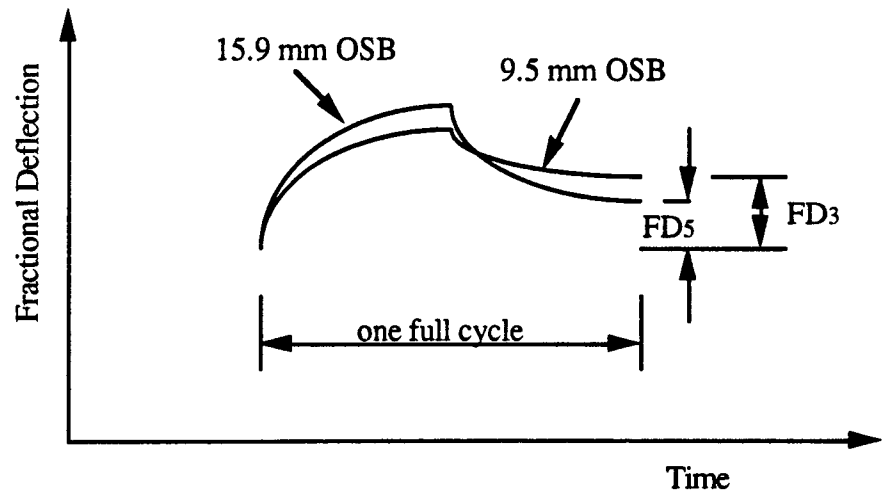

Fig. 5.10 A Schematic Plot of Creep Deflection Development of Panels with Two Different Thicknesses in One Full RH Cycle in the Cyclic RH Environment

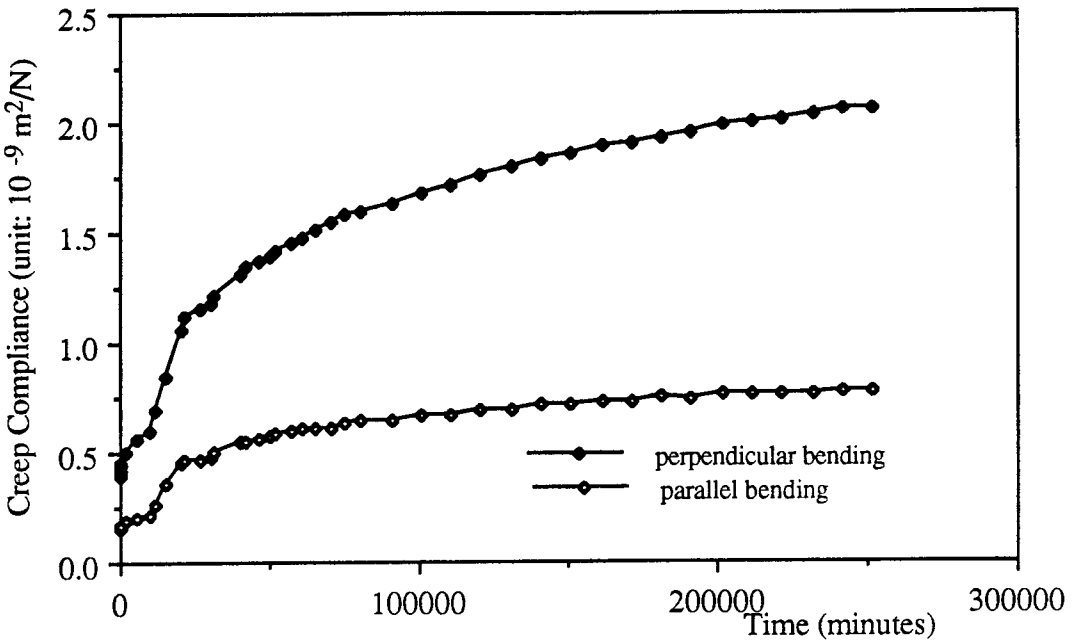

Fig. 5.11 Creep Compliance of 15.9 mm OSB Panels with Two Bending Directions under Sustained Loading for 25 Weeks in Cyclic RH Test V14

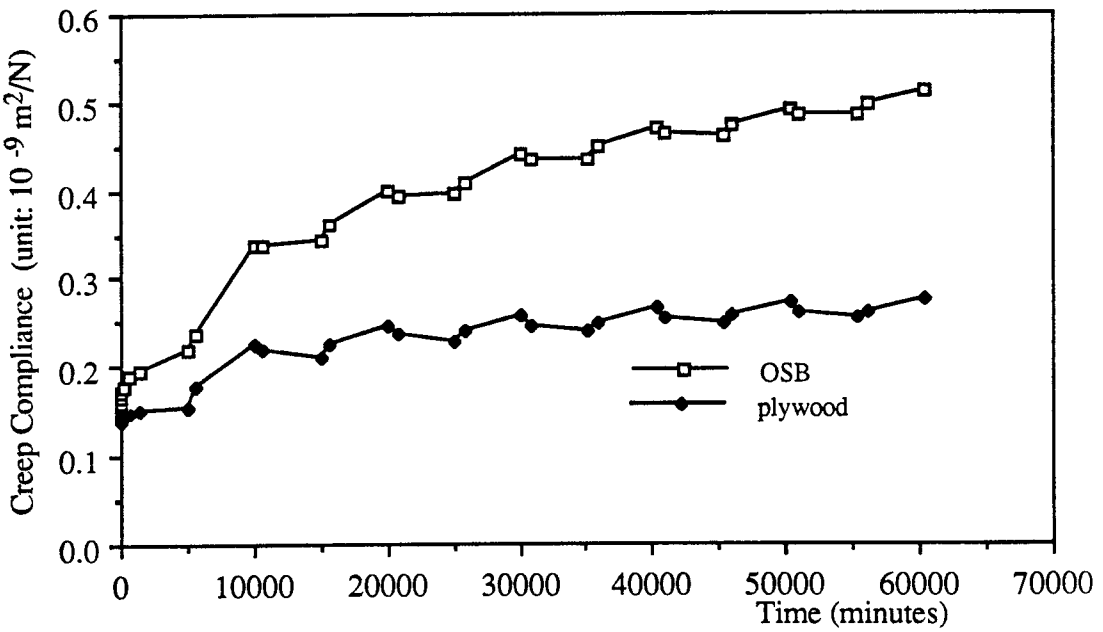

Fig. 5.12 Creep Compliance of 15.9 mm Parallel OSB and Plywood Panels in Cyclic RH Test V7

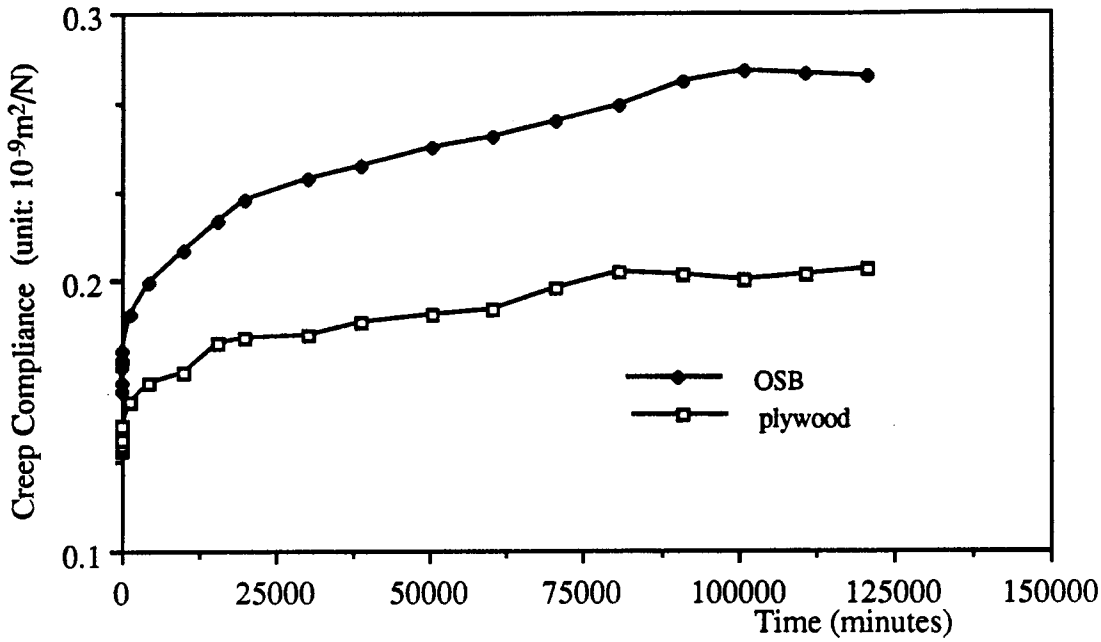

Fig. 5.13 Creep Compliance of 15.9 mm Parallel OSB and Plywood Panels in Indoor Environment Test I3

Chapter 6 Long-term Creep Deflection Prediction

6.1 General

In this chapter, curve fitting and regression analysis techniques are used to analyze the OSB creep test data. The major objective of the analyses is to predict OSB panel long-term deflections under the sustained bending load using the creep test results within a relatively short creep duration (6 or 12 weeks). In the process of both curve fitting and regression analysis, the logarithmic time scale rather than the normal time scale, is used. The reason for choosing logarithmic time is that the distance between six weeks and 10 years is fairly small. The long-term prediction results carried out on the logarithmic time scale therefore are reasonably reliable.

One advantage of the prediction method presented in this chapter is that it is easy to use in practice. In a specified environment, the OSB panel creep can be easily estimated by a simple prediction equation. To predict panel creep deflection, the contributions of each individual factor (such as MC level or panel thickness) need not necessarily be known or classified. The validity of the long-term prediction is difficult to check because of the shortage of long-term creep information, but the predictions up to 175 days are validated by the cyclic creep test V14, which lasted for 25 weeks.

In Section 6.2, OSB panels' creep under three constant RH conditions (35%, 65%, and 85% RH) are predicted by curve fitting method applied to the creep test data within six weeks. In Section 6.3, a two-line model is proposed for cyclic RH environments. To determine the parameters in the predicting curve, a stepwise regression analysis procedure is adopted. The significant variables are recognized from the regression analyses, and the final prediction equations are achieved. Long-term creep prediction can be made when information about both the panel and the environment is given.

Section 6.4 gives creep predictions about OSB panels in normal indoor environment by a curve fitting equation based on the twelve week creep test results. Finally, in Section 6.5 the long-term deflections under the various climatic conditions estimated in this chapter are compared with the current Canadian code (CAN-O86.1-M89) and Eurocode No. 5 (1991).

6.2 Creep Prediction for Constant RH Conditions

6.2.1 Multiple Linear Regression Model

The observed fractional deflections of OSB panels can be plotted on a logarithmic time scale, such as shown in Fig. 6.1 for 9.5 mm parallel bending OSB panels in test C35 (35% RH constant). A multiple linear regression technique is used to achieve the regression equations for the creep of OSB panels in constant RH environments. The regression model proposed here includes both linear and quadratic polynomial terms. With the definition of fractional deflection, the regression curves should go through 1.0 at $t = 1.0$ minute ($log(t) = 0.0$). The proposed regression equation is

$$\hat{F} = 1.0 + b_1 log(t) + b_2 log^2(t) \qquad (6.1)$$

where $\hat{F}$ = the expected value at any time t ($t > 1$ *min.*) for fractional deflection of OSB panels

b_1, b_2 = the partial regression coefficients

t = creep time elapsed from uploading, minute.

The observed fractional deflection, F_i, can be expressed as

$$F_i = \hat{F} + e_i = 1.0 + b_1 log(t) + b_2 log^2(t) + e_i \qquad (6.2)$$

where e_i is the experimental error or residual, which is the difference or deviation between the measured and expected value.

The criterion used for best fitting the test data adopted here is the least-squares criterion. This requires the sum of squares of the deviation (e_i) to be a minimum; that is, $\sum_i (F_i - \hat{F})^2$ or $\sum_i (e_i)^2$ is a minimum. A parameter to measure how well the regression model fits the experimental data is R^2 , which is defined as the sum of the squares of the regression model divided by the total sum of the squares. The R^2 can be expressed as

$$R^2 = \frac{\sum (\hat{F} - \overline{F})^2}{\sum_i (F_i - \overline{F})^2} \tag{6.3}$$

where $\overline{F}$ = the mean of the observed fractional deflection

F_i, $\hat{F}$ = the same as defined before.

Usually, the larger the R^2, the better the model fits the test data. Theoretically, $R^2 = 1.0$ for perfect fitting, which means no error ($e_i = 0$), but it never happens in practice because the experimental error always exists.

6.2.2 Regression Equations for Constant RH

According to the regression model given by Eqn. (6.1), the regression equations are obtained for 9.5 mm OSB parallel loaded panels under constant RH environments in test C35, C65, and C85. The estimated parameters b_i's and R^2 are given in Table 6.1. As shown in the table, the R^2's for the three regression equations are all very close to 1.0, which means that the equations fit the test results very well.

As discussed in Chapter 5, the fractional creep differences between panels with

different strand orientations/thicknesses are small in constant RH environments. For easy long-term prediction, the test data of OSB is not separated according to panel thicknesses and strand orientations in a constant RH environment. A "least square regression" curve is based on the data from all types of tested OSB panel under one RH condition. The estimated parameters (b_i's) for the three regression equations, the equation R^2's, and the panel predicted fractional deflections at ten years are all listed in Table 6.2. The R^2's in Table 6.2 are smaller than R^2's in Table 6.1 because of the existing creep differences between different types of OSB panels. The test data with fitted curves are plotted in Fig. 6.2 for the three RH levels. It is noticed that the parabolic curves may have negative slope for the early creep stage, which is not realistic. However, the overall regression equations could still give good long-term predictions as shown in Fig.6.2.

The results of the creep tests show that the OSB panels exposed to 85% RH had much larger fractional deflections after six week creep duration, and the low (35%) or intermediate (65%) RH produced much less creep during six weeks than did 85% RH. The same conclusion can be extended to the panel long-term deflection according to the predictions given in Table 6.2, which shows that OSB panels exposed to 85% RH have very high long-term fractional deflection values. The deflection after ten years could be about nine times that of its initial elastic deflection. The predicted long-term creep under low or intermediate RH is relatively small.

6.3 Creep Prediction for Cyclic RH Conditions

6.3.1 Bilinear Prediction Model

The fractional deflection curves of 15.9 mm parallel OSB panel under cyclic RH are shown in Fig. 6.3 on a logarithmic time plot. The fractional deflections can be modeled

as two straight lines, one for the first half cycle and the other for the creep time longer than the first half cycle. The observed fractional deflections for other types of panel have a similar tendency during cyclic RH when plotted on a logarithmic time scale, as shown schematically in Fig. 6.4, where the second straight line can be portrayed by a linear equation, $F = A + K\,log(t)$. The parameters (A and K) determined by panel creep behavior are different for various environmental/panel conditions. To achieve an empirical expression of the second straight line for various situations, the linear equation for calculating creep at time t, which is longer than the first half cycle, can be rewritten as

$$F(t) = F(t_1) + K(\log t - \log t_1) \tag{6.4}$$

where $F(t_1)$ = the fractional deflection at time t_1, which is longer than the first half cycle, for the anticipated OSB panel and the environmental conditions; if not available, an estimate of $F(t_1)$ for $t_1 = 6$ weeks (60480 minutes) can be calculated by the following regression equation obtained from the creep data of OSB panels in the four cyclic tests

$F(t_1) = F(60480\,min) = 2.953 + 1.408\log p - 0.049\log h$

K = the slope of the straight line; if not available, an estimate of K can be calculated by the regression formula based on the cyclic creep tests results

$K = 1.026 + 0.180p - 0.042h$

p = period of cyclic RH (between 35% and 85%), days

h = nominal thickness of OSB panels, mm.

For creep time less than the first half of the cyclic period, an interpolation can be made to estimate the fractional deflection on a logarithmic time plot, as shown in Fig. 6.4. It should be noted that the prediction equations are obtained from the creep test

results within six weeks. The validity of the model's long-term prediction after six weeks needs to be checked by creep tests with a longer creep duration.

6.3.2 Stepwise Regression Analyses

A physical variable may be affected by many independent variables. Sometimes, it is hard to tell whether or how each independent variable affects this physical variable. A multiple regression analysis technique provides an approach to recognize the significant variables among a set of independent variables and their effects on the dependent variable. *The "best" regression equation* (Draper and Smith, 1981) is expected to make the equation useful for prediction purposes, and includes as few independent variables as possible.

There are many procedures to select the "best" regression equation. The stepwise regression procedure (Draper and Smith, 1981) is carried out here to select the "best" regression equations for both $F(t_1)$ and K. In general, let Y be a dependent variable and X_i ($i = 1,2,\ldots,n$) be independent variables. $\hat{Y}$ is the expected or predicted value. $\overline{Y}$ is the mean of Ys. The basic procedure for stepwise regression analysis is as follows.

First, select the X, which is most correlated with Y (suppose it is X_1), and find the linear equation $\hat{Y} = f(X_1)$. Whether the variable is significant is then checked. If it is not significant, the model $\hat{Y} = \overline{Y}$ is adopted as best; otherwise the second variable to enter regression is searched for.

Secondly, the X_j with the highest partial correlation coefficient with Y is now selected (suppose it is X_2) and a second regression equation $\hat{Y} = f(X_1,X_2)$ is found. The overall regression equation is checked for significance and the two F-values for both variables (X_1,X_2) now in the equation are examined. The lower of the F's is

then compared with a specified F value (25% significant level is chosen here), and the corresponding independent variable is retained or rejected according to whether or not the test is significant.

Thirdly, repeat the process described above until all the variables left in the equation are significant and no other variables meet the significant level for entry into the model. The "best" regression equation is then obtained.

To assure a valid regression analysis, the basic assumption involved is that the error (or residual) of the regression model is random. Therefore, the randomization of the error should be checked after the regression equation is achieved.

6.3.3 Regression Analyses for $F(t_1)$ and K

In the prediction model given by Eqn. (6.4), both $F(t_1)$ and K must be known to specify the prediction line. The $F(t_1)$ and K are a specified point and slope of the straight line in Fig. 6.4. When the creep data ($F(t_1)$ and K) of the panel are not known, the estimation of those two variables could be computed by the following regression equations.

Regression Equation for $F(t_1)$

The six week fractional deflection is taken as $F(t_1)$ ($t_1 = 60480$ minutes) in the following discussion. The data used for regression analysis are fractional deflections at six weeks, which consist of four different cyclic frequency tests, panels with two thicknesses, and two different strand orientations. In each case, there are four replicated panels, and therefore a total sixty-four observations ($4 \times 2 \times 2 \times 4$) in the regression analysis. The independent variables include cyclic frequency, panel thickness, strand orientation, and also functions of those variables, such as inverses

and logarithms, etc. thought to be desired and necessary. Several regression models, including different sets of independent variables, are tried by stepwise regression procedure using SAS. By examining regression model's R^2 and the validity of the obtained model (checking the residuals), the Eqn. (6.5) is achieved as an expression for computing fractional deflection at six weeks or 60480 minutes:

$$F(t_1) = F(60480\,min) = 2.953 + 1.408 \log p - 0.049 \log h \qquad (6.5)$$

where p = period of cyclic RH, days/cycle

h = nominal thickness of OSB panels, mm.

The regression analysis yields $R^2 = 0.96$ for the regression model, and the independent variables ($log\ p$, $log\ h$) in the equation are all significant at 0.01% level. A normal probability plot of the residuals from SAS output shows a close to straight line trend, which implies that the residuals are random and the regression model is therefore valid.

Regression Equation for K

To obtain a regression equation for the slope K, the slopes from the creep tests should first be obtained. As shown in Fig. 6.3, the observed fractional deflections after the first half cycle in cyclic RH tests are close to a straight line on a logarithmic time plot. A straight line fitting is undertaken for observed fractional deflections from four replicated panels with the same nominal thickness and the same strand orientations. The slope from the straight line fitting is taken as an experimental observation under the specified cyclic RH, panel thickness, and strand orientation combination. The data set used for regression analysis consists of 16 observed slopes for four cyclic RH periods, two panel thicknesses, and two strand orientations.

The same analyzing procedure as for $F(t_1)$ is carried out to get the "best" regression equation for the slope K. The regression equation is selected after trying several models with different independent variables. The "best" regression equation is chosen as

$$K = 1.026 + 0.180p - 0.042h \tag{6.6}$$

where p, h are the same as in Eqn. (6.5).

This regression equation has $R^2 = 0.98$. The basic assumption for a valid regression analysis is also satisfied. The independent variables entered in the regression equation are all significant at 0.2% level.

6.3.4 Predicting Results from the Bilinear Model

When creep time is larger than half of the cyclic period, the fractional deflection of a panel can be estimated by combining Eqns. (6.4), (6.5), and (6.6). The prediction equations for a specific cyclic frequency and a panel thickness can be obtained by giving p and h in Eqns. (6.5) and (6.6). Such prediction equations are summarized in Table 6.3.

For creep time less than half of the cyclic period, an interpolation could be made to estimate the fractional deflection on a logarithmic time plot. Considering that the fractional deflection is defined as 1.0 at 1 minute ($\log t = 0.0$) and the fractional deflection at the end of the first half cycle can be estimated by using Eqns. (6.4), (6.5), (6.6), the fractional deflection within the first half cycle could be estimated by linear interpolation.

The fractional deflection curves of 15.9 mm OSB panels under four different cyclic frequencies predicted by the proposed model are plotted in Fig. 6.5. Long-term

prediction, such as that for ten years, is also shown in the figure. A comparison of the predicted curves with the test results (Fig. 6.3) shows them to be in a good agreement, especially when the creep time is longer than the first half cycle.

The validity and accuracy of the bilinear creep prediction model can be examined. The difference between the predicted fractional deflection and the experimentally observed fractional deflection is called a residual. The residual vs. panel thickness for all test samples in cyclic creep tests after 4 and 6 weeks' sustained loading are plotted in Figs. 6.6(a) and 6.6(b) respectively, and the figures show that the variations of residuals for two panel thicknesses are homogeneous. The residual vs. cyclic period for all test samples in cyclic creep tests after four and six weeks of sustained loading are plotted in Figs. 6.7(a) and 6.7(b), respectively. These figures also show that variations of residuals for four cyclic periods are homogeneous. The homogeneous residuals show the validity of the proposed regression model. In addition, the fractional deflection residuals are all within a range of $\pm$ 0.5, and most residuals are within the range of $\pm$ 0.2. Considering the variation of panels, the error is fairly small and the creep prediction made by the given model agrees, with reasonable accuracy, with the creep test results.

It should be noted that the prediction equations are based on the six week creep tests. The model's validity for long-term prediction after six weeks needs be checked by creep tests with a longer creep duration. As shown by Fig. 6.5, the validity of the model can be checked up to twenty-five weeks by creep test V14. The error at 175 days are - 0.1 and - 0.7 for 9.5 mm and 15.9 mm OSB panels, respectively.

6.4 Creep Prediction for Indoor Environment

The fractional deflections of OSB panels in indoor environment creep test series are

plotted in Fig. 6.8 on a logarithmic time scale. Parabolic curves are also drawn to fit the test data for each test series. Since the three indoor creep test series were conducted during different seasons, the indoor climates were also different from one another. The observed creep is therefore slightly different. To achieve a general prediction equation for the creep of OSB panels in normal indoor environment, the creep test results of the three series are plotted together in Fig. 6.9 to represent the overall indoor climatic conditions for all seasons, and a parabolic curve is drawn to fit the data. Though climatic conditions did fluctuate throughout each creep test, those fluctuations were relatively smooth compared to the cyclic RH. Therefore, the creep differences among panels with different thicknesses and strand orientations are neglected for the prediction purpose. The regression equation for fractional deflection $F(t)$ in a normal indoor environment is obtained as

$$F(t) = 1.0 - 0.084 \log t + 0.056 (\log t)^2 \qquad (6.7)$$

where t = creep time for calculated fractional deflection, minutes

R^2 = sum of squares for the regression model divided by the total sum of squares = 0.88 for the regression equation (6.7).

To predict creep beyond the test duration (12 weeks), an extrapolation can be made by using Eqn. (6.7). Given the 25% increase or decrease in the slope of the predicted curve from Eqn. (6.7), another two curves are obtained, as dashed curves shown in Fig.6.9. Most observed fractional deflections fall within the two dashed curves. The widths of the band are reasonably narrow considering the variations of panels and environment. Therefore, Eqn. (6.7) can be used to predict the creep of OSB panels in indoor conditions with reasonable accuracy. For example, the calculated fractional deflection of OSB at ten years ($t = 5.256 \times 10^6$ minutes) would be approximately 3.0

with a fluctuation between 2.5 and 3.5.

6.5 Comparison of Long-term Creep Prediction Results

Long-term creep prediction can be based upon the prediction models obtained for various climatic conditions. In Table 6.4, ten year creep predictions are made for constant, cyclic, and indoor climates and are also compared to the fractional deflection factors used in the Canadian code (CAN/CSA-O86.1-M89, 1989) and the Eurocode (1991). As mentioned in Chapter 1, the Canadian code does not have explicit expression for creep calculation and a number of two is interpreted for long-term fractional deflection. The European code gives explicit factors for creep calculation for environments with RH mostly less than 65% or 85%. No creep factor is given for RH higher than 85% in the Eurocode (1991).

From Table 6.4, the criteria to limit deflection under sustained loads in the Canadian code becomes inadequate when the loading history and the exposed environment are considered. In the Eurocode No. 5 (1991), the proposed creep factor K_{def} agrees well with the predictions for environmental RH not greater than 65%. When cyclic or high RH climate are encountered, the creep of OSB panels becomes very severe. Neither code gives an adequate description of the amount of creep.

In engineering design, the actual deflection is checked to meet the serviceability requirement. Therefore, not only the fractional deflection should be concerned, but also the MOE of panels should be taken into account.

Table 6.1 Parabolic Curve Fitting Models and Their Fractional Deflection Predictions for 9.5 mm Parallel loaded OSB Panel in Three Constant RH Environments (Valid for t > 1 minute)

		Estimated Parameters [a]		
Test ID	(R^2) [b]	b_1	b_2	F (10years)[c]
C35	0.999	-0.0017	0.03555	2.6
C65	0.976	-0.0141	0.0191	1.8
C85	0.991	-0.3519	0.1948	7.4

[a] The estimated parameters for regression models are obtained based on the Eqn. (6.1).

[b] R^2 is defined by Eqn. (6.3).

[c] The estimated fractional deflection for panels are calculated from the obtained regression equations according to b_i's.

Table 6.2 Parabolic Curve Fitting Models and Their Predictions for Fractional Deflection of All OSB Panels in Three Constant RH Environments (Valid for t > 1 minute)

		Estimated Parameters [a]		
Test ID	(R^2) [b]	b_1	b_2	F (10years)[c]
C35	0.87	-0.014	0.041	2.8
C65	0.77	-0.09	0.052	2.8
C85	0.94	-0.46	0.231	8.3

[a] The estimated parameters for regression models are obtained based on the Eqn. (6.1).

[b] R^2 is defined by Eqn. (6.3).

[c] The estimated fractional deflection for panels are calculated from the obtained regression equations according to b_i's.

Table 6.3 Prediction Equations for Fractional Deflection of OSB Panel under the Four Cyclic RH Conditions

Cyclic Period "p"	Nominal Thickness "h"	Fractional Deflection F(t) at Time "t" (in minutes)	Valid for Time "t"
1 day/cycle	9.5 mm	F(t) = -1.36496 + 0.8061 log t	>0.5 day
	15.9 mm	F(t) = -0.3878 + 0.5365 log t	>0.5 day
2 days/cycle	9.5 mm	F(t) = -1.8028 + 0.9863 log t	>1 day
	15.9 mm	F(t) = -0.82568 + 0.7167 log t	>1 day
7 days/cycle	9.5 mm	F(t) = -5.3451 + 1.8873 log t	>3.5 days
	15.9 mm	F(t) = -4.3679 + 1.6177 log t	>3.5 days
14 days/cycle	9.5 mm	F(t) = -10.9529 + 3.1487 log t	>7 days
	15.9 mm	F(t) = -9.9757 + 2.8791 log t	>7 days

Table 6.4 Comparison of Predicted Ten Year Fractional Deflection with the Canadian and European Codes

	Fractional Deflection at 10-year		
Climates	Canadian code(1989)	European code(1991)	Prediction model
35% Constant	2.0	3.0	2.8
65% Constant	2.0	4.0[b]	2.8
85% Constant	2.0	-	8.3
35-85-35%, 1 day/cycle	2.0	-	4.0[a]
35-85-35%, 2 days/cycle	2.0	-	4.8[a]
35-85-35%, 7 days/cycle	2.0	-	7.3[a]
35-85-35%, 14 days/cycle	2.0	-	10.2[a]
indoor environment	2.0	3.0	3.0

[a] The fractional deflections are calculated for OSB panels with 9.5 mm thickness.

[b] No Creep factor is given for RH higher than 85%.

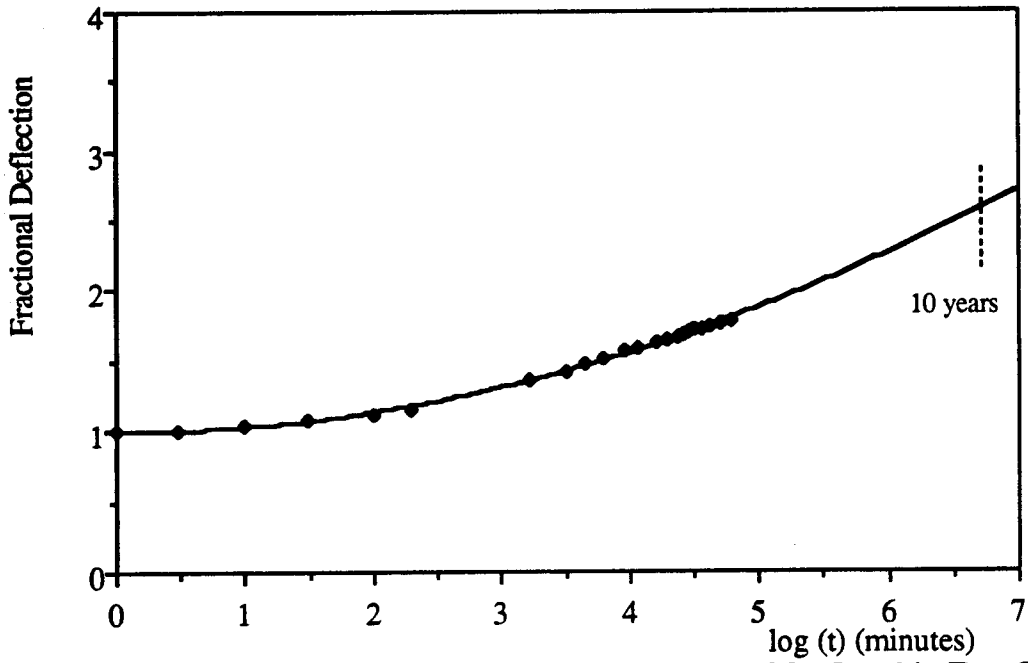

Fig. 6.1 Fractional Deflection of the 9.5 mm Parallel Loaded OSB Panel in Test C35 (35% RH Constant) and the Parabolic Regression Curve

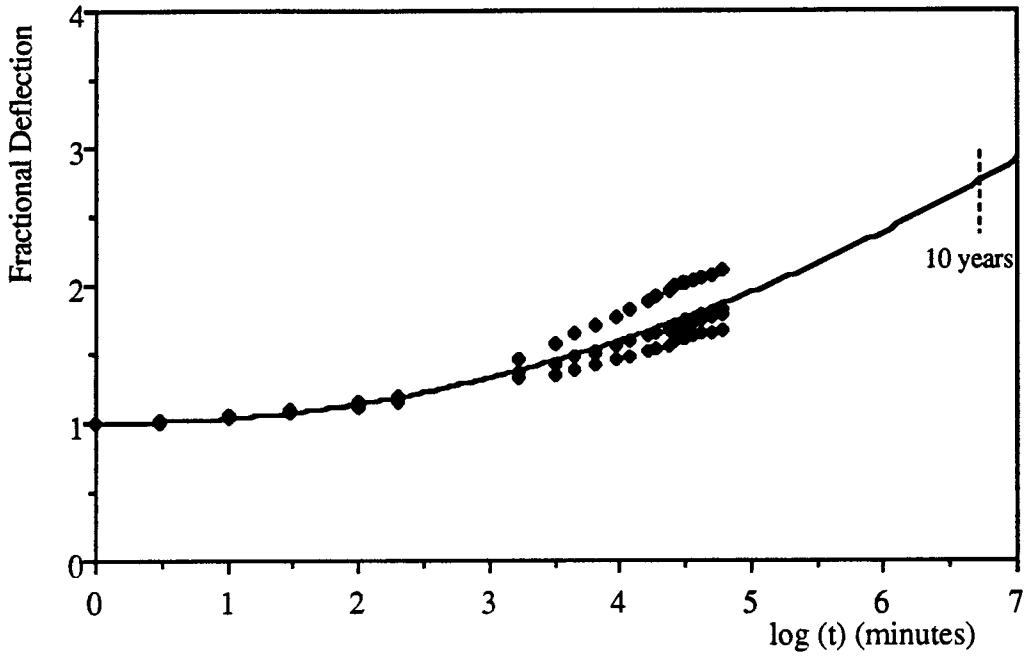

(a) Test C35 (35% RH Constant)

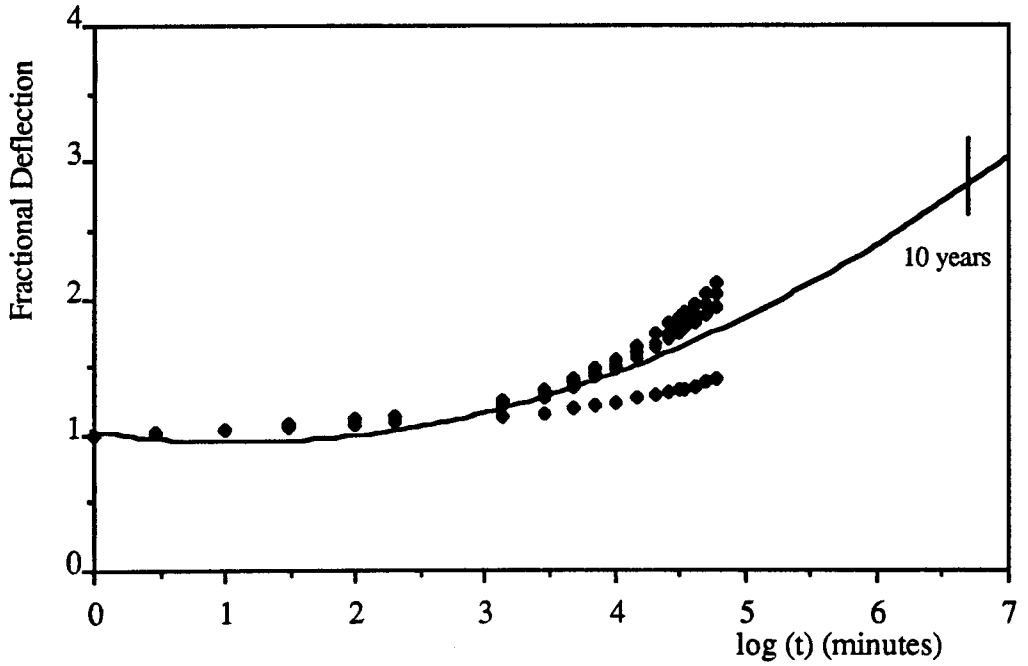

(b) Test C65 (65% RH Constant)

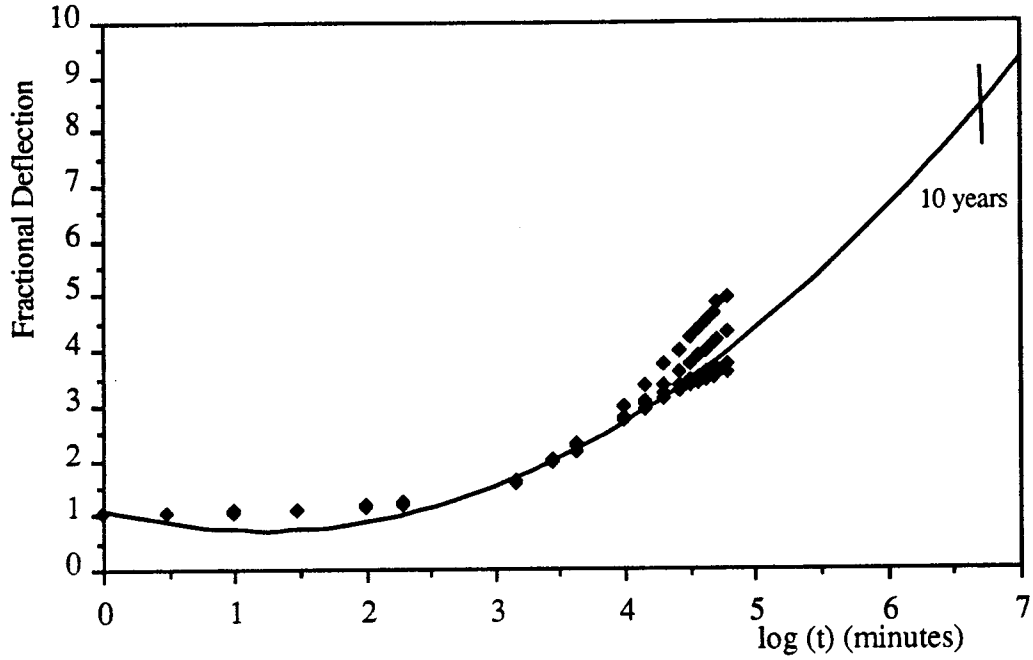

(c) Test C85 (85% RH Constant)

Fig. 6.2 Fractional Deflection of All OSB Panels in Tests C35, C65, C85 and Their Parabolic Regression Curves

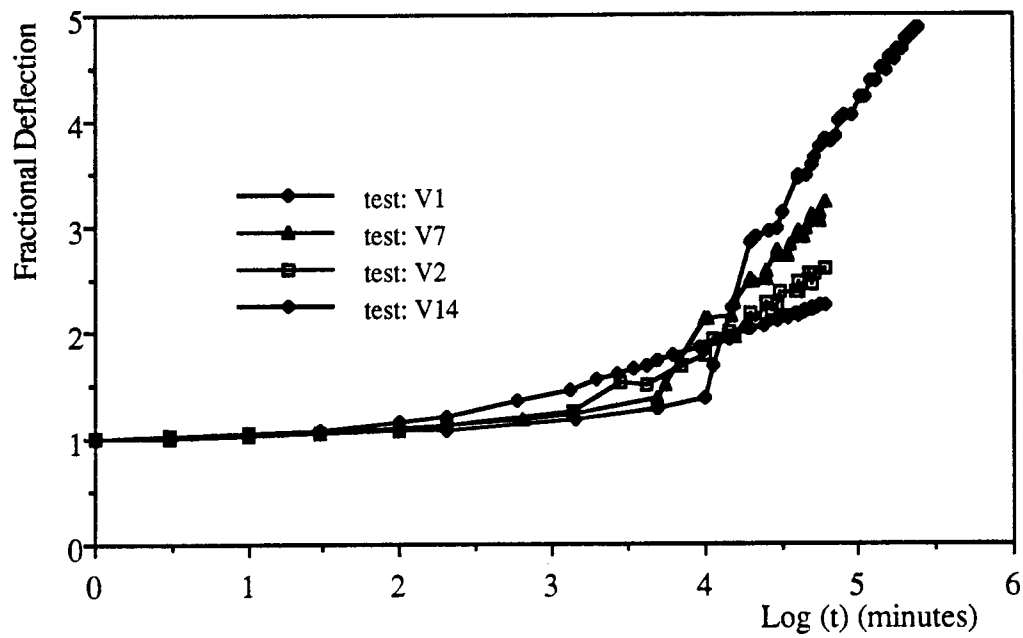

Fig. 6.3 Fractional Deflection vs. Log (t) Curves for the 15.9 mm Parallel Loaded OSB Panel in the Four Cyclic RH Tests

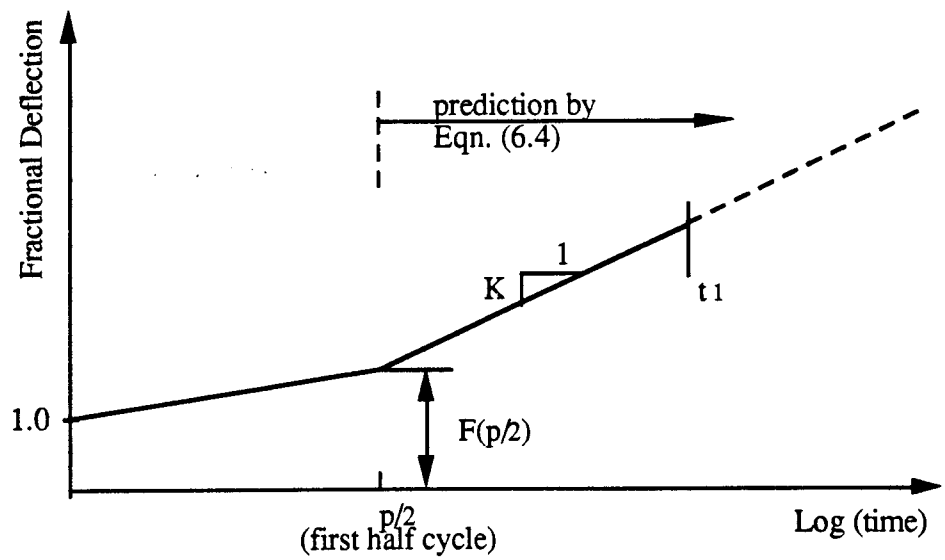

Fig. 6.4 Schematic Plot of Bilinear Creep Prediction Model for the OSB Panel under Cyclic Humidity

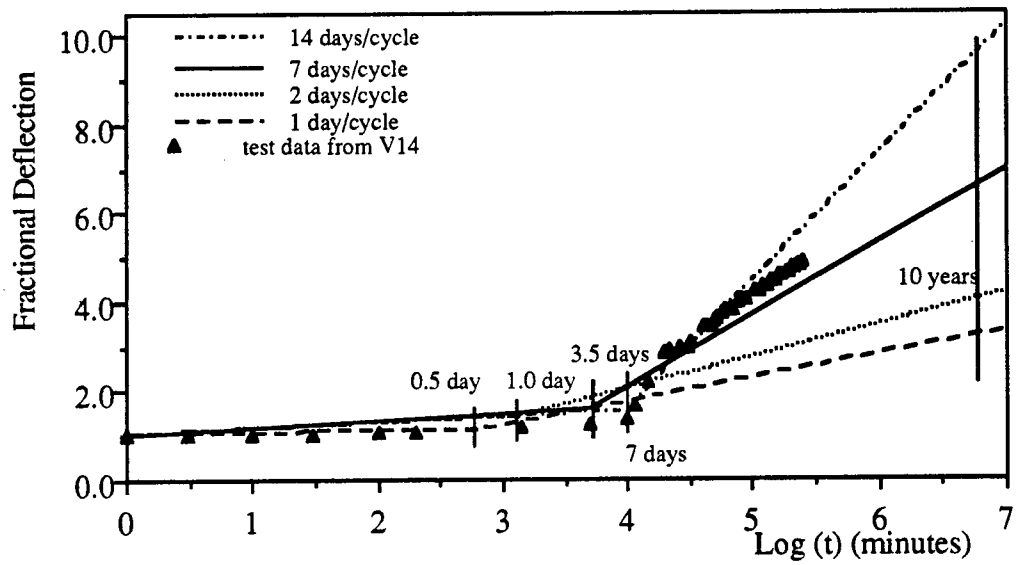

Fig. 6.5 The Predicted Fractional Deflection vs. Log (time) Curves for the 15.9 mm OSB Panel under the Four Cyclic Conditions

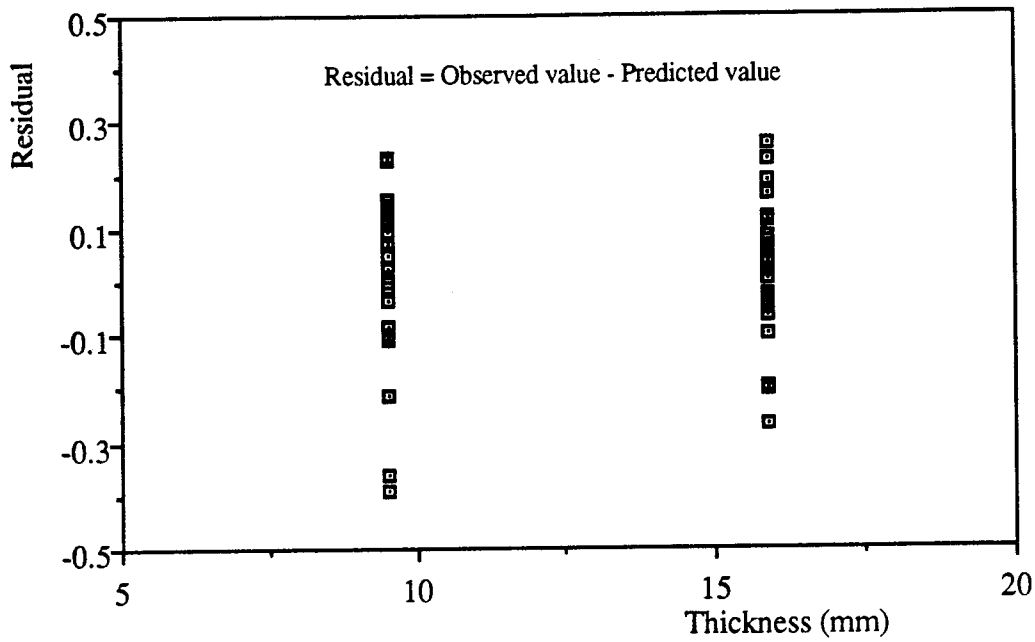

(a) Residual at 4-week

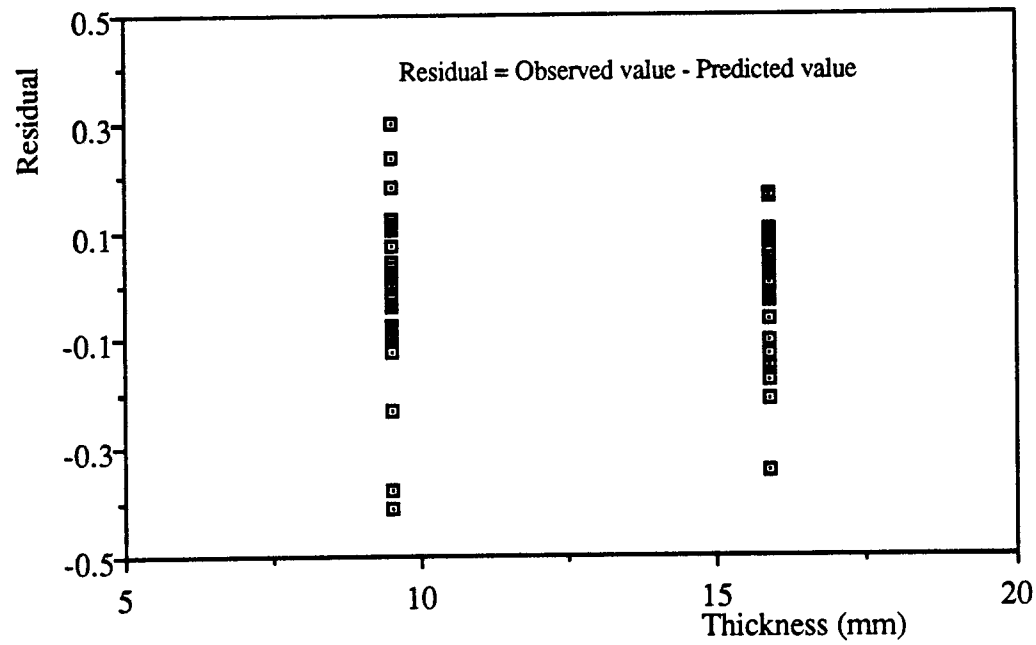

(b) Residual at 6-week

Fig. 6.6 Residual of Fractional Deflection at 4- and 6-weeks vs. OSB Panel Thickness

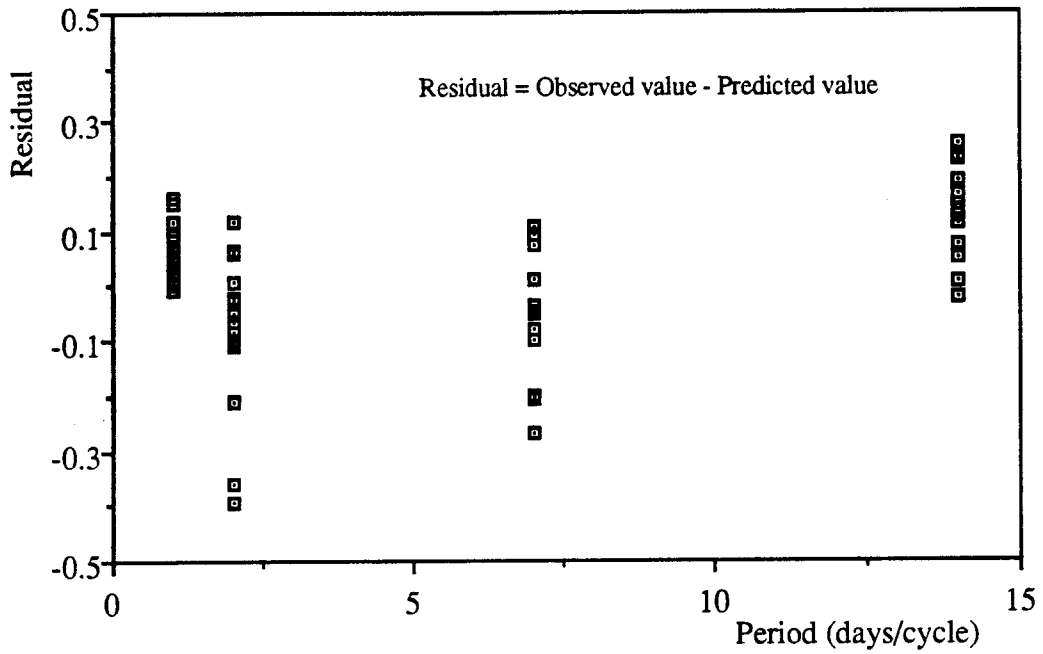

(a) Residual at 4-week

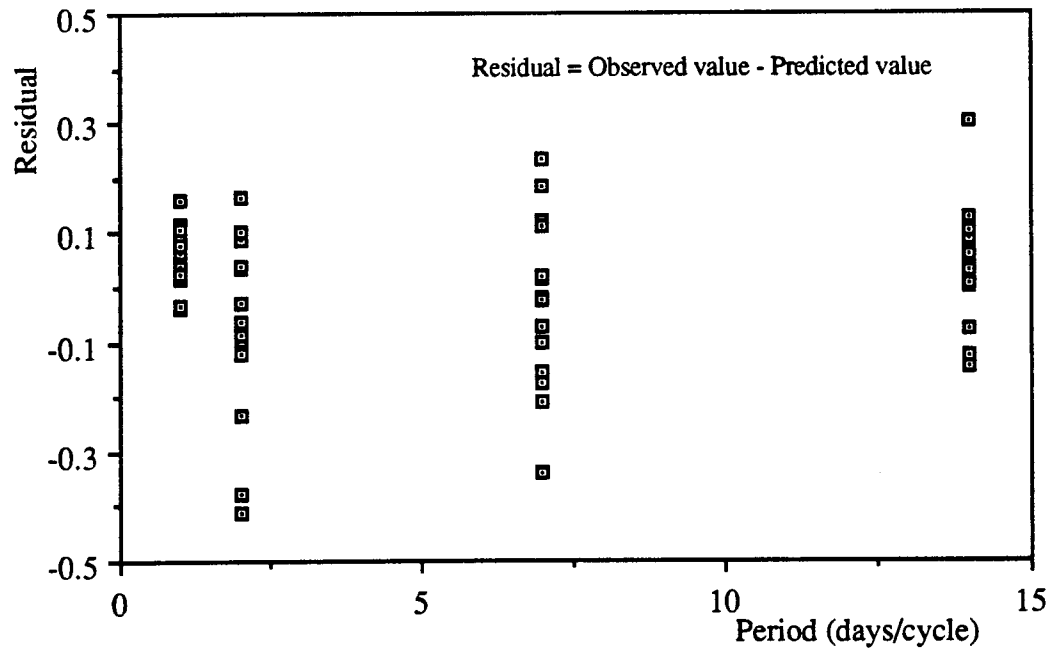

(b) Residual at 6-week

Fig. 6.7 Residual of Fractional Deflection at 4- and 6-weeks vs. Cyclic RH Period

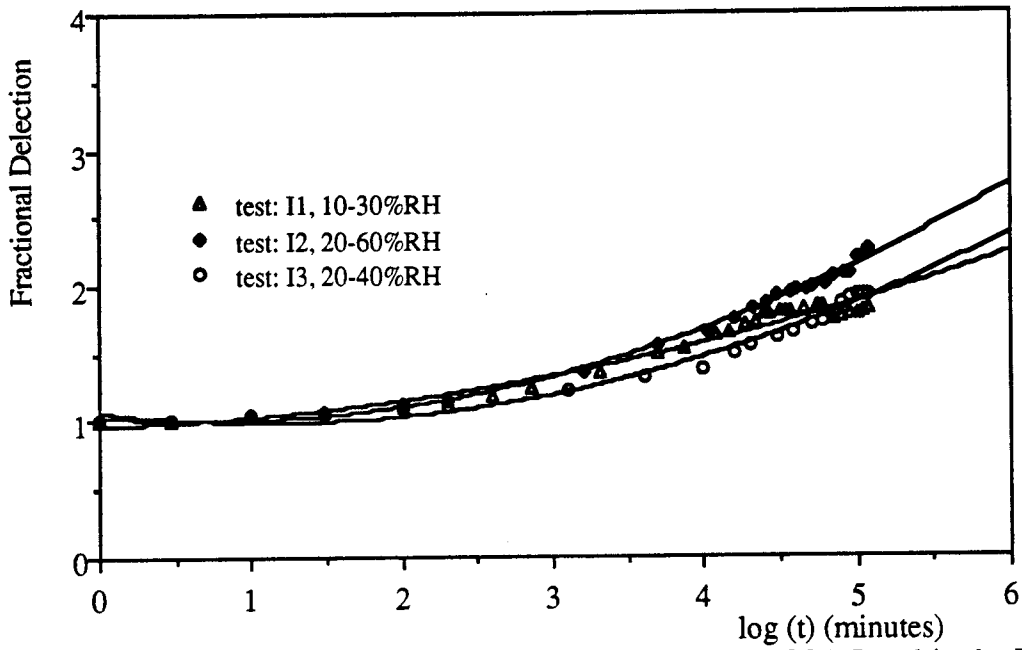

Fig. 6.8 Fractional Deflection of the 9.5 mm Parallel Loaded OSB Panel in the Three Indoor Creep Tests and Their Parabolic Fitting Curves

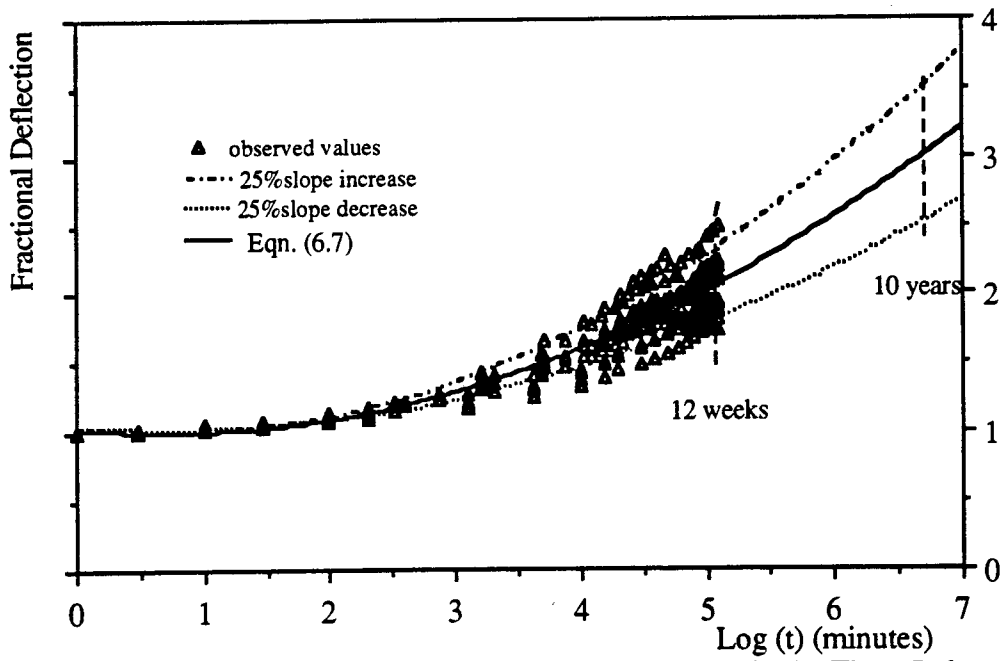

Fig. 6.9 Log (t) vs. Fractional Deflection for All OSB Panels in the Three Indoor Creep Tests and The Predicting Curve

Chapter 7 One-dimension Moisture Diffusion Analysis by Finite Difference Method

In this chapter, diffusion equations for modeling moisture movement in wood panels are introduced. The finite difference method is used to solve the diffusion differential equations with arbitrary boundary conditions. The numerical analysis results are compared with what is obtained from the tests. The moisture diffusion coefficients are calculated from the various test series for OSB panels. Some characteristics of the moisture diffusion coefficient are also discussed.

Fundamental knowledge about the diffusion process and the mathematical modeling for one-dimension diffusion are introduced in Section 7.1. Section 7.2 gives the method for calculating the moisture diffusion coefficient from desorption or adsorption, as well as the diffusion coefficients computed from each test series. The finite difference method used to solve the differential equation of moisture diffusion is introduced in Section 7.3, where both accuracy and convergence of the method are discussed briefly. In Section 7.4 the moisture movements through panels are obtained by the diffusion model for all creep test environments (cyclic and constant RH) and are compared with the results from the experiment. Finally, some properties of the moisture diffusion coefficient are discussed in Section 7.5.

7.1 Introduction of Diffusion Equation

Diffusion is the process by which matter is transported from one part of a system to another as a result of random molecular motions (Crank, 1956). The molecular motion occurs under the influence of a concentration gradient. In the cases where wood is heated, or impregnated with water, or dried, the flux and gradient are variable in both space and time, and an unsteady-state flow occurs.

The unsteady-state diffusion equation may be derived from a steady-state relationship that is known as Fick's First Law, which states that the rate of transfer of the diffusion substance through the unit area of a section is proportional to the concentration gradient normal to the section; that is,

$$Q = -D_m \frac{\partial V}{\partial x} \tag{7.1}$$

where Q = the rate of transfer per unit area of section

V = the concentration of diffusion substance

x = the space coordinate measured normal to the section

D_m = the diffusion coefficient

The negative sign in the above equation shows that the flow is from high to low concentration.

For the unsteady-state problem, Eqn. (7.1) can be translated into a differential equation (Siau 1984):

$$\frac{\partial V}{\partial t} = D_m \frac{\partial^2 V}{\partial x^2} \tag{7.2}$$

where t is the diffusion time.

For problems of moisture diffusion in wood, the concentration V is often replaced by the moisture content (MC), which has been defined in Chapter 3. Diffusion Eqn. (7.2) becomes

$$\frac{\partial MC}{\partial t} = D_m \frac{\partial^2 MC}{\partial x^2} \tag{7.3}$$

In the above equations, the diffusion coefficient (D_m) is assumed constant. However, the coefficient usually increases significantly with moisture content (Siau 1984). An exact form of Eqn. (7.3) is derived by differentiating the coefficient (Siau 1984):

$$\frac{\partial MC}{\partial t} = \frac{\partial}{\partial x}(D_m \frac{\partial MC}{\partial x}) \tag{7.4}$$

For convenience and generality, non-dimensional variables are introduced. Dimensionless time, called relative time τ, is defined as

$$\tau = \frac{D_m t}{(L/2)^2} \tag{7.5}$$

where t = actual diffusion time, minutes (min)

D_m = the diffusion coefficient, mm^2/min

$L/2$ = half thickness of wood panel, mm

The fractional moisture content, Z, is defined as

$$Z = \frac{MC(t) - MC_i}{MC_0 - MC_i} \tag{7.6}$$

where $MC(t)$ = moisture content at time t

MC_i = initial equilibrium moisture content

MC_0 = the outside surface moisture content

Now, the general diffusion differential equation (7.3) may be written as

$$\frac{\partial Z}{\partial \tau} = \frac{\partial^2 Z}{\partial X^2} \tag{7.7}$$

where X = dimensionless distance = $x/(L/2)$.

In the following few sections, the diffusion coefficient is assumed constant for simplicity. Therefore, Eqn. (7.3) will be the governing equation for the unsteady-state moisture diffusion problems. Close form solutions of the equation can only be obtained for a limited number of instances. For general situations such as arbitrary given boundary conditions, solution of the equation can however be obtained by numerical methods such as finite difference method.

7.2 Determination of Diffusion Coefficient for OSB Panels

7.2.1 Calculation of Diffusion Coefficient from Sorptions

When wood panels are exposed to environmental RH changes, the moisture diffusion will take place in three dimensions. Because of the geometrical dimensions of the test specimens (the panel thickness is much less than that of the other two dimensions), an one-dimensional diffusion model could be used to approximate the moisture diffusion process in the test specimens. The analytical solution of Eqn. (7.3) is given by Crank (1956) for a parallel-sided panel that suddenly change from one equilibrium state to another environment. The following assumptions are involved for the solution:

1. The diffusion coefficient is constant.

2. The initial value of MC is uniform within the specimen.

3. The surface of the specimen reach equilibrium immediately when exposed to the uniform relative humidity of the surroundings. Therefore, the surface MC is the EMC corresponding to the environmental RH.

4. The moisture transport process is symmetrical in space through the panel.

From Eqn. (7.7), the fractional change in average moisture content within entire thickness of the panel, $\bar{Z}$, may be calculated from the solution given by Crank (1956) and Siau (1984)

$$\bar{Z} = 1.0 - 0.811 exp(-2.47\tau) \tag{7.8}$$

where $\tau > 0.2$ and $\bar{Z}$ is calculated by Eqn. (7.6) when $MC(t)$ represents the panel's average MC.

The value of $\bar{Z}$ for short terms may be determined as

$$\bar{Z} = 1.13\sqrt{\tau} \tag{7.9}$$

where $\tau < 0.3$.

Eqn. (7.9) may be rearranged so that the moisture coefficient can be determined. With $\tau < 0.3$, the diffusion coefficient can be determined by (Siau 1984)

$$D_m = \frac{\bar{Z}^2 L^2}{5.10t} \tag{7.10}$$

When the moisture content of a specimen is increased or decreased over relatively small time intervals ($\tau < 0.3$), the values of $\bar{Z}$ at successive times may be calculated from the specimen MC by Eqn. (7.6). The diffusion coefficient may then be calculated by Eqn. (7.10).

7.2.2 Diffusion Coefficients of OSB Panels from the Creep Tests

According to the experimental program, all test specimens were at equilibrium MC corresponding to 65% RH before the beginning of the creep tests. The surrounding RH

changed from 65% to 35% at the first half cycle of the cyclic test series (V1, V2, V7, V14), and in test C35. The four assumptions given in the previous section are assumed to be true. The panel diffusion coefficients are calculated from the desorptive processes. In test C85, the surrounding RH changed from 65% to 85% at the beginning of the creep test, therefore, the panel diffusion coefficients are calculated from the adsorption.

The calculated diffusion coefficients at successive times from desorptions and the adsorption in the cyclic and constant RH creep tests are listed in Table 7.1, where time is the moisture diffusion time for adsorption or desorption. Since specimens of a test series were not weighed continuously, the table is not completed.

The following observations can be drawn from the values summarized in the table:

1. The diffusion coefficients calculated from desorptions are mostly larger than those from adsorption. The diffusion coefficients from the adsorption (in Test C85) are all less than 1.0×10^{-3} mm^2/minute, but most diffusion coefficients from desorption are lager than that value. This fact agrees with what is observed in solid wood (Comstock, 1963). The results given by Comstock show that the diffusion coefficients calculated from desorptions are appreciably greater than those from adsorptions in solid wood specimens. As suggested by Comstock, the difference is probably due to the effect of stresses on the equilibrium MC attained at the surface of the specimens.

2. In each test series, the diffusion coefficients calculated from successive diffusion time intervals are very consistent. The panels with different nominal thicknesses (9.5 mm and 15.9 mm) also have consistent moisture diffusion coefficients in each individual test series. One exception is test C35, in which the calculated diffusion coefficients for 15.9 mm OSB panels are much larger than for the 9.5 mm OSB

panels.

3. Although the diffusion coefficients computed from the cyclic tests and the 35% RH test are all based on the desorptive process, the variations between test series are fairly large. This may imply that the calculated diffusion coefficient is very sensitive to the measured MC of the panels. Slight differences of the measured MC may cause fairly large differences in the calculated diffusion coefficients. Later in the chapter, the numerical analysis results will show that the different diffusion coefficients yield fairly close MC results in OSB panels. A detailed discussion about the relation between measured MC and the calculated diffusion coefficients is given in Section 7.5. It is noticed here that the values from test V1 as listed in Table 7.1 are extremely large and the reason is not clear.

7.3 Finite Difference Method

7.3.1 Finite Difference Solution for Diffusion Equation

The general moisture diffusion equation (7.3) may be solved by finite difference method for arbitrary changes of the surrounding environment, which is considered as the boundary conditions of the equation. The method can be explained as the following procedures. Let the diffusion range x be divided into a number of equal intervals δx, and the time into intervals δt, then MC_{m-1}, MC_m, MC_{m+1} represent the moisture contents at the points $(m-1)\delta x$, $m\delta x$, $(m+1)\delta x$, respectively at time $n\delta t$. Let MC_m^+, MC_m^- correspond to moisture content at $x = m\delta x$ at time $(n+1)\delta t$ and $(n-1)\delta t$, respectively. The Taylor's expansion theorem gives

$$MC_{m+1} = MC_m + \delta x(\frac{\partial MC}{\partial x})_m + \frac{1}{2}(\delta x)^2(\frac{\partial^2 MC}{\partial x^2})_m + \cdots \tag{7.11}$$

$$MC_{m-1} = MC_m - \delta x(\frac{\partial MC}{\partial x})_m + \frac{1}{2}(\delta x)^2(\frac{\partial^2 MC}{\partial x^2})_m - \cdots \tag{7.12}$$

By adding the above two equations and neglecting the high-order terms, an approximation for $\frac{\partial^2 MC}{\partial x^2}$ at the point $m\delta x$ at time $n\delta t$ is

$$(\frac{\partial^2 MC}{\partial x^2})_m = \frac{MC_{m+1} - 2MC_m + MC_{m-1}}{(\delta x)^2} \tag{7.13}$$

And the approximation for $\frac{\partial MC}{\partial t}$ is

$$(\frac{\partial MC}{\partial t})_m = \frac{MC_m^+ - MC_m}{\delta t} \tag{7.14}$$

The above approximations may be used in different ways to solve the differential Eqn. (7.3). The method used here is called the Schmidt method (Crank, 1956).

By substituting Eqns. (7.13) and (7.14) into Eqn. (7.3), the moisture content at point $m\delta x$ at time $(n+1)\delta t$ may be obtained

$$MC_m^+ = MC_m + \frac{\delta t D_m}{(\delta x)^2}(MC_{m+1} - 2MC_m + MC_{m-1}) \tag{7.15}$$

Assuming that a panel's surfaces reach equilibrium MC with the surrounding RH immediately, and that the moisture diffusion is symmetric from both surfaces of a panel, an OSB panel may be divided into several layers through half of the panel's thickness. The moisture contents at the planes of layers could be calculated by Eqn. (7.15) layer by layer from the panel's surface in successive time step.

Similarly, for the general diffusion equation (7.4) with dimensionless variables, the corresponding formula to calculate fractional moisture content for the next time step is

$$Z_m^+ = Z_m + \frac{\delta \tau}{(\delta X)^2}(Z_{m+1} - 2Z_m + Z_{m-1}) \tag{7.16}$$

where X is the dimensionless distance as defined in Eqn. (7.7).

7.3.2 Accuracy and Convergence of Finite Difference Solution

The accuracy and convergence of the solution obtained by the finite difference method given above depend largely on the ratio $\frac{\delta t D_m}{(\delta x)^2}$ or $\frac{\delta \tau}{(\delta X)^2}$ (Crank 1956). The smaller the ratio, the more rapidly the solution converges. For the Schmidt method, the solution is conditionally stable; the ratio must be less than 0.5. A value of 0.1 was suggested by Nielsen and Bach (1975).

The accuracy of a finite difference solution could be estimated and improved in many ways (Crank, 1956). In practice, the accuracy of a solution may be estimated by repeating the process using smaller δx and δt ; for example, half the δx and δt. If the result obtained is within the desired accuracy, the solution is complete. Otherwise, a smaller δx or/and δt should be tried.

7.4 Finite Difference Solution to Moisture Movement in OSB Panels

A computer program to solve the diffusion equation using the Schmidt method was originally written by Bach and Nielsen (1974) in FORTRAN IV and later rewritten by Leitch (1990) who used FORTRAN 77. The program is modified in this study to fit the analysis requirements of this study. The modifications involve mostly details such as input, output, and the limitation for $\frac{\delta t D_m}{(\delta x)^2}$. The analytical results are also presented in graphic format by using the software SAS (1990).

When using the program to model the moisture movement in OSB panels with the simulated creep tests environment, the half panel thickness is, in most cases, divided into ten layers with eleven planes. After trying several numerical analysis examples for the test panels, a limit of 0.2 for $\frac{\delta t D_m}{(\delta x)^2}$, is found to be adequate. The time intervals (δt) are usually equal to, or less than, 60 minutes.

7.4.1 Moisture Movement Modeling in Constant RH Tests

In the creep test C35 (35% RH constant), the environmental RH changed from 65% to 35% and then remained constant. Only one desorption process occurred during the entire creep test duration. To model the moisture movement through panels, the diffusion coefficient calculated from that test series (as listed in Table 7.1) was used in the program computation. D_m = 1.42 x 10^{-3} mm^2/minute was chosen for 9.5 mm OSB panels, which is the average of the four calculated diffusion coefficients in Table 7.1 from test C35. The calculated panel average MC curve vs. time is plotted in Fig. 7.1 for 9.5 mm OSB. The F.D.M. in the figure refers to the solution obtained from the Finite Difference Method (F.D.M.). The measured MC of the panel is also shown in the same figure. Although the diffusion coefficient used was the average of the values from the first 3.5 days, the analytical results fit well with the measured MC during the entire test duration.

For 15.9 mm OSB panels, the desorption curve from the finite difference program (using D_m = 4.0 x 10^{-3} mm^2/minute from Table 7.1) is also close to the measured MC. The results are similar to 9.5 mm OSB panels (in Fig.7.1) and are not plotted.

Similar to desorption in test C35, the moisture movement during adsorption in test C85 is plotted in Fig. 7.2 for 9.5 mm OSB panels with D_m = 0.94 x 10^{-3} mm^2/minute; the moisture diffusion program results agree very well with the MC measured from test C85 in the entire test duration.

In Fig. 7.3 the moisture movement during adsorption in test C85 is plotted together with the measured MC. The diffusion coefficient used for the computation is also taken from Table 7.1 (D_m = 0.65 x 10^{-3} mm^2/minute). The calculated curve fits well with the test data for about 10 days, but later, the calculated curve underestimates the measured

MC. A larger diffusion coefficient would give a better overall fit of the test results. There are two possible reasons for the underestimation of the MC. First, the panel's original thickness, which is measured at 65% RH environment, is taken to calculate the diffusion coefficients in Table 7.1, and its thickness increases about 7-8% during the adsorption from 65% RH to 85% RH, as shown in Fig. 4.4. The calculated diffusion coefficient would be larger if the actual panel's thickness is used for the calculation of the diffusion coefficient as shown by Eqn. (7.10). Secondly, the diffusion coefficient itself is not a constant and becomes larger at a higher MC level (described in Section 7.1), which means that the diffusion process is faster when the panel's MC increases. Therefore, the actual MC is higher than the prediction based on the diffusion coefficient at a lower MC level.

A better way to solve the problem is to use a varying diffusion coefficient instead of a constant one. Then Eqn. (7.4) should be used, but the solution to Eqn. (7.4) is more complex (Crank 1956) and will not be used in this study.

7.4.2 Moisture Movement Modeling in Cyclic RH Tests

As the results given in Section 7.2.2, the values of the diffusion coefficient are different when they are calculated from desorption and adsorption. In the four cyclic RH tests, desorption and adsorption occurred consecutively, but the diffusion coefficients shown in Table 7.1 were all calculated from the first desorption. The values listed in the table under each test series are therefore not necessary appropriate for modeling the moisture movement in that cyclic RH test, since both desorption and adsorption were involved in a cyclic RH test. For this reason, as well as for the convenience of comparing moisture movement in the cyclic RH environments with four frequencies, one diffusion coefficient (D_m = 1.0 x 10^{-3} mm^2/minute) is used for all OSB panels and cyclic test series in the analysis. The moisture movement in panels vs.

time (in minute) curves obtained from the analytical modeling are shown in Figs. 7.4 to 7.11.

7.4.2.1 Modeling Results and Test Measurement in Cyclic RH Tests

During RH cycling, panel surfaces are assumed to have the same square wave changes as the surrounding environment, that is, the panel surfaces reach EMC immediately. The MC at a point inside a panel also fluctuates during the cyclic changes. However, there are differences between the locations with different depths from the surfaces. The larger the depth, the less the MC fluctuation at that location. There may also be phase lag between outside layers and inside layers , which means that the MC of inside layers may be increasing when the outside layers start to drop the MC. These phenomenon can be observed in Figs. 7.4 to 7.11. For example, the MC vs. time are plotted in Fig. 7.9 for 15.9 mm OSB panels at several depths in test V7. The magnitude and the phase difference of MC fluctuations at various depths are clearly shown.

The moisture content gradient through the panel thickness at any time during sorptions can be calculated, although the gradients were not measured in the experiment to verify the accuracy. The moisture gradient may be important to the internal stress and creep development of wood panel. A series of moisture content through panel thickness curves are drawn in Fig. 7.12 for 9.5 mm and 15.9 mm OSB in cyclic test V2 (2 days/cycle) when the first drying is from a uniform initial MC of 9.4% to 7.05% MC of the surface environment. In Fig. 7.13, another series of moisture content through thickness curves is plotted for the same panel during the last adsorption in six weeks.

When the surrounding RH has a cyclic change between 35% and 85%, panel weight or average MC would also fluctuate. The comparison between calculation and measurement can also be found in Table 7.2. The MC in the table is the panel average

MC. In the table, ΔMC is the panel MC fluctuations during the last few cycles of creep tests (close to six weeks). MC_{max} represents the maximum MC of panel during cyclic RH. The subscripts "c" and "m" represent values from program calculation and test measurement, respectively. The table indicates that the finite difference method tends to give better results when compared with the measurement for a slower cyclic test such as V14 (14 days/cycle). Also, the MC fluctuations from the calculation are close to the test measurement. A higher overall MC level however is given by the model analysis for a fast cyclic test such as V1 (1 day/cycle). The comparison between model analysis and the experimental measurement is also shown by Fig. 7.14 where the average MC of 15.9 mm OSB panel vs. time (in minute) curve from the finite difference method and the actual measured MC values are plotted.

The difference between the modeling results and measurement may come mainly from the assumptions made in Section 7.2.1. First of all, the moisture diffusion coefficient is not an exact constant. The actual diffusion coefficient becomes larger at higher MC levels and is different for desorption and adsorption. Secondly, the surfaces of the panel do not reach equilibrium MC with surrounding RH immediately, as assumed in the model. Surface resistance does exist. Although the numerical model does not precisely portray the moisture diffusion in wood panels, it still works very well from a practical point of view.

7.4.2.2 The Effect of Cyclic Frequency and Panel Thickness on the Moisture Diffusion

As described in Chapter 5, it was observed from the experiment that the MC fluctuated more in 9.5 mm panels than in 15.9 mm panels. The moisture movement in panels were different for the cyclic environments with different frequencies. To study the moisture diffusion in panels with different thicknesses and cyclic frequencies, the

results from the finite difference method are summarized in Table 7.3. The calculations use D_m = 1.0 x 10^{-3} mm^2/minute, and the panel half thicknesses are equal to 5.2 mm and 8.5 mm from measurements for OSB of two different nominal thicknesses. The moisture content in the table refers to the average moisture content throughout panel thicknesses. The panel average moisture content changes in the four cyclic RH conditions are also plotted in Figs. 7.15 and 7.16 for 9.5 mm and 15.9 mm OSB, respectively. The following observations are drawn from the modeling results:

1. In the cyclic frequency range tested, the slowest cyclic environment V14 (14 days/cycle) gives the most MC fluctuations (ΔMC in the table). The MC fluctuation of 9.5 mm panel in test V14 is 5.1% points, but only 1.3% points in test V1.

2. The maximum MC reached during cycling is different for different cyclic frequencies. The slower RH cycling gives the larger maximum MC at the end of an adsorption.

3. For the panels with different thicknesses, the MC fluctuations of thicker panels are less than those of the thinner panels. For example, the MC changed about 3.1% points in 15.9 mm OSB panels, but 5.1% points in 9.5 mm panels in one sorptive process in test V14.

4. Thinner panels give a little larger maximum MC level than do thicker panels. For example, the maximum MCs in test V14 are 14.0% and 12.7% for 9.5 mm and 15.9 mm OSB panels, respectively.

5. The average MC change rate ($\Delta MC/\Delta t$) in one sorptive process is larger in a faster cyclic RH environment. Panel MC changes very fast in the early stage of desorption or adsorption and gradually slows down, which can also be observed from the moisture diffusion curve in Fig. 7.14. The overall MC rate during an entire sorption

must therefore be less in slower cyclic tests.

6. The average MC in one full cycle is close for panels with two nominal thicknesses.

7. The average MC in one full cycle is close for panels in a different cyclic RH frequency environment.

All of the above observations, except the observation number 7, are consistent with what was found in the experiment. The observation number 7 does not agree with what is given in Section 4.3.2.

7.5 Discussions about The Diffusion Coefficient

The moisture diffusion coefficient D_m for wood is wood's internal resistance to moisture movement. It depends on several factors such as wood MC, temperature, and internal stress (Comstock, 1963). Movement of water through the surface of wood also affects the rate of moisture movement. This external resistance is characterized by surface emission coefficient, which depends on factors including temperature and air velocity. In the numerical analysis carried out in this chapter, the boundary conditions assume that the surfaces reach equilibrium MC with the surrounding environment immediately. Simpson et al.(1991) show that the apparent diffusion coefficient is less than the true diffusion coefficient determined by methods which consider the surface resistance.

In a fast cyclic test such as V1, the wood panel surfaces undergo more environmental changes than in a slow cyclic test such as V14. The cumulated effect of ignoring the surface resistance is expected to be larger in the faster cyclic test than in the slower one. This might explain the calculation results presented in Section 7.4.2.1, where the calculation agrees better with the slow cyclic test than with the fast test.

The diffusion coefficients calculated from the series of tests as listed in Table 7.1 have large differences in some cases. This may result from the experimental error in measuring panel MC. Slight difference in panel MC will introduce the same order of difference in the fractional moisture content difference as shown by Eqn. (7.6). However, the calculated diffusion coefficient D_m is proportional to the square of the fractional moisture content from Eqn. (7.10). A small experimental error in panel MC measurement could lead to a relatively large difference in the calculated diffusion coefficient.

The effect of the magnitude of diffusion coefficient on the calculated MC of panel is examined for cyclic RH. Several diffusion coefficients ranging from 0.2 x 10^{-3} mm^2/minute to 5 x 10^{-3} mm^2/minute are tried for environmental conditions as in tests V1 and V14. Numerical calculations are made on 15.9 mm OSB panel, and the maximum and minimum values of the panel's average MC across thickness during the last cycle of six week duration are listed in Table 7.4. The half thickness of panels is taken as 8.5 mm in the calculations. The measured MC values are also shown in the table. The D_{m1} to D_{m4} in the table are four values assigned to the diffusion coefficient for carrying out the numerical analysis. The following notes are made from the results shown in the table with respect to the calculated moisture movement and the assumed diffusion coefficient in the cyclic RH environment.

1. The diffusion coefficient D_{m1} is 1/5 of D_{m2}. For slow cyclic test V14, both coefficients give very close minimum MC during cycling. The only difference is that the maximum MC is about 1.7% points higher when using D_{m2}. As the diffusion coefficient gets large (D_{m4} is five times D_{m2}) the calculated MC is very different for both the maximum and the minimum value during cyclic changes. This may imply that for slow cyclic RH, the calculated moisture movement in the panel is not

sensitive to the value of the diffusion coefficient up to a certain extent, and becomes very sensitive to the diffusion coefficient when the coefficient reaches a sufficiently large value.

2. For fast cyclic test V1, the ratios between D_{m4} to D_{m2}, and D_{m2} to D_{m1} are both equal to 5, the calculated MC differences between using D_{m4} and D_{m2} is close to those between using D_{m2} and D_{m1}. There are no big differences between D_{m1} and D_{m4} considering that the coefficients are 25 times different.

The above observations show that the calculated moisture movement is less sensitive to the value of the diffusion coefficient in fast cyclic RH than it is in slow cyclic RH, and the calculation results become sensitive to the diffusion coefficient in slow cyclic RH only when the diffusion coefficient is large enough.

Table 7.1 Moisture Diffusion Coefficients D_m Calculated from the Cyclic and Constant RH Tests (unit: 10^{-3} mm^2/minute)

		Desorption (65% to 35%)					Adsorption (65% to 85%)
Nominal	Time	Test ID					Test ID
Thickness	(days)	C35	V1	V2	V7	V14	C85
9.5 mm	0.5	1.23	7.07	-	0.95	-	-
	1.0	1.53	-	1.80	1.19	1.16	0.93
	2.5	1.59	-	-	-	-	0.94
	3.5	1.34	-	-	1.20	1.13	-
	7.0	-	-	-	-	0.85	-
15.9 mm	0.5	-	5.25	-	1.71	-	-
	1.0	-	-	1.97	1.56	1.14	0.70
	2.5	4.23	-	-	-	-	0.59
	3.5	3.84	-	-	1.58	1.18	-
	7.0	-	-	-	-	1.17	-

Table 7.2 Comparison of the Panel Average MC between the Calculation and Measurement in the Cyclic RH Tests (D_m = 1.0 x 10^{-3} mm^2/minute)

Nominal		Test ID			
Thickness		V1	V2	V7	V14
9.5 mm	$((\Delta MC)_c - (\Delta MC)_m)$	~ 0%	0.4%	0.7%	0.9%
	$((MC_{max})_c - (MC_{max})_m)$	2.2%	2.0%	1.1%	0.1%
15.9 mm	$((\Delta MC)_c - (\Delta MC)_m)$	~ 0.%	0.3%	0.2%	-0.2%
	$((MC_{max})_c - (MC_{max})_m)$	2.0%	1.8%	1.0%	-0.1%

Table 7.3 Comparison of Moisture Diffusion in the Panel with Different Thicknesses during the Last cycle of 6 week Duration

Nominal Thickness		Test ID			
		V1	V2	V7	V14
9.5 mm	ΔMC (%) [a]	1.3	1.8	3.5	5.1
	ΔMC/Δt (%/day) [b]	2.6	1.8	1.0	0.73
	$(MC)_{max}$ (%) [c]	12.3	12.6	13.3	14.0
	$(MC)_{ave}$ (%) [d]	11.7	11.7	11.6	11.5
15.9 mm	ΔMC (%)	0.9	1.3	2.1	3.1
	ΔMC/Δt (%/day)	1.8	1.3	0.6	0.44
	$(MC)_{max}$ (%)	11.9	12.0	12.3	12.7
	$(MC)_{ave}$ (%)	11.5	11.4	11.3	11.2

[a] ΔMC = MC fluctuation during the last cycle in 6 week duration.

[b] ΔMC/Δt = the average MC change rate in the last half cycle.

[c] $(MC)_{max}$ = the maximum panel MC during the last cycle.

[d] $(MC)_{ave}$ = the average value of panel MC during the last cycle = $(MC)_{max}$ - ΔMC/2.

Table 7.4 The Calculated MC (%) Fluctuation Rangers for 15.9 mm OSB Panel using Different Diffusion Coefficients

Test ID	Measured Value	Diffusion Coefficient D_m (10^{-3} mm^2/minute)			
		D_{m1} = 0.2	D_{m2} = 1.0	D_{m3} = 2.5	D_{m4} = 5.0
V14	9.8 ~ 13.0	9.5 ~ 11.0	9.7 ~ 12.7	8.9 ~ 14.1	8.0 ~ 15.1
V1	8.8 ~ 9.5	10.2 ~ 10.7	10.8 ~ 11.5	-	10.8 ~ 12.5

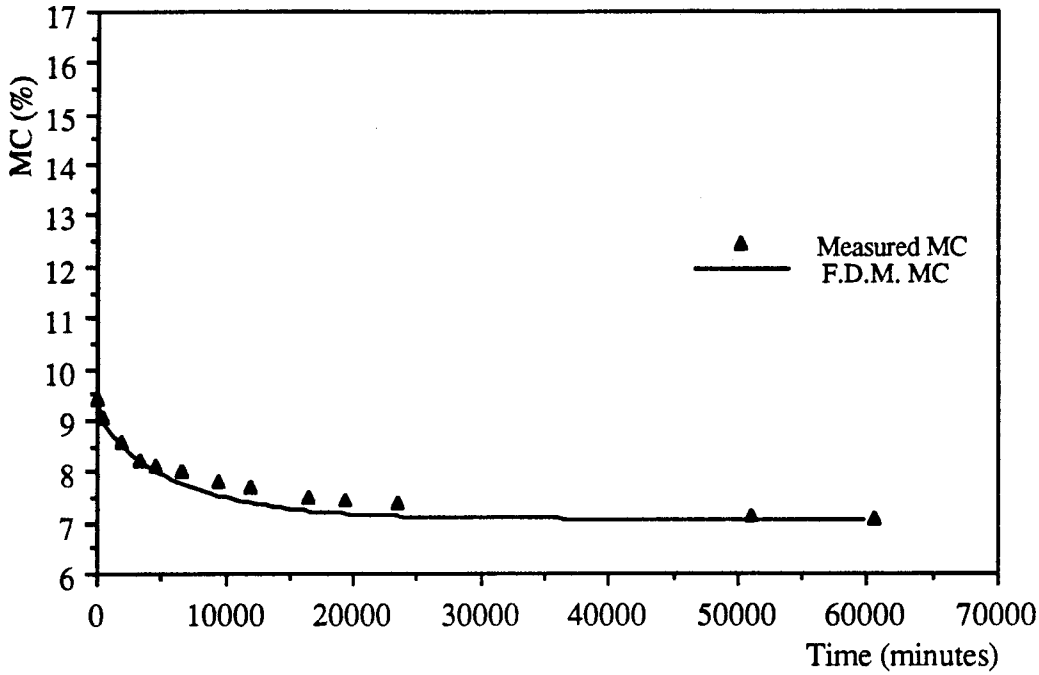

Fig. 7.1 Comparison of MC from the Finite Difference Method and Test Measurement for the 9.5 mm OSB Panels in Test C35

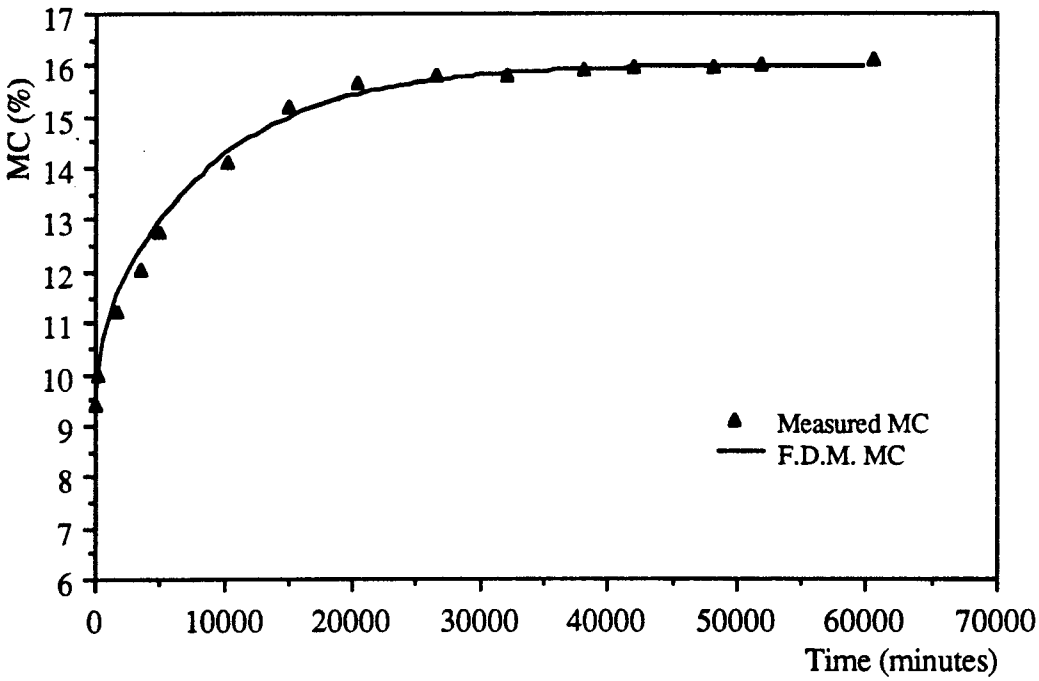

Fig. 7.2 Comparison of MC from the Finite Difference Method and Test Measurement for the 9.5 mm OSB Panels in Test C85

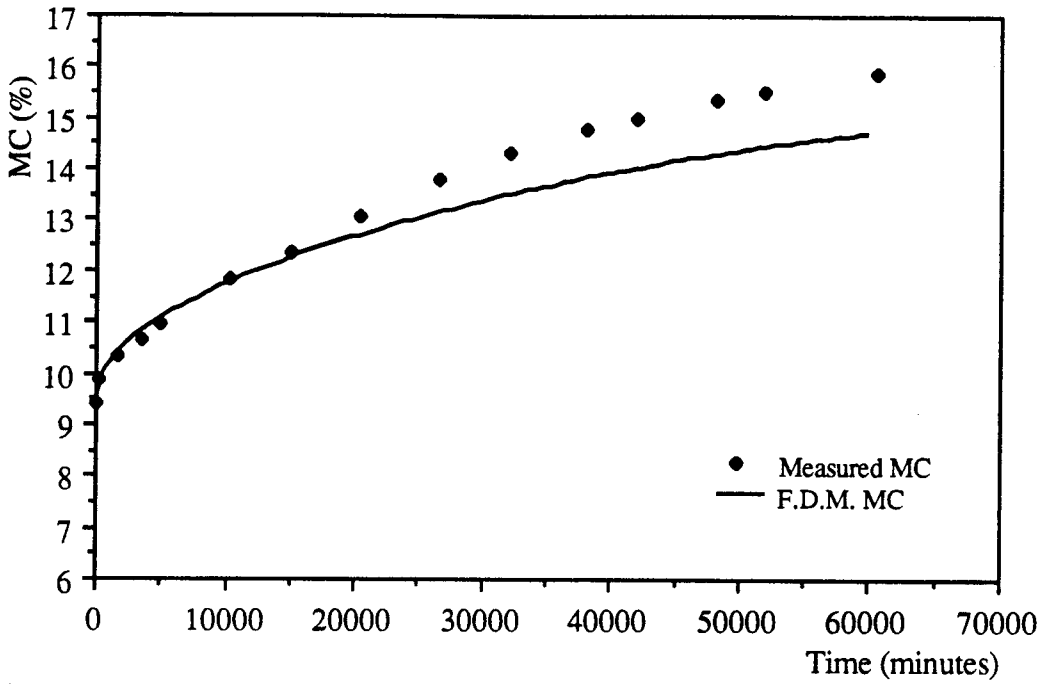

Fig. 7.3 Comparison of MC from the Finite Difference Method and Test Measurement for the 15.9 mm OSB Panels in Test C85

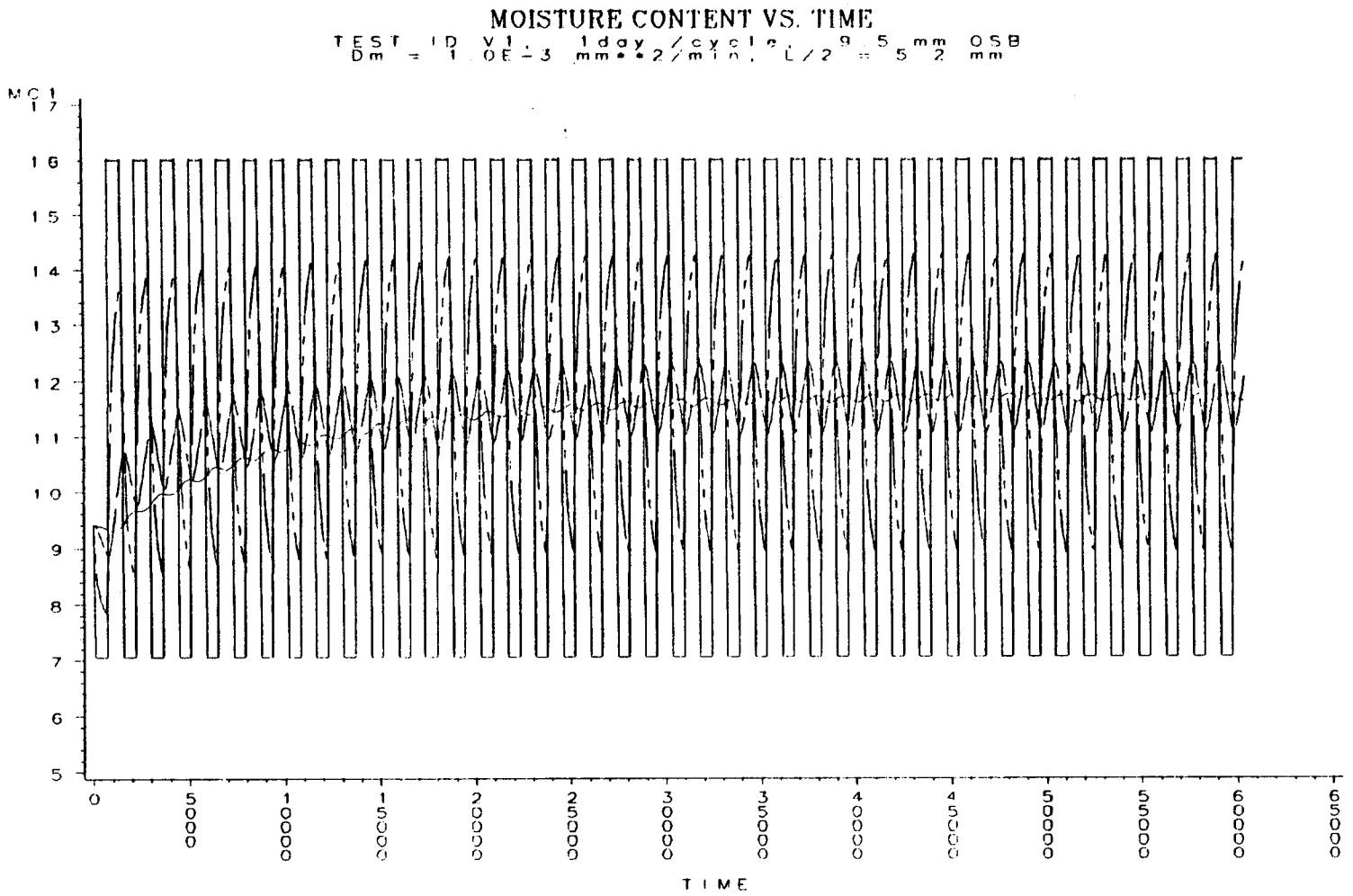

Fig. 7.4 Moisture Diffusion of the 9.5 mm OSB Panels at Various Depths in Cyclic RH Test V1

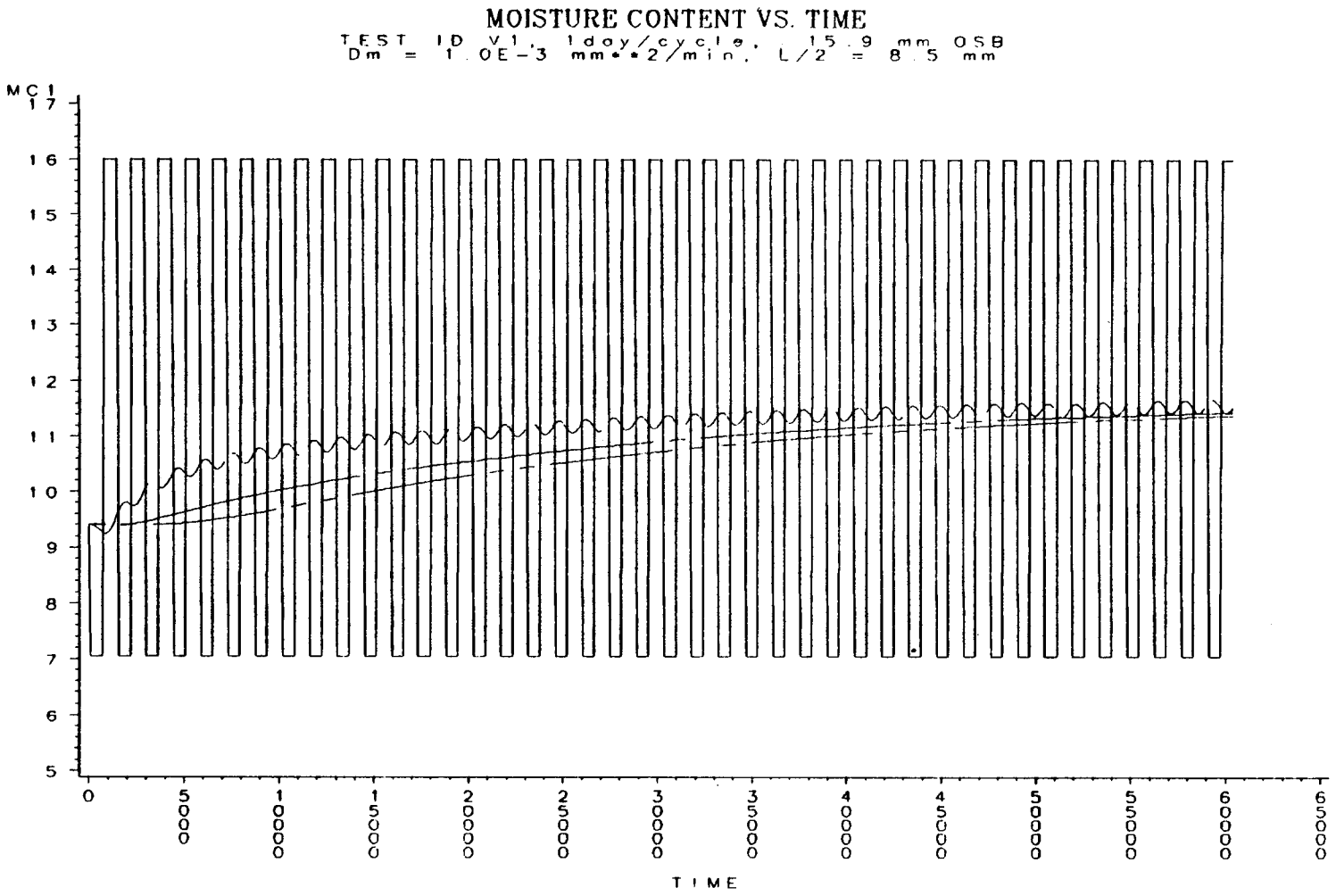

Fig. 7.5 Moisture Diffusion of the 15.9 mm OSB Panels at Various Depths in Cyclic RH Test V1

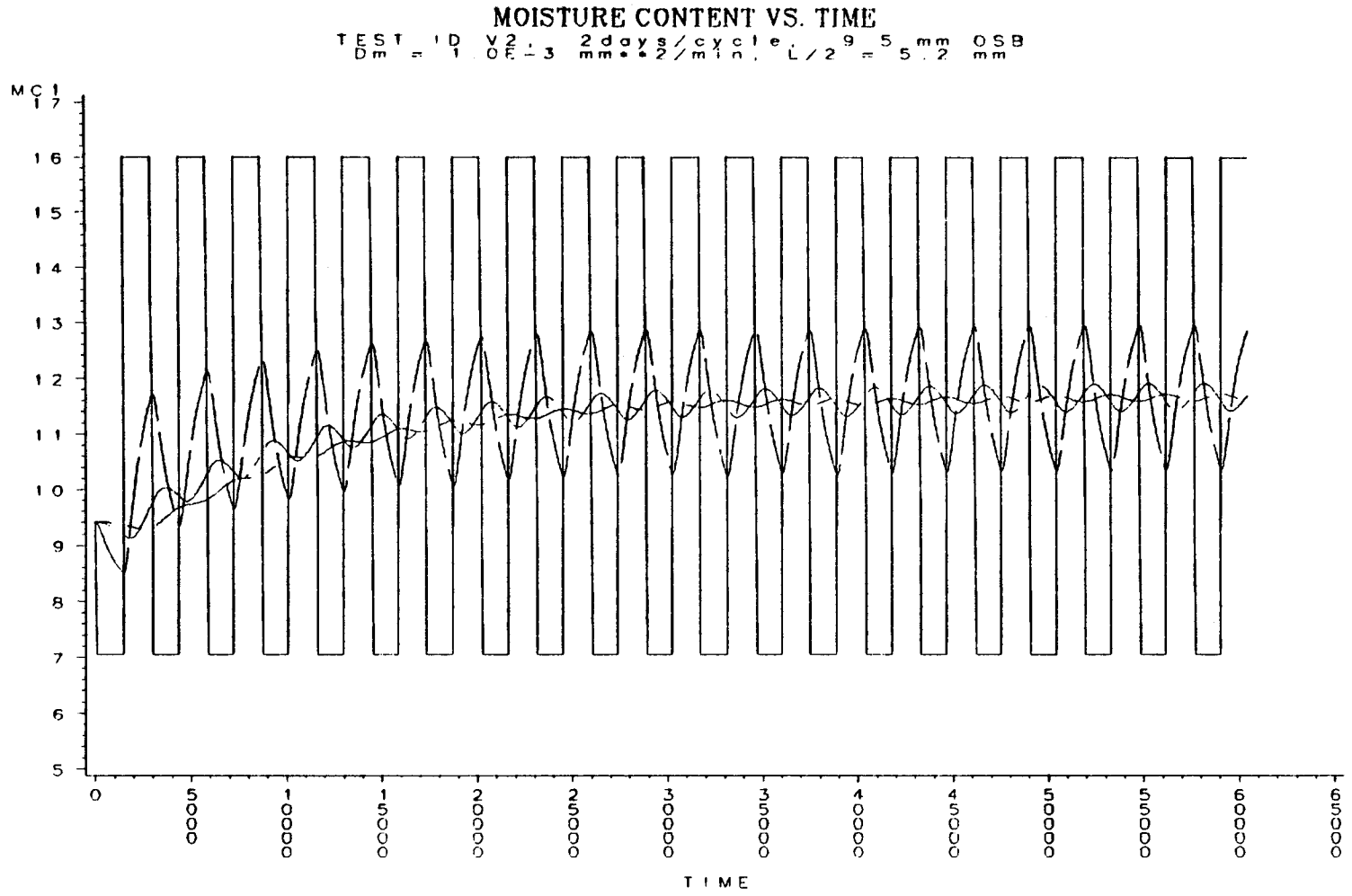

Fig. 7.6 Moisture Diffusion of the 9.5 mm OSB Panels at Various Depths in Cyclic RH Test V2

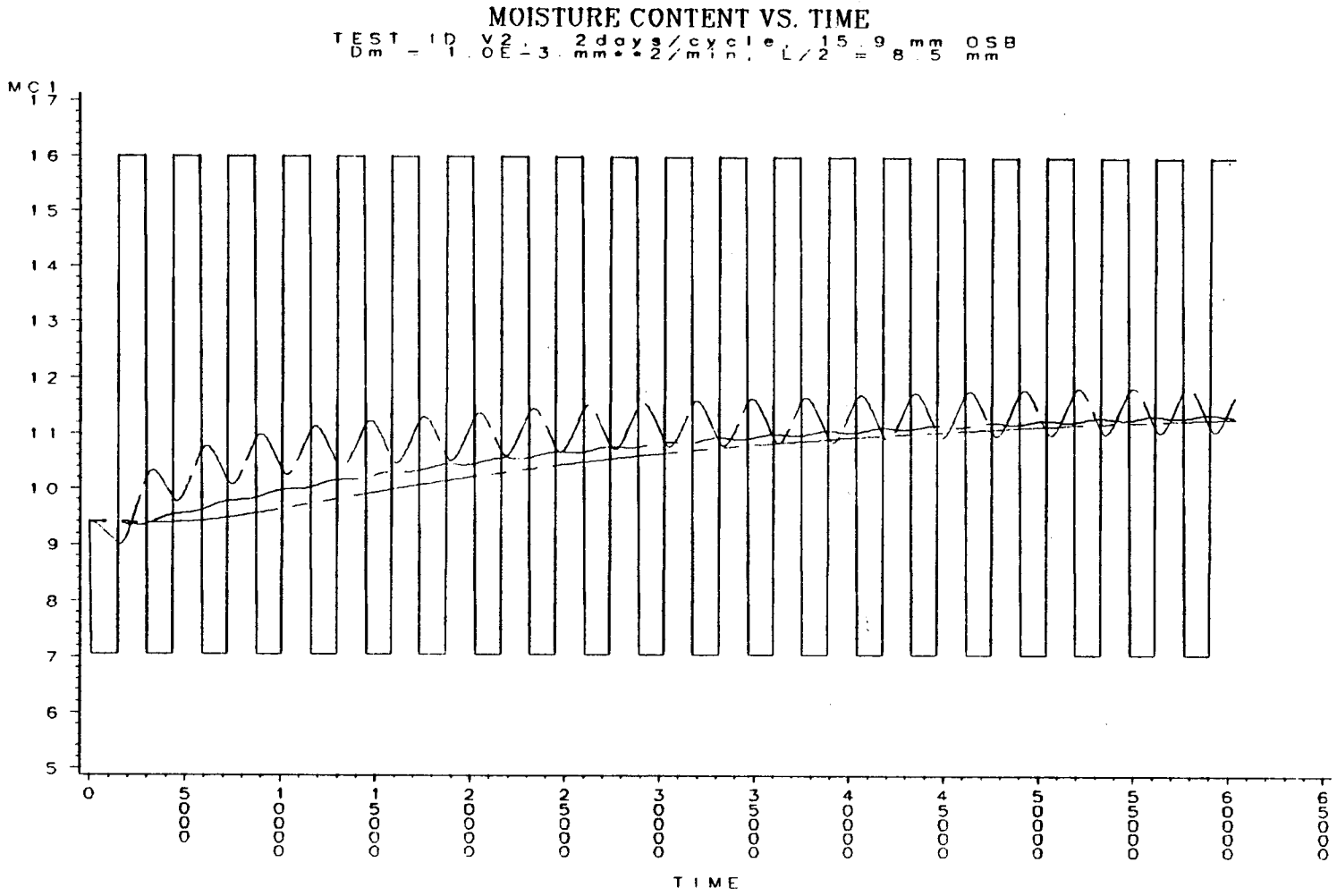

Fig. 7.7 Moisture Diffusion of the 15.9 mm OSB Panels at Various Depths in Cyclic RH Test V2

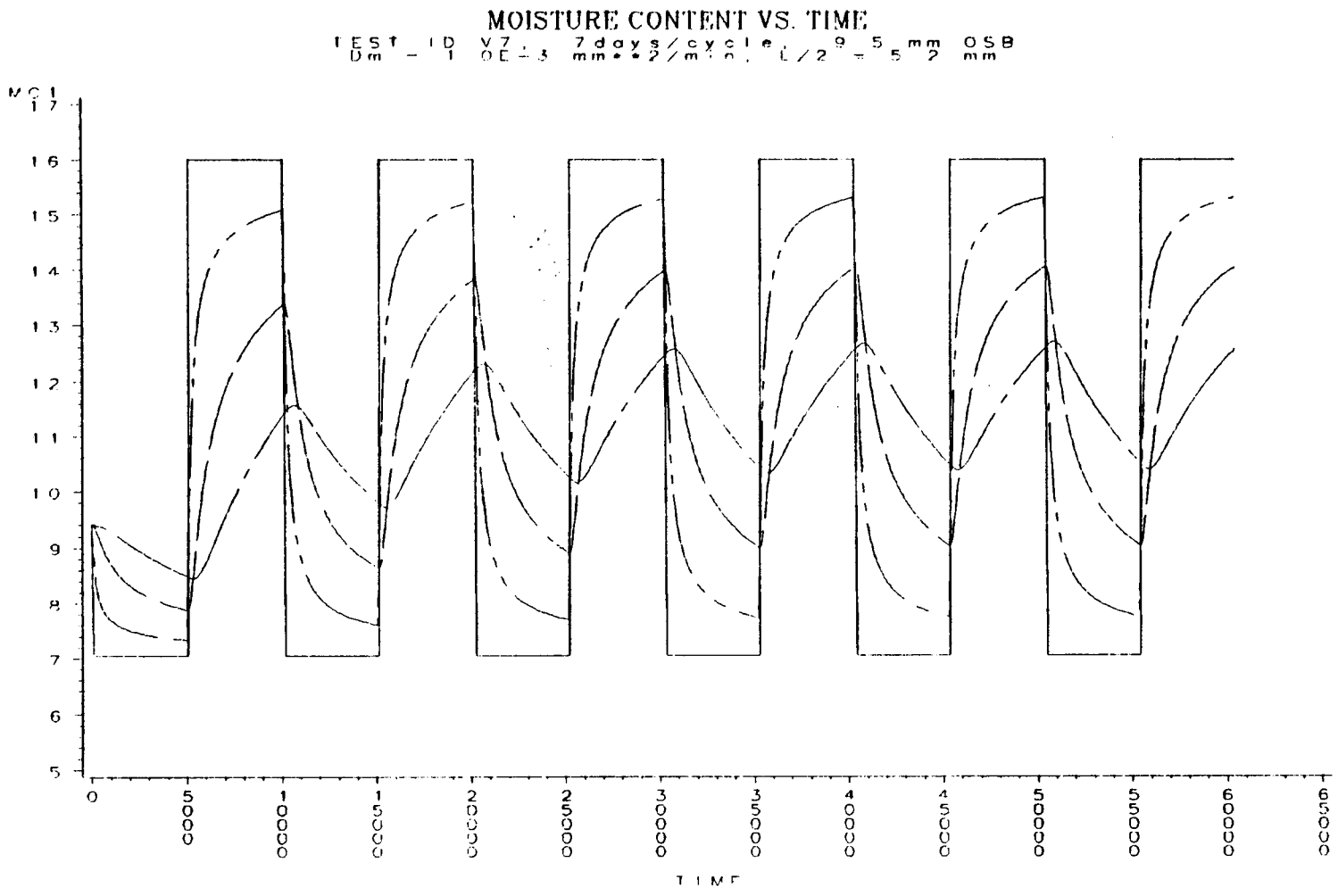

Fig. 7.8 Moisture Diffusion of the 9.5 mm OSB Panels at Various Depths in Cyclic RH Test V7

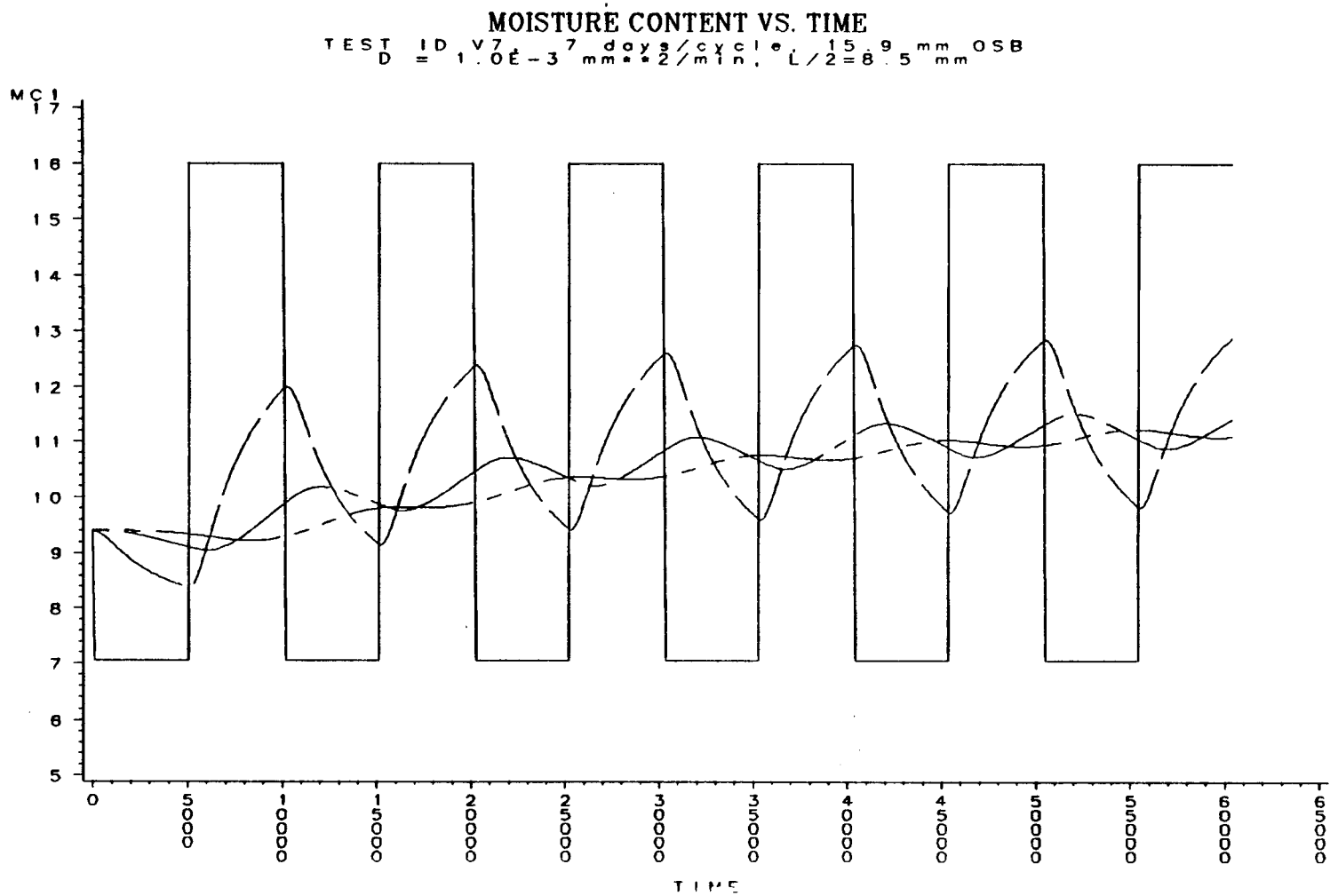

Fig. 7.9 Moisture Diffusion of the 15.9 mm OSB Panels at Various Depths in Cyclic RH Test V7

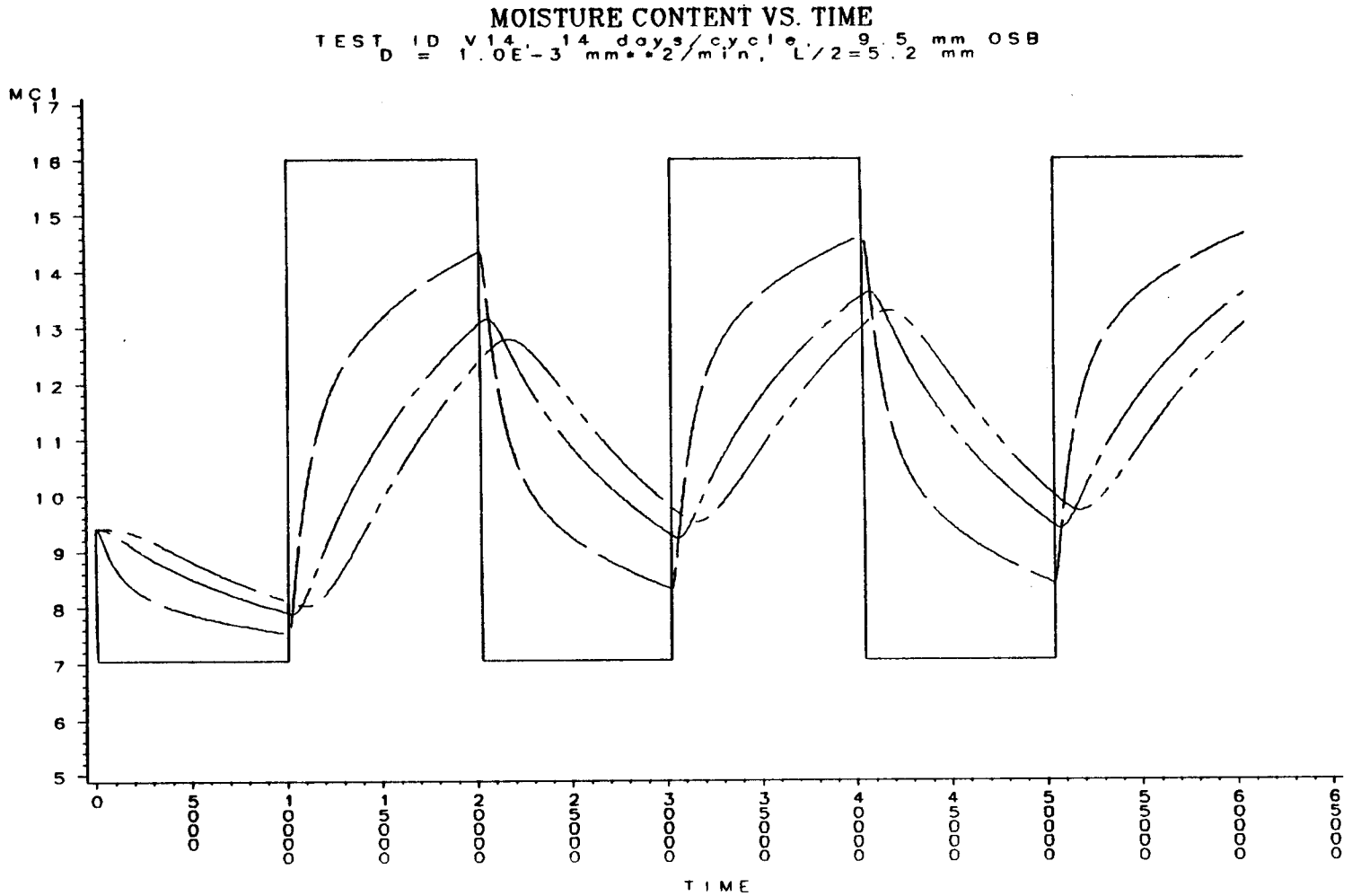

Fig. 7.10 Moisture Diffusion of the 9.5 mm OSB Panels at Various Depths in Cyclic RH Test V14

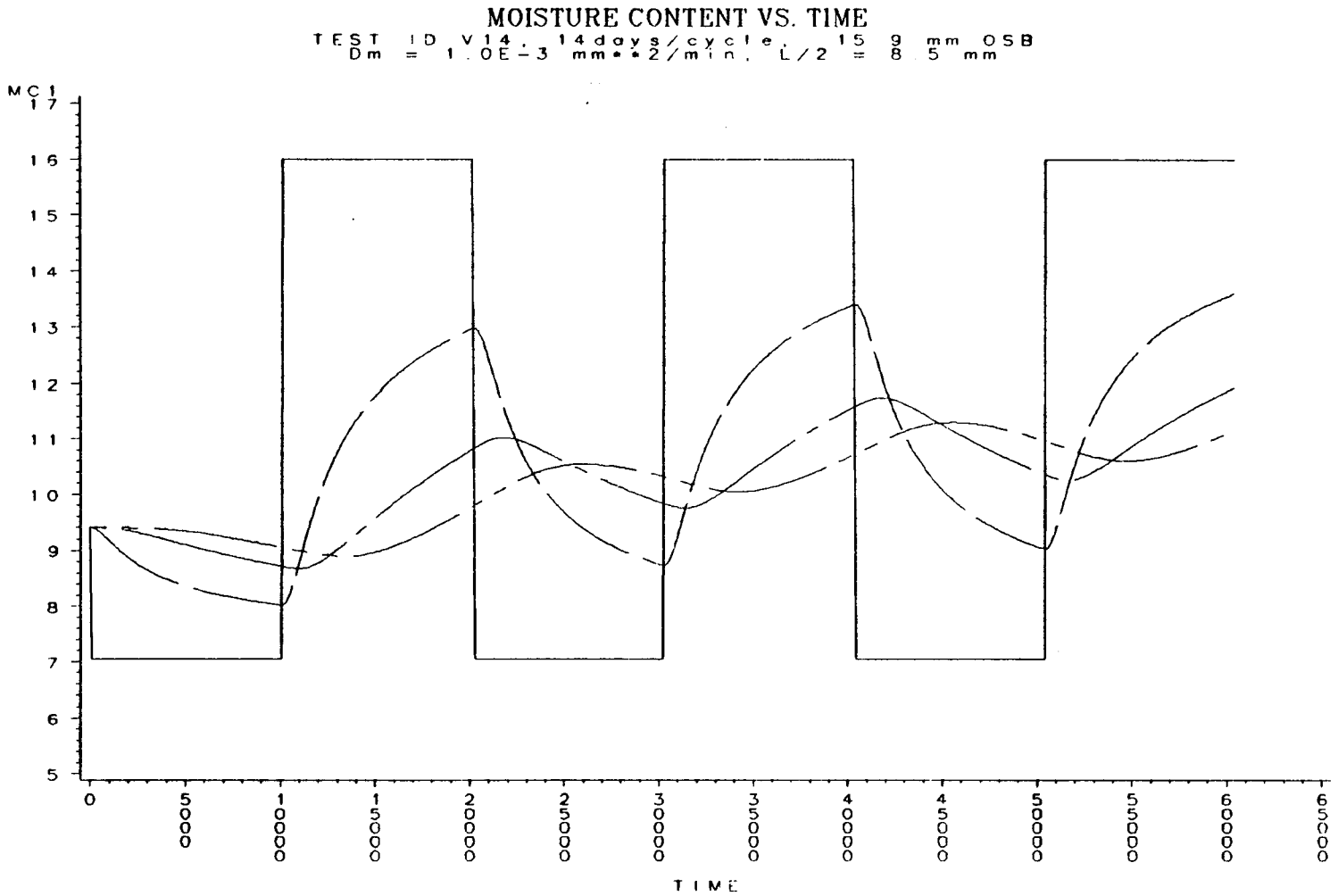

Fig. 7.11 Moisture Diffusion of the 15.9 mm OSB Panels at Various Depths in Cyclic RH Test V14

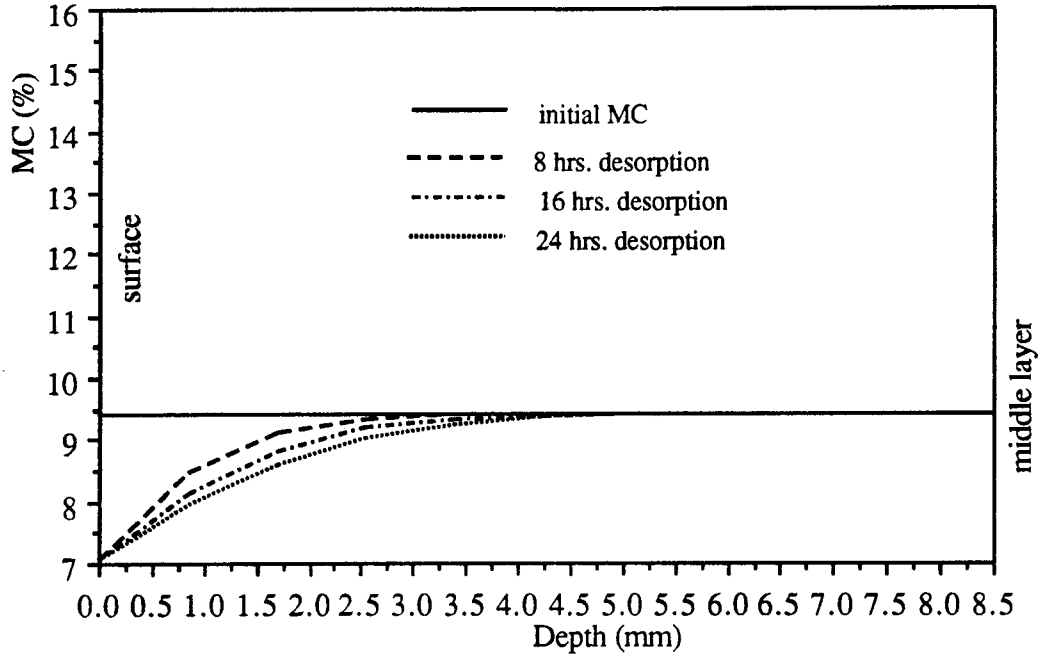

Fig. 7.12(a) Calculated Moisture Content through Thickness when Drying from 65% RH (at Equilibrium MC) to 35% RH for the 15.9 mm OSB Panels in Test V2 (D_m = 1.0 x 10^{-3} mm^2/minute)

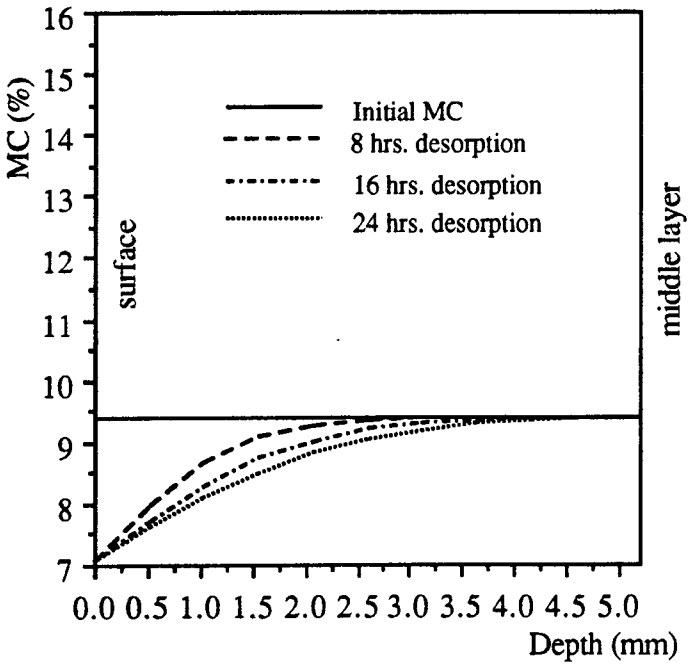

Fig. 7.12 (b) Calculated Moisture Content through Thickness when Drying from 65% RH (at Equilibrium MC) to 35% RH for the 9.5 mm OSB Panels in Test V2 (D_m = 1.0 x 10^{-3} mm^2/minute)

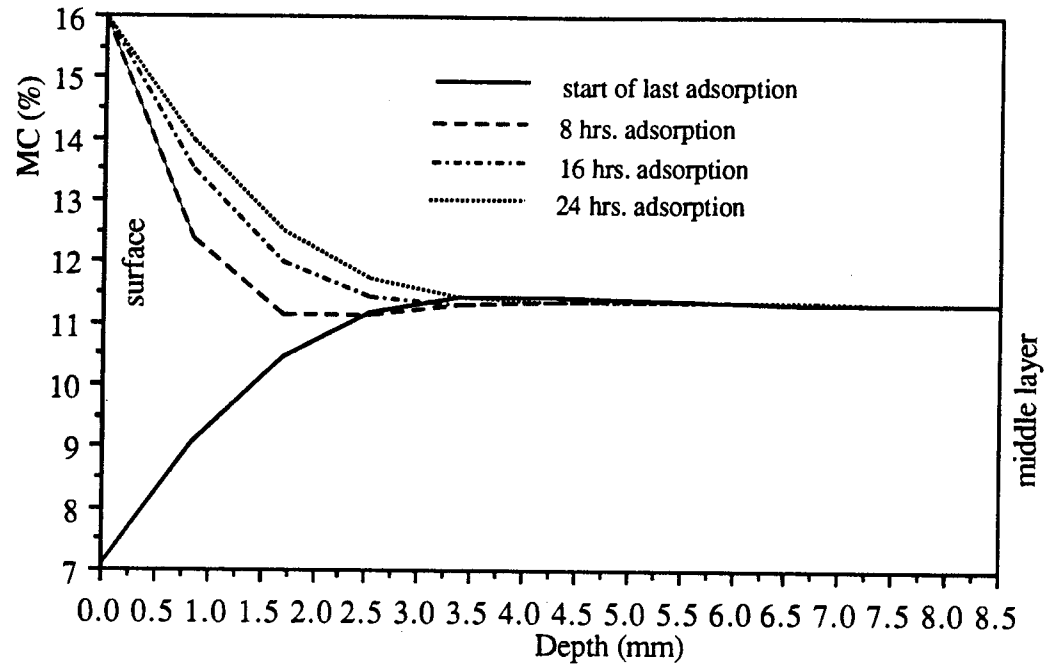

Fig. 7.13 (a) Calculated Moisture Content through Thickness when Wettng from 35% RH to 85% RH for the 15.9 mm OSB Panels in the Last Cycle of Test V2 (D_m = 1.0 x 10^{-3} mm^2/minute)

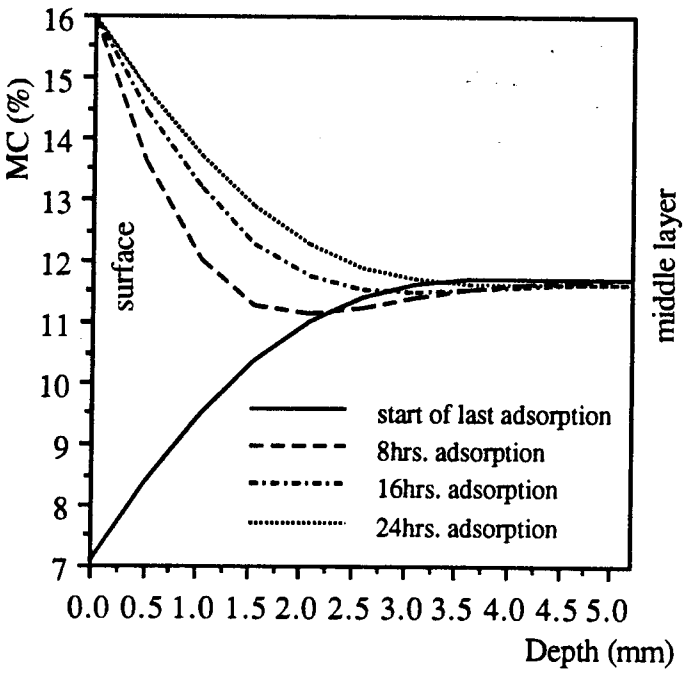

Fig. 7.13 (b) Calculated Moisture Content through Thickness when Wettng from 35% RH to 85% RH for the 9.5 mm OSB Panels in the Last Cycle of Test V2 (D_m = 1.0 x 10^{-3} mm^2/minute)

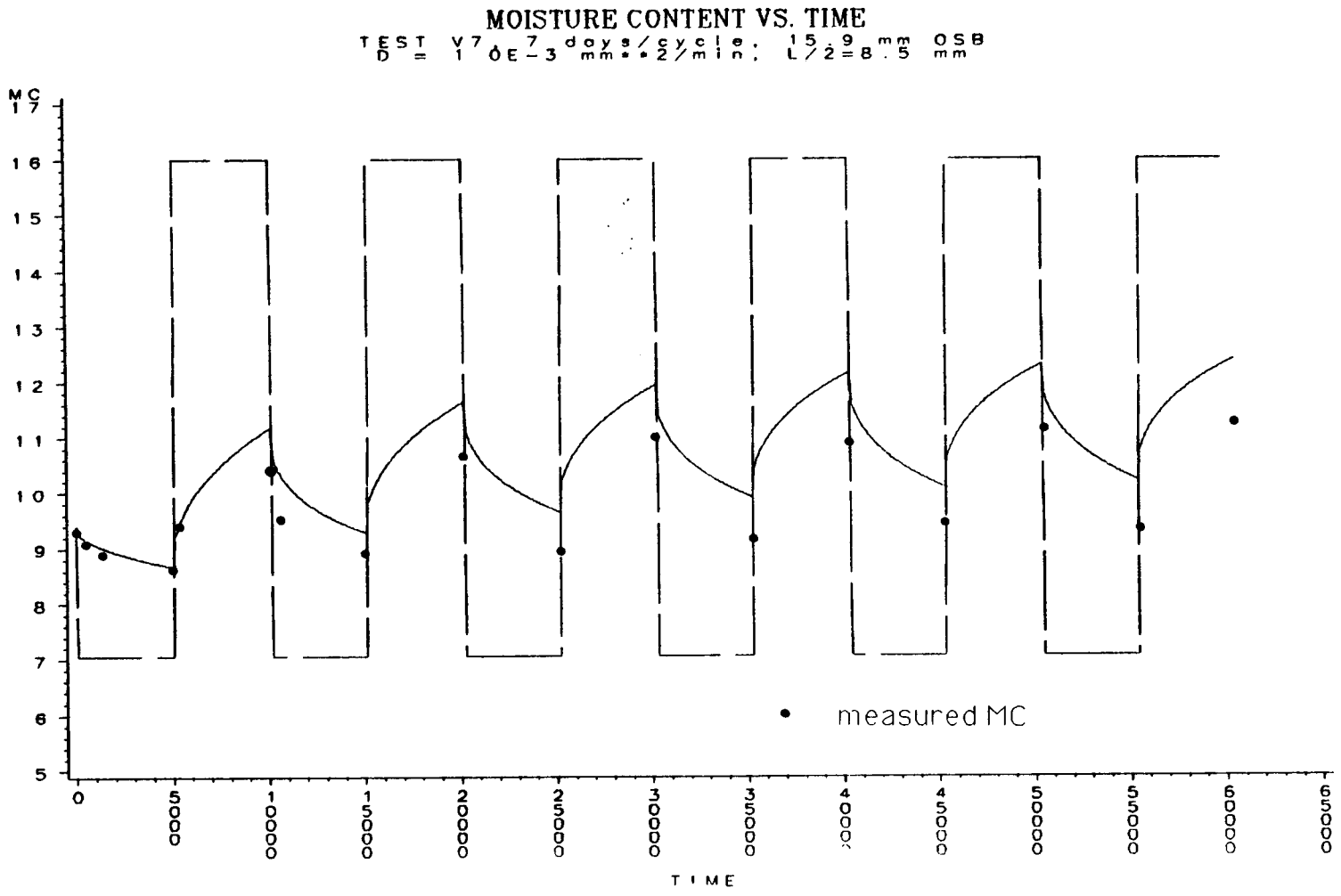

Fig. 7.14 The Average Moisture Content of the 15.9 mm OSB Panels vs. Time and the Measured Moisture Content in Test V7 (D = 1.0 x 10^{-3} mm^2/minute)

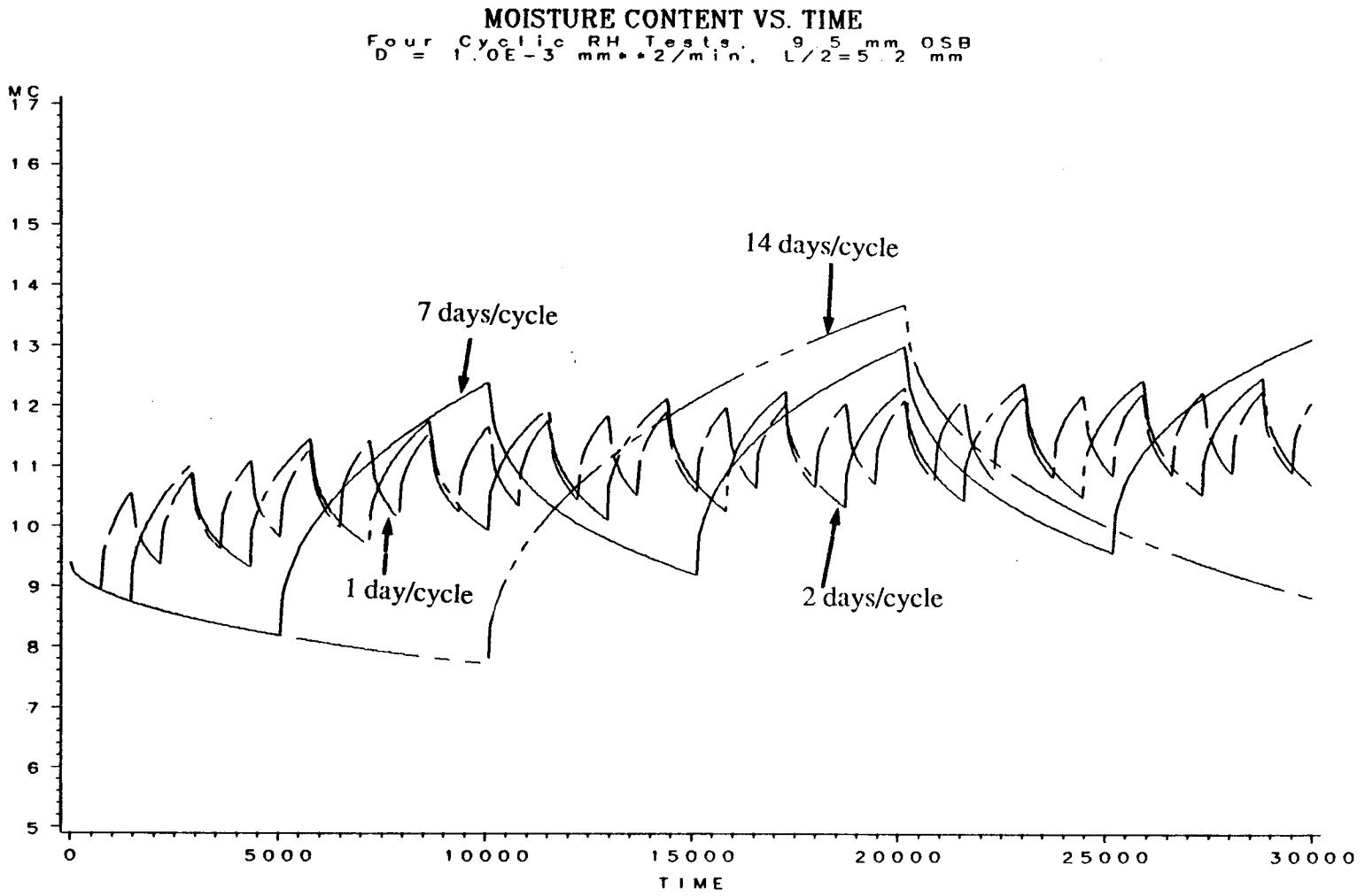

Fig. 7.15 The Average Moisture Content of the 9.5 mm OSB Panels vs. Time Curves in the Four Cyclic RH Tests

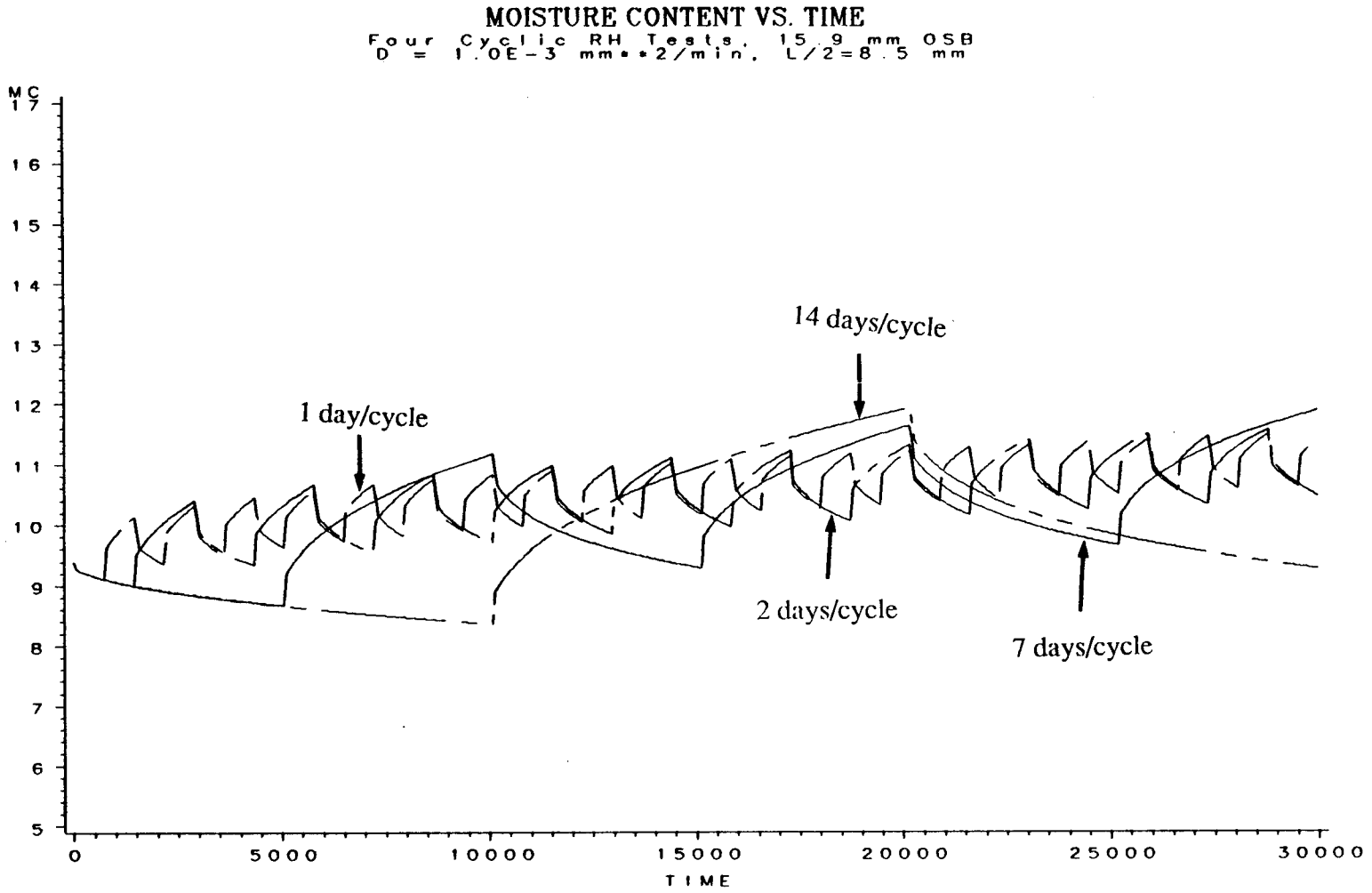

Fig. 7.16 The Average Moisture Content of the 15.9 mm OSB Panels vs. Time Curves in the Four Cyclic RH Tests

Chapter 8 Creep Calculation Model

8.1 General

In this chapter, the constitutive relationship describing the time-dependent flexural behavior of OSB panels under the influence of moisture changes is derived. The derivation is based on observations and speculations made from the creep test results. A number of assumptions and simplifications are proposed to develop a creep model which can be easily approached in practice, as well as with satisfactory accuracy.

As summarized in the literature review found in Chapter 2, the creep behaviors observed for the same type of materials are sometimes different from one study to another. Differences, and sometimes even contradictions, also exist between solid wood and wood composite products. Because of the inconsistency of observations reported and the complications of both time and moisture dependency of the deformation under sustained loading, no model can cover all the test results available in literature. The major objective of this modeling study is to simulate the OSB flexural deflection development during the square wave cyclic environmental RH changes under sustained loading. The model derived in this chapter is an experimentally based model. The model is extended to predict long-term deflection and deflections under other RH changes such as normal indoor conditions.

In Section 8.2, the creep test results are briefly reviewed and discussed. Some basic assumptions are made and the flexural deflection of the bending panel is divided into several components. Models evaluating each component and the related material parameters are then derived in Section 8.3. The restrictions and limitations of the model are also discussed in that section. In Section 8.4, the derived model is verified by comparing the model prediction with cyclic creep test results. Section 8.5 discusses the

applications of the model; long-term predictions are made and parametric study is carried out for the RH levels, creep under annual fluctuations, the effect of cyclic frequencies, and the influence of panel thicknesses. Finally, a summary and some remarks about the model study are made in Section 8.6.

8.2 Assumptions and Simplifications

8.2.1 Creep Behavior during RH Variation: A Brief Review

Although the experimental program and the test results are presented in Chapters 3 and 4, they are briefly reviewed here to facilitate understanding of the construction of the creep calculation model. In the experiment, all specimens were preconditioned at 65% RH/20 ^{o}C before the creep tests started. The environmental RH dropped from 65% to 35% as soon as the creep tests began. Besides the instantaneous deflection that occurred under the applied load, the deflection continually developed during the first desorption. When the RH changed from 35% to 85% after the first half cycle, a panel's deflection increased dramatically during this first adsorptive process; large amounts of creep deflection developed during the first full RH cycle with both desorption and adsorption. In the subsequent cycles, the creep accelerated during adsorptions, which also had a RH level as high as 85%; and the creep leveled off, or even partially recovered, during desorptions. Compared with the subsequent cycles, the first cycle generated much more creep.

The frequency of RH cycling definitely affected panels' creep as observed from the experiment. Among the four cyclic frequencies, the slowest cycling (14 days/cycle) yielded the most creep during the creep test duration (6 weeks). The accelerating effect of cyclic RH environments was also related to the geometric dimension of the panels. The thinner panels (9.5 mm) crept more than the thicker panels (15.9 mm) with respect

to the four frequencies adopted in the experiment.

The creep tests with three constant RH levels showed that the panel creep became very sensitive to the RH level when subjected to a high RH level such as 85%; a dry environment generated little creep.

8.2.2 Panel's Bending Deflection: A Conceptional Discussion

In the linear range, the curvature or deflection of a bending panel in a constant environment is proportional to the applied moment at a specified time. When the environmental RH changes, the panel shrinks or swells. The shrinking/swelling differs across the panel thickness due to the moisture gradient, and it may also be different from free shrinking/swelling because of the existence of the stress across the thickness. This imposed deformation (shrinking/swelling) could cause self-equilibrated stresses on the cross section. The self-equilibrated stress would further introduce strain on the cross section. The final strain profile is therefore different from the original. As a result, the resultant bending deflection may also be different from the original due to the sorptive processes in a cyclic RH environment.

Because the stress and/or strain distributions, as well as the panel deflections may change during environmental RH variations, the whole process during sorptions is very complicated. Some assumptions (as illustrated below) are made, and the stress and strain profiles during a desorptive process are shown in Figs. 8.1 and 8.2. These assumptions are proposed for discussing and constructing the creep model. The bending cross section must have double symmetric axes, such as a rectangular cross section, to fit the discussion. The assumptions are:

Assumption 1. The plane cross section remains plane.

This assumption implies that the strain distribution under applied moment (M) is a straight line, as in Fig. 8.2(a). In the figure, Φ_1 is the curvature of the bending panel corresponding to the applied moment before sorption happens.

Assumption 2. The modulus of elasticity for both compression and tension sections are identical.

When this is true, the neutral axis in Figs. 8.1(a) or 8.2(a) is passing through the symmetric axis of the cross section.

Assumption 3. Compression and tension have the same creep function and the creep function is not affected by sorptions; that is, creep behavior is not related to signs of the stress. This can be expressed as

$$\text{if} \quad \varepsilon_{creep} = f(\sigma,t), \qquad \text{then} \quad -\varepsilon_{creep} = f(-\sigma,t)$$

While the above assumption is true, the neutral axis keeps passing through the symmetric axis of the cross section under the sustained loading. If the creep function f was not affected by sorptions, the uniaxial creep curve would be a smooth curve without fluctuation during the abrupt environmental changes. However, this behavior is not what is usually observed in experiments.

Assumption 4. The creep strain is proportional to the stress applied.

When the linear assumption is valid, the stress distribution in Fig. 8.1(a) will remain a straight line, as in the linear elastic case.

Assumption 5. The moisture diffusion and the introduced shrinking or swelling are not affected by the applied stress.

With this assumption, the shrinking/swelling in Fig. 8.2(b) is symmetric about the

symmetric axis of the cross section.

If all assumptions given above are satisfied, there is no additional deflection generated or recovered during sorptions; that is, Φ_1 is equal to Φ_2 in Fig. 8.2. However, this is not what was observed in the tests, where the panel deflection accelerated or decelerated during sorptions. The facts therefore indicate that one (or some) of the above assumptions must not be valid. Some speculations are discussed as follows and the detailed discussion about these speculations is given in Appendix A.

1. The non-linear creep behavior may exist (referring to strain vs. stress not linear); therefore, the fourth assumption listed above is not valid. For the non-linear creep behavior, the resultant stress profile shown in Fig. 8.1(c) gives a strain profile different from what is shown in Fig. 8.2 (e).

2. Shrinking and/or swelling of a specimen with applied stresses may be different from that of a specimen with free dimension changes; that is, the fifth assumption is not true. Therefore, the shrinking/swelling introduced deformation is not symmetric about the neutral axis.

3. Different stress states (compression and tension) may have different creep functions, especially during sorptions; that is, the creep function for compression (f_c in assumption 3) and the creep function for tension (f_t in assumption 3) are different. Therefore, the neutral axis may move upwards or downwards during the sorptions.

4. Compression and tension have the same creep compliance (f_c is the same as f_t), but the creep compliance may change during desorptions and adsorptions; that is f changes during sorption. In such cases, the flexural deflection or the curvature changes during sorptions.

Under low stress levels, the linear assumption is usually a reasonable assumption (as reviewed in Chapter 2). The linear creep behavior assumption is kept for this model study.

Although some studies show that moisture introduced deformation changes are stress dependent, and that different stress states might have different effects on the shrinking or swelling, the creep behaviors under compression and tension might also be different for the two stress states as reported in literature.

The last possibility (No. 4) listed above is picked up as a reason for the deflection fluctuations of OSB panel during sorptions; that is., all five basic assumptions presented in the beginning of this section, except for part of the third assumption, are adopted to derive the creep model.

8.2.3 Creep Components

Many efforts have been made to construct a model to evaluate creep during sorptive processes. Lists of requirements to construct such a model are given by Grossman (1976), Hoffmeyer (1990), and Hunt (1989). There are some differences among these requirements, which result from the differences in interpretation of test results and/or from inconsistency between the test results themselves. The model proposed here is mainly based on the test results obtained from the experiment of this study, as presented in the earlier chapters (Chapters 4 and 5).The derivation, which is based upon the assumptions presented above and which will be suitable for bending cases, begins with the uniaxial case as it is introduced to bending.

The terms used for the following derivation are defined here. In the uniaxial case, strain (ε) is chosen as a measurement of deformation. Upon the application of the load, an instantaneous deformation is produced in a specimen. This deformation is usually

referred to as elastic deformation. Under sustained loading, the deformation of the specimen will increase with time; some of the deformation can be recovered upon unloading and the remaining is unrecoverable. Those time-dependent deformations are called creep. If the climatic condition of the specimen is thereafter kept constant, the creep deformation is called pure creep.

If the test specimen is subjected to environmental humidity changes, the specimen's total deformation ε will increase. The deformation increment can be divided into two parts; the first part is the deformation change by shrinking or swelling of the specimen due to the moisture changes in the specimen. As discussed above, the amount of the moisture introduced shrinking or swelling under an applied load may be different from the free shrinking or swelling ε_f, which is the deformation change of a similar specimen subjected to the same humidity changes, but with no loading. According to the given assumptions, the shrinking or swelling of a creep specimen is assumed equal to that of a specimen without loading. Besides the free shrinking or swelling, the deformation left from the total moisture deformation, called mechano-sorptive creep strain ε_{ms}, is the second part of the deformation increment during environmental humidity changes. The mechano-sorptive deformation is the deformation generated in the specimen due to the coexistence of both humidity changes and sustained loading. Such deformation (M-S creep) can not occur if only one of these factors is present; the mechano-sorptive deformation happens only when a loaded specimen is subjected to environmental humidity changes.

When the deformation in a loaded specimen caused by humidity changes is divided into two components as above, whether or not the shrinking/swelling is affected by the applied load is not important. Even if the shrinking/swelling under applied load does differ from the free shrinking/swelling, the difference between the two is therefore

included in the component of mechano-sorptive deformation.

The total strain of a specimen under sustained loading and humidity variations is expressed as

$$\varepsilon = \varepsilon_e + \varepsilon_c + \varepsilon_f + \varepsilon_{ms} \tag{8.1}$$

where ε = the total strain of a specimen at any time t

ε_e = the elastic strain under applied load

ε_c = the pure creep strain (both viscoelastic and viscous) due to the sustained loading under a constant climatic condition

ε_f = the free shrinkage or swelling strain due to the climatic humidity changes

ε_{ms} = the mechano-sorptive strain of a specimen with sustained loading and simultaneous climatic humidity changes.

The deformation of a bending specimen is usually measured by deflection. The deflection development of a bending specimen is related to the behaviors of both compression and tension zones on the cross section. As discussed in Section 8.2.2, the free shrinkage/swelling of a bending cross section with two symmetric axes will not cause extra bending deflection. Therefore, in the uniaxial case given by Eqn. (8.1), the deflection of a bending specimen subjected to sustained loading and simultaneous moisture variations can be taken as

$$\Delta = \Delta_e + \Delta_c + \Delta_{ms} \tag{8.2}$$

where Δ = the total deflection of a bending specimen at any time t

Δ_e = the elastic deflection under applied load

Δ_c = the pure creep deflection due to the sustained loading under a constant climatic condition, which includes recoverable and unrecovrable components

Δ_{ms} = the mechano-sorptive deflection of a bending specimen with sustained loading and subjected to climatic humidity changes, which may also include recoverable and unrecovrable components.

It should be noted that the deflection here denotes flexural deformation by applied moment only. With the test set-up (Figs. 3.2 and 3.7), the measured deflection results only from flexural deformation.

8.3 The Proposed Model

8.3.1 Components in the Proposed Model

Time-dependent deflection of an OSB panel under constant applied moment and subjected to humidity variations could be divided into three components as illustrated by Eqn.(8.2). In the proposed model, the elastic deflection Δ_e is taken as the instantaneous deflection measured in the tests. Since all panels were preconditioned at 65% RH/20 ^{o}C, the elastic measured deflections corresponded to the elastic moduli at that climatic condition. The pure creep deflection Δ_c is the deflection increment with time under the constant climate (65% RH/20 ^{o}C). When the environmental humidity changes, the extra deflection generated is the mechano-sorptive creep deflection Δ_{ms}. When wood panels are exposed to various environmental RH conditions, the first two components of the total deflection in Eqn. (8.2) remain unchanged, and the resulting difference from the different humidity changes is the third component, that is, the mechano-sorptive creep deflection. The summation of the first two components is the total deflection of a creep specimen in 65% constant RH environment, which is the

climatic condition for test series C65 as described in the experimental chapters. The creep curves obtained from test C65 are here referred to as basic creep curves.

Because the first two components are already known from the creep test C65, the mechano-sorptive creep deflection Δ_{ms} is the one which is different for different humidity changes and it needs to be modeled. The following study mainly focuses on modeling this component.

If Eqn.(8.2) is rewritten to use creep compliance (defined by Eqn. (5.1)) instead of creep deflection, and to specify the 65% constant RH as the pure creep (or the basic creep) environmental condition, the total creep compliance during humidity variations becomes

$$J(t) = J_e + J_c + J_{ms} \tag{8.3}$$

where $J(t)$ = the total creep compliance of a bending specimen at any time t

J_e = the elastic compliance of a specimen at equilibrium condition as 65% RH/20 ^{o}C

J_c = the creep compliance corresponding to the creep deflection increment at 65% RH/20 ^{o}C environment under sustained loading

J_{ms} = the creep compliance corresponding to the climatic humidity changes.

If both sides of Eqn. (8.3) are divided by J_e, then the panel's time and moisture dependent behavior could be expressed by fractional deflection

$$F(t) = F_{65} + F_{ms} \tag{8.4}$$

where $F(t) = J(t)/J_e$ = the fractional deflection of a bending specimen at any time t

$F_{65} = (J_e + J_c)/J_e$ = the fractional deflection of a specimen under constant climatic condition as 65% RH/20 ^{o}C. The values for F_{65} are taken or predicted from test C65 as described in Chapter 6

$F_{ms} = J_{ms}/J_e$ = the mechano-sorptive fractional deflection due to moisture changes and sustained loading.

8.3.2 Modeling of Mechano-sorptive Creep

Based on the experimental observations and the above proposed method of separating creep components, the rate of the mechano-sorptive fractional deflection is assumed to depend on the rate of moisture changes, as well as to the current moisture state, and yields

$$\dot{F}_{ms} = \dot{F}_{ms}(u, \dot{u}) \tag{8.5}$$

where $\dot{F}_{ms} = \frac{dF_{ms}}{dt}$ = the change rate of mechano-sorptive fractional deflection with respect to time t

u = the panel's average moisture content (%) at time t

$\dot{u} = \frac{du}{dt}$ = the panel's moisture content change rate with respect to time t

As observed from the tests, the deflection development during the first desorption and adsorption is much more than in the subsequent cycles. The mechano-sorptive creep calculation model should also show the difference. For the first RH cycle, the creep deflection increment was found proportional to the magnitude of the moisture change in panels. The creep rate can be written as follows:

For the first desorption

$$\dot{F}_{ms} = A\dot{u} \tag{8.6}$$

where A = a material constant for calculating the effect of the first desorption; it is different for panels with different thicknesses. The value is given later in this section.

$\dot{F}_{ms}$ and $\dot{u}$ are the same as in Eqn. (8.5).

For the first adsorption

$$\dot{F}_{ms} = B\dot{u} \tag{8.7}$$

where B = a material constant for calculating the effect of the first adsorption; it is different for panels with different thicknesses. The value is given later in this section.

$\dot{F}_{ms}$ and $\dot{u}$ are the same as in Eqn. (8.5).

For the subsequent sorptions, it is expected that both the moisture change rate and the current moisture level, especially high moisture levels, will affect the mechano-sorptive creep rate. The creep rate is expressed as

$$\dot{F}_{ms} = C\dot{u} + Du/\bar{n}^m \tag{8.8}$$

where C = a material constant which reflects the fluctuation of creep deflection during the moisture changes; it is different for panels with different thicknesses. The value is given later in this section.

$D = 5.5 \times 10^{-6}$ minute^{-1} = a material constant which accounts for the effect of panel moisture level on mechano-sorptive creep and which is not relevant to panel thickness

$\bar{n} = 2,3,\cdots$ = number of RH cycles the panel is exposed to

m = a material constant which accounts for the creep rate decreases when the number of RH cycles increases. The value is given later in this section.

The total mechano-sorptive fractional deflection at time t (t > one full cycle with time p could be obtained from Eqns. (8.6), (8.7), and (8.8):

$$F_{ms}(t) = \int_0^{p/2} A\dot{u}dt + \int_{p/2}^{p} B\dot{u}dt + \int_p^t C\dot{u}dt + \int_p^t Du/\bar{n}^m dt \qquad (8.9)$$

or

$$F_{ms}(t) = A \times (u(p/2) - u(0)) + B \times (u(p) - u(p/2)) + C \times (u(t) - u(p)) + D\int_p^t u/\bar{n}^m dt \qquad (8.10)$$

where t= the time when the mechano-sorptive fractional deflection is calculated in minutes

$F_{ms}(t)$ = the total mechano-sorptive fractional deflection at time t, with t longer than one full cycle

p = time for one full cycle in minutes

$u(0)$ = the initial moisture content (%) = 9.4 (%) for OSB at 65% RH/20 ^{o}C

$u(p/2)$ = panel's average moisture content (%) at the end of the first desorption or half cycle

$u(p)$ = panel's average moisture content (%) at the end of the first adsorption or one full cycle

$u(t)$ = panel's average moisture content (%) at time t.

A,B,C,D,m, and $\bar{n}$ are the same as defined on the previous two pages.

To actually calculate the values of mechano-sorptive fractional deflection, the material constants need to be known. Those constants are evaluated from the cyclic creep tests (shown in Appendix B), and are given below:

A = material constant for calculations during the first desorption;

= -0.194 for 9.5 mm (3/8") OSB; or

= 0.0 for 15.9 mm (5/8") OSB

B = material constant for calculations during the first adsorption;

= 0.204 for 9.5 mm (3/8") OSB; or

= 0.267 for 15.9 mm (5/8") OSB

C = mechano-sorptive deflection fluctuation coefficient;

= 0.01 for 9.5 mm (3/8") OSB; or

= 0.06 for 15.9 mm (5/8") OSB

m = constant accounting for decreasing of mechano-sorptive creep rate;

= 0.925 for 9.5 mm (3/8") OSB; or

= 1.10 for 15.9 mm (5/8") OSB

With Eqns. (8.6) to (8.10), and the material constants given above, the mechano-sorptive fractional deflections of OSB panels can be calculated easily. However, some restrictions must be placed on the model. Recalling from the experimental results that

the mechano-sorptive creep in subsequent cycles was much less than that of the first cycle, and that the mechano-sorptive creep was less at lower moisture content levels, the mechano-sorptive creep rate in subsequent cycles is set at zero when the panel's moisture content is less than the panel's initial moisture content (9.4%); that is, for Eqn. (8.8), $\dot{F}_{ms} = 0$ when $u(t) < u(0) = 9.4\%$ during subsequent cycles.

The second restriction is applied to very slow environmental changes. In slow RH cycling, panels reach equilibrium moisture content (EMC) in each RH duration. There should be little mechano-sorptive creep after equilibrium moisture content is reached. Therefore, $\dot{F}_{ms} = 0$ for Eqn. (8.8) when $u(t) \cong EMC$. The EMC is the equilibrium moisture content corresponding to the RH level to which the panel is exposed.

With the model given in this section, it is easy to calculate the fractional deflections of panels tested in cyclic RH environments. Comparisons between the results from the calculation and the experiment verify the model proposed here. This consistency will be examined in the next section.

8.4 Verification of the Creep Model

The total fractional deflection of bending OSB panel can be estimated by adding a mechano-sorptive creep component to the basic creep curve corresponding to 65% constant RH at 20 ^{o}C as expressed by Eqn. (8.4). Within the creep test duration (6 weeks), the basic creep is directly taken from experiment. After the creep test duration, values of the basic creep are estimated by curve fitting predictions that are made on the measured values during the six weeks on a logarithmic time plot. The curve fitting predictions are presented in Chapter 6.

To estimate the mechano-sorptive creep component, a panel's moisture content and its change rate must be evaluated first. They are calculated by the method presented in

the diffusion analysis of Chapter 7. Another small program was written and connected to the moisture diffusion analysis program during the study to evaluate the mechano-sorptive creep component according to the proposed model.

To verify the proposed model, the four cyclic and one indoor environmental RH creep tests conducted in the experiment are analyzed by the model. The analytical results are compared with the experimental results.

8.4.1 Comparison of the Calculated Results with the Test Results for the Four Cyclic RH Creep Tests

The actual RH profiles of the four cyclic tests are inputted as environmental excitations to calculate the fractional deflection of 9.5 mm and 15.9 mm OSB panels. Results from the calculation and experiment are listed in Tables 8.1 and 8.2 for 9.5 mm and 15.9 mm OSB panels, respectively. The calculated fractional deflections after one full cycle and after 6 weeks are all very close to the experimental results as listed in Tables 8.1 and 8.2, which shows that the model can very well fit the overall tests results within the creep test duration for both panel thicknesses. The calculated mechano-sorptive fractional deflection (F_{ms}) vs. time curves are plotted in Figs. 8.3 to 8.10 for both 9.5 mm and 15.9 mm panels in the four cyclic RH environments. During cyclic test V14, the M-S fractional deflection data taken from the tests are plotted together with the predicted curves for 9.5 mm and 15.9 mm panels in Figs. 8.6 and 8.10, respectively. The experimental values of M-S fractional deflection is the difference between cyclic test and the constant test C65.

The figures show that the mechano - sorptive creep accelerates during adsorptions and slows down, or even partially recovers, during desorptions. This behavior agrees with the test observations described in Chapter 4. From the plotted curves, the

magnitude of creep deflection fluctuations during sorptive processes is also found to be close to what was observed from the tests.

The comparison between the modeling and the test results shows that the model provides not only good overall creep estimation, but also creep fluctuations during sorptions. The calculated creep at 150 days and 10 years is also compared with the predictions made by Eqn. (6.4) in Chapter 6. The results are summarized in Tables 8.1 and 8.2 for both thicknesses.

In the modeling analysis, the basic creep component F_{65} is predicted by the curve fitting equation, which is based on the six week creep data, with a fitting equation like $F_{65} = a + b\log t + c(\log t)^2$. However, the mechano-sorptive creep component F_{ms} is calculated by Eqns. (8.6), (8.7), and (8.8).

The predicted and modeling values at 150 days and ten years are fairly close to each other It should be noted that the prediction by Eqn. (6.4) or Table 6.3 is just an extrapolation of the six week test data. The model proposed in this chapter is to model mechano-sorptive creep based on the moisture content state of the panels. The model given here and by Eqn. (6.4) provides two different prediction approaches. Therefore, the model is verified to some extend by the close long-term results given by the two different methods, even though there are no real long-term test results available to support the prediction.

8.4.2 Comparison of the Calculated Results with the Test Results for the Indoor Creep Tests

Three creep test series were conducted in a normal indoor environment. In Edmonton, the indoor humidity in a warehouse building is usually very low in the winter (much less than 65%). However, sometimes the RH may be higher than 65%

during summer; therefore, panel creep in an indoor environment is usually less than the basic creep defined earlier.

Among the three indoor creep test series, the second series I2 was tested during April to July 1991, gave the most creep, and the creep was a little larger than the basic creep (under 65% RH/20 ^{o}C). To model the creep test I2, the environmental record of the test is read carefully and the RH is simplified as a two-step square wave cycling. In the early stage of the creep test, the RH was very low, but became higher during summer. The simulated RH profile is shown in Fig. 8.11. Since the RH in the figure is always less than 65%, the mechano-sorptive creep F_{ms} is assumed to be zero after the first desorption and adsorption according to the proposed model; that is, after the first full cycle, the creep rate is assumed to be the same as the basic creep curve.

The panel's initial MC is 9.4%. The panels' EMCs at 25% and 50% RH are extrapolated or interpolated from the EMCs at 65% and 35% RH which are listed in Tables 4.12 and 4.13. The fractional deflection is calculated by the model for the RH profile shown in Fig. 8.11. The results are listed in Table 4.3 together with the values obtained from the tests. The modeling results fit well with the test data, and demonstrate that the model can also give approximate creep values as long as the environmental RH can be reasonably simplified into square wave cycles. In the cases which have very low RH, the panel creep can be conservatively estimated by the basic creep curve.

8.5 Parametric Study by the Model

As mentioned above, the proposed model provides a tool to calculate creep of OSB. This section provides a parametric study on various parameters such as the RH fluctuating amplitude, the level of the fluctuation center, the frequency of cycling, and

the panel thickness. It should be noted that the parametric study only provides speculations on some factors which were not studied in the experimental program. Whether or not they are correct needs to be verified by further experiments.

8.5.1 RH Fluctuation Range

All the cyclic RH creep tests were conducted with RH fluctuating between 35% and 85%. The fluctuations with larger or smaller amplitudes are studied here, and fluctuations with the same amplitude, but different center levels, are also examined.

For the 35-85% RH cycling, the corresponding panel equilibrium surface moisture contents are 7% and 16%. This can be expressed as (11.5 ± 4.5) %MC fluctuation, where 4.5% represents the amplitude of the fluctuation. Amplitude values other than 4.5% MC are studied, and the creep for those environmental conditions are calculated by the model. Some results are summarized in Table 8.4. Since the basic creep component F_{65} is always the same for the different environmental fluctuation amplitudes, only the calculated mechano-sorptive fractional deflections are compared for cyclic fluctuations with different ranges.

Different MC fluctuating amplitudes yield different amount of creep. Table 8.4 shows that the larger amplitude (AM = 4.5 % MC) yields more mechano-sorptive creep than does the smaller amplitude (AM = 2 % MC) when the fluctuations are around the same center (11.5% MC), as is shown by comparing the first two columns of fractional deflections in the table. The same conclusion can be reached for the two fluctuations with the same center at 10% MC. The results for these two cases are listed in the last two columns of the table.

Furthermore, the mechano-sorptive creep difference caused by the fluctuation amplitude difference is mostly contributed to the first full cycle. After the first full

cycle, there is little creep differences between the first (AM_1) and the second (AM_2) amplitude; that is, the amplitude has little influence on the later creep duration.

It can therefore be concluded that larger fluctuation amplitudes give more mechano-sorptive creep in OSB panel, and that this happens mostly at the early creep stage.

The different fluctuation center level also seems to make a difference to panel creep, as is shown by comparing the cycling with center levels at 10.0% or 11.5% MC in Table 8.4. The higher fluctuation center level (11.5% MC) produces more long-term (ten years) mechano-sorptive creep than the lower fluctuation center level (10.0% MC). This result also agrees with the constant RH creep test results, which show that the higher RH gives more creep.

8.5.2 RH Cyclic Frequency

The creep experimental results indicated that OSB panel creep was affected by the frequency of cyclic RH environmental changes. Within the frequency range adopted by the tests, from a 1 day/cycle to a 14 days/cycle, it was found that the panels generated more creep during slower cyclic RH variations. This conclusion may change when the RH cycling becomes very fast or very slow. Because of the limitations of the experiment, the very fast or slow cyclic RH environment was not tested. The effect of these situations is investigated by the model developed in this chapter.

The frequencies studied range from 4 hours/cycle to 1 year/cycle, and the environmental RH changes between 35% and 85%. The panels are assumed in equilibrium with 65% RH before the RH excitation. Such environmental conditions simulate the experimental conditions, except that more cyclic frequencies are investigated. The calculated long-term creep at ten years are summarized in Table 8.5 for both 9.5 mm and 15.9 mm OSB panels. The values listed in the table are the

mechano-sorptive fractional deflections, which do not include the basic creep component. The cyclic period vs. the ten year mechano-sorptive fractional deflection is also plotted in Fig. 8.12 for 9.5 mm OSB panels. For the four cyclic frequencies adopted in the experiment, the analytical model shows that the slower RH cycling yields the more creep, which agrees with the test results. The model analysis also shows that beyond a certain value, the slower cyclic RH generates less creep. The particular frequency that generates the most creep changes may be different for different panel thicknesses and/or for different RH fluctuation ranges.

As shown in Table 8.5, the crucial frequencies for 9.5 mm and 15.9 mm OSB panels are about 60 days/cycle and 100 days/cycle, respectively, for 35%-85% cyclic RH changes.

For very fast RH cycling, such as 4 hours/cycle, the environmental changes are too fast for OSB panel to respond. Therefore, the calculated mechano-sorptive creep is small as shown in the Table 8.5 and Fig. 8.3. For the slow cycling of 1 year/cycle, OSB panels reach EMC before the RH changes to the next step. There is also little mechano-sorptive creep after that because of the small amount of moisture movement in the panels. This is why the slower cycling produces less creep when the cyclic frequency is slow enough.

8.5.3 Panel Thickness

The experimental results showed that the OSB panel with different thicknesses yielded a different amount of creep in cyclic RH environments. From the four cyclic RH tests, it was found that the thinner panels (9.5 mm) produced more creep than did the thicker panels (15.9 mm). This fact agrees with the results from the modeling. When the cyclic frequencies are between 1 day/cycle to 14 days/cycle, the calculated

creep for 9.5 mm panels in Table 8.5 is larger than for 15.9 mm panels. Fig. 8.13, which is a plot of panel mechano-sorptive fractional deflection at ten years with different cyclic RH frequencies for panels with both thicknesses, shows the same conclusion.

The model analysis shows that the thicker panels begin to creep more than the thinner panels when the cyclic RH changes are slower than a certain value. As shown in Table 8.5 or Fig. 8.13, the 9.5 mm panels creep more than the 15.9 mm panels when the cyclic RH changes are faster than 28 days/cycle. When the cyclic RH changes are slower than 60 days/cycle, the 15.9 mm panels begin to creep more. The reason for this may be that in a fairly slow cyclic environment, there may still be much moisture movement in the thicker panels while the moisture in the thinner panels is reaching equilibrium. In such cases, the thicker panels may generate more mechano-sorptive creep than do the thinner panels.

The long-term creep of OSB panels with thicknesses other than 9.5 mm or 15.9 mm could be analyzed by the model if the material constants for those panels are known. However, they are not analyzed here because of the shortage of the material constants.

8.6 Summary and Remarks

The time and moisture dependent deformation of OSB panels under sustained loading has been modeled in this chapter. When the total deformation is divided into several components, those for bending deflection are obtained through a theoretical deduction. Finally, the mechano-sorptive creep component, which is the time dependent deflection resulting from simultaneous moisture changes and mechanical loading, is defined and extracted from the total bending deflection and modeled by

Eqns. (8.6) to (8.8).

The proposed model is verified by comparing the modeling results with the cyclic creep test and the indoor creep test. A parametric study, including the RH fluctuation ranges, the different cyclic frequencies, and the effect of panel thickness, has been carried out by the model. The long-term creep under the annual cycling is also predicted by the model.

The model developed in this chapter is derived from experimental results. The material constants still need to be known for wood panels other than 9.5 mm and 15.9 mm OSB. These constants could be obtained from relatively short creep tests for a particular material. All the calculations carried out by the model are for square wave RH cycling. Whether the model fits other cyclic RH changing patterns should be verified by tests with that environment.

It should also be mentioned that the mechano-sorptive creep in the model is set at zero when the panel reaches to EMC. The numerical analysis by the computer program shows that the calculated creep is sensitive to the tolerance criteria used to judge whether or not EMC has been reached. This happens when the RH cycling is slow. The model can further be refined if the creep behavior under such environments is actually known.

Table 8.1 Comparison of the Fractional Deflection between Modeling and Experiment in the Cyclic RH Tests for the 9.5 mm OSB Panel

		Test ID			
Creep Time		V1	V2	V7	V14
one full cycle	Measured [a]	1.7	1.5	2.3	3.1
	Modeling [b]	1.6	1.8	2.3	2.8
6 weeks	Measured [a]	2.5	2.6	3.7	4.2
	Modeling [b]	2.2	2.5	3.5	4.0
150 days	Predicted [c]	2.9	3.1	4.7	5.8 [d]
	Modeling [b]	2.4	2.9	4.5	5.5
10 years	Predicted [c]	4.0	4.8	7.3	10.2
	Modeling [b]	3.2	4.1	7.7	10.8

[a] The measured fractional deflection is from the creep tests as given in Chapter 4.

[b] The fractional deflection is calculated by the proposed model in this chapter.

[c] The predicted fractional deflection is calculated by Eqn. (6.4) or Table 6.3.

[d] The fractional deflection for test V14 at 150 days is obtained from the creep test.

Table 8.2 Comparison of the Fractional Deflection between Modeling and Experiment in the Cyclic RH Tests for the 15.9 mm OSB Panel

		Test ID			
Creep Time		V1	V2	V7	V14
one full cycle	Measured [a]	1.6	1.5	2.1	2.8
	Modeling [b]	1.5	1.7	2.2	2.6
6 weeks	Measured [a]	2.3	2.6	3.2	3.8
	Modeling [b]	2.5	2.8	3.4	3.8
150 days	Predicted [c]	2.5	3.0	4.0	4.8 [d]
	Modeling [b]	2.8	3.2	4.2	5.2
10 years	Predicted [c]	3.2	4.0	6.4	9.4
	Modeling [b]	3.9	4.4	6.4	8.8

[a] The measured fractional deflection is from the creep tests as given in Chapter 4.

[b] The fractional deflection is calculated by the proposed model in this chapter.

[c] The predicted fractional deflection is calculated by Eqn. (6.4) or Table 6.3.

[d] The fractional deflection for test V14 at 150 days is obtained from the creep test.

Table 8.3 Comparison of the OSB Panel Fractional Deflection between Modeling and Experiment for Indoor Creep Test I2

Nominal Thickness(mm)		Creep Time	
		6 weeks	12 weeks
9.5	Measured [a]	2.0	2.3
	Modeling [b]	2.0	2.5
15.9	Measured [a]	1.9	2.1
	Modeling [b]	1.9	2.4

[a] The measured fractional deflection is from the creep tests as given in Chapter 4.

[b] The fractional deflection is calculated by the proposed model in this chapter.

Table 8.4 The Mechano-sorptive Fractional Deflection (F_{ms}) of 9.5 mm OSB Panels Exposed to Different Cyclic Climate Fluctuation Ranges

		$(11.5 \pm AM_i)$%MC[a]		$(10.0 \pm AM_i)$%MC[b]	
Creep Time	Cyclic Period	$AM_1 = 2.0$	$AM_2 = 4.5$	$AM_1 = 2.0$	$AM_2 = 4.5$
10 years	1 day/cycle	1.2	1.4	1.0	1.2
	2 days/cycle	2.1	2.3	1.7	1.8
	7 days/cycle	5.3	5.9	4.0	4.0
	14 days/cycle	8.9	9.0	6.1	6.4
	28 days/cycle	12.5	13.0	8.1	10.3
	1 year/cycle	6.0	7.8	4.2	6.7
one full cycle	1 day/cycle	0.2	0.4	0.2	0.5
	2 days/cycle	0.2	0.6	0.3	0.6
	7 days/cycle	0.4	1.1	0.5	1.2
	14 days/cycle	0.6	1.6	0.7	1.7
	28 days/cycle	0.8	2.0	1.0	2.3
	1 year/cycle	0.8	2.3	1.3	2.6

[a] Square wave RH cycling with panel's surface EMC at either $(11.5 + AM_i)$% or $(11.5 - AM_i)$%.

[b] Square wave RH cycling with panel's surface EMC at either $(10.0 + AM_i)$% or $(10.0 - AM_i)$%.

Table 8.5 The Ten Year Mechano-sorptive Fractional Deflection (F_{ms}) for OSB Panels Exposed to Climate Fluctuations with Different Cyclic Frequencies [a]

	F_{ms} at 10 Years	
Cyclic Frequency	9.5 mm OSB	15.9 mm OSB
4 hours/cycle	0.5	0.3
1 day/cycle	1.4	0.8
2 days/cycle	2.3	1.3
7 days/cycle	5.9	3.3
14 days/cycle	9.0	5.7
28 days/cycle	13.0	9.8
60 days/cycle	13.3	15.0
100 days/cycle	11.7	19.3
200 days/cycle	9.5	17.0
300 days/cycle	8.3	15.1
365 days/cycle	7.8	14.0

[a] The square wave RH cycles are between 35% and 85% RH.

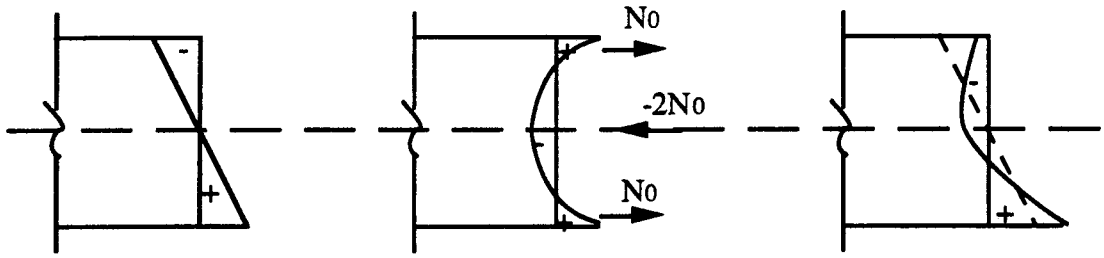

(a) applied M (b) self-equilibrated stress by drying (c)the resultant stress

Fig. 8.1 The Stress Profiles of Bending Cross Section during Desorption

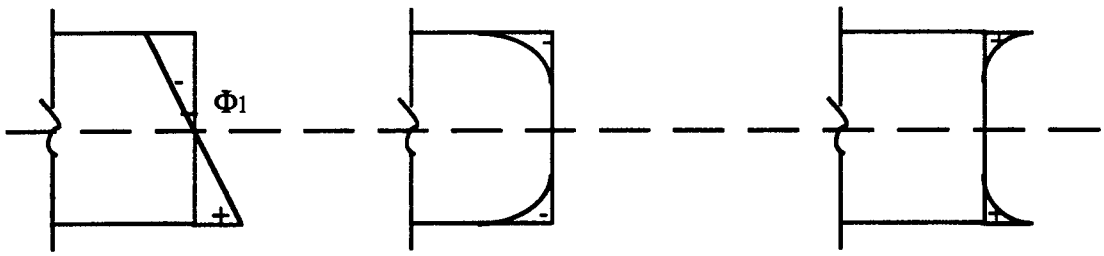

(a) applied M (b) shrinking by free drying $\varepsilon=\Delta MC\ \alpha$ (c) strain by restrainingstress No and

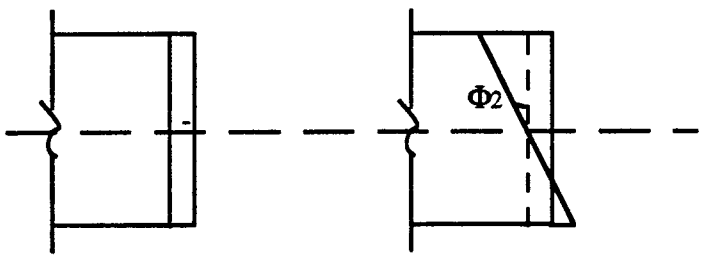

(d) strain by theopposite force (e) the resultant strain

Fig. 8.2 The Strain Profiles of Bending Cross Section during Desorption

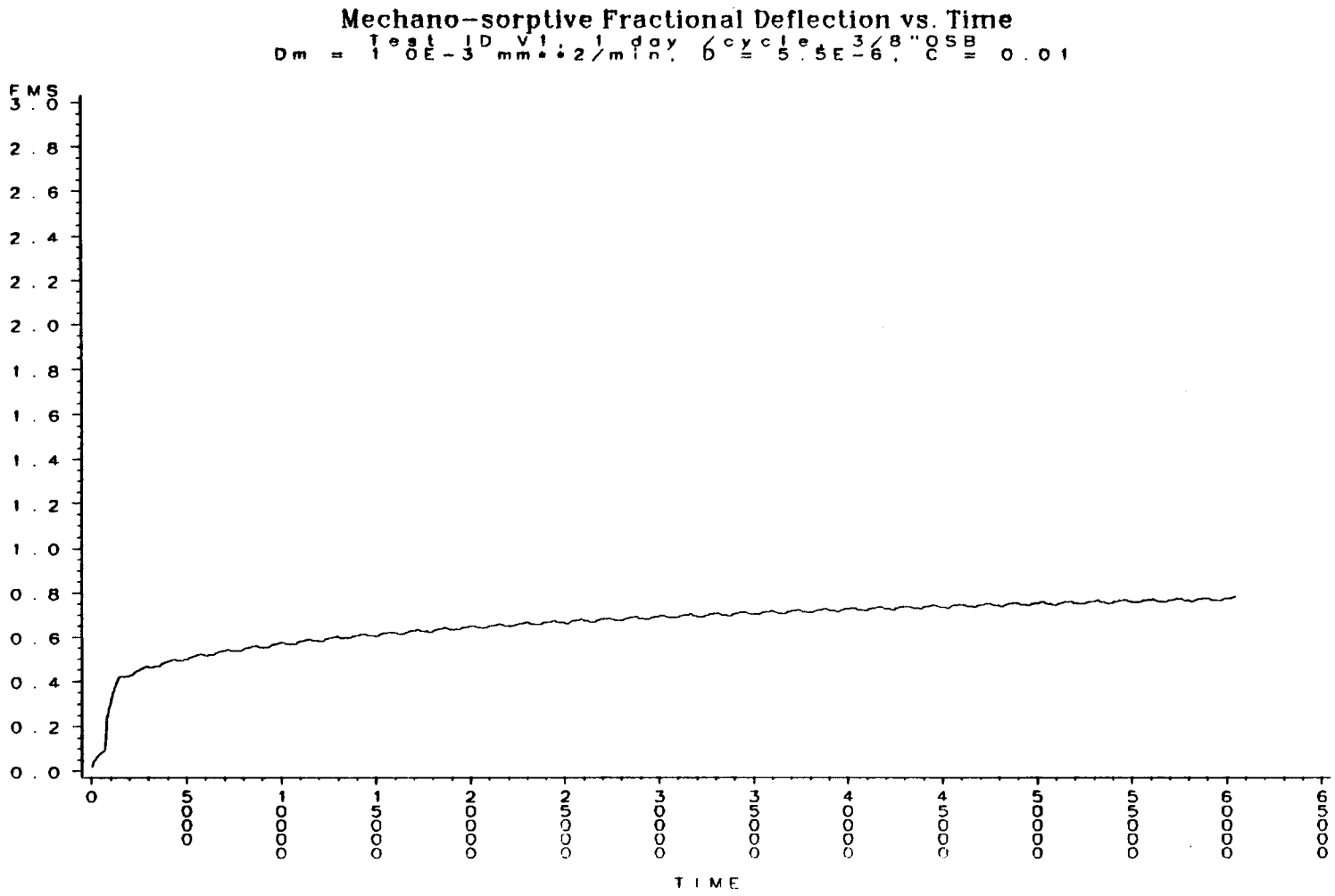

Fig. 8.3 The Mechano-sorptive Fractional Deflection (Fms) vs.Time Curve for the 9.5 mm OSB Panels in Test V1

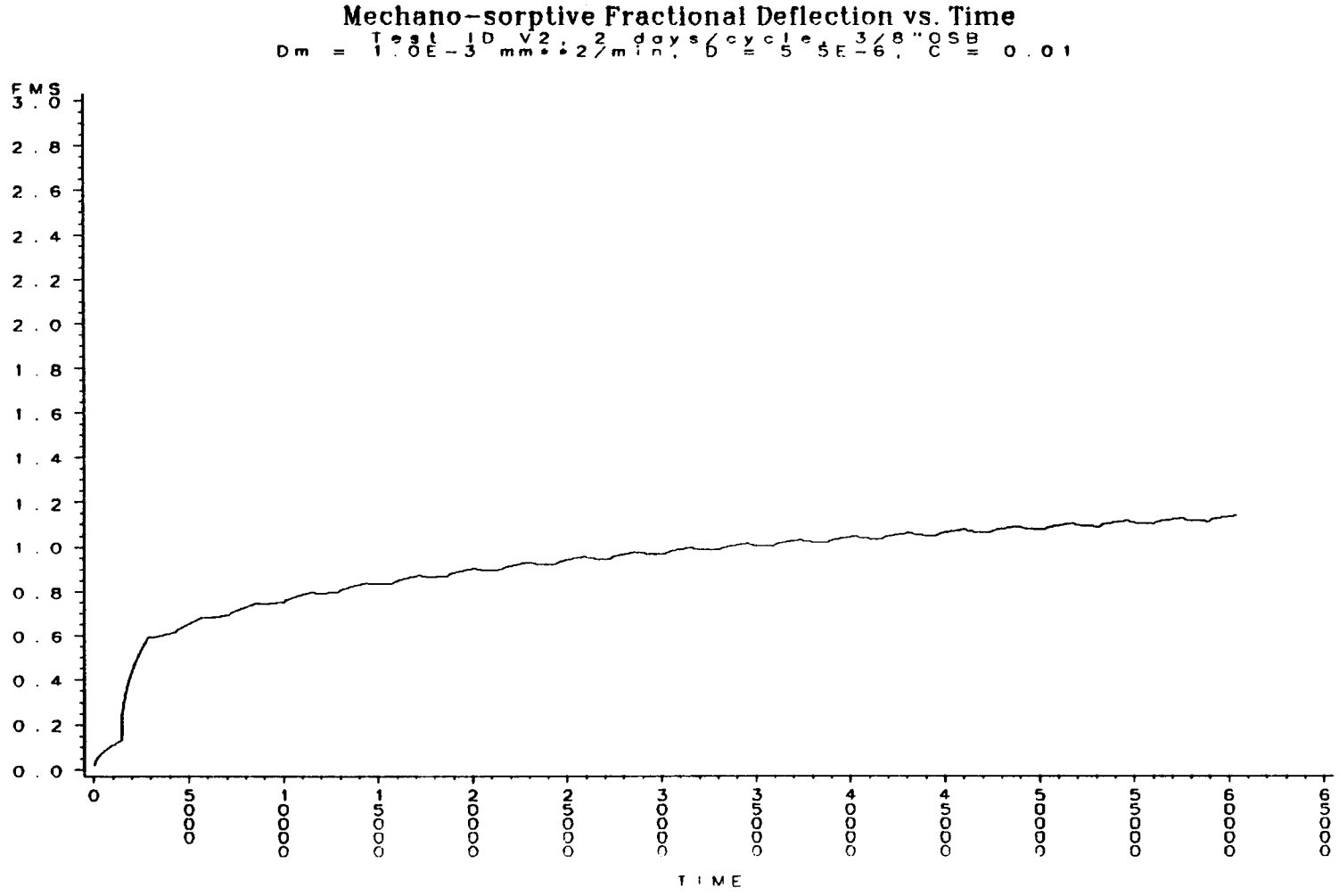

Fig. 8.4 The Mechano-sorptive Fractional Deflection (Fms) vs.Time Curve for the 9.5 mm OSB Panels in Test V2

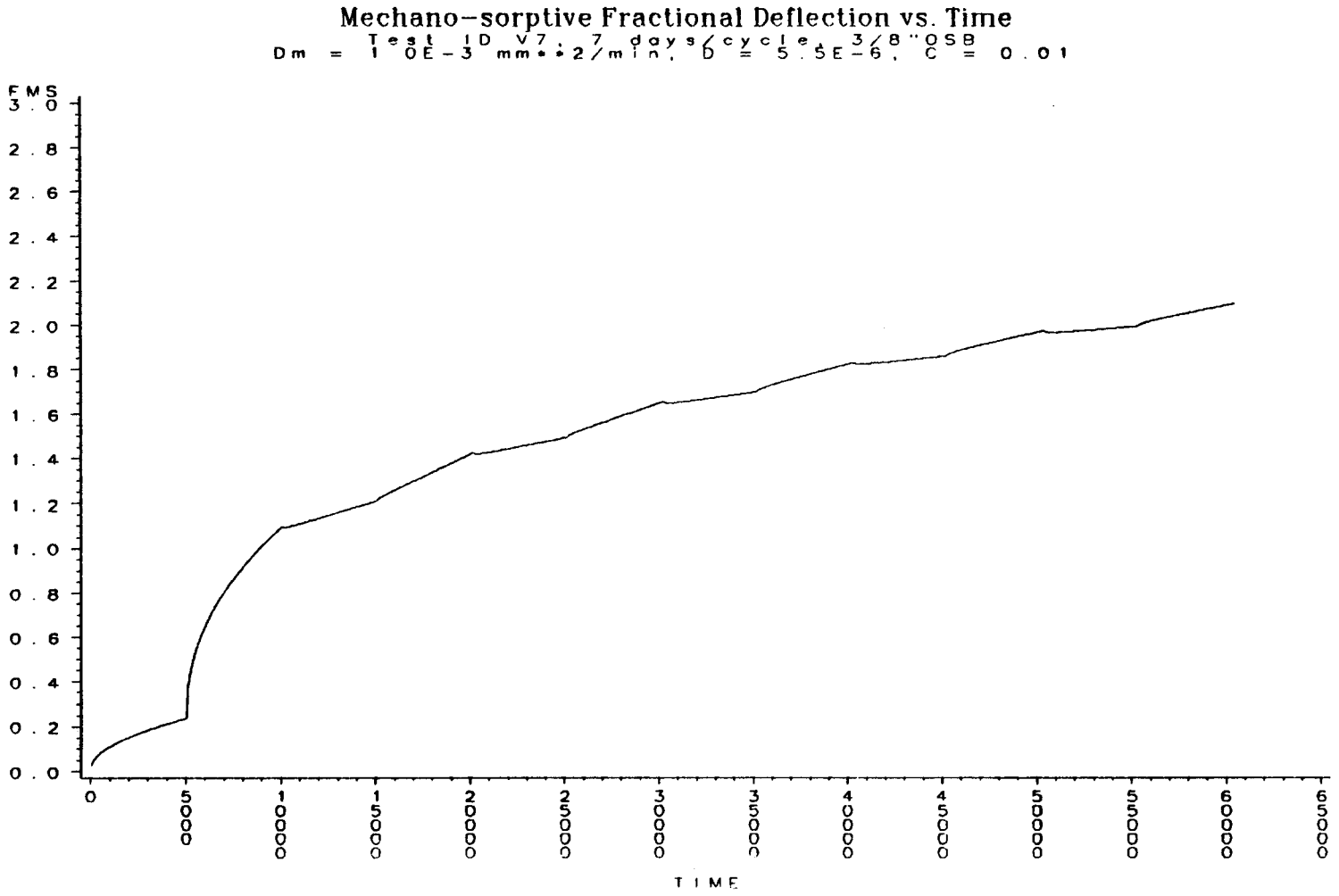

Fig. 8.5 The Mechano-sorptive Fractional Deflection (Fms) vs. Time Curve for the 9.5 mm OSB Panels in Test V7

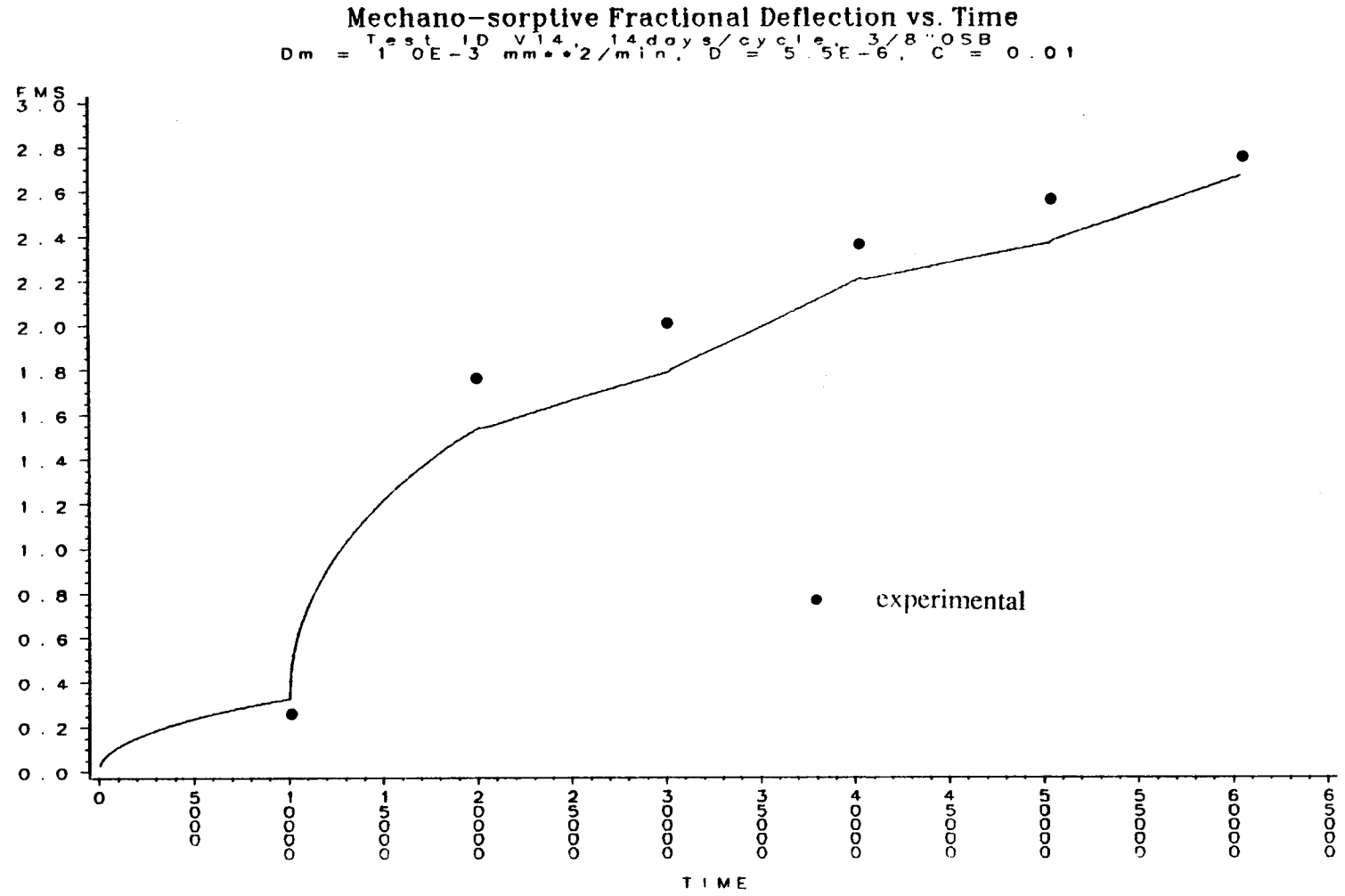

Fig. 8.6 The Mechano-sorptive Fractional Deflection (Fms) vs.Time Curve for the 9.5 mm OSB Panels in Test V14

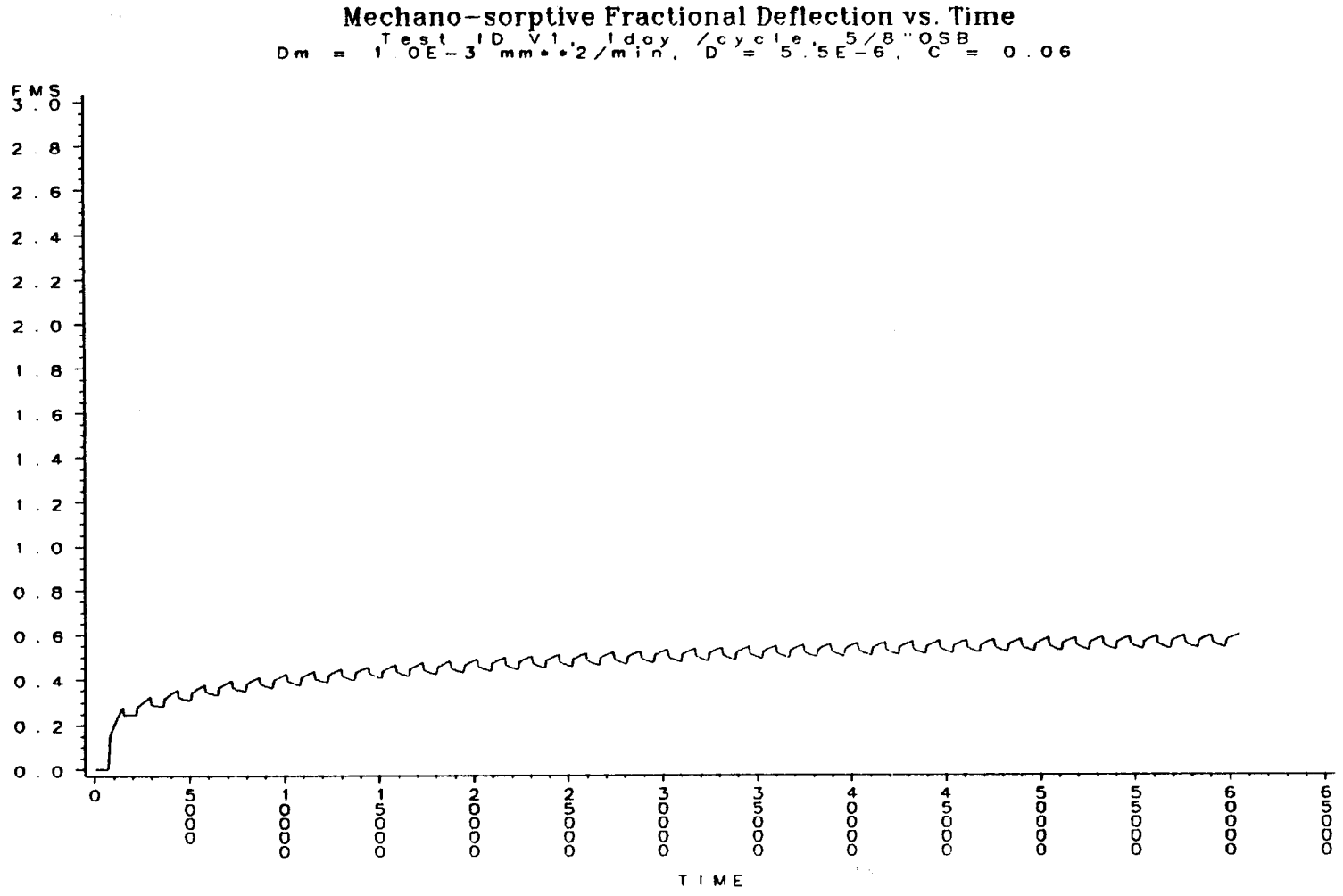

Fig. 8.7 The Mechano-sorptive Fractioral Deflection (Fms) vs.Time Curve for the 15.9 mm OSB Panels in Test V1

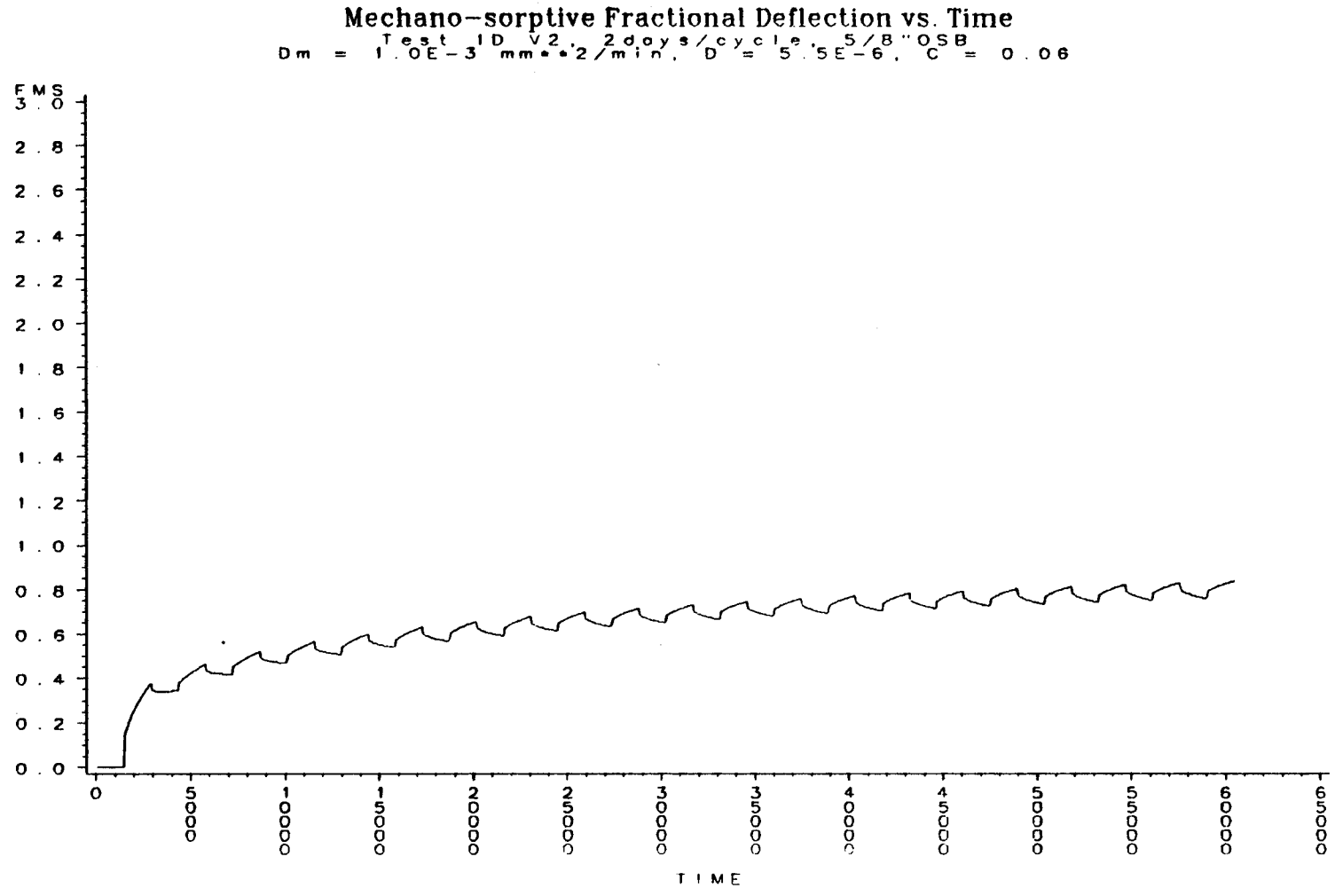

Fig. 8.8 The Mechano-sorptive Fractional Deflection (Fms) vs. Time Curve for the 15.9 mm OSB Panels in Test V2

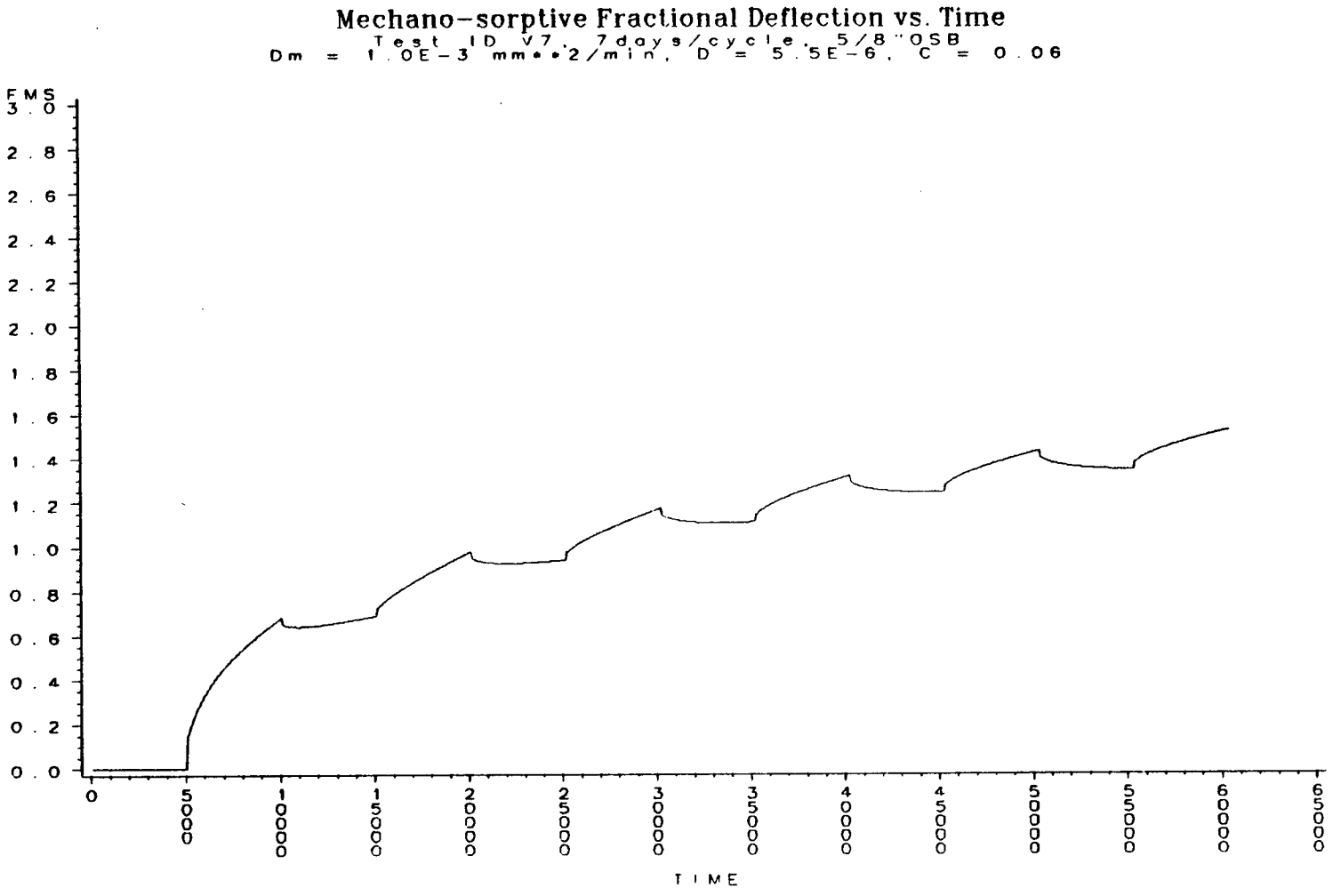

Fig. 8.9 The Mechano-sorptive Fractional Deflection (Fms) vs.Time Curve for the 15.9 mm OSB Panels in Test V7

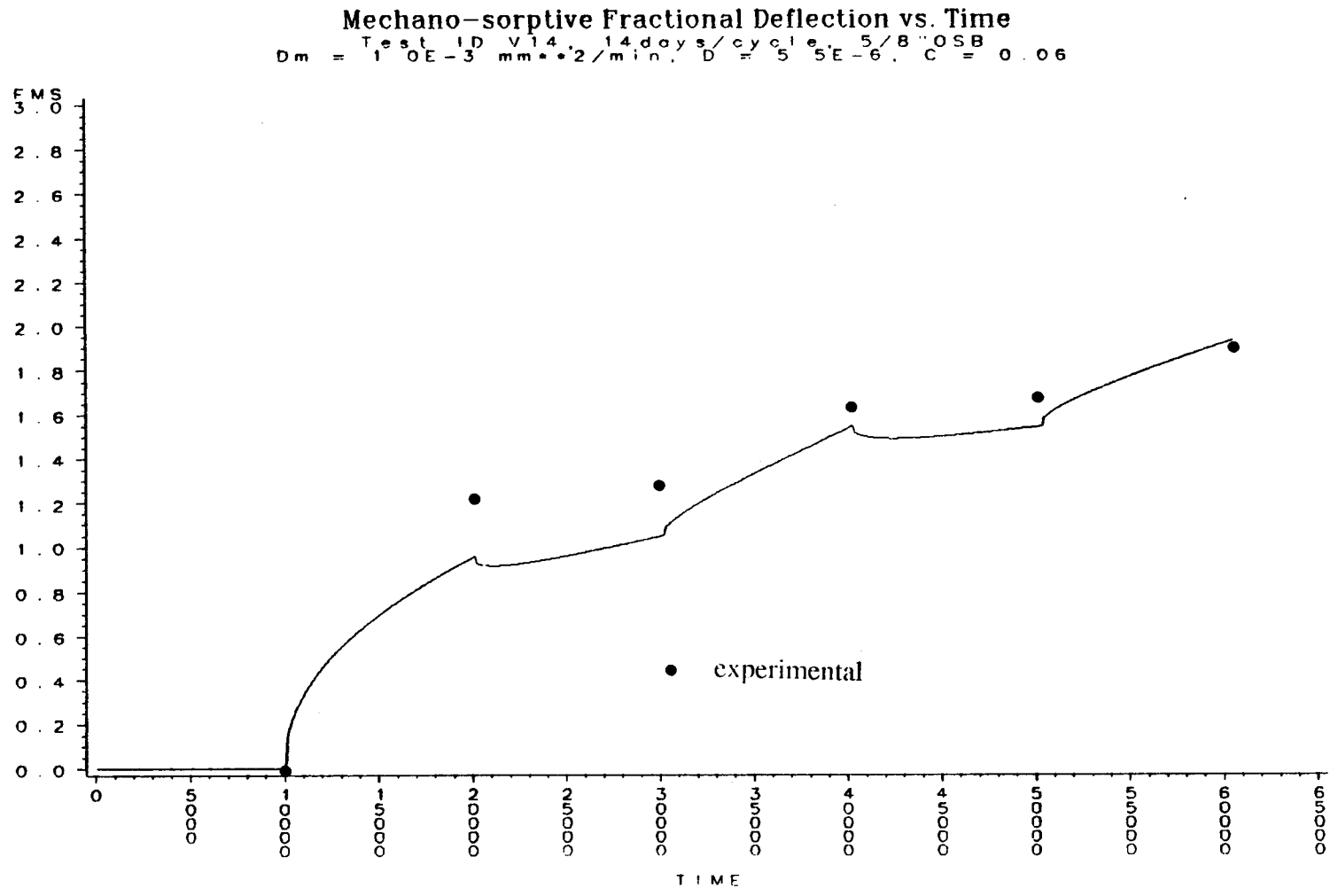

Fig. 8.10 The Mechano-sorptive Fractional Deflection (Fms) vs.Time Curve for the 15.9 mm OSB Panels in Test V14

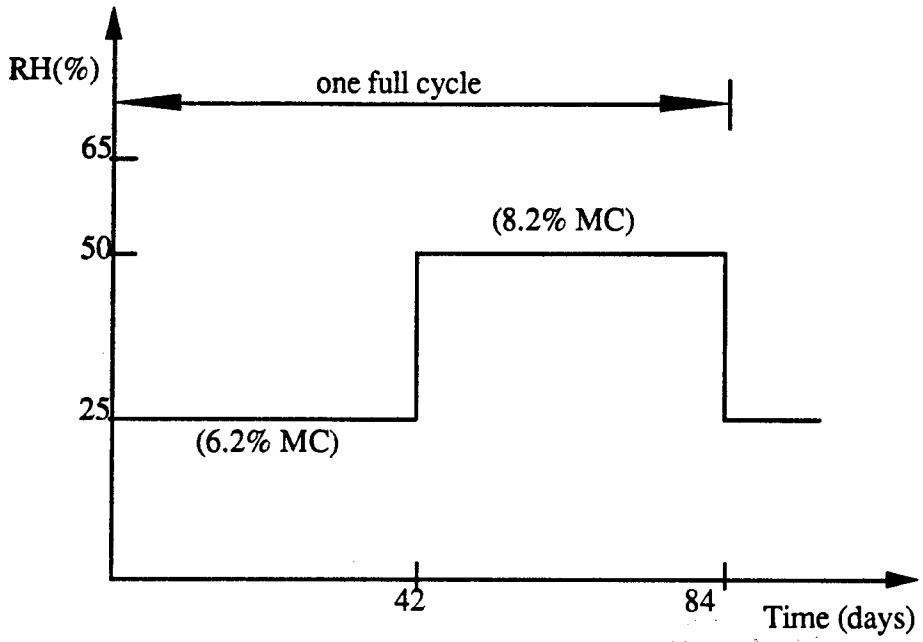

Fig. 8.11 The Simulated Stepwise RH Cycling for Indoor Creep Test I2

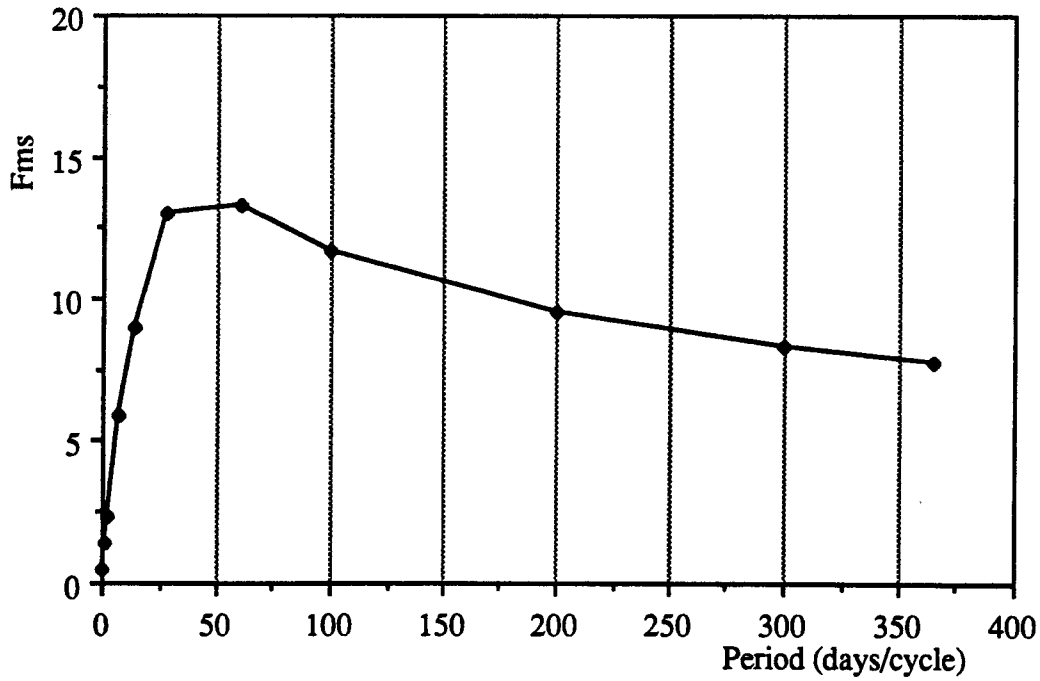

Fig. 8.12 The Ten Year Mechano-sorptive Fractional Deflection (F_{ms}) vs.Cyclic Period when the 9.5 mm OSB Panels Exposed to 35-85% RH Fluctuations

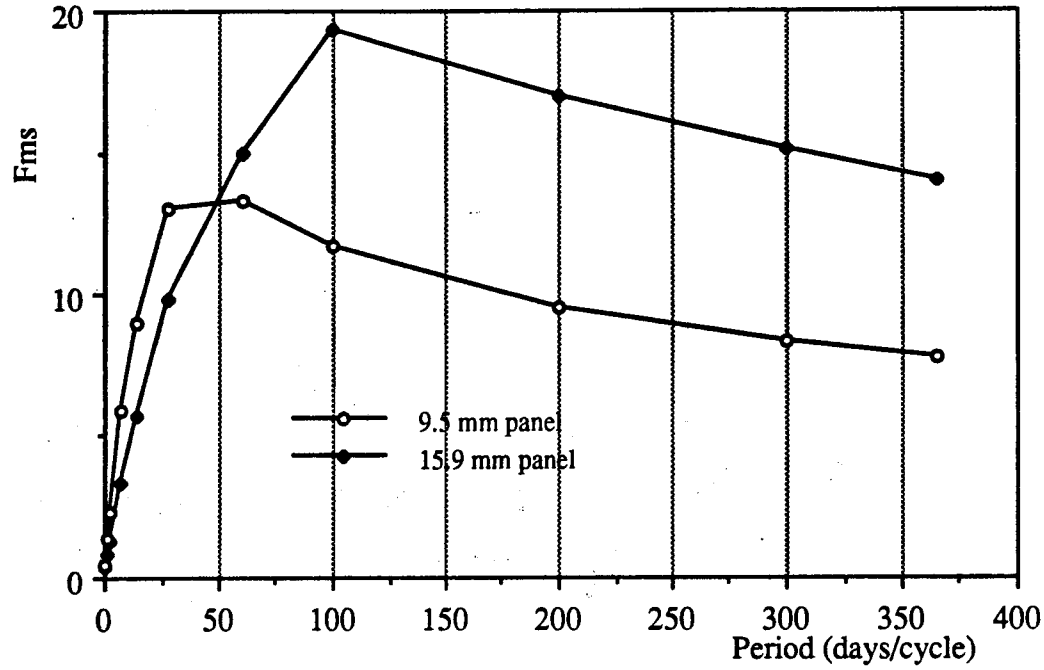

Fig. 8.13 The Ten Year Mechano-sorptive Fractional Deflection (F_{ms}) vs.Cyclic Period for OSB Panels with Two Thicknesses Exposed to 35-85% RH Variations

Chapter 9 Summary, Conclusions, and Recommendations

9.1 Summary

The research conducted in this program consists of three major parts: experimental study, regression analysis, and numerical model construction. The experimental program is carried out to study the time-dependent flexural behavior of OSB panel that is exposed to various climatic conditions under sustained loads. Regression equations of the creep test results are obtained to predict the long-term performance of the OSB panels. A numerical model is constructed to portray the mechano-sorptive (M-S) creep development during square wave relative humidity (RH) cycling.

The RH level, frequency of humidity cycling, thickness of the panel, and the panel surface strand orientation are major variables studied in the experiment. A total of ten test series, each with 24 creep specimens, were studied under four frequencies of humidity cycling (1 day, 2 days, 7 days, and 14 days per cycle), three constant humidities (35%, 65%, and 85%), and three uncontrolled indoor conditions. The creep tests lasted twelve weeks for the three uncontrolled indoor conditions and six weeks for the cyclic and constant RH tests, with the exception of test V14 (14 days/cycle), which lasted for 25 weeks. The applied load was at a 20% stress level, and the same magnitude of humidity cycling (35%-85%) was used for the cyclic RH tests with different frequencies. The temperature was kept constant around 20 ^{o}C for all of the RH controlled test series. The specimens had two nominal thicknesses: 9.5 mm and 15.9 mm, and plywood panels with the same nominal thickness were also tested in the same environment for comparison with OSB panels. There were four and two replications for OSB and plywood creep specimens, respectively.

Creep panel flexural deflections, as well as weights and thicknesses of the unloaded

MC specimens, were measured during the creep tests; the recovery was observed for 3 days upon unloading. The panel fractional deflection (assuming the stress-strain relationship is linear at 20% stress level) and the MC was obtained, and discussions and conclusions are drawn from the test results. The effects of variables, such as cyclic frequency and panel thickness, on the creep behavior are deduced, and the influence of these variables are measured by statistical methods.

Regression equations based on the creep data from the indoor and constant RH tests are approached with a logarithmic time scale, as is a bilinear model proposed to portray the OSB panel fractional deflection in the cyclic RH environment. The parameters used to determine the linear equation in the model are approached by stepwise regression analysis based upon the available data from the experiment. Long-term prediction is made by extrapolations of the obtained regression equations

Diffusion coefficients are calculated according to the MC obtained from the first desorption or adsorption in the controlled RH tests. One-dimensional difference analysis is carried out to explore the moisture movement through the OSB panel during environmental RH changes. A numerical model describing the panel mechano-sorptive (M-S) creep development is constructed upon the obtained moisture movement results, and a parametric study is carried out by using the developed numerical model; that is, the M-S creep is investigated by the model for parameters not studied in the experimental program.

9.2 Conclusions

The results of this study provide a good understanding of the flexural creep behavior of OSB (3/8" and 5/8") under various RH conditions. The following conclusions can be drawn from the experimental study program:

1. Creep for both OSB and plywood panels is accelerated by the cyclic RH environments at isotherm conditions (20 ^{o}C). The slowest cycling among the four frequencies yields the most creep (both the most viscoelastic and viscous deformation) for all specimens.
2. The accelerating effect of cyclic RH environments is also related to the geometric dimension of panels. The thinner panels creep more than the thicker panels.
3. The relative direction parallel and perpendicular to face strand orientation has little effect on the panel fractional deflection of creep panels.
4. The creep of OSB panels becomes very sensitive to the RH level when subjected to a high RH level such as 85% RH.
5. The first desorption (65% RH to 35% RH) and adsorption (35% RH to 85% RH) yields much more creep than do the subsequent sorptions.
6. The plywood panels exhibit less fractional deflection than the OSB panels under the same environmental and geometric conditions.

According to parametric investigation (Chapter 8), some additional conclusions may be reached:

7. As found from the experiment, the analytical model (Chapter 8) shows that the thinner panels (9.5 mm) creep more than the thicker panels (15.9 mm) for the humidity cyclic frequencies 1-2-7-14 days/cycle. When the cyclic RH changes are slower than 60 days/cycle, the thinner panels creep less than the thicker panels according to the parametric study.
8. As observed from the experiment for 1 to 14 days/cycle environment, the analytical model shows that the OSB panel creeps more in a slower cyclic RH environment. When the cyclic frequency is lower than some values, the OSB panel creeps less in a slower cyclic RH environment. These frequencies are approximately 60 days/cycle

and 100 days/cycle for 9.5 mm and 15.9 mm OSB panels, respectively.

9. The larger amplitude of the RH fluctuation gives the larger M-S creep during the early creep stage. The amplitude has little influence on creep in the later creep duration.

From the long-term prediction made by regression equations, it is found that the current Canadian code (CSA/CAN O86.1-M89) for creep deflection may be insufficient for OSB panels when a high RH or large RH fluctuations are encountered. The results from the proposed models agree fairly well with the Eurocode (1991) for RH less than 85%.

9.3 Recommendations

To use OSB as a structural material, an extensive data bank needs to be established for both the short- and long-term properties under different environmental conditions. The following research is recommended:

1. The effects of process variables, such as resin type, resin content, and strand species, on the short- and long-term performances should be identified so that the engineering performance of OSB can be improved.
2. High stress long-term creep test should be studied more intensively to observe the ultimate strength (creep rupture) and duration of load factors.
3. More tests need to be carried out to verify the linearity of creep behavior in various climatic environments or to identify the stress range of linearity, which is important to the validity of using fractional deflection to describe the long-term performances.
4. The short- and long-term properties in tension and in compression at various climatic environments need to be studied.
5. Verify the numerical model and the parametric study results for RH cycling slower than 14 days/cycle and creep duration longer than six weeks.

Bibliography

Aklonis, J.J., and MacKnight, W.J. 1983. Introduction to Polymer Viscoelasticity. 2nd Ed., A Wiley - Interscience Publication.

American Society for Testing Material. 1987. Standard Methods of Testing Structural Panels in Flexure. ASTM D3043-87. Annual Book of ASTM Standards Vol. 04.09.

American Society for Testing Material. 1992. Standard Test Methods for Direct Moisture Content Measurement of Wood and Wood Based Materials. ASTM D4442-92. 1992 Annual Book of ASTM Standards Vol. 04.09.

Arimat, T., and Grossman, P.U.A. 1978. Recovery of Wood After Mechano-sorptive Deformation. J. Inst. Wood. Sci. Vol. 8, 47-52.

Armstrong, L.D., and Christensen, G.N. 1961. Influence of Moisture Changes on Deformation of Wood Under Stress. Nature (London) Vol. 191 No.4791, 869-870.

Armstrong, L.D., and Grossman, P.U.A. 1972. The Behavior of Particle Board and Hardboard Beams during Moisture Cycling. Wood Sci. Tech. Vol. 6 128-137.

Bach, L. 1965. Non-linear Mechanical Behavior of Wood in Longitudinal Tension. Ph.D. Dissertation. State University, College of Forestry at Syracuse University.

Bach, L., and Nielsen, A.F. 1975. A Numerical Method for Calculation of Moisture Content in Wood Exposed to Cyclic Conditions. Technical University of Denmark.

Bach, L., and McNatt, J.D. 1990. Creep of OSB with Various Strand Alignments. IUFRO Wood engineering Conference Proceeding. St. John N.B.

Bach, L., and Leitch, R. 1991. Modeling of Moisture Movements in Composite Building Panels Manufactured from Alberta Grown Wood. International Symposium on Cold Region Development. Edmonton Convention Center, Edmonton, Alberta, Canada.

Bazant, Z.P. 1985. Constitutive Equation of Wood at Variable Humidity and

Temperature. Wood Sci. Tech. Vol. 19 159-177.

Bazant, Z.P., and Meiri, S. 1985. Measurements of Compression Creep of Wood at Humidity Changes. Wood Sci. Tech. Vol. 19 179-182.

Bodig, J. 1966. Stress-Strain Relationship of Wood in Transverse Compression. J. Mat. Vol. 1 No.33 645-666.

Bodig, J., and Jayne, B.A. 1982 Mechanics of Wood and Wood Composites. Van Nostrand Reinhold Co.

Bryan, E.L., and Schniewind, A.P. 1965. Strength and Rheological Properties of Particleboard as Affected by Moisture content and sorption. For. Prod. J. Vol. 15 No.4, 143-148.

Canadian Standards Association. 1988. Construction Sheathing. CAN/CSA-O325.0-M88.

Canadian Standards Association. 1989. Engineering Design in Wood CAN/CSA-O86.1-M89.

Canadian Standards Association. 1993. Strandboard and Waferboard CAN/CSA-O437.0-M93.

Canadian Standards Association. 1994. Design Rated OSB CAN/CSA-O452 (draft).

Cheng, J.C., and Schniewind A.P. 1985. Creep Buckling of Small Slender Wood Columns under Cyclic Environment. Wood Fiber Sci. Vol.17 No.2, 159-169.

Christensen, G.N. 1962. The Use of Small Specimens for Studying the Effect of Moisture Content Changes on the Deformation of Wood under Load. Austr. J. Appl. Sci. Vol. 13 No.4, 242-256.

Comstock, G.L. 1963. Moisture Diffusion Coefficients in Wood as Calculated from Adsorption, Desorption, and Steady State Data. For. Prod. J. Vol. 13 No.3, 97-103.

Crank, J. 1956. The Mathematics of Diffusion. Oxford University Press.

Draper, N.R., and Smith, H. 1981. Applied Regression Analysis. John Wiley & Sons, Inc. New York.

Eriksson, L., and Norén, B. 1965. The Effect of Moisture Changes on the Deformation of Wood with Tension in Fiber Direction (in German). Holz als Roh und Werkstoff 23. 201-209.

Eurocode No. 5, 1991, Design of Timber Structures, unpublished.

Flügge, W. 1967. Viscoelasticity. Blaisdell Publishing Company.

Fridley, K.J., and Tang, R.C. 1992. Shear Effects on the Creep Behavior of Wood Composite I-beams. For. Prod. J. Vol. 42 No.6, 17-22.

Garoder, R., Gibson, E.J., and Laidlaw, R.A. 1967. Effects of Organic Vapors on the Swelling of Wood and on its Deformation Under Load. For. Prod. J. Vol. 17 No.4, 50-51.

Gibson, E.J. 1965. Creep of Wood: Role of Water and Effect of a Changing Moisture Content. Nature Vol. 206 No.4980, 213-215.

Griffiths, D.R., and Robertson, B. 1991. Towards Design Stresses for Oriented Strand Board in Europe. 1991 International Timber Engineering Conference, London. 3.450-3.456.

Grossman, P.U.A. 1976. Requirement for a model that Exhibits Mechano-sorptive Behavior. wood Sci. and Tech. Vol. 27, 163-168.

Hall, H., Haygreen, J., and Neisse, B. 1977. Creep of Particleboard and Plywood Floor Deck Under Concentrated Loading. For. Prod. J. Vol. 27 No.5, 23-32.

Hanhijarvi, A., and Ranta-Maunus, A. 1990. A Three-Dimension Analysis of Wooden Beams in Bending under Changing Humidity Condition. IUFRO Wood engineering Conference Proceeding. St. John N.B.

Hall, H., Haygreen, J., and Neisse, B. 1977. Creep of Particleboard and Plywood Floor Deck under Concentrated Loading. For. Prod. J. Vol. 27 No.5, 23-32.

Hall, H., and Haygreen, J. 1978. Flexural Creep of 5/8-inch Particleboard and

Plywood During 2 Years of Concentrated Loading. For. Prod. J. Vol. 28 No.6,19-22.

Halligan, A.F., and Schniewind, A.P. 1972. Effect of Moisture on Physical and Creep Properties of Particleboard. For. Prod. J. Vol. 22 No.4, 41-48

Haygreen, J.G., and Sauer, D.J. 1969. Prediction of Flexural Creep and Stress Rupture in Hardboard by Use of a Time-temperature Relationship. Wood Sci. Vol. 1 No.4, 241-249.

Haygreen, J., Hall, H., Yang, K.N., and Sawicki, R. 1975. Studies of Flexural Creep Behavior in Particleboard Under Changing Humidity Conditions. Wood and Fiber Vol. 7 No.2, 74-90.

Haygreen, J.G., and Bowyer, J.L. 1989. Forest Products and Wood Science: An Introduction. 2nd Ed., Iowa State University Press.

Hearmon, R.F.S., and Paton, J.M. 1964. Moisture Content Changes and Creep in Wood. For. Prod. J. Vol. 14 No.8, 357-379.

Hoffmeyer, P. 1990. Failure of Wood as Influenced by Moisture and Duration of Load. Ph.D. Dissertation. State University of New York, College of Environmental Science and Forestry .

Holzer, S.M., Loferski, J.R., and Dillard, D.A. 1989. A Review of Creep in Wood: Concepts Relevant to Develop Long-term Behavior Predictions for Wood Structures. Wood Fiber Sci. Vol.21 No.4, 376-392.

Hoyle, R.J., Itani, R.Y., and Eckard, J.J. 1986. Creep of Douglas-fir Beams due to Cyclic Humidity Fluctuations. Wood Fiber Sci. Vol.18 No.3, 468-477.

Hunt, D.G. 1986. The Mechano-sorptive Creep Susceptibility of Two Softwoods and its relation to Some Other Materials Properties. J. of Materi. Sci.. Vol.21, 2088-2096.

Hunt, D.G., and Shelton, C.F. 1987. Progress in the Analysis of Creep in Wood during Concurrent Moisture Changes. J. of Materi. Sci.. Vol.22 313-320.

Hunt, D.G., and Shelton, C.F. 1988. Longitudinal Moisture-shrinkage Coefficients of Softwood at the Mechano-sorptive Creep Limit. Wood Sci. Tech. Vol.22 129-144.

Hunt, D.G. 1989. Linearity and Non-linearity in Mechano-sorptive Creep of Softwood in Compression and Bending. Wood Sci. Tech. Vol.23 323-333.

Kingston, R.S.T., and Budgen, B. 1972. Some Aspects of the Rheological Behavior of Wood, Part iv: Nonlinear Behavior at High Stresses in Bending and Compression. Wood Sci. Tech. Vol.6 230-238.

Kingston, R.S.T., and Perkitny, T. 1972. On the Relationship between Active Swelling Pressure of Wood and Passive Compressibility by External Forces (in German). Holz als Roh- und Werkstoff 30, No.1 18-28.

Kliger, I.R., and Edlund, B.L.O. 1991. Creep in Particleboard - Prediction of Long-term Behavior from Primary Creep Data. 1991 International Timber Engineering Conference, London. 3.465-3.472.

Lee, W.C., and Biblis, E.J. 1976. Effects of a High and Low Relative Humidity Cycle on Properties of Southern Yellow Pine Particleboard. For. Prod. J. Vol. 26 No.6.

Leicester, R.H. 1971. A Rheological Model for Mechano-sorptive Deflection of Beams. Wood Sci. Tech. Vol.5, 211-220.

Leitch, R.1990. Mathematical Modelling of One Dimensional Diffusion in Wood. Report: FPLI 81, Alberta Research Council, Edmonton.

Libby, T.B., and Haygreen, J.G. 1964. Moisture Content Change Induced by Tensile Stress in Whole Wood. J. Inst. Wood Sci. Vol.18 54-60.

Lyon, D.E., and Schniewind, A.P. 1978. Prediction of Creep in Plywood. Part I: Prediction Models for Creep in Plywood. Wood Sci. Tech. Vol.10 No.1, 28-38.

Martensson, A., and Thelanderson, S. 1987. Wood Materials under combined Mechanical and Hygral Loading. Report TVSM-703., London Institute of Technology, Sweden.

Martensson, A. 1988. Tensile Behavior of Hardboard under Combined Mechanical

and Moisture Loading. Wood Sci. Tech. Vol.22 199-210.

Martensson, A., and Thelanderson, S. 1990. Effect of Moisture and Mechanical Loading on Wooden Materials. Wood Sci. Tech. Vol.24 247-261.

Martensson, A. 1992. Mechanical Behavior of Wood Exposed to Humidity Variations. Report TVBK-1006. London Institute of Technology, Sweden.

McKnight, T.S. (Ed.) 1974. Wood Composite Products Evaluation, Major Demands and Opportunities.

McNatt, J.D., and Hunt, M.O. 1982. Creep of Thick Structural Flakeboards in Constant and Cyclic Humidity. For. Prod. J. Vol. 32 No.5, 49-54.

McNatt, J.D., and Laufenberg, T.L. 1991. Creep and Creep-Rupture of Plywood and Oriented Strandboard. 1991 International Timber Engineering Conference, London. 3.457-3.464.

McNatt, J.D., Bach, L., and Wellwood R.W. 1992. Contribution of Flake Alignment to Performance of Strandboard. For. Prod. J. Vol. 42 No.3, 45-50.

Mohager, S. 1987. Studies of Creep in Wood (in Swedish) The Royal Institute of Technology. TRITA-BYMA, No.8, Stockholm.

National Research Council of Canada. 1990. National Building Code of Canada. The Associate Committee on the National Building Code, Ottawa.

Nemeth, L.L.J. 1964. The Influence of Moisture on Creep in Wood. M.S. Thesis. Univ. of Calif., Berkeley.

Nielsen, A. 1972. Rheology of Building Materials. National Swedish Building Research Document D6:1972.

Nielsen, A.F., and Bach, L. 1975. Computer Program for Non-stationary Moisture Variations. Technical University of Denmark, Thermal Institution Laboratory, Rept. No. 34.

Nielsen, L.E. 1962. Mechanical Properties of Polymers. Reinhold Publishing Corporation.

Ota, M., and Tsubota, Y. 1966. Studies on the Fatigue of 2 - ply Laminated Wood. I. Several Investigations on the Static Viscoelasticity Behaviors of Wood Subjected to Bending Test. J. Japan Wood Res. Soc. Vol. 12 No.1, 26-29.

Palka, L.C. 1991. A Graphical Summary of the Short Term Properties of 5/8-inch Thick Canadian commercial Waferboard Panels in Bending Determined at the Western Laboratory of Forintek Canada Corp. (confidential).

Pierce, C.B., and Dinwoodie, J.M. 1977. Creep in Chipboard. Part 1: Fitting 3- and 4- Element Response Curves to Creep Data. J. of Materi. Sci Vol. 12 , 1955-1960.

Pierce, C.B., Dinwoodie, J.M., and Paxton, B.H. 1979. Creep in Chipboard. Part 2: The Use of the Fitted Response Curves for Comparative and Prediction Purposes. Wood Sci. and Tech. Vol. 13, 265-282.

Pierce, C.B., Dinwoodie, J.M., and Paxton, B.H. 1985. Creep in Chipboard. Part 5: An Improved Model for Prediction of Creep Deflection. Wood Sci. and Tech. Vol. 19, 83-91.

Pipkin, A.C. 1972. Lectures on Viscoelasticity Theory. New York, Springler.

Pu, J., Tang, R.C., and Davis, W.C. 1992a. Creep Behavior of Commercial Oriented Strandboard under High Relative Humidity. For. Prod. J. Vol. 42 No.4, 49-54.

Pu, J., Tang, R.C., and Price, E.W. 1992b. The Effect of Hot and Humid Environmental Conditions on the Creep Behavior of Commercial Structural Oriented Strandbords. For. Prod. J. Vol. 42 No.11, 9-14.

Ranta-Maunus, A. 1975. The Viscoelasticity of Wood at Varying Moisture Content. Wood Sci. Tech. Vol.9 189-205.

Ranta-Maunus, A. 1990. Impact of Mechano-sorptive Creep to the Long-term Strength of timber. Holz als Roh und Werkstoff 48. 67-71.

Rybarczyk, W., and Ganowicz, R. 1974. A Theoretical Description of the Swelling Pressure of Woos. Wood Sci. Tech. Vol.8 233-241.

Sauer, D.J., and Haygreen, J.G. 1968. Effect of Sorption on the Flexural Creep

Behavior of Hardboard. For. Prod. J. Vol. 18 No.10, 57-63.

Schniewind, A.P. 1967. Creep-rupture Life of Douglas Fir under Cyclic Environmental Conditions. Wood Sci. Tech. Vol.1 No.4, 278-288.

Schniewind, A.P., and Richmond, C. 1968. Recent Progress in the Study of the Rheology of Wood. Wood Sci. Tech. Vol.2 188-206.

Schniewind, A.P., and Lyon, D.E. 1973. Further Experiments on Creep-rupture Life under Cyclic Environmental Conditions. Wood and Fiber Sci. Vol.4 No.4, 334-341.

Siau, J.F. 1984. Transport Processes in Wood. Springer - Verlag.

Simpson, W.T., and Liu, J.Y. 1991. Dependence of the Water Vapor Diffusion Coefficient of Aspen (*Populus Spec.*) on Moisture Content. Wood Sci. Tech. Vol.25 9-21.

Stamm, A.J. 1964. Wood and Cellulose Science. New York: Ronald Press.

The SAS Institute Inc. 1990. SAS/STAT User's Guide. Version 6. 4th Ed. The SAS Institute Inc., Cary, North Carolina.

Tong, L., and Öden, K. 1989. Rheological Behavior of Wood and Wood Structures: Review of Literature, Theories and Research Need. Dept. of Building Material, The Royal Institute of Technology, Sweden.

Toratti, T. 1990. A Cross Section Creep Analysis. IUFRO Wood Engineering Conference Proceeding. St. John N.B.

Wong, P.C.K., Bach, L., and Cheng, J.J. 1988. The Flexural Creep Behavior of OSB Stressed Skin Panels. Structural Engineering Report, No.158, University of Alberta.

Yeh, M.C., Tang, R.C., Hse, C.Y., and Chen, T.Y. 1988. Effect of Relative Humidity on the Creep Behavior of Flakeboards I: Constant Stress Level. Proc. of the 1988 International Conference on Timber Engineering. Seattle, Wash. Vol.1, 538-546.

Yeh, M.C., Tang, R.C., and Hse, C.Y. 1990. Flexural Creep of Structural Flakeboards Under Cyclic Humidity. For. Prod. J. Vol. 40 No.10, 51-57.

Youngs, R.L. 1957. The Perpendicular-to-grain Mechanical Properties of Red Oak as Related to Temperature, Moisture Content, and Time. U.S. for. Prod. Lab., Madison, Wisc. Rept. No. 2079.

Appendix A

Discussion of the Flexural Deflection during Sorptions

The assumptions for creep modeling presented in Sect. 8.2.2 are fully discussion in the following. For completion of the content, the assumptions are repeated before the discussion is carried out.

A.1 Assumptions

Assumption 1. The plane cross section remains plane.

This assumption implies that the strain distribution under applied moment (M) is a straight line, as in Fig. 8.2(a). In the figure, Φ_1 is the curvature of the bending panel corresponding to the applied moment before sorption happens.

Assumption 2. The modulus of elasticity for both compression and tension sections are identical.

When this is true, the neutral axis in Figs. 8.1(a) or 8.2(a) is passing through the symmetric axis of the cross section.

Assumption 3. Compression and tension have the same creep function and the creep function is not affected by sorptions; that is, creep behavior is not related to signs of the stress. This can be expressed as

$$\text{if} \quad \varepsilon_{creep} = f(\sigma,t), \qquad \text{then} \quad -\varepsilon_{creep} = f(-\sigma,t)$$

While the above assumption is true, the neutral axis keeps passing through the symmetric axis of the cross section under the sustained loading. If the creep function f was not affected by sorptions, the uniaxial creep curve would be a smooth curve

without fluctuation during the abrupt environmental changes. However, this behavior is not what is usually observed in experiments.

Assumption 4. The creep strain is proportional to the stress applied.

When the linear assumption is valid, the stress distribution in Fig. 8.1(a) will remain a straight line, as in the linear elastic case.

Assumption 5. The moisture diffusion and the introduced shrinking or swelling are not affected by the applied stress.

With this assumption, the shrinking/swelling in Fig. 8.2(b) is symmetric about the symmetric axis of the cross section.

If all assumptions given above are satisfied, there is no additional deflection generated or recovered during sorptions; that is Φ_1 is equal to Φ_2 in Fig. 8.2. However, this is not what was observed in the tests, where the panel deflection accelerated or decelerated during sorptions. The facts therefore indicate that one (or some) of the above assumptions must not be valid. The speculations are given in the following discussions.

A.2 Discussions

I. If Assumption 2 is not satisfied, that is, the modulus of elasticity for tension (E_t) and compression (E_c) are not the same . For example,

$$E_t \geq E_c$$

The strain and stress profiles are shown in Fig. A.1.

From equilibrium, $N_c = N_t$,

$$\frac{b}{2} \times \sigma_t \times h_t = \frac{b}{2} \times \sigma_c \times h_c$$

$$\sigma_t \times h_t = \sigma_c \times h_c \tag{A.1}$$

and the bending moment

$$M = \frac{b}{2} \times \sigma_t \times h_t \times \frac{2}{3} h = \frac{1}{3} \times b \times h \times \sigma_t \times h_t \tag{A.2}$$

From Compatibility:

$$\frac{h_c}{h_t} = \frac{\varepsilon_c'}{\varepsilon_t} = \frac{\sigma_c / E_c}{\sigma_t / E_t} = \frac{\sigma_c E_t}{\sigma_t E_c} \tag{A.3}$$

and

$$h_c + h_t = h \tag{A.4}$$

From Eqns. (A.1) - (A.4),

$$h_c = \frac{E_t - \sqrt{E_t E_c}}{E_t - E_c} h$$

$$h_t = \frac{E_c - \sqrt{E_t E_c}}{E_c - E_t} h$$

$$\sigma_t = \frac{3M(E_c - E_t)}{bh^2(E_c - \sqrt{E_t E_c})}$$

$$\sigma_c = \frac{3M(E_t - E_c)}{bh^2(E_t - \sqrt{E_t E_c})}$$

The bending curvature Φ is

$$\Phi = \frac{\varepsilon_c'}{h_c} = \frac{\sigma_c}{E_c h_c}$$

Then

$$\Phi = \frac{3M(E_t - E_c)^2}{bh^3 E_c (E_c - \sqrt{E_t E_c})^2} \qquad \text{(A.5)}$$

During sorptions, if the self-equilibrated stress and the resultant strain are remaining symmetry; no flexural deflection would happen.

II. Discussion about Assumption 3

II(a). When compression and tension follow the same creep behavior, the creep moduli are

$$E_t(t) = f_t(t) \cdot E_t$$

$$E_c(t) = f_c(t) \cdot E_c$$

where $E_t(t)$, $E_c(t)$= creep modulus for tension and compression, respectively, at time 't'

$f_t(t)$, $f_c(t)$= creep function for tension and compression, respectively, at time 't'

E_t , E_c= elastic modulus for tension and compression, respectively

Assumption 3 implies that the creep function $f(t)$ is

$$f(t) = f_c(t) = f_c(t)$$

From Eqn. (A.5), the curvature at time 't' is

$$\Phi(t) = \frac{\Phi(0)}{f(t)}$$

Therefore, the bending stiffness changes in the same way as the compression/tension stiffness changes during sorptions; this is schematically shown in Fig. A.2. The first plot shows the uniaxial creep modulus during sorptions, and the second plot is the corresponding bending deformation.

From the figure, it can be found that the bending deflection could fluctuate during sorptions even without the effects of shrinking/swelling and the self-equilibrated stresses.

II(b). When creep function for tension and compression is not the same, that is, $f_t(t) \neq f_c(t)$, the bending deflection will fluctuate during creep test.

III. About Assumption 4

When stress reaches certain level, the nonlinear stress-strain relationship appears. In Fig. 8.1 (c), the tension stress in the bottom of the cross section may lead to extra creep strain in that place, and extra bending deflection may be introduced. However, his behavior is opposite to what was observed in the experiment during desorptions.

IV. About Assumption 5

If Assumption 5 is not valid, for example, tensile side shrinks more than the compressive side during drying, the bending deflection recovery is introduced as shown in FIg. A.3.

When tensile side swells more than the compressive side during wetting, an extra bending deflection is introduced as shown in FIg. A.4.

A.3 Summary

According to the above discussions, at least one of the following facts must exist

because of the observed deflection fluctuation during the creep experiment:

1. Non linear creep behavior could lead to creep recovery during adsorption.

2. Shrinking/swelling is affected by applied load.

3. Compressive and tensile creep behavior is different ($f_t(t) \neq f_c(t)$).

4. Compressive and tensile creep behavior is the same ($f_t(t) = f_c(t)$), but they change during sorptions.

The last reason is picked up as the explanation of the fluctuation of the bending deflection during sorptions.

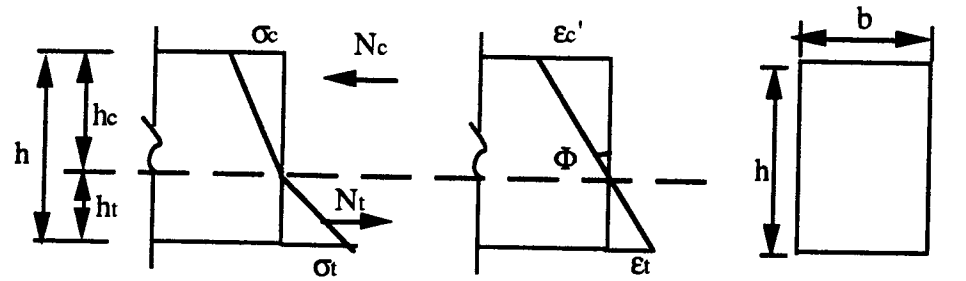

Fig. A.1 Stress and Strain Profiles for Unequal Compressive and Tensile Stiffness

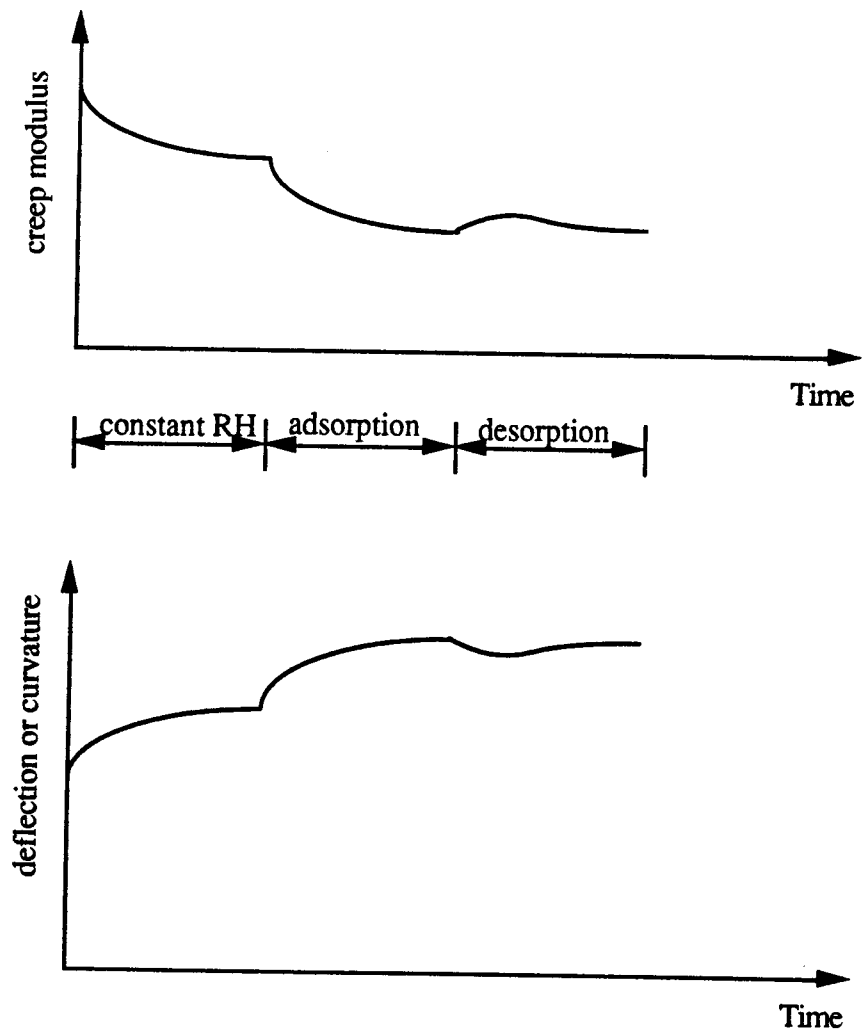

Fig. A.2 Schematic Plots of Uniaxial Creep Modulus and the Corresponding Panel Deflection

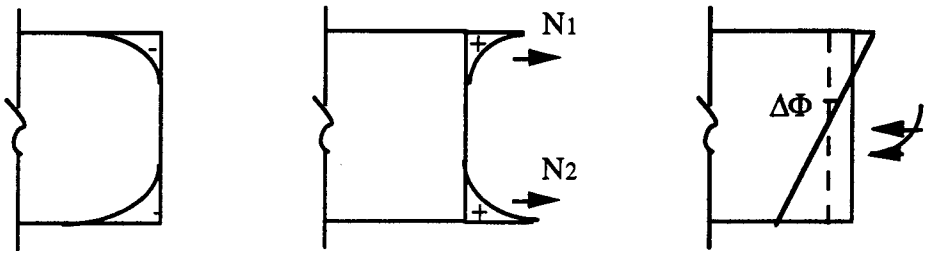

(a) shrinking by drying (b) restrained stress($N_2 > N_1$) (c) strain by theopposite

Fig. A.3 Illustration of Cross Section Deformation due to Drying

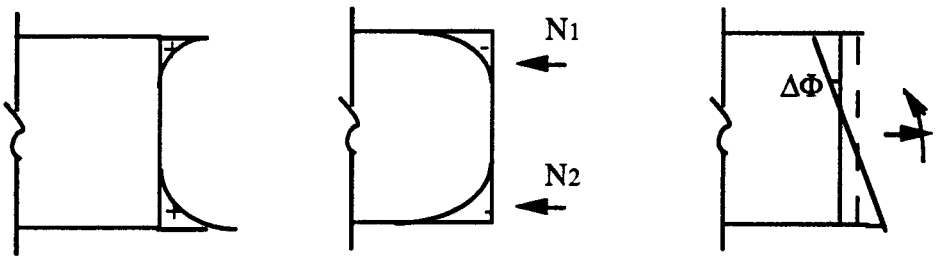

(a) swelling by wetting (b) restrained stress($N_2 > N_1$) (c) strain by theopposite

Fig. A.4 Illustration of Cross Section Deformation due to Wetting

Appendix B

Evaluation of the Material Constant in the Creep Calculation Model

The material constants used to calculate OSB mechano-sorptive creep during RH cycling are evaluated from both the creep and MC measured during the experiment. Those constants may be different for materials other than OSB. When extended to other materials, the validity of the model should be examined by more tests. The experimental mechano-sorptive creep is obtained by subtracting the constant test creep curve (C65) from the cyclic creep curve as those plotted in Figs. 8.6 and 8.10.

B.1 The Material Constants for the First RH Cycle

By careful study of the test results, it is found that the increase of the fractional deflection during the first desorption/adsorption is proportional to the panel's average MC change. It is true for all the cyclic test. Therefore, a constant A is obtained for the first desorption as

$$A = \frac{\Delta F_{ms}}{\Delta u} \tag{B.1}$$

where ΔF_{ms} is the mechano-sorptive fractional deflection increment during the first desorptive, and Δu is the MC change during the same period. Due to the fact that the A from the four cyclic tests is close to each other, A is than calculated as a constant from the three cyclic tests (V2, V7, and V14). For 9.5 mm OSB,

$$A = \frac{\sum \Delta F_{ms}}{\sum \Delta u} = \frac{0.16 + 0.27 + 0.26}{-(0.66 + 1.22 + 1.68)} = -0.194$$

The cyclic test V1 is not used because of the experimental error involve in fast cyclic test is relatively large.

For 15.9 mm OSB, the ΔF_{ms} for the first desorption is very little. Therefore, A is set at zero.

For the first adsorption (85% to 35% RH), a constant B is obtained in a similar way as for A.. For 9.5 mm OSB,

$$B = \frac{\sum \Delta F_{ms}}{\sum \Delta u} = \frac{0.19 + 0.84 + 1.51}{2.27 + 4.21 + 5.97} = 0.204$$

where ΔF_{ms} or Δu is the increment of M-S fractional deflection or MC during the first adsorption. Similarly, $B=0.267$ can be obtained for 15.9 mm OSB.

B.2 The Material Constant for the Subsequent RH Cycles

For the subsequent RH cycles, the M-S creep rate is expressed by Eqn. (8.8). The first term in the equation reflects the fluctuation of creep deflection due to the moisture changes. The constant C can be obtained from fluctuations of both M-S creep curve and MC during sorptions. Similar to A or B, $C = \frac{\Delta F_{ms}}{\Delta u}$. The values of C are 0.01 and 0.06 for 9.5 mm and 15.9 mm OSB panels, respectively. The different C values for panels with different thicknesses agree with the test results as shown in Fig. 5.10.

The second term in Eqn. (8.8) accounts for the effect of panel's MC level on the M-S creep. The produced M-S fractional deflection is an integration of panel's MC multiplied by a constant D. Considering the decreasing of M-S creep rate with time, a factor $\bar{n}^m$ is introduced, where $\bar{n}$ is the number of cycling. A large m implies that the creep increases slowly and a small m means that the creep develops quickly.

The M-S creep rate is mostly determined by the factor $\bar{n}^m$. Therefore, m is evaluated from the M-S creep rate, which is found close to 1.0. A value of 0.925 is

given to the 9.5 mm OSB panel and *1.10* is assigned to the 15.9 mm OSB panel, respectively.

The constant D is then evaluated by

$$D = \bar{n}^m \frac{\Delta F_{ms}}{\int u dt} \tag{B.3}$$

The D is calculated for different cycles ($\bar{n}$), panels, and test series. The obtained values are close to 5.5×10^{-6}. The number is assigned to D.

It should be noted that the constants are all based on the cyclic and constant (C65) test results during six weeks. However, the proposed model seems to work for creep with longer duration. The creep at 25th weeks (test V14) are close between the model calculation and the test measurement as shown in Tables 8.1 and 8.2.

Recent Structural Engineering Reports

Department of Civil Engineering

University of Alberta

172. *The Effective Modulus of Elasticity of Concrete in Tension* by Atif F. Shaker and D.J. Laurie Kennedy, April 1991.

173. *Slenderness Effects in Eccentrically Loaded Masonry Walls* by Muqtadir, Mohammad A., Warwaruk, J. and Hatzinikolas, M.A., June 1991.

174. *Bond Model For Strength of Slab-Column Joints* by S.D.B. Alexander and Sidney H. Simmonds, June 1991.

175. *Modelling and Design of Unbraced Reinforced Concrete Frames* by Yehia K. Elezaby and Sidney H. Simmonds, February 1992.

176. *Strength and Stability of Reinforced Concrete Plates Under Combined Inplane and Lateral Loads* by Mashhour G. Ghoneim and James G. MacGregor, February 1992.

177. *A Field Study of Fastener Tension in High-Strength Bolts* by G.L. Kulak and K. H Obaia, April 1992.

178. *Flexural Behaviour of Concrete-Filled Hollow Structural Sections* by Yue Qing Lu and D.J. Laurie Kennedy, April 1992.

179. *Finite Element Analysis of Distributed Discrete Concrete Cracking* by Budan Yao and D.W. Murray, May 1992.

180. *Finite Element Analysis of Composite Ice Resisting Walls* by R.A. Link and A.E. Elwi, June 1992.

181. *Numerical Analysis of Buried Pipelines* by Zhilong Zhou and David W. Murray, January 1993.

182. *Shear Connected Cavity Walls Under Vertical Loads* by A. Goyal, M.A. Hatzinikolas and J. Warwaruk, January 1993.

183. *Frame Methods for Analysis of Two-Way Slabs* by M. Mulenga and S.H. Simmonds, January 1993.

184. *Evaluation of Design Procedures for Torsion in Reinforced and Prestressed Concrete* by Mashour G. Ghoneim and J.G. MacGregor, February 1993.

185. *Distortional Buckling of Steel Beams* by Hesham S. Essa and D.J. Laurie Kennedy, April 1993.

186. *Effect of Size on Flexural Behaviour of High Strength Concrete Beams* by N. Alca and J.G. MacGregor, May 1993.

187. *Shear Lag in Bolted Single and Double Angle Tension Members* by Yue Wu and Geoffrey L. Kulak, June 1993.

188. *A Shear-Friction Truss Model for Reinforced Concrete Beams Subjected to Shear* by S.A. Chen and J.G. MacGregor, June 1993.

189. *An Investigation of Hoist-Induced Dynamic Loads* by Douglas A. Barrett and Terry M. Hrudey, July 1993.

190. *Analysis and Design of Fabricated Steel Structures for Fatigue: A Primer for Civil Engineers* by Geoffrey L. Kulak and Ian F.C. Smith, July 1993.

191. *Cyclic Behavior of Steel Gusset Plate Connections* by Jeffrey S. Rabinovitch and J.J. Roger Cheng, August 1993.

192. *Bending Strength of Longitudinally Stiffened Steel Cylinders* by Qishi Chen, Alla E. Elwi and Geoffrey L. Kulak, August 1993.

193. *Web Behaviour in Wood Composite Box Beams* by E. Thomas Lewicke, J.J. Roger Cheng and Lars Bach, August 1993.

194. *Experimental Investigation of the Compressive Behavior of Gusset Plate Connections* by Michael C.H. Yam and J.J. Roger Cheng, September 1993.

195. *Some Behavioural Aspects of Composite Trusses* by Berhanu Woldegiorgis and D.J. Laurie Kennedy, January 1994.

196. *Flexural Behavior of High Strength Concrete Columns* by Hisham H.H. Ibrahim and James G. MacGregor, March 1994.

197. *Prediction of Wrinkling Behavior of Girth-Welded Line Pipe* by L.T. Souza, A.E. Elwi, and D.W. Murray, April 1994.

198. *Assessment of Concrete Strength in Existing Structures* by F. Michael Bartlett and J.G. MacGregor, May 1994.

199. *The Flexural Creep Behavior of OSB Panels Under Various Climatic Conditions* by Naiwen Zhao, J.J. Roger Cheng, and Lars Bach, June 1994.